NTRCI

NATIONAL TRANSPORTATION RESEARCH CENTER, INCORPORATED
University Transportation Center

U24: Heavy Truck Rollover Characterization (Phase C)

This project was funded by the NTRCI University Transportation Center under a grant from the U.S. Department of Transportation Research and Innovative Technology Administration (#DTRT-06-G-0043-03-U24-01-01)

Oak Ridge National Laboratory: Tim LaClair, Helmut Knee, Oscar Franzese
Clemson University International Center for Automotive Research: Michael Arant
Western Michigan University: Richard Hathaway, Mitch Keil
Battelle: Doug Pape, Dale Rhoda

August 2010

Technical Report Documentation Page

1. Report No.	2. Government Accession No.	3. Recipient's Catalog No.
4. Title and Subtitle **U24: Heavy Truck Rollover Characterization (Phase C)**		5. Report Date **August 2010** 6. Performing Organization Code
7. Author(s) **Oak Ridge National Laboratory: Tim LaClair, Helmut Knee, Oscar Franzese** **Clemson University International Center for Automotive Research: Michael Arant** **Western Michigan University: Richard Hathaway, Mitch Keil** **Battelle: Doug Pape, Dale Rhoda**		8. Performing Organization Report No.
9. Performing Organization Name and Address **National Transportation Research Center, Inc.** **University Transportation Center** **2360 Cherahala Blvd.** **Knoxville, TN 37932**		10. Work Unit No. (TRAIS) 11. Contract or Grant No. **RITA Grant – DTRT06G-0043**
12. Sponsoring Agency Name and Address **U.S. Department of Transportation** **Research and Innovative Technology Administration** **1200 New Jersey Avenue, SE** **Washington, DC 20590**		13. Type of Report and Period Covered **Final Report November 2009 – August 2010** 14. Sponsoring Agency Code **RITA/FHWA**
15. Supplementary Notes		

16. Abstract

The effect of changes in the suspension of a cargo tank semitrailer on its roll stability was studied in experiments and modeling. Three configurations were considered: a typical design; a design with a wider track; and a design with wider track and greater separation between the air bags. All configurations used new generation wide base single tires (NGWBST). The experiments consisted of a steady state "ramp" steer, a transient "step" steer, and a more challenging dynamic "double lane change" maneuver. Lumped parameter and flexible body models of the combination vehicle were developed and exercised. Widening the track of the semitrailer's axles raised the threshold for lifting a tire from the pavement, as predicted. Moving the suspension's air bags farther apart changed several characteristics of the behavior, with no consistently measurable changes in wheel liftoff threshold. Limited testing with electronic stability control (ESC) showed that the suspension changes did not affect ESC performance. The damping of the trailer roll oscillation provided by the suspension itself was greater than the damping provided by the shock absorbers. This auxiliary damping was generated, at least in part, by the restricted movement of air between the suspension air bags.

This work is the final in a series of studies funded by NTRCI to characterize the roll behavior of heavy vehicles and develop computer simulation models to explain that behavior. Previous studies have explored the behavior of a van semitrailer, a flatbed semitrailer, and a tank semitrailer.

17. Key Word	18. Distribution Statement		
Roll stability, heavy truck rollover; cargo tank semitrailer; vehicle dynamics model, suspension	**No restrictions**		
19. Security Classif. (of this report) **Unclassified**	20. Security Classif. (of this page) **Unclassified**	21. No. of Pages **340**	22. Price

Form DOT F 1700.7 (8-72) Reproduction of completed page authorized

Table of Contents

List of Figures

List of Tables

List of Abbreviations and Acronyms

Abbreviation or Acronym	Definition
a_y	Lateral acceleration
Battelle	Battelle Memorial Institute
Bendix	Bendix Commercial Vehicle Systems, LLC
CAN	Controller area network
CG	Center of gravity
CU-ICAR	Clemson University International Center for Automotive Research
DAS	Data acquisition system
DOE	US Department of Energy
DOT	US Department of Transportation
eDAQ	Brand of data acquisition system used at the test track
ESC	Electronic stability control. In this report, ESC is used as a generic term for any electronic system that automatically applies brakes on the tractor or semitrailer to enhance the stability of the vehicle in any way.
FEA	Finite element analysis
FEM	Finite element model
FHWA	Federal Highway Administration
GPS	Global positioning system
FOT	Field operational test
GVW	Gross vehicle weight
Hendrickson	Hendrickson Trailer Suspension Systems division of Hendrickson International Corporation
HTRC	Heavy truck rollover characterization
ISO	International Organization for Standards
K&C	Kinematics and compliance test
LBT	LBT, Inc.
Link	Link Commercial Vehicle Testing, Inc.
Michelin	Michelin Americas Research Company
NGWBS	New generation wide base single [tire]
NTRCI	National Transportation Research Center, Inc.
ORNL	Oak Ridge National Laboratory
RC	Roll compliance (a calculated quantity)
RSP®	Bendix proprietary roll stability program
RT unit	Oxford inertial and GPS measurement system, Model RT2500 or RT 3100
TRC, Inc.	Transportation Research Center, Inc.
Volvo	Volvo Trucks North America
WMU	Western Michigan University

Units of Measurement

Unit	Meaning
deg	degree of angle
deg/s	degree per second
deg/s^2	degree per second squared
g	gravitational unit, 9.8 m/s^2
kg	kilogram
km/h	kilometer per hour
kPa	kilopascal
m	meter
m/s	meter per second
m/s^2	meter per second squared
mm	millimeter
N•m	Newton-meter
N•m/deg	Newton-meter per degree
N•m•s	Newton-meter-second
s	second

Executive Summary

Background

The Heavy Truck Rollover Characterization (HTRC) Program is a major research effort conducted by the National Transportation Research Center, Inc. (NTRCI) in partnership with the Oak Ridge National Laboratory (ORNL), Michelin Americas Research Company (MARC or Michelin), Western Michigan University (WMU), Battelle Memorial Institute (Battelle), LBT, Inc. (LBT), Hendrickson Trailer Suspension Systems (Hendrickson), and Bendix Commercial Vehicle Systems (Bendix). This research is one of the major projects conducted by the NTRCI in its role as a University Transportation Center (UTC) for the Research and Innovative Technology Administration (RITA), an agency within the U.S. Department of Transportation (DOT). This research also involved, via subcontract, Volvo Trucks North America, Inc., and Link Commercial Vehicle Testing, Inc. (Link). In addition, Clemson University – International Center for Automotive Research (CU-ICAR) contributed technically to this effort.

This work is the final in a series of studies funded by NTRCI to characterize the roll behavior of heavy vehicles and develop computer simulation models to explain that behavior. This phase continued the development and validation of models and included experiments with changes in semitrailer suspension design. Previous studies have explored the behavior of a van semitrailer, a flatbed semitrailer, and a tank semitrailer.

Initiated in 2004, the HTRC Program has identified and studied designs and technologies having a potential to improve the roll stability and safety of heavy-duty tractor-trailer combinations. These options have included design changes including wider tire spacing and a lower center of gravity (CG) of the trailer; components such as New Generation Wide Base Single (NGWBS) Tires; and technologies such as tractor and trailer electronic stability control (ESC) systems. The long-term goal of the effort is to develop a concept for a completely new highway vehicle (class-8 tractor-semitrailer) in which all of the components affecting stability have been designed and optimized to function as a system to improve stability.

Brief Overview

The overall objectives of this research program were to:

- Contribute to the understanding of the dynamics of heavy-duty commercial vehicle rollover and stability,
- Contribute to the development and validation of advanced computer models of heavy truck vehicle dynamics that reflect project experiences, and
- Develop recommendations for the improvement of the roll stability of heavy vehicles in preparation for realizing and testing such concepts in future phases of related research.

The specific objectives of the current phase were to:

- Modify a tank semitrailer to implement two different trailer suspension designs selected by the research team,
- Conduct track testing of the modified test vehicle to generate data for use in model validation,
- Analyze the test track data to estimate stability and safety benefits of the selected suspensions,
- Complete the development of the TruckSim® and Adams models initiated in prior phases of the HTRC research program,
- Validate the completed TruckSim® and Adams models by comparing model predictions with data from two phases of track testing,
- Apply the validated models to other designs and technologies to estimate stability benefits,
- Prepare a final report, and
- Prepare a Statement of Work (SOW) for future, related research.

The goals for this phase were to have a validated set of TruckSim® and Adams models available to the research team that could be confidently applied to evaluate designs and technologies that are aimed at improving the stability and safety of heavy-duty commercial vehicles. Future efforts could quantify the expected benefits from specific design technology options, support the prioritization of design technology options for specific heavy-duty commercial operations, and could provide data and information to support early adoption of high value design technology options by private industry.

Research Strategy

The strategy for the HTRC research program has been to develop a strong research base for conducting heavy-duty commercial vehicle stability and safety research. This research base involves three primary elements:

- The development of a deep understanding of heavy-duty commercial vehicle dynamics and stability,
- The development of state-of-the-art tools and analysis techniques for heavy-duty commercial vehicle stability studies, and
- Research team building to include national laboratory, academic and industry organizations interested in heavy-duty commercial vehicle stability improvements.

Efforts in the Current Phase

The research interest in this phase was to complete the TruckSim® and Adams modeling efforts, and to demonstrate that the models can reliably predict the magnitude of improvements that specific design changes actually provide. Two simple design modifications were made to the

tank semitrailer used in the previous phase, and they were tested on a test track in various maneuvers that induce wheel lift events, similar to maneuvers in the real world that can lead to rollover of a tractor-trailer. Data from the test track was compared with the results of the TruckSim® and Adams models to validate the models.

A photograph of the test vehicle is in Figure ES-1.

Figure ES-1. Photo. This tractor and tank semitrailer were used in the experiments. In this phase's work, two different suspensions were mounted under the semitrailer. Experiments with different tires and semitrailer CG heights were conducted in a previous phase.

Tank Semitrailer Modification

The tank trailer used in the previous phase was outfitted with new suspensions for this phase. The first modification was a wider axle that increased the track width by 160 mm (6 in.). The second modification was to increase the spacing between the beams (similar to trailing arms) in the suspension. The suspension with the greater beam spacing also had the wider axle. The photograph of a Hendrickson trailer suspension in Figure ES-2 names the parts. The sketch in Figure ES-3 shows the key dimensions that were varied between the three suspensions configurations.

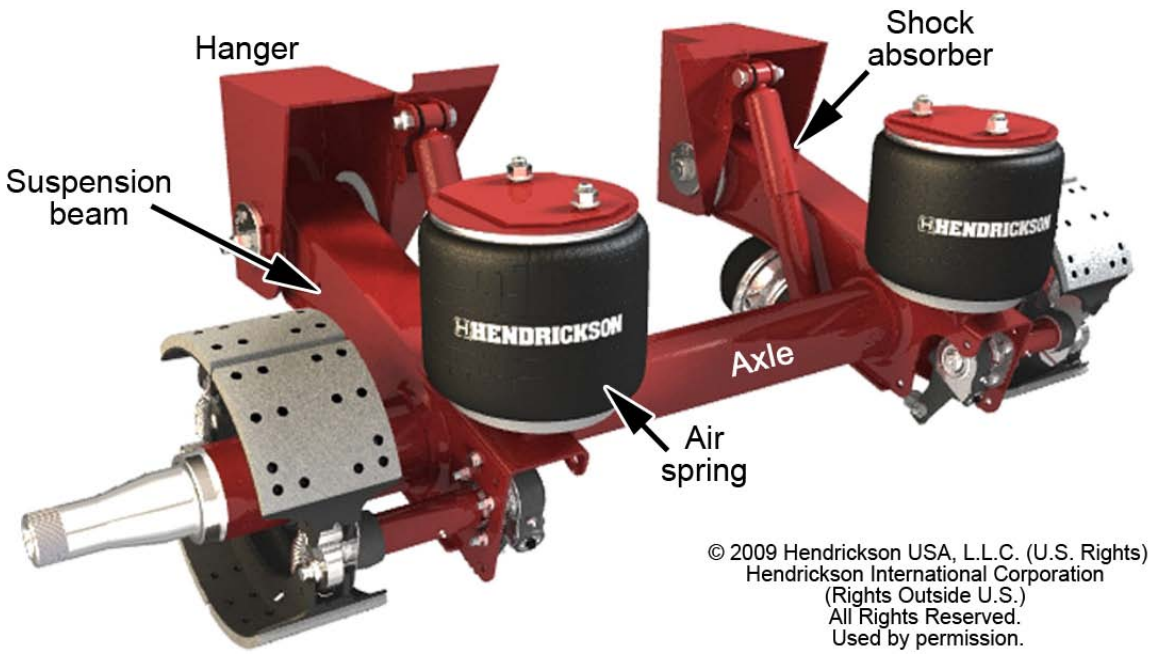

Figure ES-2. Photo. Suspensions of this design were installed on the semitrailer

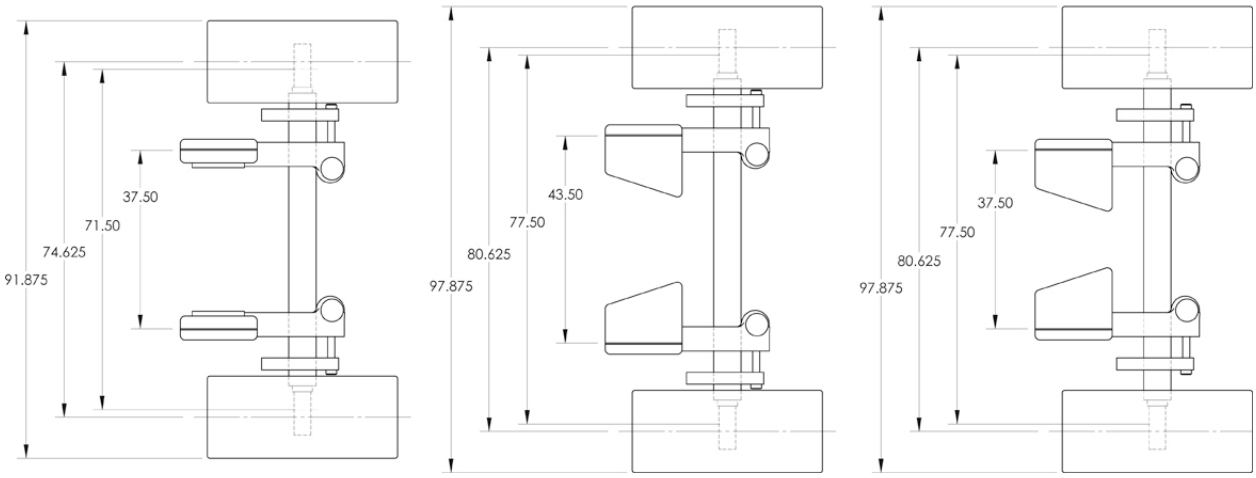

Figure ES-3. Drawing. Key dimensions of the suspensions used in this experiment. The view is looking down at the suspension. Top to bottom in the sketch is left to right on the trailer. Dimensions are in inches. The suspension at the left was used in the previous phase. The suspension on the right has the wider axle but the same beam spacing as the previous phase.

All other design features were maintained the same. As such, direct comparisons evaluating single factor design parameter changes could be made. Specifically, the results from the previous phase were compared with those of the wider axle design with the same beam spacing to measure the effect of the track width change alone. Similarly, test results of the narrower and wider beam spacings isolated the effect of that change. The tank trailer modifications to accommodate the wider axle configurations were graciously donated by LBT and both of the suspensions were generously donated by Hendrickson. Michelin contributed a set of NGWBS tires. Only NGWBS tires were used because the tire fitments were not the subject of study in this phase.

K&C Testing

After the suspension modification was completed by LBT and Hendrickson, the modified tank trailer was sent to Michelin for K&C testing at their heavy vehicle test rig located in Greenville, South Carolina. The K&C testing encompassed the evaluation of the semitrailer's response to applied loads and motions in vertical, lateral, and longitudinal directions and in roll. The tank trailer chassis was also evaluated for torsional compliance. The data collected consisted of kinematics curves (such as toe change under jounce), and compliance curves (such as wheel deflection under load). The characterization was necessary to generate data for use in the TruckSim® modeling.

Track Testing

The track testing was conducted from April 8-13, 2010. As in the previous phase, Link Commercial Vehicle Testing, Inc., of East Liberty, Ohio mounted and configured all test instrumentation (other than the strain gages) and conducted the testing on the test track. WMU donated, installed, and calibrated the strain gages on the test vehicle. The test vehicle was instrumented to collect data from a total of 150 separate channels at 100 Hz, including individual sensors, inertial global positioning system (GPS) devices, and quantities read from the tractor controller area network (CAN) bus. Representatives from most of the HTRC research team organizations were present for some or all of the testing. A steering robot was used for all maneuvers to assure repeatability and consistency. The tractor and trailer ESC systems were enabled for some of the maneuvers. Unlike the previous phase, however, the tractor and trailer ESC systems were either both enabled or both disabled. Prior to the testing, the HTRC research team also worked to refine software developed in prior phases of this program, to be used for data reduction and analysis. This software allowed rapid review of the test data in the field. Coordination of the test track efforts was led by ORNL but was ultimately shared among the team members for the project. The on-track testing was successfully conducted and was possible due to thorough planning and a solid commitment from the HTRC team and Link; with excellent teamwork between everyone involved.

Data Analyses

The test data was analyzed by ORNL, WMU, and CU-ICAR. Data analysis of each selected maneuver was accomplished by the organizations indicated below:

- Steady-State Ramp Steer Maneuver (WMU and CU-ICAR),
- Step Steer Maneuver (CU-ICAR and ORNL),
- Open-Loop Double Lane Change Maneuver, dry surface (ORNL and WMU)
- Modified Step Steer - Auxiliary Roll Damping Maneuver (WMU)

The wider axles required higher lateral accelerations to generate wheel lift for all of the maneuvers tested, and the results were statistically significant. The beam spacing played a much smaller and less consistent role.

Table ES-1 is a simplified comparison of the experimental results in the previous phase and the current phase. The nominal case in the first row has a CG height typical of a gasoline-carrying tank semitrailer, fitted with NGWBS tires. Subsequent rows are for conditions that are changed from the nominal, with entries in bold to make changes easier to identify. The next row was the same condition but with dual tires instead. When mounted on the same axle, dual tires have a greater overall width than NGWBS tires. The third row is an identical vehicle but with the ballast lowered to represent a semitrailer CG height that is about 4-1/2 in. lower. The next row in the table is the same as the first row, but the suspension has been replaced with one having a wider axle, so the overall tire width is increased by 5-1/2 in. The final row differs from the next-to-last row in that the suspension beams have been moved apart 6 in.

The “lift threshold” in the table is the lateral acceleration (“cornering force”) at which the rear inside tire of the trailer begins to lift off the ground in a high-speed steady curve. This is but one of several measures of roll stability analyzed in the main report. The change from NGWBS tires on the tractor and trailer to dual tires on the drive and trailer axles lowered the lift threshold by a barely measurable amount. Lowering the trailer CG and spreading the tires apart both significantly benefitted the vehicle’s ability to keep all of its tires on the pavement. The difference in results between the two beam spacings was not repeatable across different measures of lift threshold.

The three suspensions were modeled with finite elements before the testing. Widening the beam spacing was predicted to increase the roll stiffness of the suspension by 23%, and strain gages on the axle tube measured an increase in the roll stiffness of 28% on the test track. Higher roll stiffness helps to stabilize the vehicle, but the improvement in semitrailer roll stiffness is diluted by the other compliances, notably the semitrailer tires and the tractor’s suspension and tires. When these effects were considered, the change in roll stiffness was calculated to produce a barely perceptible improvement in wheel lift threshold.

Table ES-1. Simplified Comparison of Experimental Results

Condition	Beam Center Spacing in. *mm*	Tire		CG Height in. *mm*	Lift Threshold in a Steady Curve	
		Type	Overall Width in. *mm*		g	Change from nominal
Nominal	37.5 *953*	NGWBS	92.2 *2342*	81.4 *2067*	.364	--
Dual Tires (note the accompanying increased overall width)	37.5 *953*	**dual**	**96.6** ***2454***	81.4 *2067*	.361	-0.9%
Dual Tires and lower CG height	37.5 *953*	**dual**	**96.6** ***2454***	**76.8** ***1952***	.380	+4.1%
Wider Track	37.5 *953*	NGWBS	**97.875** ***2486***	81.4 *2067*	.388	+6.4%
Wider Track, Greater Beam Spacing	**43.5** ***1105***	NGWBS	**97.875** ***2486***	81.4 *2067*	.389	+6.7%

The ESC system performance was also evaluated for a limited number of cases to verify that no anomalous results were observed with the modified suspensions. The ESC system performance was fully consistent with expectations, and wheel lift was not observed for any of the maneuvers performed with the ESC systems enabled.

Modeling

The modeling suite included both TruckSim® and Adams models. TruckSim® is a rigid-body model, and suspensions are modeled by a few parameters rather than explicitly accounting for a number of components. TruckSim® uses characterization data such as the K&C and torsional compliance to model the dynamic behavior of the tractor-trailer. On the other hand, Adams is a flexible body model that models individual components down to the bushing level. As such, it is more complex geometrically and requires measurements on a more detailed level than TruckSim®. Together, these models provide a powerful suite for analyzing options for improved stability.

TruckSim® modeling involved a number of activities. First, the TruckSim® model was run with the wider axle and wider beam spacing to predict stability benefits of these changes. After the K&C data was received, the TruckSim® model was updated and the runs were repeated for the maneuvers to be run on the test track.

A finding that involved the track testing, modeling, and data analysis was the identification of an auxiliary roll damping effect. The results of the TruckSim® simulation of the previous phase's lane change maneuver did not match the test track results. Specifically, the roll oscillation of the trailer following the maneuver was much more damped in the experiment than in the simulation. To achieve similar damping in the model, an auxiliary roll damping factor had to be added to the

damping provided by the shock absorbers. An additional track test in the current phase illuminated this phenomenon, showing that the auxiliary roll damping was generated, at least in part, by the restricted movement of air between the suspension air bags. The additional knowledge gained through this testing led to the improvement of the TruckSim® model, and suggested a possible means to improve roll stability during transient maneuvers.

Lastly, the TruckSim® model was applied to other selected design and technology options to quantify their stability benefits. These assessments serve as a precursor to a more comprehensive evaluation in future research. More elaborate design changes require that an auxiliary model be used to estimate the changes in kinematics and compliance. The Adams model will be available to provide these estimates. Although the results were not delimitative, they indicated likely future design technologies for enhancing heavy-duty commercial vehicle stability. These areas include considerations and options related to:

- Trailer CG height,
- Trailer axle suspension,
- Trailer frame and structure,
- Tractor front suspension,
- Tractor frame and structure,
- Wheel and tires, and
- Electronic stability

The Adams model was run for two of the experimentally tested vehicles to compare with experimental results. It was also run for one hypothetical vehicle to predict the change in wheel lift threshold produced by a change in frame stiffness.

Future Program Efforts

Completion of this phase has resulted in the validation and increased confidence in the advanced TruckSim® model of the tank semitrailer, and has demonstrated the ability of the HTRC research team to effectively design and conduct test track-based experiments that are sufficiently controlled to address difficult heavy-duty commercial vehicle stability issues, and to analyze the associated data. This research has also resulted in the identification of new heavy-duty commercial vehicle stability options, such as the auxiliary damping effect, that are relatively easy to study in more depth and that offer significant stability benefits. With the tank semitrailer research base and the advanced flatbed model validated in an earlier phase of this program, future efforts will be turned toward the development of a new heavy-duty commercial vehicle stability concept that could be achievable in the near-term future. Such a concept will not necessarily involve a revolutionary new tractor-trailer design, but will focus initially on the integration and exploitation of design technology options that can more readily be embraced by industry. Solid research and effective demonstration of high-value stability design options can result in enhanced safety on our highways, reduced risk in the movement of freight, and the

achievement of technical solutions for freight movement fuel efficiencies without reducing safety. With this perspective, new research in heavy-duty commercial vehicle stability can continue. In particular, the following research is recommended:

- Comprehensive identification of possible design and technology options for class-8 combination vehicles and selection of specific options for future assessment,
- Quantitative assessment, via modeling, of the stability benefits of selected design or technology candidates,
- Identification of designs and technologies that could be included within a "Buildable Concept," i.e., a concept that is not radically different from the design of today's commercial vehicles, but that offers a significantly improved stability profile – and is not prohibitively expensive,
- Study of the vehicle dynamics of multi-trailer commercial vehicles, which offer enhanced fuel efficiencies per ton of payload, and
- Enhancement of ESC systems to support the coordination of the tractor and the trailer's (or multiple trailers') ESC systems. This can begin by co-simulation of an ESC system and the vehicle. Areas to consider include considering total stability and not only roll stability, developing ESC controllers, integrating hardware improvements in the ESC controller and moving from a tractor-only toward a full-vehicle control system

Chapter 1 – Introduction and Background

This work is the final in a series of studies performed by the Heavy Truck Rollover Characterization (HTRC) Program. Initiated in 2004 and funded by the National Transportation Research Center, Inc. (NTRCI) by partner organizations, the HTRC has characterized the roll behavior of heavy vehicles and developed computer simulation models to explain that behavior. The long-term goal of the effort is to develop a completely new highway vehicle (class-8 tractor-semitrailer) in which all of the components affecting stability have been designed and optimized to function as a system to improve stability. Previous studies have explored the behavior of a van semitrailer (Knee et al. 2005), a flatbed semitrailer (Pape et al. 2008), and a tank semitrailer (Arant et al. 2009).

The HTRC Program has identified and studied designs and technologies having a potential to improve the roll stability and safety of heavy-duty tractor-trailer combinations. These options have included New Generation Wide Base Single (NGWBS) Tires; tractor and trailer electronic stability control (ESC) systems (with combinations of the tractor and trailer ESC being on or off); wider-slider suspensions; and variations in the center of gravity (CG) of trailer. Table 1-1 summarizes these phases of research.

The research involved design and execution of test track testing; kinematics and compliance (K&C) testing; analysis of track testing data; and model development in TruckSim® and Adams. It also involved supporting activities such as instrumentation acquisition; development of data quality assurance software; test planning; partnership building; and report preparation. As this research progressed, the HTRC team gained significant experience and expertise in the design and execution of the track testing and in the development and application of the TruckSim® and Adams models to the maneuvers conducted during track testing.

The primary technology insights gained over the past six years include:

- Improvements to stability provided by ESC systems (studied for the tractor-flatbed trailer and tractor-tank trailer).
- Quantification of the improvement in stability by lowering the CG height
- Enhanced stability of a tractor-van trailer combination when a wider-slider suspension was used in conjunction with NGWBS tires.
- Improved model of the behavior of tractor-trailer combinations with high torsional compliance (i.e., the tractor-flatbed trailer combination).

The model validation and suspension testing formed the basis for the activities conducted in the current phase (Phase C) of the program.

Table 1-1. HTRC Program phases and subjects

Phase	Year	Semitrailer Body Style	Subject	Reference
1 and 2	2005	Van	Tire selection (dual vs. NGWBS) Track (slider) width CG height	Knee et al. 2005
A	2008	Flatbed	Tire selection (dual vs. NGWBS) Torsional compliance CG height Electronic Stability Control	Pape et al. 2008
B	2009	Tank	Tire selection (dual vs. NGWBS) CG Height Electronic Stability Control	Arant et al. 2009
C	2010	Tank	Suspension properties Electronic Stability Control (secondary)	(this report)

Chapter 2 – Project Overview

This chapter provides a high-level overview of the activities undertaken in Phase C of the HTRC Program. The research conducted in this phase continues the work of Phases 1, 2, A, and B. The primary Phase C goal was to validate the TruckSim® and Adams models by comparing the results from controlled test track experiments with the modeling results for the same maneuvers. The second goal was to study the effect of two suspension designs on the vehicle's roll stability. The effect was characterized in maneuvers ranging from simple steady state maneuvers to others that were quite dynamic.

The primary activities in Phase C were:

- Completion of the development of the TruckSim® and Adams models,
- Identification of two design technology options that could be easily implemented on the tank-trailer (the same physical tank-trailer used in Phase B research),
- K&C testing of the modified tank-trailer to generate the data required by TruckSim®,
- Design and accomplishment of track testing to generate new performance data,
- Track testing with the tractor and trailer modified using the selected options,
- Modification of the completed TruckSim® and Adams models to reflect the selected modifications and to simulate the maneuvers conducted on the track,
- Comparison of the TruckSim® and Adams modeling results to the track testing results to validate the models,
- Application of the validated TruckSim® and Adams models to additional selected design technology options to assess their potential benefit to stability and safety, and
- Analysis of the track testing data to estimate the stability benefits of the additional selected design technology options.

This chapter contains highlights of these major activities. Each is described in more detail below.

2.1 Pre-Test Activities

Before performing the track testing, the HTRC project team prepared by:

- Developing and refining the test plan,
- Selecting the maneuvers to be performed and how to best perform them,
- Determining the vehicle configurations for which track testing should be conducted,
- Specifying the measurement channels to be measured during track testing,
- Refining the software for data collection and quality assurance,
- Manufacturing the axles for the different vehicle configurations to be tested,
- Reconfiguring the tank trailer to accept both sets of axles, and
- Conducting the K&C testing to characterize the tank trailer in the TC1 configuration before track testing.

Input was solicited and gathered from all team members during this process to achieve consensus among the members of the HTRC team.

At a kickoff meeting in November 2009, the team discussed vehicle configuration variations that could be included in the Phase C testing. Follow-up telephone conferences were held to finalize the selection of the design variations that would be tested. The team decided to focus on suspension design modifications and selected two axle design variations as the primary parameters to test. Two suspension designs, designated TC1 and TC2, were selected. They are similar in construction to the suspension of "Tanker T" that was used in the Phase B track testing, but they are 152 mm (6 in.) wider. In this way, the performance of the three suspension configurations (i.e., Tanker T, Tanker TC1 and Tanker TC2) could be compared in a fairly "clean" manner, enhancing the utility of the test data for model validation. A shock absorber with high rebound damping was planned to be studied as a lower priority, but was shown to be unnecessary based on test results from other maneuvers, as described in Section 7.2.4. The CG height of the tank trailer during testing was selected to be as close as possible to that used in the Phase B track testing performed with the NGWBS tires, enabling direct comparison with the test results from Phase B. The three suspensions are described more fully in Section 6.11.

The team worked to further refine and streamline the software for data reduction and analysis to enable rapid review of track testing data in the field. An approach similar to that which was developed in previous phases of testing was followed, and pre-existing software code was used and modified for this activity. For example, the team rewrote the software used to convert the eDAQ data acquisition output files to text files so that they can be read directly by the Matlab-based post-processing software routines. This software now runs directly from within Matlab enabling a single user to perform all of the data conversion steps necessary to review and analyze the data. Additional post-processing software was written to allow members of the HTRC team to rapidly scan the test results of all data channels in succession. During track testing, three of the HTRC team members dedicated their time to reviewing the data using the enhanced software. This division of labor enabled the HTRC team to quickly identify problems with a test run so that any needed retesting could occur promptly and efficiently.

2.2 Phase C Test Plan

The Phase C Test Plan provided guidance to the project research team and the test contractor, Link Commercial Vehicle Testing, Inc. (Link), for conducting track testing at the Transportation Research Center, Inc. (TRC, Inc.), and for describing the related tractor-trailer configurations, data acquisition configurations, equipment, and test events. The test plan included descriptions of the:

- Maneuvers to be performed,
- Suspension designs to be addressed,
- Logistics of changing the suspensions,
- Tractor and trailer ESC systems,
- Instructions to the driver and steering robot program for executing each maneuver,
- The speeds at which each maneuver was to be executed,
- Number of repetitions,

- Direction of travel for the maneuvers (clockwise or counter-clockwise; left or right),
- Vehicle configuration,
- Data channels, and
- Frequency of data sampling.

The final Phase C Test Plan appears in Appendix A of this report.

The Phase C Test Plan was developed over a period of several months. It built upon the Phase B test plan but included information related to the design technology options to be addressed in Phase C. The Phase C test plan resulted from an iterative process among the members of the HTRC team. These iterations involved decisions related to the data channels; how best to collect the data; positioning of sensors; management of the test data; use of the steering robot; the nature of the options to address in the track testing; and data quality assurance. The test plan was agreed upon by the HTRC team and was provided to Link in a request for a price quotation in executing the test plan. The test plan was modified, as required, to assure that the efforts could be conducted within the time and budget of the Program.

2.3 Test Vehicle

The tractor used for the Phase C testing was a 2007 Volvo VT 830, model VT64T830, with a full sleeper cab, and was the same tractor used in the Phase A and Phase B testing. The LBT tank trailer used for Phase C testing was the same physical tank trailer (i.e., Tanker T) that was used in the Phase B track testing. The tank semitrailer is based on a typical petroleum tank with a total nominal volume of 9,200 gallons. The test unit had the same barrel configuration as a standard model, including cross-sectional shape, length, height, placement of heads and baffles. However, to facilitate shifting the center of gravity and to achieve the proper ground loads with the extremely heavy test tractor, the second baffle in the first compartment was replaced with a bulkhead. The extra bulkhead made a sixth compartment, which is not common. Except for the sixth compartment, the test semitrailer, LBT Model TAG-HA2-ESF9200x6SD, is quite representative of aluminum tanks in use today meeting the “DOT 406” specification (49 CFR 178.346, *Specification DOT 406; cargo tank motor vehicle*).

The semitrailer was modified from its Phase B configuration by replacing its suspension with other suspensions having wider axles. Two suspensions were tested that had different left-to-right spacing between the points at which the suspension connects to the chassis. Figure 2-1 shows the test vehicle. Details of the configurations and associated changes during the track testing are provided in Section 6.1.

Figure 2-1. Photo. The Volvo tractor and LBT tank trailer used in testing

2.4 Track Testing

As in previous phases of this Program, track testing was conducted at TRC, Inc., located in East Liberty, Ohio. As with the efforts conducted in Phase B, the test track activities were executed by Link. The testing was performed from April 8 through April 13, 2010, and involved representatives from all of the HTRC member organizations.

The testing involved two suspension designs (Tankers TC1 and TC2). These two variants, tested in Phase C, can be studied in conjunction with the "Tanker T" data from Phase B to provide the opportunity for a three-way comparison of the effect of the suspension on roll behavior. For consistency with the track testing of Phase B, the same test track maneuvers were performed (Ramp Steer, Step Steer and Open Loop Double Lane Change). For the Phase C track testing, the ESC systems for the tractor and for the trailer were either both enabled or both disabled. No CG variations were studied in Phase C. One set of tires, which included NGWBS tires on the drive and tank trailer axles, was used throughout Phase C.

One additional test was conducted during Phase C that had not been done in prior phases of the Program. The additional test was conducted to assess the auxiliary roll damping of the tank trailer. This was done because the results of the simulation of the Phase B lane change maneuver in TruckSim® did not match the Phase B track testing results. Specifically, the roll oscillation of the trailer following the maneuver was much more damped in the test track experiments than in the simulation. To achieve similar damping in the model, an auxiliary roll damping factor had to be added to the damping provided by the shock absorbers. The additional test in Phase C illuminated this phenomenon, showing that the auxiliary roll damping was generated, at least in part, by the movement of air between the suspension air bags. The additional knowledge gained through this testing led to the improvement of the TruckSim® model, and suggested a possible means to improve roll stability. The results of this additional testing appear in section 7.2.4.

2.4.1 Instrumentation

The instrumentation used for the Phase C testing was selected to allow the HTRC team to characterize the tractor tank trailer for its rollover and steady-state understeer performance. The data channels selected for the testing were agreed to by the HTRC team based on the primary data needs; considerations of budget constraints; and consistency with Phase B testing so that direct comparisons could be made with previous test results. Many of the channels used during the Phase B track testing were included in the Phase C track testing, but some differences existed. For example, Phase B testing included a series of measurements to characterize the ESC system, while Phase C testing emphasized suspension differences with the ESC system playing only a minor part. Accordingly, many of the brake pressure sensors used in the Phase B testing were not installed for the Phase C testing. With Phase C's emphasis on the suspension's contribution to roll stability, however, sensors were added to characterize how the suspension reacted during the maneuvers. Strain gages to quantify the bending and torsion of the axles were included, and pressure sensors were included at different air bag locations to allow for an understanding of how the pressure changed in the suspension during the maneuvers.

The instrumentation was selected to monitor the motions of the two chassis units (the tractor and the tank trailer) as well as the first drive axle (axle 2), the rear drive axle (axle 3), the lead tank trailer axle (axle 4), and the rear tank trailer axle (axle 5). The steer axle is designed to maintain contact with the road and is almost always the last axle to leave the ground. For this reason, it was not instrumented to identify wheel lift. Table 6-3 summarizes the measurements made during the track testing.

2.4.2 Overview of the Data Analysis

CU-ICAR, ORNL, and WMU each analyzed the data generated during the Phase C track testing, with results that are presented in Chapter 7. The primary objective of the data analysis was to quantify and compare the differences in roll performance between the two tank trailer suspensions (i.e., using configurations TC1 and TC2) that were tested in Phase C and to compare the test track results for configurations Tankers TC1 and TC2 with the results of the testing with the Phase B trailer configuration (i.e., Tanker T, with NGWBS tires and similar CG height). Each organization analyzed two maneuvers, providing a duplicate analysis of each maneuver to ensure that similar results were obtained when different researchers analyzed the same test data. As noted above, special testing was performed to assess the auxiliary roll damping of the trailer, and a detailed analysis of the roll damping was completed.

CU-ICAR analyzed the low-speed ramp steer maneuver to evaluate the basic steady-state performance for the tractor-semitrailer in the configurations tested in Phase C. CU-ICAR also conducted a statistical analysis to evaluate wheel lift in the high-speed ramp steer and the step steer maneuvers.

ORNL compared the three vehicle configurations in the step steer and open-loop double lane change maneuvers.

WMU conducted a detailed analysis of the track data from the open-loop double lane change and both the low- and high-speed ramp steer maneuvers. The analysis directly compared the measured temporal data, including lateral accelerations, roll angle, and articulation angle, of the two vehicle configurations tested in Phase C, and a physical interpretation was provided for many of these results. Differences in fifth wheel separation during testing were examined for the TC1 and TC2 suspensions. WMU analyzed the data to characterize the auxiliary roll damping and developed a much-enhanced understanding of the contributions of the suspension air bags to the auxiliary roll damping.

Although the analysis approaches used by ORNL, CU-ICAR, and WMU were different, the primary conclusions were similar, as detailed in Chapter 7.

The ESC system performance was evaluated for a limited number of cases during the Phase C testing, to verify that no anomalous results were observed with the modified tank trailer axle designs. ESC system performance was fully consistent with expectations, and wheel lift was not observed for any of the maneuvers performed with the ESC systems activated.

2.5 Kinematics and Compliance (K&C) Testing

K&C testing (Figure 2-2) is an essential element for development of functional vehicle dynamic simulation models such as TruckSim®. Functional simulation models use the descriptions of relative motion between each wheel plane relative to the chassis as a function of suspension and steering displacement (kinematics) and deflections (compliance). The K&C testing monitors the body and wheel planes so the relationship of the vehicle to the wheel, and the wheel to the ground, can be determined. Michelin conducted K&C testing on both the Volvo tractor and the LBT tank trailer used in Phase C (i.e., the Tanker TC1 with wide beam spacing). Data from these tests were used in the WMU TruckSim® models.

Figure 2-2. Photo. LBT tanker in kinematics and compliance (K&C) testing

2.6 Overview of the Modeling

TruckSim® and Adams models were initiated in prior phases of research. TruckSim® modeling is important because of its ability to reflect vehicle dynamics from a systems perspective. For more detailed analyses that involve vehicle design at the component level, Adams modeling was chosen. Together, they provide a strong modeling suite that can be used to investigate the stability and safety benefits of design technology options.

Development of the TruckSim® and Adams models has been a primary thrust in this Program. The experience of attempting to adequately model a vehicle with high torsional compliance led to the model validation efforts conducted in the current phase of the research. Additionally, differences between the modeling results and the results of the data collected during track testing led to the identification of the auxiliary roll damping effect. After this effect was understood and appropriately reflected in the TruckSim® model, good agreement between the TruckSim® modeling results and the data from the track testing was achieved. This good agreement established strong confidence in the TruckSim® model and as a result, it is considered to be a validated model. The validated TruckSim® model was also applied to a set of selected design technology options to generate estimates of stability and safety benefits. Details regarding the TruckSim® validation efforts and results of the application of the validated TruckSim® model are in Section 7.7.

2.7 Team Members

The Phase C research was conducted by the HTRC team, which is composed of organizational participants from national laboratories, academia, non-profit research organizations and private industry. This section briefly describes the roles of each of the HTRC partners in the Phase C research.

ORNL Roles and Responsibilities

ORNL was the primary technical lead and Project Manager for Phase C efforts. ORNL performed a similar role in Phases 1, 2, A and B of the HTRC efforts for NTRCI. ORNL has significant vehicle instrumentation and testing experience (especially with regard to heavy trucks), and has been involved in numerous projects that included on-track testing and FOTs for various agencies of DOT, DOE and for NTRCI. ORNL has also conducted in-depth and unique data analysis of field-test and on-track testing data for various agencies of the DOT, the DOE and the NTRCI, and has been the lead author on numerous field-test and on-track testing technical reports. ORNL applied its Program Management expertise of large, real-world, multi-year, multi-million dollar and multi-organizational projects along with its technical depth of vehicle and fleet instrumentation, real-world testing, and its expertise in data analysis capabilities, to the execution of this project.

Michelin Americas Research Company (Michelin) Roles and Responsibilities

Michelin was a primary industry technical lead for the Phase C research. Michelin was one of two primary industry participants in the Phase 1 and 2 HTRC efforts, and the primary industrial participant in Phases A and B. In addition to providing NGWBS tires and rims for testing, Michelin‘s roles included conducting the K&C and torsional stiffness testing for Tanker TC1.

WMU Roles and Responsibilities

WMU provided experience in vehicle dynamics and computer modeling, and was the lead in conducting the TruckSim® and Adams modeling efforts. WMU identified a number of design technology options some of which were modeled with TruckSim®, and benefits to stability and safety were identified. Phase C modeling efforts concluded with a TruckSim® model that is considered validated (i.e., it replicated well the data and information generated during the on-track testing).

Battelle Roles and Responsibilities

Battelle provided analysis and consulting support for the HTRC‘s Phase C on-track experiments, participated in the data analyses, and lead the compilation and production of this final report. Engineers at Battelle with experience in vehicle dynamics and instrumentation reviewed the test plans and participated in an advisory role in the data collection and analysis efforts. A Battelle statistician performed most of the statistical analysis. A statistician from Battelle performed the statistical comparisons (i.e., hypothesis tests) and generated figures to facilitate the interpretation of comparison results. Battelle supported efforts to assure the project‘s continuity with prior and anticipated future data collection efforts.

LBT Roles and Responsibilities

LBT participated in the planning of the test track activities and contributed to the selection of the TC1 and TC2 suspensions. LBT modified Tanker T (used for track testing in Phase B) to accept a wider axle and suspension beam spacing provided by Hendrickson. LBT also arranged for the logistics of the tank trailer for the K&C testing at Michelin. LBT provided extensive and deep expertise regarding tank trailer design and dynamics for Phase C efforts, participated in numerous technical discussions, and provided technical insights for the on-track testing.

Bendix Roles and Responsibilities

Bendix provided and installed an ESC system for at no charge to the project. Bendix also participated in several of the Phase C HTRC technical discussions bringing their extensive heavy-duty vehicle testing experience to the team.

Volvo Roles and Responsibilities

Volvo provided access to the same tractor as that which was used in the Phase B test track testing. Volvo also provided significant real-world experience with regard to tractor trailer dynamics and participated in Phase C HTRC technical discussions.

Hendrickson Roles and Responsibilities

Hendrickson graciously provided the TC1 and TC2 suspensions, which were the focus of the track testing. Hendrickson also participated in many of the technical discussions and at the test track, bringing their extensive axle and suspension experience to defining the test plan and specifying test data that should be collected.

CU-ICAR Roles and Responsibilities

CU-ICAR became a partner with the HTRC team in May 2010. Throughout Phase C, close coordination was maintained with CU-ICAR's Co-Sim project, another NTRCI-funded project. CU-ICAR participated in the on-track testing, conducted data analyses for two of the three maneuvers conducted at the test track, and contributed to a number of HTRC Planning meetings. Their participation provided extensive vehicle dynamics experience to the research team in Phase C.

2.8 Project Schedule

The prior phase of research, Phase B, was concluded on September 30, 2009. Phase C planning began in July 2009, and Phase C itself began in November 2009. The statement of work consisted of 12 tasks conducted over nine months, November 1, 2009 through July 31, 2010. A project schedule, list of tasks, and lead organizations per task are provided below.

Tasks	Months of the Project								
	11/09	12/09	01/10	02/10	03/10	04/10	05/10	06/10	07/10
1	■	■	■	■	■	■	■	■	■
2	■	■	■	■	■				
3	■	■	■	■	■	■			
4			■	■					
5					■				
6			■	■	■				
7						■			
8							■	■	
9						■	■	■	
10								■	■
11							■	■	■
12							■	■	■

Figure 2-3. Chart. Schedule of tasks in Phase C

Task 1: Program Management (ORNL Lead)
Task 2: Completion of the Tractor Tank Trailer Modeling (WMU Lead)
Task 3: Identification and Selection of Candidate Design and Technology Options for Roll Stability Enhancement and Model Validation (WMU Lead)
Task 4: Modifying Tanker T to Tanker TC1 (LBT Lead)
Task 5: Physical Testing of Tanker TC1 (Michelin Lead)
Task 6: Developing a Test Plan for On-Track Testing for Model Validation (ORNL Lead)
Task 7: On-Track Testing for Model Validation (ORNL Lead)
Task 8: Analyzing On-Track Testing Data (ORNL, Michelin and WMU Co-Leads)
Task 9: Modeling Runs for Validation and Benefits of Design and Technology (WMU Lead)
Task 10: Design and Technology Recommendations for SafeTruck (WMU Lead)
Task 11: Planning for Phase D and Beyond (ORNL Lead)
Task 12: Phase C Final Report and Executive Summary (Battelle Lead)

Some Phase C events involving the modification of the Phase B tank trailer (Tanker T) and the on-track testing are described below.

LBT modified the same semitrailer (Tanker T) that was tested in Phase B to accommodate the axle and beam spacing supplied by Hendrickson. The first suspension (TC1) was shipped to LBT

on January 25, 2010. LBT installed the first set of suspensions (TC1) with the wide beam spacing.

Tanker TC1 was shipped to Michelin in Greenville, South Carolina, for K&C testing on February 23, 2010. The trailer was delivered to Michelin with the TC1 axles in place, and Michelin performed their K&C characterization of the trailer. When the K&C testing was completed, Tanker TC1 was sent to Link in East Liberty, Ohio, on March 22, 2010. The second suspension (TC2) was shipped to Link in early March 2010. Link installed the instrumentation and prepared the tractor tank trailer for track testing from March 15 to April 7, 2010. Link modified the mounting interface to fit the TC2 axle.

While the tank trailer was at Link, prior to testing, WMU personnel visited Link's facilities on two occasions to instrument and calibrate all of the strain gages for the Phase C testing, both for the tractor and on the TC1 and TC2 axles.

The test vehicle was instrumented to collect data from a total of 150 channels, including individual sensors, inertial global positioning system (GPS) devices, and quantities read from the tractor and tank trailer controller area network (CAN) buses. The large number of data channels was necessary to meet the needs of the project.

As in previous phases of this Program, track testing was conducted at TRC, Inc., located in East Liberty, Ohio; and like the efforts conducted in Phase B, the track test activities were executed by Link. The testing was performed from April 8 through April 13, 2010, and involved representatives from all of the HTRC member organizations. Data from the track testing was quality assured and was distributed to the HTRC member organizations shortly after the testing.

CU-ICAR, ORNL, and WMU each analyzed the data generated during the Phase C track testing. The primary objective of the data analysis was to quantify and compare the differences in the roll performance among the two tank trailer configurations (i.e., using axles TC1 and TC2) that were tested in Phase C, and to compare the track results for configurations Tankers TC1 and TC2 with the results of testing with the Phase B tank trailer configuration (i.e., Tanker T, with NGWBS tires and similar CG height). Data analysis was a primary activity of the Phase C efforts. The analysts met during the track testing to formulate analysis strategy, and met again on May 12 and 13, 2010, to discuss the results of the analysis, to date. The data analyses reports were completed in late May 2010.

Modeling development efforts were carried out throughout the Phase C period. In February 2010, TruckSim® modeling was done with modified Phase B K&C data to estimate the impact of the design technology options selected for test-track testing. When the K&C testing was completed in March 2010, the TruckSim® model was rerun in order to estimate the stability benefits of the design technology options. In late April, TruckSim® was applied to the maneuvers conducted on the test track as well as to other selected design technology options.

This work was carried out through June, 2010. Adams modeling continued to the end of the project.

A series of Statements of Work (SOW) for subsequent research was prepared in May and June, 2010, with a draft SOW provided to NTRCI on June 30, 2010.

The Phase C final report was outlined early in Phase C including writing assignments and delivery dates. The Phase C final report was delivered to NTRCI on August 30, 2010

Chapter 3 – Theoretical Concepts

This chapter presents the basic theoretical concepts of a vehicle's roll stability. It explains the equations that predict when a vehicle's tire will lift off the pavement in a steady state curve, and it discusses how the multiple axles on a vehicle share the overturning moment. The chapter goes on to explain some of the cornering characteristics of an articulated tractor-semitrailer combination.

The TruckSim® model discussed in the next chapter incorporates this theory as well as some other, more subtle effects. Because it is a time-domain model, TruckSim® predicts the dynamic effects of a transient maneuver.

3.1 Wheel Lift Threshold

Wheel lift threshold is defined as the maximum lateral acceleration, usually specified in gravitational units (g), that the vehicle can experience before wheel lift occurs. Many factors affect the wheel lift threshold of a tractor-trailer combination (Figure 3-1). Wheel lift threshold is affected most directly by the height of the CG and the track width. When a vehicle's path changes from one direction to another, it experiences a lateral acceleration (a_y) or cornering force. The effort acting to turn a vehicle over is called the overturning moment. In its simplest form, the overturning moment is the product of the lateral acceleration at the CG, the height of the CG, and the mass of the vehicle. The overturning moment can increase to such a magnitude that the wheels on the inside of the turn lift from the road surface. If the weight is equally distributed from side-to-side on straight, level road, then the weight on the inside tires during a maneuver is shown in Equation 1.

$$\frac{w}{2} - m \cdot a_y \frac{h}{t} = w_{inside}$$

Equation 1

Where: w = weight of the vehicle supported by the axle
m = mass of the vehicle supported by the axle
t = track width
a_y = lateral acceleration of the vehicle
h = height of the CG

The weight on the inside wheels (w_{inside}) cannot drop below zero. Therefore, the lateral acceleration required to produce wheel lift is shown in its simplest form in Equation 2.

$$\frac{a_y}{g} = \frac{t}{2h}$$

Equation 2

Although the assumptions for this derivation are rather simplistic, this equation demonstrates the critical nature of the geometry of the truck in terms of track width and CG height. Their ratio is the most important factor in determining the wheel lift threshold, and other factors are generally of secondary importance to this ratio. Nonetheless, the t/h ratio is largely constrained by current operational practices and established standards and regulations, and other design parameters of the tractor and trailer may be the only tools available to improve the roll propensity of a tractor-trailer. The remainder of this chapter addresses real deviations from the above model in order to demonstrate some of the secondary design factors influencing roll stability.

One factor that affects the lateral acceleration at wheel lift is the roll angle between the sprung mass and the road surface. This roll angle is the sum of (1) the axle roll generated by tire deflection as a result of the tire radial stiffness being acted on by differential loading on opposite sides of the axle and (2) the suspension roll angle. The roll angle has a degenerative effect on the lateral acceleration for wheel lift due to the CG moving away from the inside wheels as the overturning moment rotates the payload's CG toward the outside wheels of the turn, shown in Figure 3-1 and Figure 3-2.

As a result of the associated roll angles of the axle and the suspension, the CG of the sprung mass is displaced toward the outside wheels of the turn. The axle roll displaces the suspension roll center toward the outside wheels of the turn similarly to the movement of the payload's CG.

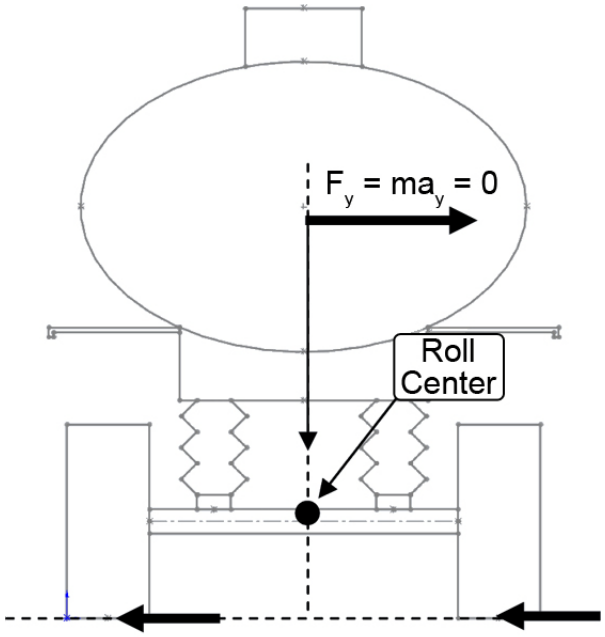

Figure 3-1. Diagram. Trailer prior to cornering

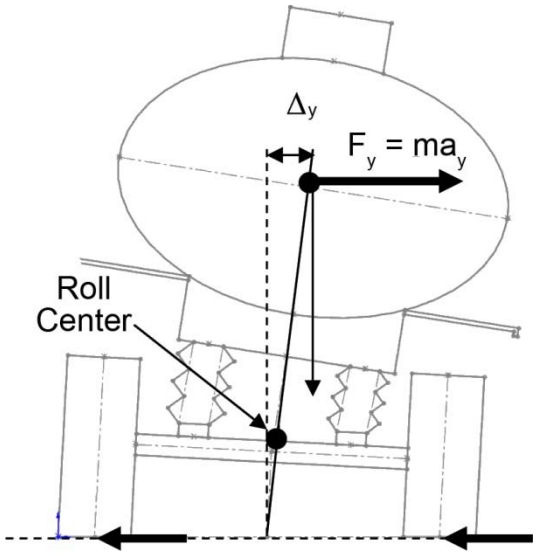

Figure 3-2. Diagram. Trailer with lateral acceleration

The equations and figures before this point describe an idealized single-axle vehicle. With a multi-axle vehicle, the roll moment may be shared with the other axles of the vehicle, which may delay lift on one axle while promoting lift on another axle depending on the weight distribution and a host of other factors. One factor that affects the amount of sharing which occurs is the stiffness of the chassis that couples one suspension system to another suspension system. On a tractor trailer, the trailer roll angle caused by the roll overturning moment is resisted by the trailer suspension roll stiffness and fifth wheel. The frame roll angle produced at the rear suspension may be resisted by the tractor drive axle suspension depending on the torsional stiffness of the frame and the fifth wheel through which the moment must pass. If the roll angles of the tractor and trailer are equal, due to the height of the CG of each unit and the suspension characteristics, there is no roll moment shared between the tractor and trailer through the fifth wheel.

Analytical simplification of rollover can be used to obtain insights into the rollover phenomenon, even if these simplified solutions may not accurately predict the actual vehicle behavior. It is reasonable to assume a torsionally rigid frame for tank trailers; however, some trailer configurations, such as a flatbed trailer, have much more torsionally flexible frames. If the load carried by a flatbed trailer is not uniform along the length of the trailer, the resulting roll moment can be translated to different axles at different magnitudes or at different times in the maneuver. In a transient maneuver, overturning moment can vary from axle to axle even if the load is uniformly distributed. For a torsionally rigid frame, such as a tank trailer, it is much easier to predict the roll behavior even if the load is not uniform along the length of the trailer.

Because all cornering forces (F_c) act at the ground (Figure 3-3), the overturning moment (M_o) is established by the CG height (h), the lateral acceleration that the CG experiences (a_y) and the

magnitude of the load (m) as presented in Equation 3. A restoring moment (M_R), counters the overturning moment and ultimately is established by the radial load on the tires (F_r) and the vehicle track width (t). The restoring moment (M_R) is also shown to be the product of the vertical load and the distance between the vertical load and the outside tire in the turn as shown in Equation 4. The variable Δy defines the lateral shift in center of gravity and affects the instantaneous lateral load position. This simplified analysis of Equations 4 and 5 only considers a load as distributed on a single axle in a turn. However, Equation 4 can provide insight into variables affecting lift. Complex vehicles with multiple axles and flexible coupling devices such as fifth wheels involve a much more sophisticated approach to fully understand stability, roll couple distribution and wheel lift thresholds.

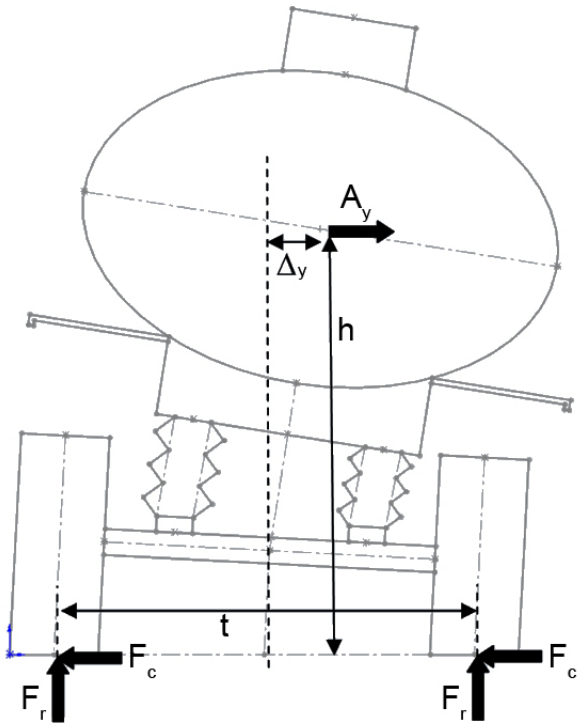

Figure 3-3. Diagram. Trailer overturning moment

$$M_O = (m) * h * a_y = F_C * h$$

Equation 3

$$M_R = (m * g) * \left(\frac{t}{2} - \Delta y \right) = w * \left(\frac{t}{2} - \Delta y \right)$$

Equation 4

3.2 Roll compliance analysis

The roll compliance of the tire and suspension components that affect the roll angle provide a more comprehensive understanding of the factors contributing to roll. Figure 3-4 shows a simplified trailer axle to demonstrate its roll behavior. Axle roll stiffness is a function of tire radial stiffness and track width, as shown in Equation 5. The wider track used in Phase C increased the axle roll stiffness ($K_{\phi\text{-axle}}$) from the tire radial stiffness (k_{tire}) which should have the effect of reducing the total roll angle of the system at an equivalent roll moment as achieved in Phase B. In Phase C, the increased roll stiffness was accompanied by an increased lateral acceleration at wheel lift which in turn increased the roll moment resulting in axle roll angles, at wheel lift, similar to those experienced in Phase B. These equivalent axle roll moments were accomplished at the higher lateral accelerations.

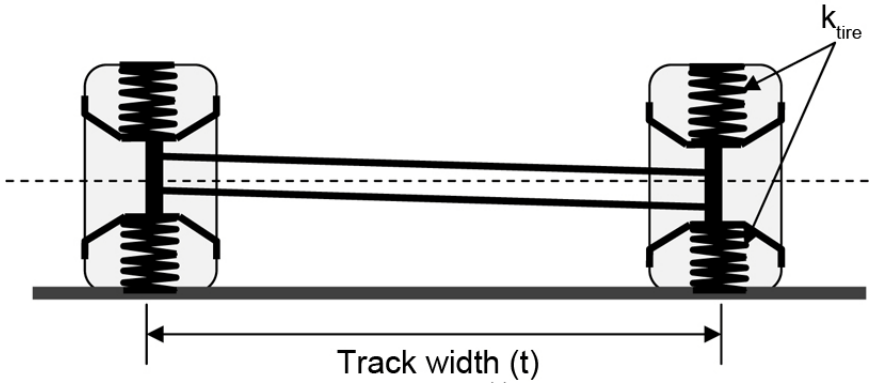

Figure 3-4. Drawing. Example of axle roll due to tire radial compliance and tire load

$$\text{Axle Roll stiffness} = K_{\phi-axle} = \frac{k_{tire} \times t^2}{2 * 57.3} (N \cdot m / \deg)$$

Equation 5

The interest in Phase C was in being able to separate the axle roll from the body-related roll to establish the suspension-related roll. Axle roll was measured on axles 3 and axle 5 with optical sensors. The optical sensors, at high lift angles, could go out of range, which limited their applicable range to roll angles prior to lift, and within a limited range after lift.

The body roll was measured with the two RT units mounted close to the CG of each of the tractor and trailer. The RT units are inertial-based global coordinate reference units which provide accurate information regarding position and angle as well as velocities and accelerations. In addition, string potentiometers were used on axles 3 and axle 5 which directly measured the suspension roll by directly measuring the change in distance between the frame and the axle.

$$\text{Suspension}_{\text{roll}} = \text{body roll} - \text{axle roll}$$

Equation 6

The suspension roll stiffness is that which is contributed by the suspension springs, any auxiliary roll devices such as anti-roll bars, and that which is contributed by the elastic deformation of suspension components. In Phase C, the axle torsion-related strain was measured, which allowed for the examination of the axle-produced roll stiffness during the transient maneuvers. The suspension spring-related roll stiffness can be determined if the spring rate and spring spacing are known, as shown in Equation 7, where k_{spring} represents the suspension-related spring and *d* represents the spacing between the suspension's springs. The relationship provided in Equation 8 demonstrates the influence of the spring spacing on the suspension roll stiffness.

$$k_{\phi-roll} = \frac{k_{spring} \times d^2}{2 * 57.3} (N \cdot m / \text{deg}) + k_{\phi-aux}$$

Equation 7

If both the axle roll stiffness and the suspension roll stiffness are known, the overall body roll stiffness at a particular location can be determined using Equation 8. Obviously, frame torsional stiffness between axle locations as well as the coupling stiffness between tractor and trailer affects the overall body roll stiffness. Additionally, roll center locations, which affect the roll moment acting on the suspension affects the roll angle.

$$K_{\varphi-body} = \frac{\left(K_{\varphi-axle}\right) \times \left(K_{\varphi-susp}\right)}{\left(K_{\varphi-axle} + K_{\varphi-susp}\right)}$$

Equation 8

The combined roll stiffness of the axle and the suspension always results in a body roll stiffness that is lower than either of the individual stiffness values. The axle roll contributed approximately 1.5 to 2 deg of roll to the system; the remaining being suspension roll (approximately 2.5 deg) and roll angles related to wheel lift. The total roll angle was approximately 10 deg at outrigger touchdown.

Roll stiffness is distributed from axle-to-axle depending upon the relative stiffness of the connecting elements. As an example, if a roll moment is applied to the fifth wheel, the tractor and the trailer contribute to the roll stiffness as shown in Equation 9. Consideration of both the tractor and trailer frame torsional stiffness must be considered in the determination of the roll stiffness at the fifth wheel (kφ-eff-5th).

$$k_{\phi-eff-5th} = \frac{1}{\frac{1}{k_{\phi-5th}} + \frac{1}{k_{\phi-Dr}}} + \frac{1}{\frac{1}{k_{\phi-TrkF}} + \frac{1}{k_{\phi-SA}}} + \frac{1}{\frac{1}{k_{\phi-TrlF}} + \frac{1}{k_{\phi-TA}}}$$

Equation 9

When a roll moment is applied through the steer axle, it is resisted by both the drive suspension and the trailer suspension. The trailer suspension acts through the fifth wheel, and both act through the compliant tractor frame. This is demonstrated with the effective roll stiffness at the steer axle ($k_{\phi\text{-eff-SA}}$) in Equation 10.

$$k_{\phi-eff-SA} = k_{\phi-SA} + \frac{1}{\frac{1}{k_{\phi-Dr} + \frac{1}{\left(\frac{1}{k_{\phi-5th}} + \frac{1}{k_{\phi-TrlF}} + \frac{1}{k_{\phi-TA}}\right)}} + \frac{1}{k_{\phi-TrkF}}}$$

Equation 10

If the resistance to a roll moment applied at the trailer suspension ($k_{\phi\text{-eff-TA}}$) is considered, the coupling of the tractor and the tractor suspension and the frame through which they act must be considered. The equation for evaluating the roll resistance to a moment applied above the trailer axles is shown in Equation 11.

$$k_{\phi-eff-TA} = k_{\phi-TA} + \frac{1}{\frac{1}{k_{\phi-Dr} + \frac{1}{\left(\frac{1}{k_{\phi-SA}} + \frac{1}{k_{\phi-TrkF}}\right)}} + \frac{1}{k_{\phi-TrlF}}}$$

Equation 11

In addition to the distribution of roll couples, the fifth wheel characteristics need to be considered. At a certain lateral acceleration, the fifth wheel may separate during a maneuver, and as a result, the sharing of the roll couples the tractor to the trailer, or the trailer to tractor, ceases. Once the fifth wheel lash is taken up, the sharing of couples re-establishes and the two units again roll together. Application of Equations 5 through 11 is demonstrated in Table 3-1 for the coupled system and in Table 3-2 when the fifth wheel is in float. Float is defined as separation prior to the point where the kingpin limits further travel. The impact of the fifth wheel lash is demonstrated as a result, and it can be seen that the roll stiffness is reduced by nearly 50% when the fifth wheel is not coupled. Equations 9 through 11 were derived to provide insight into the

roll stiffness distribution with roll moments applied at the three critical locations of steer axle, fifth wheel and trailer axle as well as how fifth wheel separation influences roll resistance.

Table 3-1. Roll resistance with moments applied at individual locations with the fifth wheel coupled

Axle roll stiffness includes tire radial stiffness effects			
Steer axle suspension roll stiffness	$k\varphi_{SA}$	5000	N•m/deg
Drive axle suspension roll stiffness	$k\varphi_{Dr}$	23000	N•m/deg
Trailer axle suspension roll stiffness	$k\varphi_{TA}$	24000	N•m/deg
Structural stiffness within the system			
Fifth wheel torsional stiffness	$k\varphi_{5th}$	258000	N•m/deg
Tractor chassis torsional stiffness	$k\varphi_{TrkC}$	1200	N•m/deg
Trailer chassis torsional stiffness	$k\varphi_{TrlC}$	1000000	N•m/deg
Is fifth wheel separated and floating	Y or N	N	1
Applied moment at the fifth wheel			
Contribution of the drive axle		21117	N•m/deg
Contribution of the steer axle		968	N•m/deg
Contribution of the trailer		23438	N•m/deg
Effective stiffness at the fifth wheel	coupled	45523	N•m/deg
Applied moment at the steer axle			
Contribution of the steer axle		5000	N•m/deg
Contribution of drive plus trailer		1168	N•m/deg
Effective stiffness at the steer axle	coupled	6168	N•m/deg
Applied moment at the tank trailer Axle			
Contribution of the trailer axle		24000	N•m/deg
Effective stiffness at trailer axle	coupled	45460	N•m/deg

Table 3-2. Roll resistance with applied moments at individual locations with the fifth wheel in float condition

Axle roll stiffness includes tire radial stiffness effects			
Steer axle suspension roll stiffness	$k\varphi_{SA}$	5000	N•m/deg
Drive axle suspension roll stiffness	$k\varphi_{Dr}$	23000	N•m/deg
Trailer axle suspension roll stiffness	$k\varphi_{TA}$	24000	N•m/deg
Structural stiffness within the system			
fifth wheel torsional stiffness	$k\varphi_{5th}$	258000	N•m/deg
Tractor chassis torsional stiffness	$k\varphi_{TrkC}$	1200	N•m/deg
Trailer chassis torsional stiffness	$k\varphi_{TrlC}$	1000000	N•m/deg
Is the fifth wheel separated and floating	Y or N	Y	0
Applied moment at the fifth wheel			
Contribution of the drive axle		21117	N•m/deg
Contribution of the steer axle		968	N•m/deg
Contribution of the trailer		0	N•m/deg
Effective stiffness at the fifth wheel	floating	22085	N•m/deg
Applied moment at the steer axle			
Contribution of the steer axle		5000	N•m/deg
Contribution of the drive plus tank trailer		1140	N•m/deg
Effective stiffness at the steer axle	floating	6140	N•m/deg
Applied moment at the tank trailer Axle			
Contribution of the tank trailer axle		24000	N•m/deg
Effective stiffness at the tank trailer axle	floating	24000	N•m/deg

3.3 Roll damping

Roll damping was of interest during Phase C because: 1) the simulation output showed final maneuver oscillations that were not present in the experimental data, and 2) some advanced concepts involving active damping had shown, in simulation, to be beneficial in raising the roll threshold. To better understand the concept of trailer roll damping, the time-dependent roll amplitude (θ) can be represented as shown in Equation 12.

$$\theta_t = \theta_0 \, e^{-\xi \omega_n t_1} \, \mathrm{Sin}\left(\sqrt{1 - \xi^2}\ \omega_n t_1 + \phi\right)$$

$$\text{undamped natural frequency} = \omega_n = \sqrt{\frac{k_\phi}{I_{xx}}} \qquad \zeta = \frac{\text{system damping present}}{\text{critical damping}}$$

t = time, θ_0 = initial angle, θ_t = angle at time t, I_{xx} = roll inertia, k_ϕ = roll stiffness

Equation 12

The decay in angular amplitude, as a function of time, was measured during testing and evaluated using a logarithmic decrement approach. Chapter 7 of this report provides an in-depth analysis of the damping tests, evaluation and results.

3.4 Steer characteristics of the tractor and trailer

3.4.1 Establishing the Equivalent Tractor and Tank Trailer Wheelbase

In establishing the steady-state dynamics of a three-axle vehicle, one of the first concerns is to establish the equivalent tractor wheelbase. Because the tractor has tandem drive axles, competing slip angles are induced between the drive wheels, even at very low velocities, when in a turn (Figure 3-5). The induced slip is a result of forcing two separated but parallel axles to rotate about a common center in a turn. This induced slip complements side slip on one drive axle (forward) and opposes it on the other (rear) drive axle, of an axle set. This induced slip acts to increase the effective wheelbase of the tractor beyond that of the conventional or customary definition, which is the center of the steer axle tire to the center of the drive axles. The increase in equivalent wheelbase (L_{equiv}) means that the front wheels need to steer into the turn further (i.e., δ increases) to negotiate a given radius.

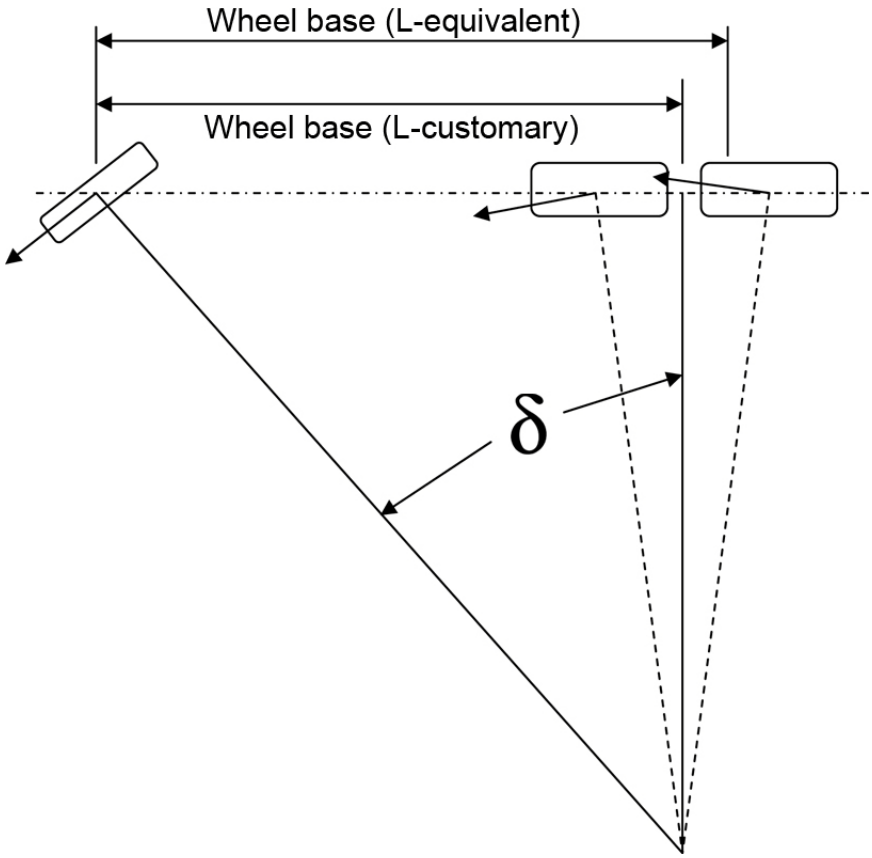

Figure 3-5. Diagram. Equivalent wheelbase of a multi-axle vehicle

The tire slip angle, as shown in Figure 3-6, indicates the relationship between the lateral force and the slip angle. This direct relationship is referred to as the cornering stiffness or the cornering coefficient. Fundamentally, a tire requires a certain slip angle to achieve a given lateral cornering force. The cornering stiffness greatly affects the cornering properties of the vehicle.

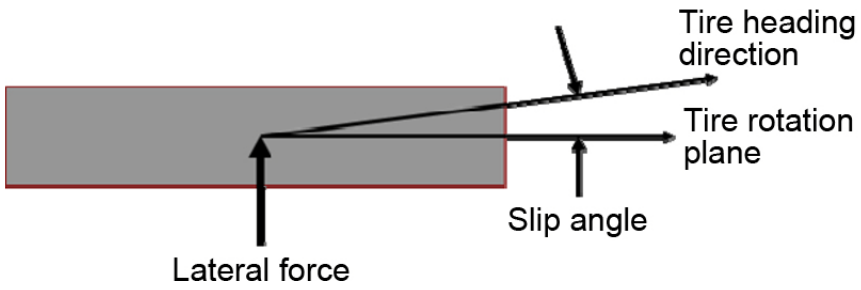

Figure 3-6. Diagram. Tire slip angle

The tandem factor (T) in Equation 13, relates the axle spacing to the mean or average position. In the case of two drive axles, the term (Δ) is equivalent to half of the spacing between the axles. The equivalent wheel-base length (L_{equiv}) is approximated by Equation 14.

$$T = \left[\frac{1}{N} \sum_{i=1}^{N} \Delta_i^{\,2} \right]$$

Equation 13

$$L_{eqiv} = L\left[1 + \frac{T}{L^2} \left(1 + \frac{C_{F\alpha 2}}{C_{F\alpha 1}} \right) \right]$$

Equation 14

Table 3-3 shows the equivalent wheelbase length factors and compares the difference in length of the customary length (L_{cust}) with the equivalent wheelbase length (L_{equiv}).

Table 3-3. Tractor equivalent wheelbase calculation

Tractor Equivalent Wheelbase				
Steer axle to drive axle 1 spacing	5.829	m	229.5	in
Steer axle to drive axle 2 spacing	7.173	m	282.4	in
Number of drive axles	2			
Steer axle to average of drive axle positions	6.501	m	255.9	in
Length rearmost drive axle to rear drive axle center (delta)	0.672	m^2	26.457	in
Tandem factor (T)	0.452	m^2	700.0	in^2
Cornering stiffness of the steer tires	3500	N/deg	785	lb/deg
	200550	N/rad	44976	lb/rad
Number of tires on the steer axle	2			
Number of tires per drive axle	2			
Cornering stiffness of the drive tires	5500	N/deg	1233	lb/deg
	315150	N/rad	70676	lb/rad
Cornering stiffness factor	4.143		4.143	
T/L^2	0.010685		0.010685	
Equivalent Wheelbase	6.789	m	267.3	in
L_{equiv}-L_{cust}	0.288	m	11.33	in

3.4.2 Understeer and Oversteer Behavior of the Tractor and Trailer

The steered wheel angle (δ) that is needed to negotiate a turn is a combination of the Ackerman steer angle, shown in Equation 15, and the collective tire steer angle resulting from the tire slip

angle differences, and any suspension-related geometry steer angles. The steered wheel angle, shown in Equation 16, includes the Ackerman Steer angle and the tire-related steer angle effects. A vehicle with multiple drive axles has a turn-induced slip angle at the drive axles, which is a function of the axle separation and the tire cornering stiffness. The force for this turn-induced slip at the tandem axles must be generated at the front steer axle. As a result, the ratio of the tire cornering stiffness between the steer axle and the tandem axles plays a large role in establishing the equivalent wheelbase.

The theoretical amount of steering needed for a vehicle to negotiate a given turn is related to the turn radius and the vehicle wheelbase (or equivalent wheelbase in this case). There is a geometric relationship defining this steering requirement. For a "zero-speed" case, or a case where no lateral forces need to be generated to force the vehicle around the turn, this relationship is between the turn radius (R) and the vehicle wheelbase (L or L_{equiv}), and is defined as the Ackerman steer angle. The Ackerman steer angle (in degrees) is defined in Equation 15.

$$\delta_{\deg} = \frac{L}{R}\left(\frac{180}{\pi}\right)$$

Equation 15

where:

L_{equiv} = equivalent wheelbase as defined above for the three-axle vehicles R = radius of the turn

L_{equiv}/R = Ackerman angle (at very low, "zero-slip angle" speeds)

Because the weight on the axle sets (W_f, W_r), multiplied times the lateral acceleration represents the cornering forces (F_{y1}, F_{y2}), in a linear model the tire steer angle can be represented as a combination of the Ackerman steer angle plus the tire slip angle relationships as shown in Equation 16. The first term on the right side of Equation 16 ([(L/R)*(57.3)]) represents the Ackerman steer angle, while the second term ($\eta\left(\frac{v^2}{Rg}\right)$) represents the dynamic steer gradient.

The sign of the dynamic steer gradient indicates either an understeer (for positive values) or oversteer (for negative values) characteristic.

$$\delta_{\deg} = \frac{L}{R}\left(\frac{180}{\pi}\right) + \left[\frac{W_f}{C_{F\alpha 1}} - \frac{W_r}{C_{F\alpha 2}}\right]\left(\frac{v^2}{Rg}\right) = \frac{L}{R}(57.3) + \eta\left(\frac{v^2}{Rg}\right) = \frac{L}{R}(57.3) + \eta(a_y)$$

Equation 16

where

η = understeer gradient (deg/g)
v = longitudinal (tangential) velocity
$C_{F\alpha 1}$, $C_{F\alpha 2}$ = total front and rear tire cornering stiffness respectively
W_f = weight over one front wheel (half of the front axle weight)

$C_{F\alpha 1}$= cornering stiffness of the front tires (force/deg)
W_r= weight over one rear wheel
$C_{F\alpha 2}$= cornering stiffness of the rear tires (force/deg)
a_y = lateral acceleration of the vehicle (g)

With the equivalent wheelbase established, the turn radius for a steady-state maneuver can be calculated from the yaw velocity (ω_y) and the longitudinal velocity (v), and can also be calculated from the roll corrected lateral acceleration as indicated in Equations 17 and 18.

$$a_y = v * \omega_y = v * \frac{v}{R} = \frac{v^2}{R}$$

Equation 17

$$R = \frac{v^2}{a_y} \qquad or \qquad R = \frac{v}{\omega}$$

Equation 18

$$R = \frac{v^2}{a_y} = \frac{v}{\omega_y}$$

With the equivalent wheelbase established, the understeer gradient (η) can be extracted from the experimental data with the relationships between yaw velocity (ω_y), forward velocity (v), and the roll corrected lateral acceleration (a_y) as shown in Equations 19 through 21. Equations 19 and 20 provide the relationships leading to the understeer gradient (η) in Equation 21.

$$\delta_{\text{deg}} = \frac{L_e}{R}\left(\frac{180}{\pi}\right) + \left[\frac{W_f}{C_{F\alpha 1}} - \frac{W_r}{C_{F\alpha 2}}\right]\left(\frac{v^2}{Rg}\right) = \frac{L_e}{R}\left(\frac{180}{\pi}\right) + \eta\left(\frac{v^2}{Rg}\right)$$

Equation 19

$$\delta_{\text{deg}} = \frac{L_e}{R}\left(\frac{180}{\pi}\right) + \eta\left(a_y\right)$$

Equation 20

$$\eta = \frac{\delta_{\text{deg}} - \frac{L_e}{R}\left(\frac{180}{\pi}\right)}{a_y} (\text{deg}/g)$$

Equation 21

Because considerable effort was focused on determining the characteristics that were different between the TC1 and TC2 suspensions, it was deemed appropriate to determine the steer characteristics of the tank trailer for each suspension. Steer analysis of the tank trailer was performed with the same equations by using the articulation angle between the tractor and tank trailer as the steer angle for the tank trailer. The calculated equivalent wheelbase of the tank

trailer and the tank trailer turn radius are used to establish the steer characteristics of the tank trailer as shown in Equation 22.

$$\textit{Articulation angle} = \text{Tank trailer ackermann angle} + \text{understeer angle}$$

$$\textit{Articulation angle} = ATAN\left(\frac{L_{equiv}}{R}\right) * 57.3 + k\left(\frac{velocity^2}{R \times g}\right)$$

Equation 22

Table 3-4. Tank trailer equivalent wheelbase

Tank Trailer Equivalent Wheelbase					
Kingpin to tank trailer axle 1	10.046	m		395.5	in.
Kingpin to tank trailer Axle 2	11.292	m		444.6	in.
Number of trailer axles	2				
Kingpin to average of tank trailer Axle positions	10.669	m		420.0	in.
Length of the rearmost tank trailer axle to the rear tank trailer axle center (delta)	0.623	m		24.5	in.
Tandem factor (T)	0.388	m^2		602	$in.^2$
Cornering stiffness of the drive tires	5500	N/deg		1233	lb/deg
	315150	N/rad		70676	lb/rad
Number of tires on the drive axle	2				
Number of tires per tank trailer axle	2				
Cornering stiffness of the tank trailer tires	5500	N/deg		1233	lb/deg
	315150	N/rad		70676	lb/rad
Cornering stiffness factor	3.000			3.000	
T/l^2 =	0.00341			0.00341	
Equivalent Wheelbase	10.778	m		424.3	in.
L_{equiv}-L_{cust}	0.109	m		4.3	in.

In general, trailer understeer increases the articulation angle between the tractor and the trailer. Trailer over steer decreases the articulation angle and the off-tracking up to the point where the articulation angle changes sign and the potential for jackknifing or spin is possible.

Chapter 4 – Tractor-Trailer Modeling

Modeling can provide valuable insight into how physical properties affect a tractor trailer's dynamic performance. Two themes were central to modeling in Phase C: 1) validate the models with data obtained in Phase C and 2) test the developed models' ability to predict performance and validate changes which could be a part of a future stable truck concept. To address this need, two approaches were employed which included; 1) building a model in a commercially available software package called TruckSim®, and using the model to predict dynamic behavior with a controlled set of variables, and 2) advancing the flexible body modeling using a software package called Adams to a useable model with predictive capabilities. The flexible body model being developed has the potential to provide increased accuracy and greater insight than is possible with the rigid body models developed in TruckSim®. However, complexity of the flexible body models requires a greater number of specific parameters to be known than is required with the rigid body models. TruckSim® uses the more global K&C data as input while the flexible body models require specific component engineering data that is used for specific component predictions and ultimately, overall dynamic response. Both methods have great value in future stable truck concept development.

4.1 Rigid Body Modeling

TruckSim® is a commercially available rigid body model of heavy-duty trucks, including combination unit vehicles. Prior work for NTRCI has used TruckSim® models extensively to plan experiments and understand their results.

4.1.1 Use of TruckSim® in this project

Prior to implementing any design changes for Phase C, the Phase B modeling results for Tanker T were compared with the Phase B experimental data. A few parameters in the models had to be refined to provide agreement between the models and the experimental results. Model comparison focused on two output quantities. The first is the wheel lift threshold, commonly evaluated in the ramp steer maneuver, and the second is the trailer body roll angle as a function of time, evaluated in the lane change maneuver. The Phase B model was then modified to implement the Phase C changes of track width and beam center spacing, which will be explained in Section 6.1.1.

4.1.2 Inherent Limits of Modeling

Precise data is not always readily available for all elements of the tractor-tank trailer combination. Estimates can be valid, valuable, and in some cases, may be all that is available. In some cases the models are highly sensitive to these estimated variables, and in other cases less sensitivity is indicated. Many parameters necessary in the TruckSim® models cannot be obtained for hypothetical changes and therefore other techniques may be needed to obtain the necessary modeling input for the prospective change. Some of the sensitive parameters that dictate the path the model will follow and its general behavior include centers of gravity, inertial properties,

suspension roll center heights, frame stiffness, tire properties, steer characteristics, suspension stiffness, suspension damping, and fifth wheel properties. These parameters are further explained below.

Center of gravity heights and respective inertial properties

Payload CG heights, sprung and unsprung mass CG heights, and the composite CG heights are difficult to measure. The CG heights of the Phase B and C vehicles were not measured, so the heights have been calculated from the known and estimated weights of the components. Changes to the vehicle during testing may make accurate measurement and calculation problematic. Examples of changes include fuel burned, driver changes, and tire pressure changes. These changes typically do not affect the CG height prediction appreciably unless gross errors are made. In many cases relative performance predictions are to be made and the small CG height errors may not affect the relative change being assessed.

The roll inertia (Ixx), pitch inertia (Iyy) and yaw inertia (Izz) values of heavy vehicles are expensive to measure and are best calculated mathematically. In many cases approximate shapes can be used with standard inertia calculations to provide the necessary inertia estimates for modeling as well as experimental data analysis. Typically the team has used experimentally measured loads at wheel locations for both the unloaded and loaded tractor and trailer to determine payload and payload lateral and longitudinal location. These lateral and longitudinal values, along with the known location of the tank payload compartments, can be used to estimate the CG and inertial properties.

Roll centers

TruckSim® uses force-based roll center determination in its calculations. A specific roll center height is not separately entered into the program. Roll centers are determined from the K&C plots that relate lateral input forces to vertical changes in load. The force-based roll center method is an effective way to perform weight transfer analysis within simulation programs.

A challenge exists if the roll centers of the suspension are a target for change, and the K&C data is not available. The relationship between lateral load and vertical response to the load will need to be approximated in either a secondary program that employs a force-based roll center approach or modeled in Adams or a similar kinematic analysis program.

Chassis torsional compliances

Trailer torsional compliance has been examined from two extremes in Phases A, B, and C. The flatbed trailer in Phase A had low torsional stiffness. (Compliance is the inverse of stiffness; if one is low, the other is high.) In Phases B and C a tank trailer with high torsional stiffness was tested. The torsional stiffness of the flatbed trailer frame and structure was measured to be approximately 1800 N·m/deg. The ratio of suspension roll stiffness to chassis torsional stiffness for the flatbed trailer is approximately 15:1. In contrast the torsional stiffness of the tank trailer frame and structure was approximately 1,000,000 N·m/deg. The tank trailer’s ratio of suspension

roll stiffness to torsional stiffness was only approximately 0.025:1. The tank trailer's chassis-to-suspension torsional stiffness ratio was 600 times greater than that of the flatbed. The high suspension roll stiffness to torsional stiffness ratio allowed the flatbed trailer to be viewed as having little coupling between the trailer suspension and the tractor drive axle suspension. Conversely the tank trailer, with its high torsional stiffness, coupled the trailer roll directly to the fifth wheel, and any difference in roll angles between the tractor and the tank trailer were reflected at the fifth wheel.

The tank trailer, due to its low torsional compliance, could simply be modeled as a rigid chassis. Previous work growing out of the HTRC program developed an improved model of a tractor-semitrailer combination where the semitrailer has a high torsional compliance (Arant 2009).

The tractor's torsional stiffness was measured to be approximately 1200 N·m/deg. The low torsional stiffness of the tractor chassis did not greatly affect the roll characteristics because the drive axle suspension roll stiffness is considerably higher than the steer axle suspension roll stiffness. Little roll moment is transferred to the steer axle, with the drive axles resisting most of the roll.

Tire properties

The tire cornering stiffness is an idealization of the ratio of the lateral force generated by the tire to the slip angle. The cornering stiffness depends on the normal (vertical) force the tire is experiencing. These properties determine the lateral acceleration achieved at any given steer input, the path that the vehicle will follow, and ultimately the conditions leading to wheel lift. Tire radial stiffness affects the roll angle axle roll and suspension roll add to produce the total body roll. Tire properties affect both steady-state and transient behavior. Properties differ between the steer tires, the drive tires, and the trailer tires, and they are different for dual tires than NGWBS tires.

Roll steer and compliance steer

Changes to the suspension design such as beam spacing and suspension pivot heights affect the steer behavior of the tractor and the trailers. Compliance, as it relates to roll steer, is critically important in building a predictive model. Roll steer of Tanker M (identical to Tanker T) and Tanker TC1 was measured on the K&C rig. Tanker TC2, which had identical beam spacing to Tanker T, was assumed to have roll steer identical to that of Tanker T.

Suspension roll stiffness

Suspension roll stiffness is the result of a combination of springs, torsional elements, suspension bushings, flexure of suspension links, as well as other mechanical and pneumatic systems.

With leaf springs, which were on the steer axle, the majority of the roll stiffness ($k_{\phi\text{-roll}}$) is a result of the spring deflection rate (k_{spring}) and spring spacing (d) as shown in Equation 23, which duplicates Equation 7. A small proportion of the steer axle roll stiffness comes from auxiliary sources ($k_{\phi\text{-aux}}$) such as spring element and suspension component twist.

$$k_{\phi-roll} = \frac{k_{spring} \times d^2}{2 * 57.3} (N \cdot m / \deg) + k_{\phi-aux}$$

Equation 23

Air bag suspensions, in contrast, typically derive little roll stiffness from the bags themselves in steady-state maneuvers. This is because air can flow from the bag on the outside of the curve to the bag on the opposite side of the axle. The trailer suspensions used in this study are typical of air bag suspensions in that most of the roll stiffness is auxiliary–the structural components provide most of the roll stiffness. The "beams" in the trailer suspension function as both trailing arms and anti-roll bars. To assist in understanding the contribution of the axle torsion and its contribution to roll stiffness strain gage rosettes were mounted on each of the tank trailer axles.

In TruckSim®, the measured roll stiffness for the drive axles and the trailer axles was input as auxiliary roll stiffness. The air bags were modeled as providing little roll stiffness in the steady-state maneuvers. The air bags do provide roll resistance, both stiffness and damping, in transient maneuvers (Sections 7.2.3 and 7.2.4).

Total system damping

Total system damping, which includes dampers (shock absorbers) and any damping inherent in the system, is largely an unknown. The damping is not measured during K&C testing because the movement of suspension, body, and tires is done in quasi-static conditions to allow for accurate position measurement. Consequently, system damping, which is rate dependent, is not precisely characterized.

The shock absorbers can be removed from the vehicle, as was done in Phase A, and their damping force vs. velocity curve can be obtained. This, when applied through the appropriate motion ratio between the damper and the suspension, can then be used to obtain their damping contribution. Modeling suggested that the damping in roll was at least partially attributable to system characteristics other than the shock absorbers. Section 7.2.4 describes tests performed in order to establish the roll damping contribution of the shock absorbers and the amount of damping to be modeled in TruckSim® as auxiliary roll damping.

4.1.3 Fifth Wheel Stiffness and Lash

Best estimates of the fifth wheel characteristics are currently being used. Fifth wheel stiffness, which controls how the trailer load is transferred to the tractor, has not been measured. Kingpin lash, which governs the period during which the trailer and tractor roll stiffness are essentially uncoupled, has been shown to have an effect. Whereas the fifth wheel provides the coupling between the roll stiffness of the tractor and the roll stiffness of the trailer, roll angles of both units are affected by these two parameters.

A variety of stiffness models were entertained prior to testing to validate the affect of both fifth wheel stiffness and lash on roll angle and lift threshold. The roll moment required to cause fifth

wheel separation is found from the trailer fifth wheel normal load acting onto the tractor times half the fifth wheel diameter. This value for the tractor tank-trailer separation moment is calculated at approximately 51600 N·m for the load on, and dimensions of, the tractor fifth wheel. This would then convey that when a moment approaches this value the plate pivots about the outer edge of the fifth wheel until the lash is taken up. After the lash is taken up, the stiffness resumes its pre-separation values as shown in Figure 4-1.

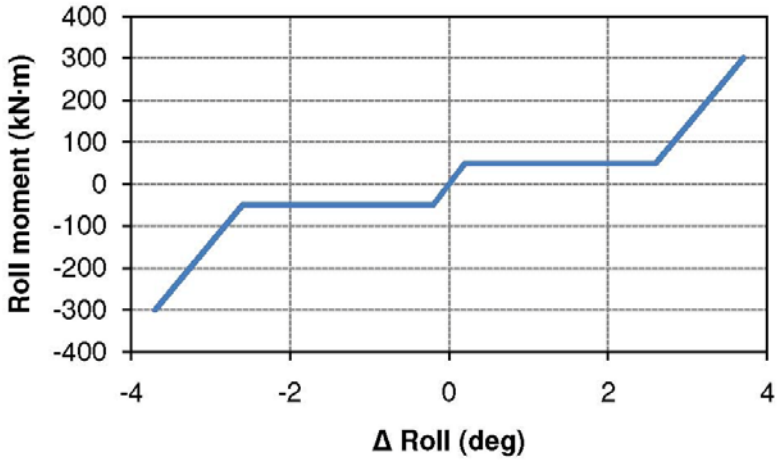

Figure 4-1. Graph. Modeling fifth wheel stiffness

Figure 4-2 and Figure 4-3 demonstrate the effects of fifth wheel stiffness on lateral acceleration and roll angle respectively. Uncoupling tractor and semitrailer roll (i.e., zero fifth wheel x-axis rotational stiffness) has influence early in the maneuver, as shown in Figure 4-3.

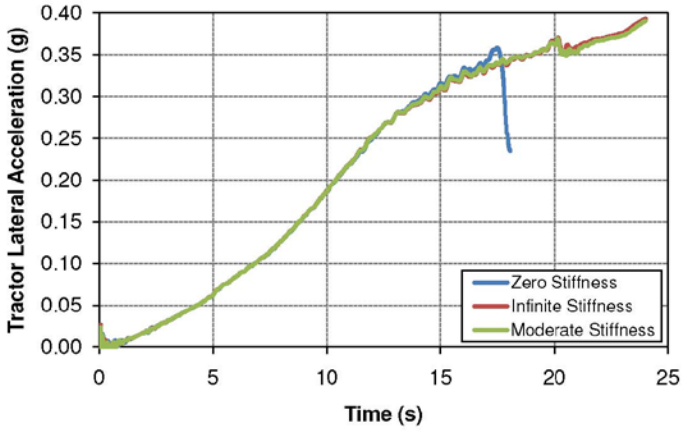

Figure 4-2. Graph. Lateral acceleration vs. time for fifth wheel stiffness variation

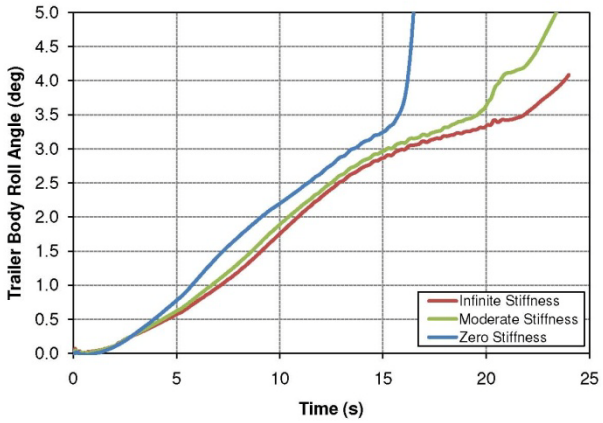

Figure 4-3. Graph. Roll angle vs. time for fifth wheel stiffness variation

Changing the lash or the stiffness affects how, and at what lateral acceleration, the trailer roll uncouples from, and re-couples with, the tractor. Modeling showed that as fifth wheel lash was minimized (a closer coupled trailer-tractor), lash played an increasingly important role in tractor trailer behavior. Above one degree of lash, less significant affect on tractor tank trailer behavior was found for this particular tractor trailer combination.

4.2 Flexible Body Modeling

Modeling of the tractor-trailer has been done primarily in TruckSim®, but Adams models have been developed more recently. TruckSim® uses a lumped parameter approach in which several lumped masses and lumped stiffness elements represent the vehicle. In contrast, Adams models are flexible body models.

Adams can model the discrete components of a tractor-trailer. This includes springs, shock absorbers, flexible frames, flexible axles, and bushings. Adams shows particular promise in modeling flatbed trailers, because the body of the trailer is not rigid.

Rigid body models have the advantage of being easier to build. Rigid body models represent frame, axles, and chassis structures as solid inflexible members with mass but no elastic or damping properties. Rigid body models must then rely on tires, suspension springs and shock absorbers for elasticity and damping. Properties of these components must often be adjusted to account for elasticity and damping present elsewhere in the vehicle structure. Furthermore, any stress that is placed on those rigid structures is then analyzed by observing the forces developed at the mount points and transferring the structure and those forces to a finite element analysis (FEA) program. Many have observed that this procedure often occludes the interactions among flexible structures in a vehicle model (Koike et al. 2004), (Azadia et al. 2010), (Zhou et al. 2007), (Ambrogi et al.2000), (Sun et al. 2007), (Guelzau 2006). As a result, the stresses in the actual vehicle and the associated vehicle responses can differ significantly from those found by isolating a single component for analysis in FEA. For these reasons, the flexible body Adams modeling approach was initiated.

The flexible body models for this phase of the project were developed in several stages. Digital scans of the tractor and semitrailer were used to develop solid models as outlined in the Phase B

Final Report (Arant et al. 2009). Using ABAQUS FEA software, these models were further refined into FEA models (as described in Appendix G of this report). However, the classic FEA model is severely limited by size in the Adams environment. To overcome this limitation, the files are further processed into “modal neutral files.” In Adams, the FEA and modal neutral models look identical though they are mathematically quite different. The modal neutral files use the Craig-Bantham method to significantly reduce the model size of a given flexible body while preserving its stiffness and mass content. Finally, the models were assembled into Adams. Figure 4-4 shows a full vehicle model in the Adams environment.

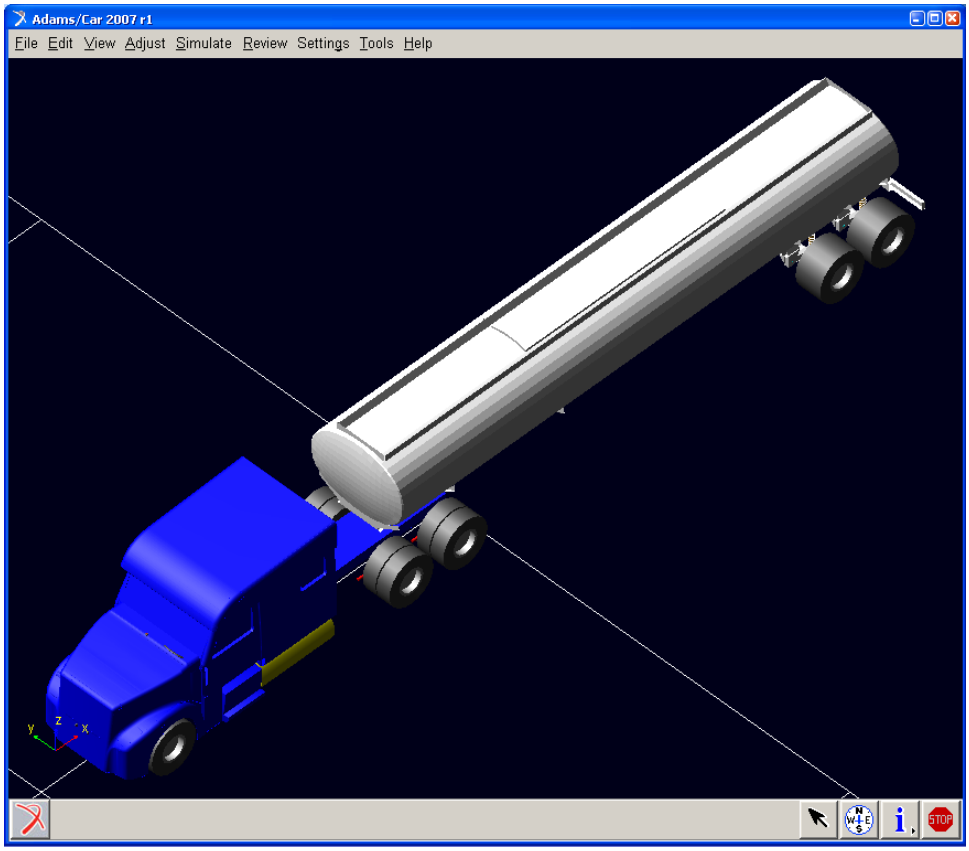

Figure 4-4. Screen capture. Tractor and tank semitrailer in Adams

Figure 4-5 show a wireframe view of the tank flex body structure derived from its modal neutral file. There are many nodes where stress or strain can be tracked individually or mapped out in a color fringe pattern to show stress or strain trends over the tank's body. Not shown in this figure are special nodes called master nodes. Master nodes are placed in locations where other structures can be attached to this flexible body. Attachments can be erroneously made to other nodes in the flex body. If this is done, unusual and incorrect results are generated. Therefore, attachments must only be made at master nodes. Master nodes are used sparingly in the model

because they strongly contribute to the size and complexity, and thus the run time, of the flex body model.

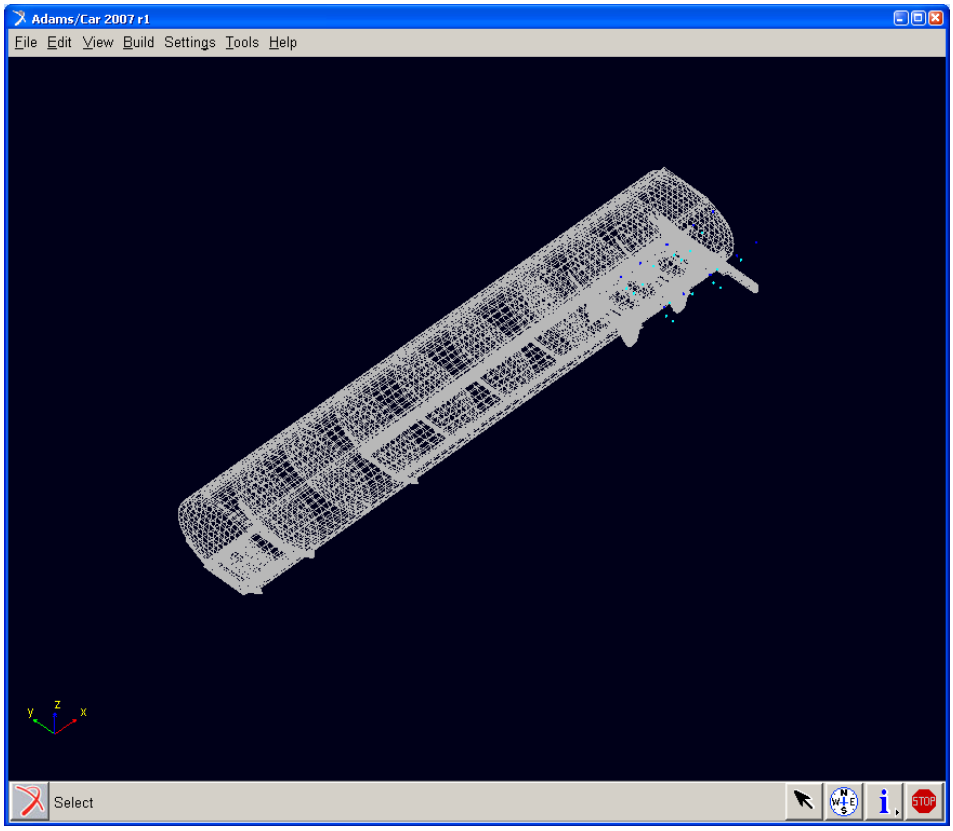

Figure 4-5. Screen capture. Wireframe view of tank showing mesh density

Some of the attachment points to the tank are obvious. The kingpin is an obvious attachment point as are the four hinge points for the suspension trailing arms. Two other master nodes have been added at locations corresponding roughly to the edges of the fifth wheel contacts. Figure 4-6 (left) shows a bottom view of the wireframe tank and Figure 4-6 (right) shows the location of these three master nodes on the shaded model.

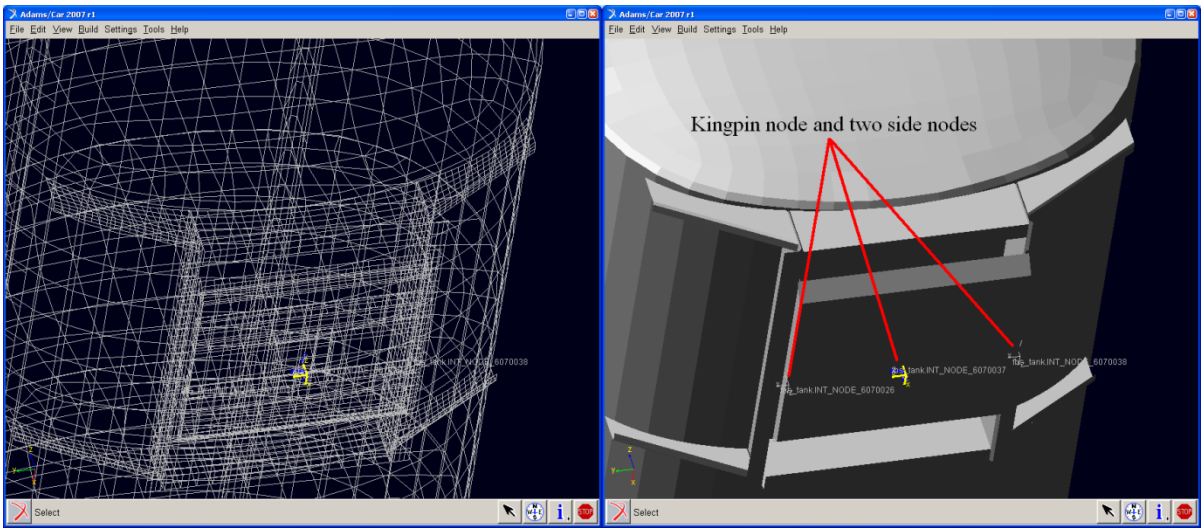

Figure 4-6. Screen capture. Center kingpin master node with two side master nodes

The master nodes of Figure 4-6 were included in the Adams model to accommodate stop limits that mimic the tilt limits seen in the fifth wheel during the Phase B track testing. Limits to downward travel were placed at these two side master nodes. A limit to upward travel was then placed on the kingpin. Figure 4-7 (left) shows the tank resting on a red representation of the tractor's kingpin plate. Figure 4-7 (right) shows the tank tilted to its limit relative the kingpin plate.

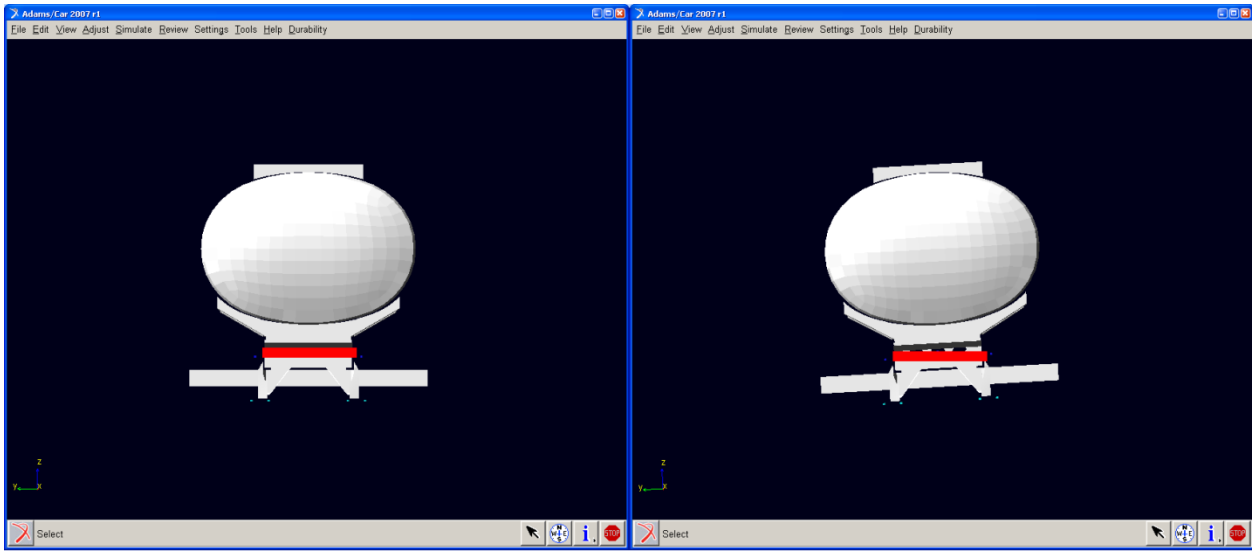

Figure 4-7. Screen capture. Tank tilting to its limit relative to kingpin plate (shown in red)

The water and sand masses in the tank were modeled with soft solid elements between the compartment ends where the sand or water was placed. This allowed for the mass distribution to be modeled correctly without a significant change in either torsional or bending stiffness of the tank. Attaching the mass directly to the tank as a rigid body would have made the tank

completely rigid in the region of those attachments, thereby making the natural frequencies of the tank artificially high. Modeling the load as soft solid elements is even more important when the liquid is gasoline, because gasoline would be distributed along the entire length of the tank, or on a flexible flatbed. The model of the load did not appreciably increase the size of the model.

The rest of the model structural elements were constructed in a similar manner. This means that the compliance and structural damping do not have to be pushed into various bushings and dampers located elsewhere on the vehicle. It also means that more attention needs to be taken in locating joints and suspension elements on the vehicle. With rigid bodies, the location of a revolute (hinge) joint does not have to be precise as long as it exists on the correct line of action. With flexible bodies joints need to be placed more precisely to prevent loads and moments from developing at the wrong location.

Most of the data for the Adams model comes from the material properties of the flex bodies. Modulus of elasticity, damping, and Poisson's ratio are basic material properties. Tire properties typically come from the manufacturer or from independent tests. Beyond that, a description of the maneuvers for simulation needs be put into the model.

Appendix G explains how the Adams model of the test vehicle was used to predict behavior in a ramp steer maneuver.

Chapter 5 – Identification and Selection of Design and Technology Options

The process used to identify design technology options was based on prior experience and knowledge gained from Phases A and B of the HTRC studies, team discussions, and a literature search. The options that were selected for Phase C testing were those expected to provide detectable experimental change, with minimum tractor or trailer modification and could be performed within the budget constraints. Additional options were selected for modeling.

The selection process began by systematically decomposing the tractor tank trailer system to highlight areas of possible change; that is, to break the major systems into subsystems. Subsequently, the subsystems were further broken down into their individual components. Interactions among subsystems and components were identified to promote an understanding of how candidate changes might affect other subsystems or parameters. For clarity, visual representations of the systems are presented in Chapter 8 of this report. Several systems were examined in the selection of candidates:

- CG height reduction through design. This included active system adjustment as well as optimizing packaging to allow a lower CG.
- Trailer axle and suspension. This included the axle roll stiffness, roll steer, roll center position, air bag positioning and other parameters that are a part of the axle design.
- Trailer frame and structure. Fundamental design factors related to torsional load transfer were examined including how the trailer axle suspension roll stiffness, the roll angle and the overturning moment are transferred to the fifth wheel.
- Fifth wheel design. The fundamental properties of the fifth wheel were examined as well as the potential for actively adjusting the fifth wheel position laterally and longitudinally.
- Tractor frame and structure. This included reviewing fundamental design factors as well as how the drive axle suspension roll stiffness is coupled to the steer axle suspension roll stiffness.
- Steer axle suspension. This included fundamental choices such as independent suspension or the usual solid axle. Other factors that change the weight transfer and roll angle relationships such as roll center heights were identified.
- Tires and wheels. This examination included parameters that play a large role in steady-state and transient handling, such as tire cornering stiffness.
- Electronic systems for stability enhancement, warning, or control. This analysis looked at active control of various components, driver alert systems, and maintenance systems such as tire inflation systems.
- Steer axle components. This included factors such as the choice of steering systems (e.g., rack and pinion steering vs. conventional recirculating ball systems with drag links).
- Steer axle steering characteristics. This analysis included roll and compliance steer, basic system geometry, and other kinematic characteristics.

An example of the evaluation process employed showing some options that may improve roll stability through trailer axle and suspension design appears in Figure 5-1.

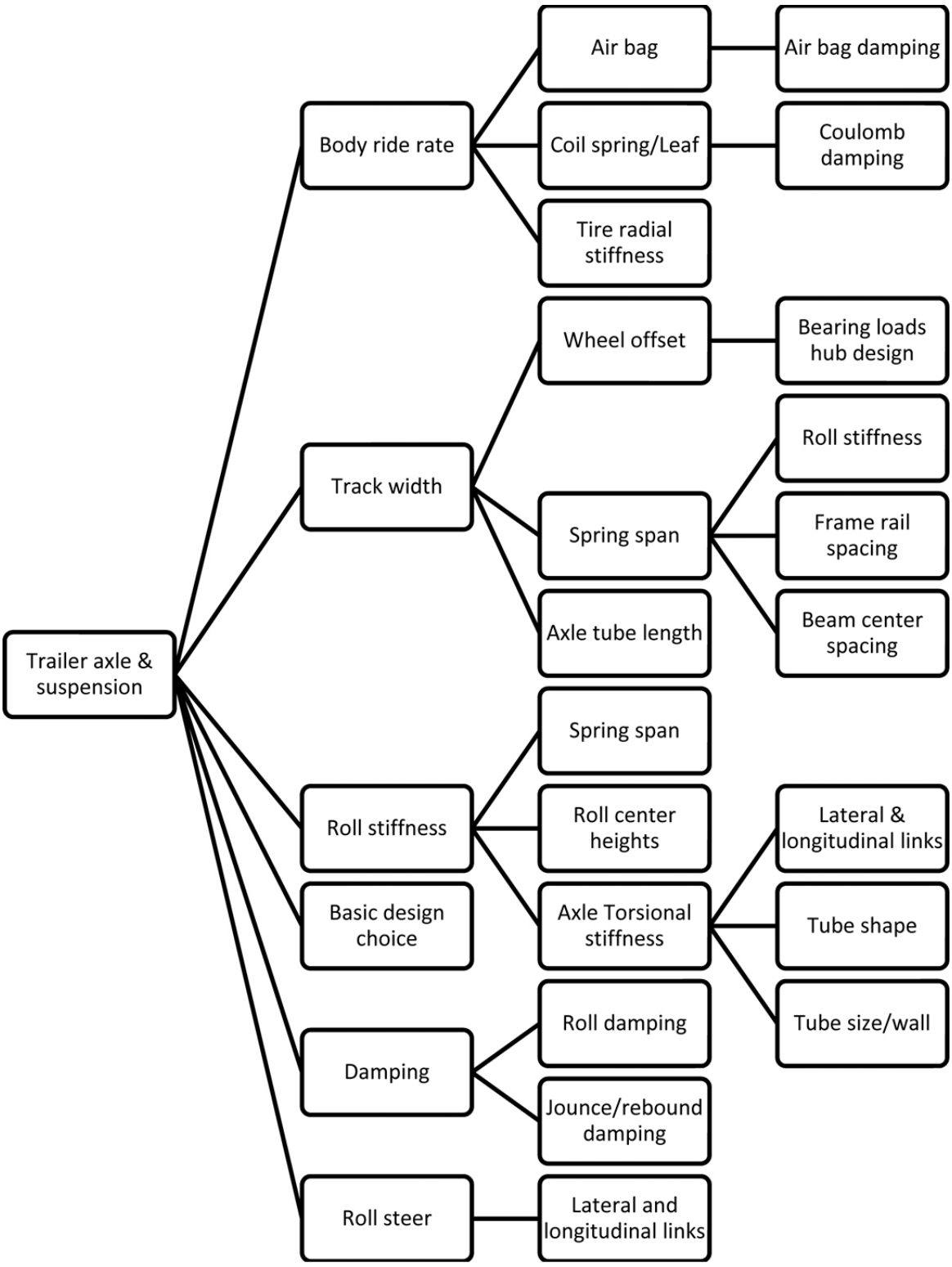

Figure 5-1. Drawing. Trailer axle and suspension options for roll stability

5.1 Options Selected for Track Testing

The design modifications selected for Phase C testing were chosen to provide additional test results that could be used for validating the vehicle simulation models. With a limited testing budget, the team decided early in the planning process to select a limited number of design changes. The selected configurations that were built and tested were specifically chosen so that they could be used to validate the fidelity of the models in both transient and steady state maneuvers.

To reduce testing time and to minimize costs, the selected changes focused on the trailer rather than the tractor. This also addressed the least stable element of the vehicle combination.

The HTRC team decided that all of the Phase C track testing would be performed with NGWBS tires (Table 5-1). Phases A and B both addressed comparisons between NGWBS and dual tires and the team is now comfortable with NGWBS tires both for the drive axles of the tractor and for the trailer axles. No new knowledge would be gained by comparing dual tires with NGWBS tires because this had already been addressed in Phase B efforts.

Table 5-1. Tractor track widths for Phase B and Phase C with NGWBS tires

Steer axle track width	2057 mm
Drive axle track width	1938 mm
Drive axle outside-outside dimension	2383 mm

The HTRC team also decided that all of the track testing would be performed with the vehicle configured with a high CG that closely matched that of Phase B. The CG height was predicted to be slightly lower for Phase C since new axle and new chassis constructions with longer axles on the tank trailer would add a small amount of weight to both the sprung and unsprung masses at heights below the Phase B loaded trailer CG height. The reduction in the height of the CG of the trailer was predicted to be less than 25 mm; because the exact weights of the components were unknown, exact determination was not possible. This was considered an insignificant change in CG height that would result in an imperceptible change in the measured vehicle response characteristics in both track testing and in modeling.

The HTRC team determined that the greatest knowledge and best validation would occur with changes focused on the trailer suspension, with consideration for axle wall thickness, axle beam spacing, track width and shock absorbers. The final decision was that the track width and other axle parameter changes obtainable from off-the-shelf hardware would yield enough variation to produce detectable and analyzable changes in vehicle rollover performance and therefore would be applicable to support model validation. The complete description of the modified suspensions is in Section 6.1.1.

Preliminary estimates based on Adams modeling by Hendrickson indicated a 22 % increase in tank trailer axle roll stiffness for suspension TC1 relative to the Tanker T suspension.

Hendrickson's model had the suspensions mounted differently than in the experiments, so the results are not directly comparable. K&C testing was later performed, but only for suspension TC1. This testing, conducted by Michelin, was performed to validate the predicted axle roll stiffness as well as to identify any changes in roll steer and compliance. The K&C testing conducted in Phase B measured the overall suspension roll stiffness by applying loads through the tires—Phase B values were therefore identified as a body roll stiffness value which included the series load path of the tires and the axle roll stiffness.

The TC1 configuration was selected for K&C testing because testing suspension with the greater beam spacing would provide new information. Table 5-2 provides the relevant axle data for comparison. The Phase B data that is presented is with NGWBS tires to allow the comparison to be compatible with the Phase C data in which NGWBS tires were also used. This table represents the design and technology options evaluated during Phase C testing, with the corresponding Phase B parameter data included for comparison.

Track testing with a special shock absorber having a high rebound damping was planned, if test time and funding permitted. This option was considered for testing because TruckSim® simulations performed in Phase B with active rebound control showed promise in raising the roll threshold in the Open-Loop Double Lane Change maneuver. The testing with different shock absorbers would provide a change in a transient parameter, not just the stiffness parameters of the suspension design. A model of shock absorber with considerable rebound change was identified. As will be explained more fully in Section 7.2.4, the shock absorbers were found to have a minor contribution to the overall damping, and therefore testing with the alternative shock absorbers was not warranted.

Early consideration was also given to lowering the CG mechanically by replacing the kingpin with an assembly that lowers the front of the semitrailer and by lowering the rear of the semitrailer by adjusting the ride height of the air suspension. Issues of clearances and air bag geometry at the trailer axles limited the magnitude of the potential change, and confidence in the TruckSim® model's ability to predict the effect of changing CG height caused the team to decide against pursuing this option.

Table 5-2. Nominal trailer track widths and relevant axle parameters

	Tanker T	Tanker TC1	Tanker TC2
	Phase B	Phase C	Phase C
Tires (drive and trailer)	NGWBS	NGWBS	NGWBS
Axle width	1816 mm (71.5 in.)	1969 mm (77.5 in.)	1969 mm (77.5 in.)
Wheel offset	51 mm	51 mm	51 mm
Track width	1900 mm	2050 mm	2050 mm
Outside-outside tire dimension	2342 mm	2486 mm	2486 mm
Suspension beam center spacing	953 mm	1105 mm	953 mm
Air bag spacing	787 mm	937 mm	787 mm
Axle wall thickness	7.9 mm	7.9 mm	7.9 mm
Axle outside diameter	146 mm	146 mm	146 mm
Increased rebound damping	Not tested	Not to be tested	Considered but found unnecessary

5.2 Options Selected for Modeling

Chapter 8 identifies numerous possible options, some of which were explored in modeling. The benefits of the widest possible track width with the lowest possible CG provided the baseline. Beyond the baseline, safety can be improved by using electronic sensing to maintain proper handling margins (that is, in the gap between electronic engagement strategies and wheel lift) to bring the vehicle under control. These margins need further exploration. All sound designs and technologies should be investigated to improve the tractor semitrailer's roll stability as much as possible.

Chapter 6 – Description of Maneuvers and Test Procedures

The testing for the project was conducted at TRC, Inc., in East Liberty, Ohio, from April 8 to April 13, 2010. All test activities were supported by Link, the testing contractor. The tractor-tank trailer was tested in two vehicle configurations in which different axles were mounted to the trailer.

The maneuvers performed in Phase B testing were also performed in Phase C so that the results of Phase B could be compared directly with those of the current Phase C test program. The test results from the previous phase of testing showed excellent repeatability and the team was fully satisfied with the approach followed in Phase B. Accordingly, the test methods and procedures from Phase B were followed as closely as possible for this testing.

Unlike the Phase B testing, the Phase C configurations focused only on variations to the suspension and did not include changes to the CG height or of the tires. Evaluation of the ESC system performance was not a primary objective for Phase C, so for each vehicle configuration tested (i.e., TC1 and TC2), only a few test conditions were performed with the ESC system activated (on both the tractor and trailer). This enabled the team to verify that the ESC operation was consistent with expectations and that there were no anomalies experienced with the modified vehicle configurations.

One additional maneuver was included to quantify the contribution to roll damping provided by the trailer shock absorbers and other sources. All maneuvers were designed to have the greatest degree of repeatability possible. Sensors were selected to permit comparisons between the test data and modeling predictions.

The vehicle's gross weight for all maneuvers was near 36,000 kg (80,000 lb). The same tractor and same tank semitrailer were used in both Phase B and Phase C. When referring to "Tanker T," "Tanker TC1," or "Tanker TC2," it is in fact the same physical tank semitrailer, with only the suspension (and its included axles) changed from one configuration to the next.

6.1 Vehicle Configurations during Testing

The variations in the vehicle configuration were much simpler during this phase of testing than during Phase B and consisted primarily of changes to the axle design of the tank trailer. The tractor and trailer used for Phase C testing had been used for Phase B testing in 2009, and the vehicle configuration variations were carefully selected so that data from Phases B and C could be readily compared.

The CG height for Phase C testing was intended to match that of the high-CG vehicle configuration of the Phase B testing, and the CG height is representative of modern gasoline-carrying tank semitrailers. Table 4-1 of the Phase B report (Arant et al. 2009) gave LBT's calculation of the loaded semitrailer's CG height as 2080 mm (81.9 in.). LBT estimates that this is 38 mm (1.5 in.) higher than the corresponding semitrailer would have in normal operations.

The tanks were loaded similarly in both phases with water in compartments 1 and 6 and sandbags placed on top of the tank trailer in the same way to achieve the maximum vehicle loading of 80,000 lb. NGWBS tires were used in Phase C, so the only intentional differences between the Phase B NGWBS tire high-CG ("Tanker T") configuration and all of the Phase C configurations were the suspension changes. The similarity of the configurations justifies comparing all three of these configurations, and the results of the testing were used to make conclusions regarding design influences among all three suspension designs. To accommodate the different suspensions, minor changes were made to the chassis and the CG height may have been altered slightly, perhaps 10 to 20 mm. The team believes that the effect on roll performance due to this change is negligible.

6.1.1 Suspension Variations

Figure 6-1 shows the type of suspensions that were installed in the trailer. Callouts show the key elements of the suspension. The suspension beams function as trailing arms with a bushing at one end and the air spring or air bag at the other. Because of stiffness in the bushings, they apply an anti-roll moment as well. The spacing between the two beams was the difference between TC1 and TC2, as explained next.

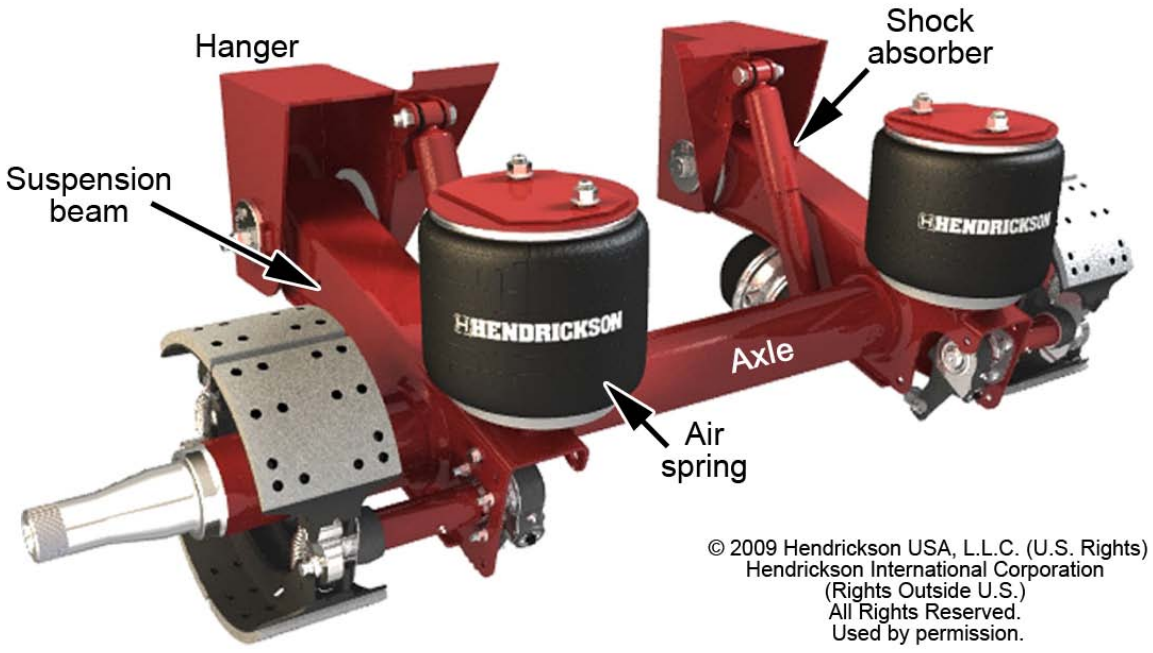

Figure 6-1. Photo. Components of the Hendrickson INTRAAX® Suspension

Phase C involved two primary vehicle configurations. The first, referred to as Tanker TC1, had trailer suspensions with an axle width of 1,969 mm and a spacing between the centers of the suspension beams of 1,105 mm. The second configuration, referred to as Tanker TC2, had axles of the same width and a beam spacing of 953 mm on center. The wall thickness of all of the axle tubes was 7.87 mm. The suspension design from the Phase B testing ("Tanker T") was narrower,

with an axle width of 1,816 mm and a beam center spacing of 953 mm, the same as that of the TC2 suspension. Though the differences between configurations TC1 and TC2 lay only in the suspensions, they are identified in this report as “Tanker TC1” and “Tanker TC2” because the whole tank semitrailer was being evaluated and for consistency with the “Tanker T” designation of Phase B.

The tank trailer configurations tested in Phase C are shown in Table 6-1 and Figure 6-2. The Tanker T configuration is included for reference.

Table 6-1. Comparison of Tanker T, TC1, and TC2 axle dimensions

Axle	Axle Specification			Tire Spacing	
	Wall Thickness in *mm*	**Beam Center Spacing** in *mm*	**Axle Width** in *mm*	**Track Width** in *mm*	**Overall Width** in *mm*
Tanker T	0.310 *7.87*	37.5 *953*	71.5 *1816*	74.625 *1895*	92.2 *2342*
Tanker TC1	0.310 *7.87*	43.5 *1105*	77.5 *1969*	80.625 *2047.9*	97.875 *2486.5*
Tanker TC2	0.310 *7.87*	37.5 *953*	77.5 *1969*	80.625 *2047.9*	97.875 *2486.5*

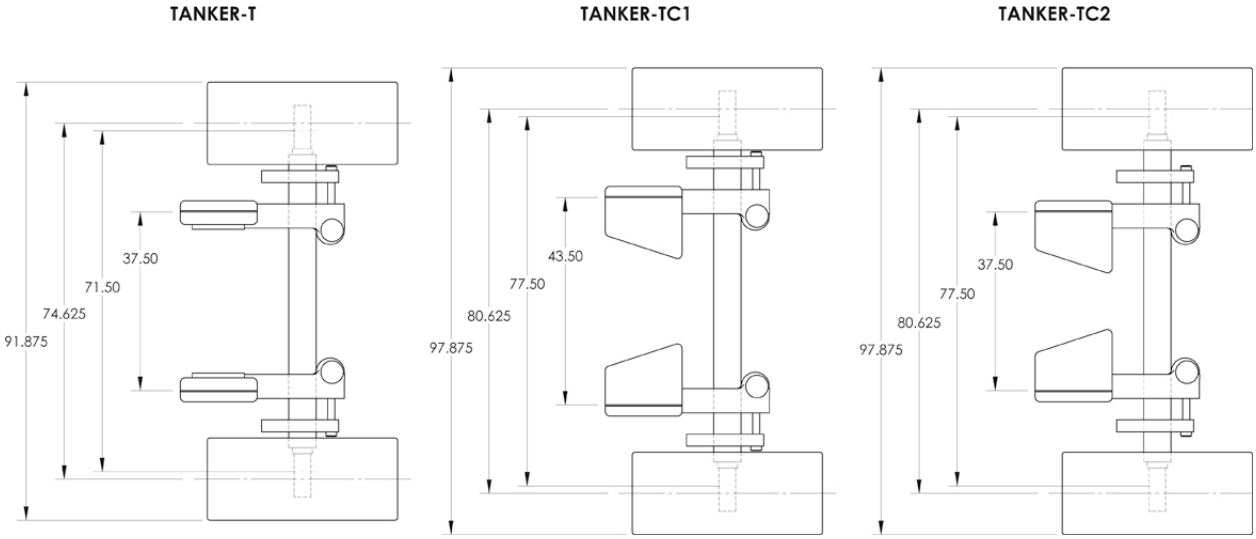

Figure 6-2. Drawing. Key dimensions (in inches) showing the differences among the three suspensions with the NGWBS tires mounted

The trailer was loaded by completely filling compartments 1 and 6 (the front-most and rear-most compartments). This minimized sloshing, thereby minimizing the uncertainty in lateral forces generated during testing. The remaining load consisted of sandbags, placed on the upper rails of the tank trailer and securely strapped in place to prevent their movement. The combined water mass in the two compartments was measured to be approximately 18,560 kg (40,840 lb), and the sand was loaded to provide a total vehicle mass—including tractor and trailer—of 36,290 kg (80,000 lb), the maximum gross vehicle weight allowable on federal highways for combination

trucks without a permit. The necessary weight of sand for the testing was found to be approximately 2,050 kg (4,510 lb). The tractor-tank trailer was equipped with outriggers and anti-jackknife chains during track testing; these were in place during the loading, so the total mass reported above corresponds to the as-tested mass of the vehicle. The only significant difference between the Phase B Tanker T high-CG configuration and the Tanker TC1 and TC2 configurations was the trailer suspension.

Table 6-2 lists the weights on the vehicles' axles as tested.

Table 6-2. Vehicle axle weight as tested

Tanker	Axle Weights lb *kg*			
	Axle 1 (steer)	**Axles 2 and 3 (drive)**	**Axles 4 and 5 (trailer)**	**Total**
T	12,040 *5,460*	34,492 *15,640*	33,532 *15,208*	80,064 *36,308*
TC1	11,940 *5,415*	34,180 *15,504*	33,360 *15,132*	79,480 *36,052*
TC2	11,940 *5,415*	34,180 *15,504*	33,360 *15,132*	79,480 *36,052*

6.1.2 Electronic Stability Control (ESC)

Phase C, as did prior phases, called for running some maneuvers with the ESC System disabled so that the behavior of the vehicle itself could be observed. In other maneuvers, the ESC system was enabled so that it would activate and apply the brakes so that its effect could be observed. Unlike prior phases, in which the ESC system might be enabled on only one unit or the other, in Phase C the ESC systems on the tractor and tank trailer were either both disabled or both enabled. In prior reports, these conditions were termed "Off-Off" or "On-On," respectively. When the ESC system is said to have "activated," it means that it applied braking to slow the vehicle during a maneuver.

6.2 Maneuvers

The test procedures for Phase C were identical to those of Phase B, and the Phase C maneuvers used the same steering programs and, wherever possible, the same speeds as used in the Phase B testing. This assured that the results would be fully comparable between the two test programs. In cases where wheel lift did not occur at the same test speed as in Phase B testing, because of configuration changes, the speed was modified.

A steering robot was used for all maneuvers, and a "drop throttle" approach (described in detail in the test plan, Appendix A) was employed for the step steer maneuver and for the modified step steer maneuver that was developed to characterize the auxiliary roll damping. For the ramp steer

and open-loop double lane change maneuvers, the driver actively controlled the speed in an effort to maintain constant speed throughout the maneuver. By using the steering robot and the drop throttle method where appropriate, the test repeatability was excellent and the number of runs for each maneuver could be minimized while providing statistically sound results.

All test maneuvers were run on a closed track using a professional driver and a programmed steering robot. Special safety precautions and devices were used, including outriggers and anti-jackknife chains. To determine wheel lift thresholds during the test maneuvers, the tractor was subjected to severe steering inputs and speeds that were specifically designed to place the tractor and tank trailer into unstable, limit conditions. The use of a steering robot provides improved test repeatability, but the robot will continue to add de-stabilizing steer inputs to the tractor past the point at which a human driver would normally intervene to recover a stable trajectory. The test maneuvers should not be construed as representative of normal inputs or of vehicle responses seen in everyday use on public roads.

Both the ramp steer and the step steer maneuvers include a low-speed and a high-speed test. The low speed was selected so that the vehicle would operate in a sub-limit manner in which the ESC would not normally intervene and wheel lift would not occur; the high speed condition was selected so that either wheel lift would occur or the ESC system would intervene. For safety, the "high" speed was determined during testing by increasing speed incrementally until wheel lift was achieved.

The low-speed ramp steer maneuver was performed in both clockwise and counter-clockwise directions. All other maneuvers were performed without varying the direction of travel employed during the test procedure.

6.2.1 Ramp Steer

A ramp steer maneuver is a decreasing radius turn performed at a nearly constant vehicle speed. The steering input increases linearly from zero to the maximum steer angle for the maneuver, resulting in a plotted steering angle that is a "ramp," hence the name of the maneuver. The steering input from the steering robot during the ramp steer maneuver is shown in Figure 6-3. During the maneuver, the driver maintains a constant speed while the steering robot controls the steering rate. By slowly decreasing the radius of the turn, the steady-state behavior of the vehicle is approximated for any given steering angle because the transient effect produced by the slow steering input is negligible. The ramp steer maneuver was performed with a steering input from the robot of 10 deg/s to the point at which an instability event occurs (e.g., wheel lift or excessive articulation).

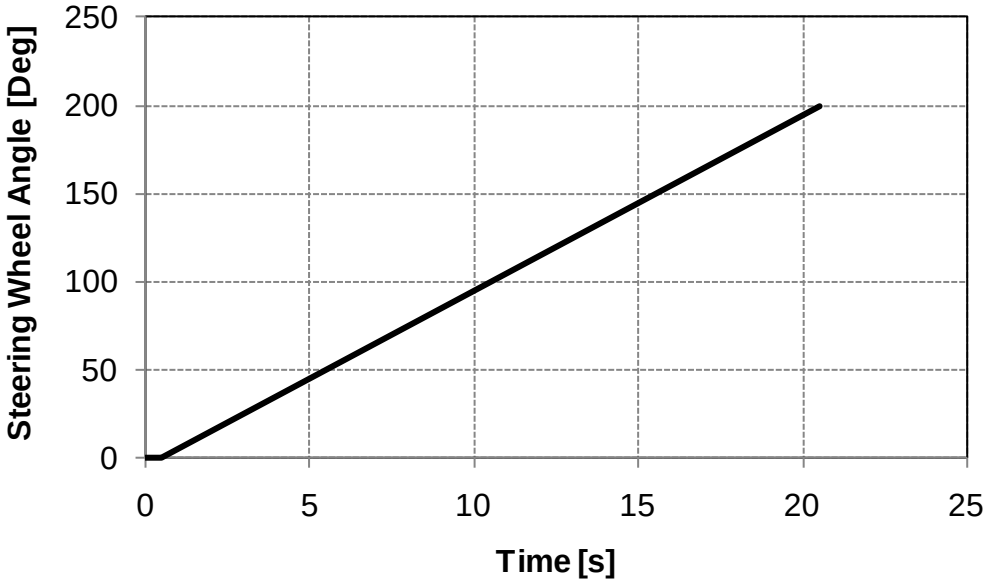

Figure 6-3. Graph. Robot steering program for the ramp steer maneuver

The benefit provided by the use of the steering robot can be well appreciated by observing (Figure 6-4) the plots of multiple runs performed for the ramp steer. This degree of repeatability would not be possible with a human driver, and the statistical quality of the data during the early phases of research could not come close to matching the results of Phase B and Phase C testing during which the steering robot was used.

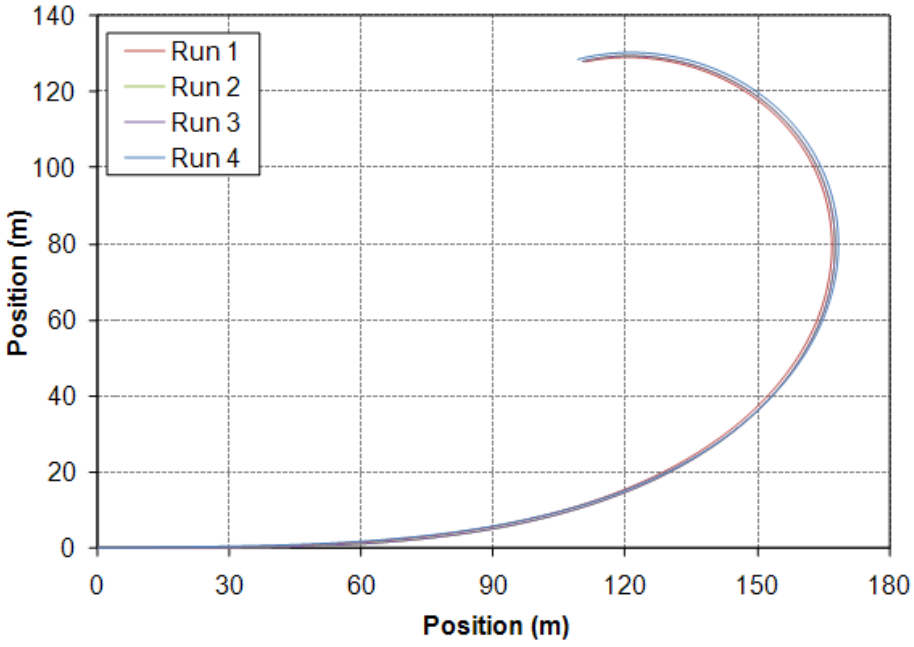

Figure 6-4. Graph. Overlay of the tractor path for four runs for the ramp steer maneuver (TC1), showing the repeatability that the steering robot provides

Because some of the data analysis required that the vehicle's path radius and the axle roll angles be known, these channels were developed using calculations from other measured data channels. A MATLAB routine was developed by CU-ICAR to provide the data. The vehicle's path radius was determined by fitting an arc through the path of the vehicle over a short (one sec) interval. The image in Figure 6-5 is from the algorithm used to analyze the path radii from both the field data and the TruckSim® model results. The blue marks are the location of the center of the radius for previous points on the vehicle's path, while the red mark and red line are the current center of curvature and radius for the vehicle. The same algorithm was used to define the radius of curvature for the track data and the modeling analysis.

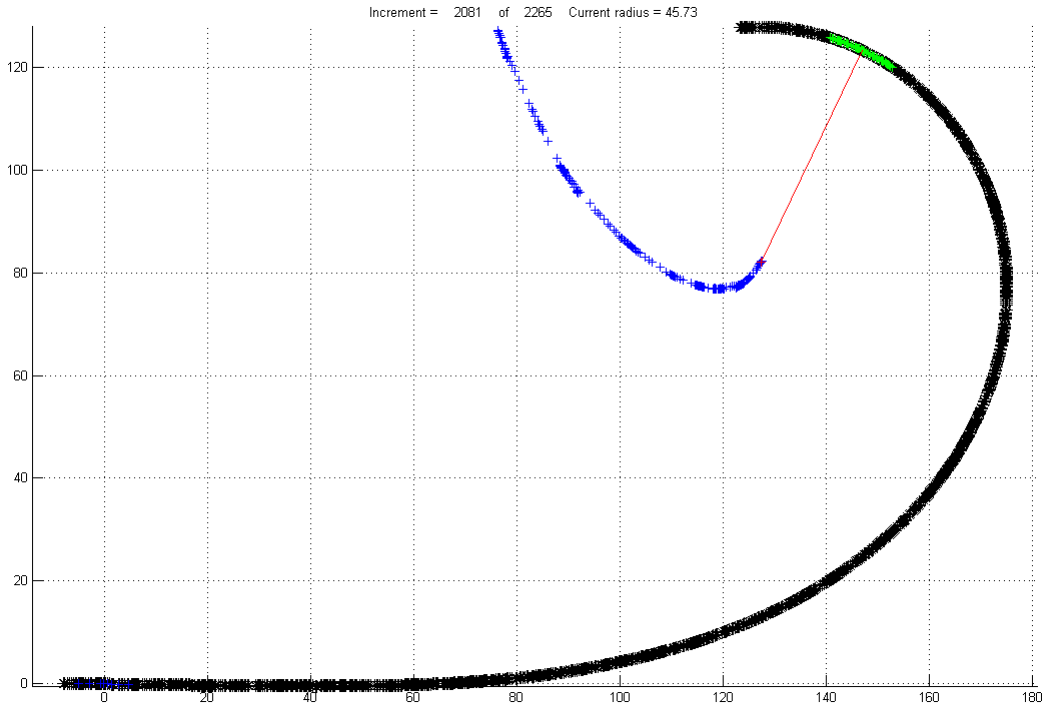

Figure 6-5. Graph. Vehicle path and radius of curvature

The ramp steer test was performed both at a low speed (sub-limit) condition—to evaluate the basic handling dynamics of the vehicle, in particular its steer characteristics—and at a high speed to quantify the rollover characteristics in steady-state operation. The low-speed test was performed at 32.4 km/h while the high-speed test was run at 48.6 km/h. The driver was able to maintain the speed within 1.1 km/h of the target speed during all of the runs performed. For the low-speed maneuver, the test was repeated in both clockwise and counter-clockwise directions, while the high-speed maneuver was only performed in a counter-clockwise direction (left turn of the tractor-trailer).

The high-speed ramp steer test was performed initially with the ESC system disabled, and was then repeated with both the tractor and tank trailer ESC systems enabled (termed “On-On” in prior reports).

6.2.2 Step Steer

The step steer maneuver was selected and executed because it provides information in a repeatable manner on the transient responses of the tractor-trailer to a change in steering input. This information contributes to the understanding of the total vehicle system response. The step steer maneuver used for this test was based on International Organization for Standards (ISO) 7401, *Road vehicles—Lateral transient response test methods—Open-loop test methods*.

The step steer maneuver, as executed, was a straight-line test with a single, rapid left turn input of 170 deg at the steering wheel at a rate of 170 deg/s. This amplitude and rate was selected because the Phase B (and Phase A) testing also used this step input profile. A sufficient test area was required to operate the tractor-trailer at a constant speed of approximately 57 km/h for approximately 30 s. The step steer maneuver was only performed with the ESC system disabled on both the tractor and trailer (termed “Off-Off” in prior reports).

The speeds for trailer-only wheel lift and tractor and trailer wheel lift were determined using a bracketing method in which the test speed was increased incrementally. Once determined, the test was repeated four times at each of these test speeds, and four times at a third speed slightly below that at which trailer wheel lift occurred but for which wheel lift did not take place. The complete set of test conditions was repeated for both the Tankers TC1 and TC2. The steering robot program used for this maneuver appears in Figure 6-6. Figure 6-7 is an overhead view of the tractor’s path in four runs of the step steer maneuver.

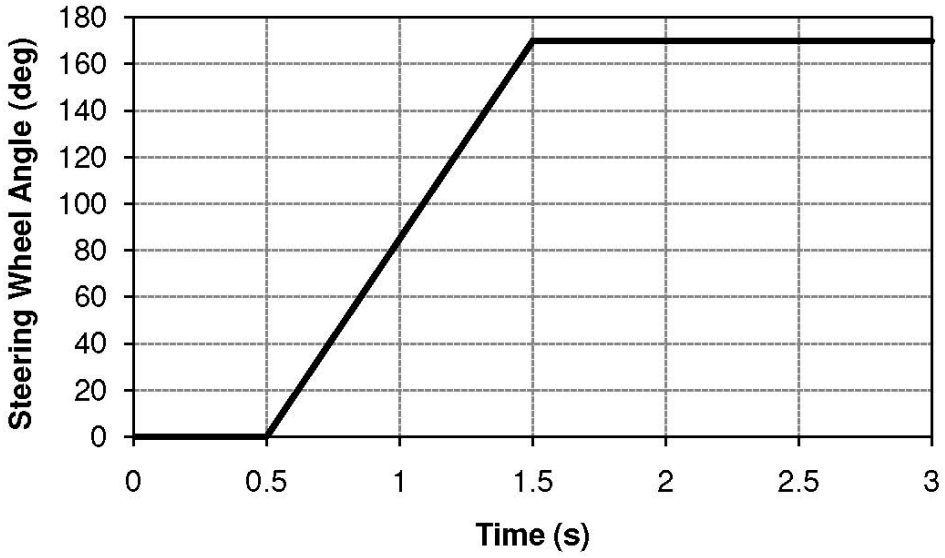

Figure 6-6. Graph. Robot steering program for the step steer maneuver

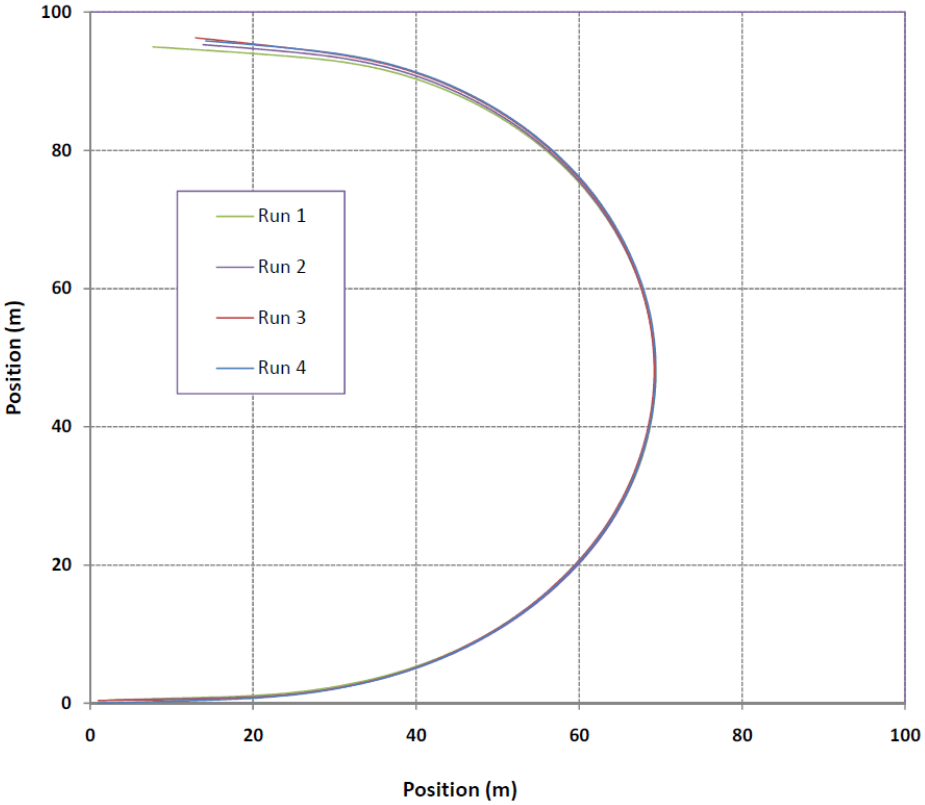

Figure 6-7. Graph. Overlay of the tractor path for four runs for the step steer maneuver (TC1), showing the repeatability that the steering robot provides

6.2.3 Open-Loop Double Lane Change

A double lane change maneuver consists of an initial abrupt lane change from the right lane to the left lane, as would occur during an evasive maneuver in which a driver attempts to avoid an obstacle that appears in the right hand lane. Following the lane change to the left, the vehicle is straightened in the left lane and then makes an abrupt lane change back to the right, returning the vehicle to its original lane of travel. Finally, the vehicle is straightened so that it is traveling in the original lane and in the same direction as before the beginning of the maneuver.

The maneuver during Phase C testing was performed by a steering robot to control the steering according to a pre-programmed maneuver, yielding far more repeatable results than can be realized by a human driver. The maneuver is characterized as an “open-loop” double lane change because steering is performed without regard to the lateral position or heading of the vehicle. For convenience, this report will often refer to simply the “lane change.”

The steering program, developed in Phase B using the TruckSim® software, is shown in Figure 6-8. The same program that was developed and used as the main lane change test in Phase B was repeated for Phase C, without modification, because the path was appropriate for a double lane change and because using the same program for Phase C meant that test results could be directly

compared with the Phase B results. The program was designed for a vehicle speed of 64 km/h, but the same program is used even for other test speeds. For different test speeds, the direction in which the tractor-trailer travels at the end of each turn may not be fully parallel with the original direction of travel, but the deviations in the travel direction have been observed to be minimal, and the benefits of using a single robot program outweigh the added complexity of modifying the steering program for different test speeds.

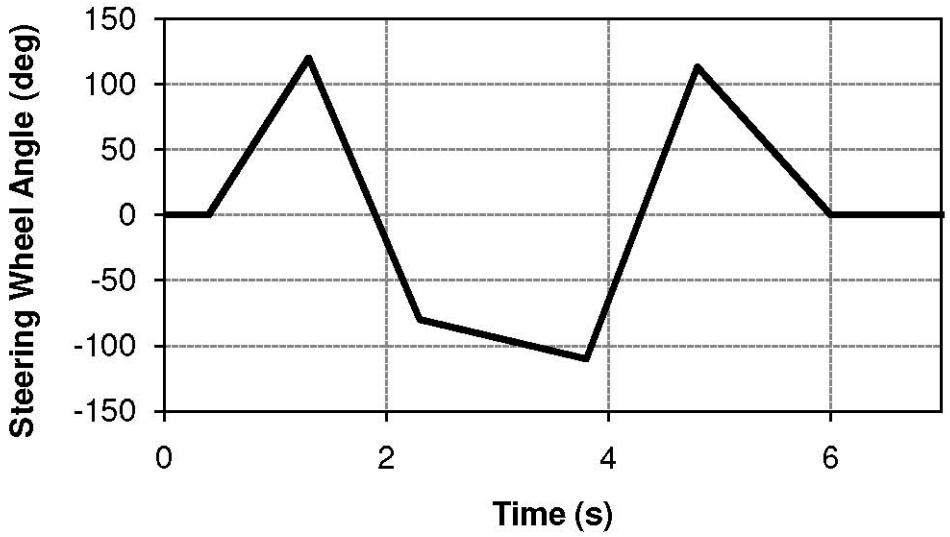

Figure 6-8. Graph. Reference steering program for the open-loop double lane change maneuver (designed for 40 mph using the drop throttle method)

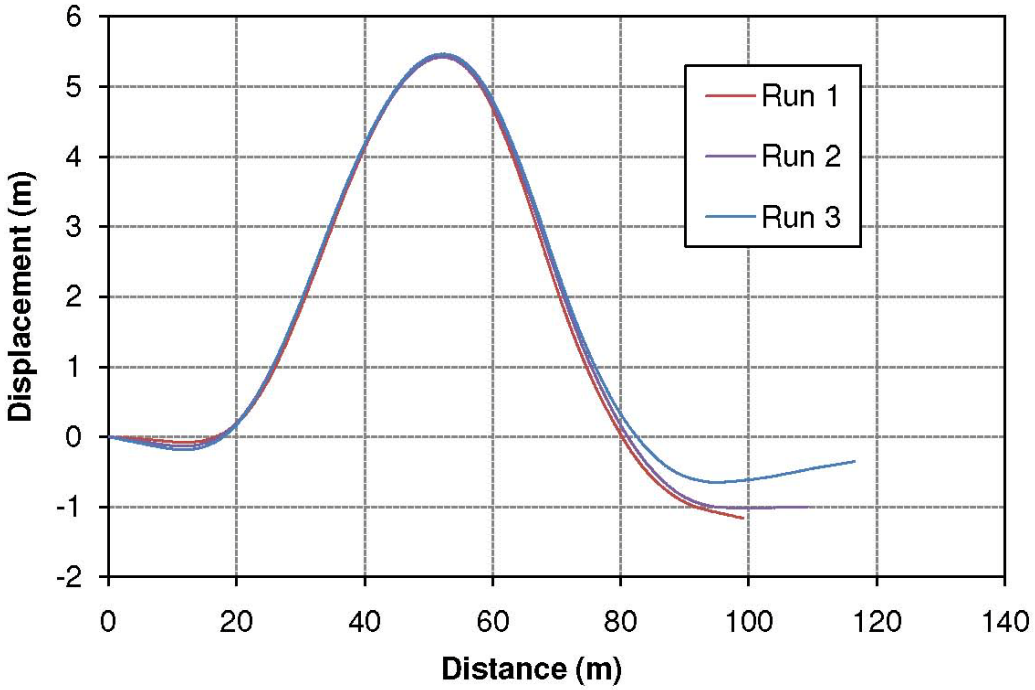

Figure 6-9. Overlay of the tractor path for three runs of the lane change maneuver (TC1), showing the repeatability that the steering robot provides

6.2.4 Modified Step Steer Maneuver

A fourth maneuver, a modification of the Step Steer, was executed to characterize roll damping in the trailer.

As part of the Phase B modeling efforts, WMU developed a TruckSim® model using input parameters that represented the test vehicle design, with all parameters based on measured vehicle characteristics or other known component parameters. Although the TruckSim® model gave relatively reasonable dynamic performance predictions in some cases, roll oscillations for certain maneuvers in the model were more significant than those observed in the track testing, indicating that the model was under-damped compared to the real vehicle. TruckSim® provides the ability to apply what is referred to as "auxiliary roll damping" in the model, in addition to the normal damping due to shock absorbers. This auxiliary roll damping was adjusted to achieve similar levels of roll oscillations for the lane change maneuver, and the predictions aligned well to the measured data.

To gain a better understanding of the auxiliary roll damping phenomenon and to see if it could be quantified indirectly through additional testing, the HTRC team sought to develop a new test that could be used to observe the auxiliary roll damping of the tractor-tank trailer. Ideally, this test would apply a roll impulse to the tank trailer and subsequently record the behavior as the vehicle came to rest. The auxiliary roll damping, then, could be characterized by testing the vehicle, using the imposed roll impulse, without shock absorbers present, since only the auxiliary roll damping would remain.

Several approaches were considered to generate a roll impulse, but many were ruled out due to the complexity or cost of safely performing them. The HTRC team determined that one more way to generate the desired roll impulse that would not compromise safety would be to drive the tractor-trailer in a maneuver that generates wheel lift, so that the vehicle would roll onto an outrigger. The vehicle would then be allowed to drop back to the ground, and the roll oscillations would be measured after the tractor-trailer re-established ground contact. The team decided that this could be accomplished by using a step steer maneuver to roll the vehicle onto its outrigger, maintaining the maximum steering input for a short period of time to allow the vehicle to stabilize, and finally returning the steering to a zero input steer angle.

Variations of this "modified step steer" maneuver, using different maximum steer angles and dwell times (i.e., the duration at the maximum steer angle), were programmed for the steering robot, and a program that worked quite well was readily obtained. Because the period of interest for data collection is the time after the tractor-trailer returns to the ground, the steering program had to include a period with zero steer angle at the end of the maneuver since the data acquisition system (DAS) was configured to record only during the period that the steering robot is executing its program. The program used (Figure 6-10) includes a 3-s dwell time and a 5-s hold time at the end of the maneuver, using the same 170 deg maximum steer angle input at 170 deg/s. as in the normal step steer maneuver.

The maneuver was repeated for both the TC1 and TC2 configurations so that the difference in the roll damping could be observed between the different configurations. In addition, a third configuration, without shock absorbers, was tested.

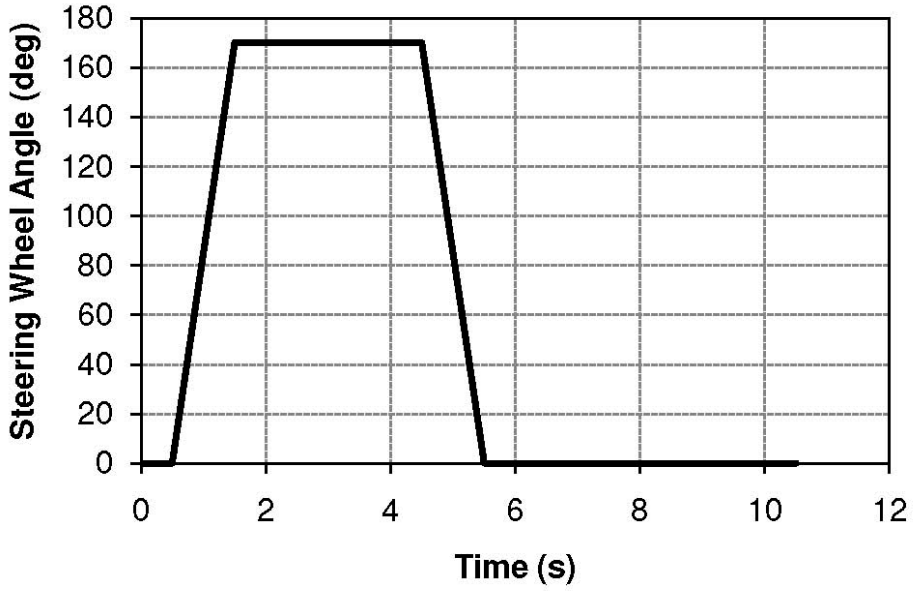

Figure 6-10. Graph. Steering program for the modified step steer maneuver, for characterizing the auxiliary roll damping

6.3 Data Collection

The test vehicle was instrumented to collect data from a total of 150 channels, including individual sensors, inertial global positioning system (GPS) devices, and quantities read from the tractor and trailer controller area network (CAN) buses.

6.3.1 Sensors Installed for These Tests

A broad range of instruments was used during testing. Commonly available sensors such as pressure gages, strain gages, and string potentiometers were used for many of the measurements required. Strain gages on the tractor drive and tank trailer axles were used to identify wheel lift (as in Phases A and B). This provided a more precise indication than could be achieved with only height sensors on the axles. The strain gages were calibrated to provide an accurate zero-load condition so that wheel lift could be identified with the strain gage measurement.

The second point in the calibration of each strain gage involved the static load of each axle end. The measurement output was load rather than micro-strain values with the conversion done directly on the eDAQ system. While complex loading of the axle during the test maneuvers may result in incorrect load outputs from the strain gages at intermediate load levels, the zero-load condition remains accurate, and thus provides a simple indication of the approach to wheel lift and the time at which wheel lift takes place. Strain gage rosettes were installed in half-bridge and

full-bridge configurations on the tank trailer axles in order to measure the bending and torsion of the axles, respectively.

A summary of the sensors on the vehicle appears in Table 6-3. A complete list of the channels recorded appears in the Test Plan in Appendix A.

Table 6-3. Vehicle Sensor Installation

Vehicle	Sensor
Tractor	GPS (Global Positioning System) location
Tractor	Vx, Vy sensors
Tractor	Roll rate
Tractor	Yaw rate
Tractor	X, Y, Z accelerations
Tractor	Steering wheel angle
Tractor	Road wheel angle (calibrated road wheel)
Tractor	2 height sensors for determining the roll of the rear tractor drive axle (axle 3)
Tractor	Strain gages for wheel lift sensing for axles 2, 3 (supplemental to height sensors)
Tractor	CAN-bus data logging for powertrain and ESC system
Tractor	4 tractor wheel speeds – “high-resolution”
Tractor	6 tractor wheel speeds – “low-resolution”
Tractor	ESC intervention signals
Tractor	Vehicle speed
Tractor	Other available CAN-bus signals for vehicle state analysis
Tractor	Brake line pressure sensor at axle 2
Trailer	GPS location
Trailer	Vx, Vy sensors
Trailer	Roll rate
Trailer	Yaw rate
Trailer	X, Y, Z accelerations
Trailer	Articulation angle
Trailer	2 height sensors for determining the roll of the rear tank trailer axle (axle 5)
Trailer	Strain gages for wheel lift sensing for axles 4, 5 (supplemental to height sensors)
Trailer	Strain gage rosettes for measurement of bending and torsion of axles 4 and 5
Trailer	Brake line pressure sensor at axle 4
Trailer	Suspension air bag pressures for left and right sides of the trailer axles (axles 4 and 5)
Trailer	2 Trailer-to-frame ride height sensors for axle 5 (left and right)

In addition to these sensors, two Oxford inertial and GPS measurement systems, models RT3100 and RT2500, were used to collect vehicle dynamics and positional information from the tractor and tank trailer, respectively. These systems provide exceptional accuracy for position, speed, acceleration and orientation data and each is equipped with a CAN-bus output interface. The CAN-bus outputs were used to provide data to the eDAQ DAS due to their speed and ease of configuration, and all of the channels available from the RT units were recorded. Other sensors included a Torque Trak drive shaft torque telemetry system, Wenglor optical height sensors, and a Stable Imaging Solutions infrared camera that was used to record the orientation of the

interface between the tractor and tank trailer at the fifth wheel, including fifth wheel separation during vehicle roll events.

The large number of data channels was necessary to meet the needs of the project. Redundant data channels were incorporated to permit verification of the results and to ensure that critical data would not be missed if one channel were lost during a test.

Link calibrated all of the sensors, as appropriate, after they were installed on the tractor-tank trailer. The calibration procedure included zeroing the sensors, as appropriate and when feasible. A few sensors required adjustments in the field, and to save set-up time, these sensors were zeroed using specially developed software after the data was collected. The calibration of the measurement was not affected by this change.

Axle-end strain gages were calibrated using statically measured wheel loads. However, during testing, the axles experience complex combinations of tension, compression, bending and torsion, and the only reliable measure of the strain gages was when the load is, at, or near zero. Therefore, data from the linear strain gages was used only to identify wheel lift. For the torsional and bending strain gage rosettes, WMU traveled to Link's facilities twice prior to the track testing to install and calibrate the sensors. Since the TC1 suspension was already installed on the trailer and the calibration procedure required that the beams (trailing arms) of the suspension be free, only the sensors for the TC2 suspension were calibrated before testing.

The sensor calibration curves from the TC2 suspension were initially used for the TC1 suspension on the vehicle. After the TC1 suspension testing was completed and the axles were exchanged, WMU completed the calibration of the sensors for the TC1 suspension. Since the strain gages were all from the same lot, the gage factors and other parameters were similar, so the calibrations were actually quite similar and the data could be reviewed qualitatively during the testing of the TC1 suspension even though the calibration was not exact. After all the testing was completed, the preliminary sensor calibrations for the TC1 suspension were corrected using software.

All data were recorded using a set of three Somat eDAQ DASs. The eDAQ systems provide a high level of reliability, accuracy and robustness for data acquisition, and the technical specifications for these devices met all requirements of the project. These devices were attached in a master-slave configuration, which guaranteed that all measurements were made simultaneously during data sampling. One system recorded the analog data channels, while the other two recorded the CAN bus inputs from the vehicle's data bus and from the Oxford RT units. Each device was placed for convenience of measurement, and various cables and input modules connected all of the sensors and devices to the eDAQ systems. All channels were sampled at a rate of 100 Hz. A complete list of the data channels recorded is provided in Appendix A.

6.3.2 CAN Bus Data

Only two channels on the eDAQ units could record CAN bus data. Because of the possibility of data collisions and bandwidth overload, the HTRC team was advised not to attach the two vehicle CAN outputs, or a vehicle CAN bus output and an RT unit output, to the same data channel. Accordingly, one channel was assigned to the tractor CAN bus and one to the Oxford RT systems. The tank trailer CAN-bus was not recorded because the trailer wheel speeds and trailer ESC intervention signals were the only signals of interest on the tank trailer CAN bus, and ESC analysis was not critical to Phase C testing. The team recorded some tractor CAN bus channels that were not critical to the project to have supplemental information available to help understand any irregularities that occurred during the testing. The recorded data from the tractor CAN bus included 39 channels, while the RT units had 78 channels total (39 channels from each of the tractor and trailer RT units).

6.3.3 Processing and Filtering

Several channels were calculated from other data, either in real-time by the Oxford RT units or by the eDAQ DAS; or during post-processing. For the real-time calculations, the calculated data appeared as additional data channels. These included a number of the acceleration and vehicle orientation channels (provided in multiple reference frames from the RT units, for convenience). These calculated channels, which were configured directly in the device setup, are described in Appendix A. The methodology of the development of the calculated channels is described in the Oxford documentation (http://www.oxts.com).

The roll angles of the rear drive and tank trailer axles (axles 3 and 5) were calculated during post-processing. Using the Wenglor optical height sensors mounted on opposite sides of each axle, the axle roll angles could be calculated trigonometrically. It was necessary to analyze the roll angle from the field data only because the modeling analysis includes vehicle roll angle. The tractor and tank trailer roll angles were available directly from the RT units that were mounted to the chassis of the tractor and trailer.

After the test data had been collected and corrected for sensor errors, it was filtered using a third-order 5 Hz low-pass Butterworth filter. This removed noise from the data so that the observed vehicle response was smoother and the trends in the data were clearer. Because any response-of-interest of the vehicle would occur below 5 Hz, this filtering did not affect the conclusions of the analysis. The filter used was bi-directional, so there was no issue with the phase lag of the filtered signals.

Chapter 7 – Test Data Analysis

Data from the test track maneuvers described in the previous chapter, as well as additional static and dynamic measurements, were analyzed in diverse ways to learn about the axles' effects on the test vehicle's stability. That analysis is in this chapter.

7.1 Chapter Overview

The first measurements to be analyzed are those that characterized individual components of the vehicle. The heart of this chapter is Sections 7.4 through 7.6, which present analysis of the three maneuvers that induced near-rollover conditions on the test track. While the different maneuvers called for different analyses, certain steps were followed in every analysis, and they are outlined in Section 7.5. Observations and conclusions are drawn at each individual analysis, with the general over-arching conclusions presented in the final section of this chapter.

7.2 Supplemental Measurements

Most of the data were collected during the three near-rollover maneuvers. The primary purpose of these maneuvers was to ascertain the roll threshold of the vehicle. Supplemental measurements were performed to characterize particular subsystems of the test vehicle. The K&C tests measured properties of the suspension in static conditions. The steer characteristics of the vehicle and the roll stiffness properties of the suspension were observed in a low-speed ramp steer maneuver. Finally, a modified step steer or "drop test" maneuver was added to measure the roll damping, with and without shock absorbers.

7.2.1 Kinematics and Compliance (K&C)

As in previous efforts, the trailer's suspension was characterized in quasi-static conditions using Michelin's K&C test equipment. The relations between loads and deflections measured in this manner were incorporated into the models of the vehicle. Both suspensions, TC1 and TC2, were tested in the dynamic maneuvers; only Tanker TC1 was characterized by the K&C testing.

In Phase B, a semitrailer designated "Tanker M" was characterized by K&C testing. Tanker M was a different vehicle than Tanker T, which was used on the test track in Phase B, but was effectively identical to Tanker T. In the comparison in the next few paragraphs, Tanker M is called Tanker T to simplify comparisons with Tanker T later in the report. Tankers T and TC1 differ in both axle width and beam spacing; differences between their K&C properties cannot be attributed with certainty to one dimension or the other.

Values from the K&C measurements of the two tank semitrailers are in Appendix H, and important points are highlighted in the following paragraphs. The vertical kinematic responses of Tanker T and Tanker TC1 are similar.

There are compliance differences between these two trailers in response to braking forces. Tanker T demonstrates more toe out under braking forces than does Tanker TC1. Wheel center

longitudinal displacement and locked wheel rotation due to braking forces are greater for Tanker TC1 than Tanker T. There is most likely more than one source of this compliance difference due to the reversal of compliance between toe out and longitudinal displacement. Despite these differences both trailers demonstrate near zero axle steer during braking.

The two trailers respond differently to lateral forces. Tanker T demonstrates more vertical load change due to lateral forces than does Tanker TC1. Tanker T's roll center height is higher than Tanker TC1's by approximately 100 mm. The difference in roll center heights was unexpected as Adams modeling (of the suspensions on a test rig, not on the semitrailer) predicted almost no change.

Tanker T demonstrates more toe change axle steer due to lateral forces than does Tanker TC1. Tanker T demonstrates a less linear lateral axle shift over center due to lateral forces than does Tanker TC1.

While the vertical suspension spring rate of the leading trailer axle is similar between these two trailers, Tanker TC1 demonstrates more hysteresis in roll stiffness than Tanker T. Tanker T has more roll steer. The leading axle of Tanker TC1 has much more camber change due to roll. Tanker TC1's axle roll stiffness is higher. Normally a wider connection point (wider beam spacing as in Tanker TC1) would result in less camber change, not more, so the result was contrary to expectations. A wider axle could go in the opposite direction for camber change, but that may not account for so large a difference.

7.2.2 Steer Characteristics

The understeer properties of the combination tractor and semitrailer vehicle were assessed using a constant velocity test with an increasing steer angle—a low-speed ramp steer. The test was run at 32 km/hr with a 10 deg/s steering input and the hand wheel. The tests were performed in both the clockwise and counter-clockwise directions as illustrated in Figure 7-1.

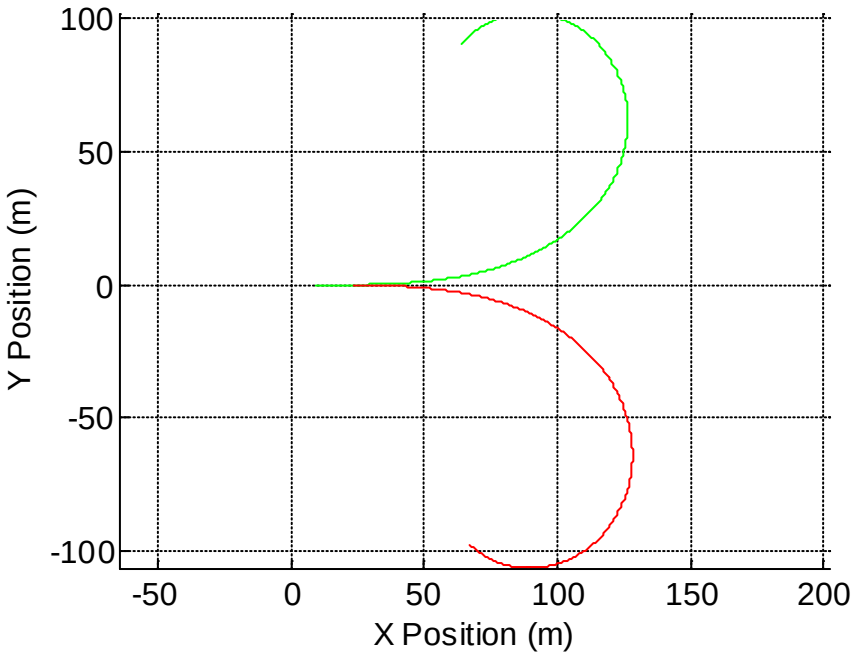

Figure 7-1. Graph. Clockwise and counter-clockwise tractor trajectory map

Steering was controlled by a steering robot while the vehicle speed was maintained by a driver. To gage the variation in driver-maintained velocity during the test, the forward speed of the tractor was reviewed for each maneuver (Figure 7-2). Because the maneuver was a ramp steer, the velocity fluctuations of 1 km/h at the beginning of the maneuvers are not significant.

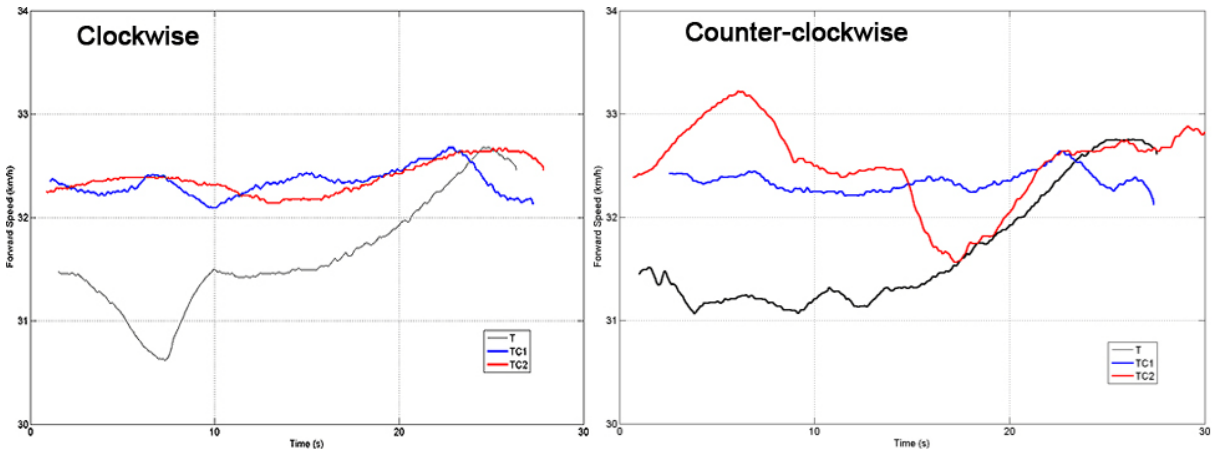

Figure 7-2. Graph. Clockwise (left) and counter-clockwise (right) speeds in the low-speed ramp maneuver.

As the maneuver progressed and more steering angle was introduced, the radius of the vehicle's path decreased. The tighter radii regions are of interest (Figure 7-3), and the noise in the measured path radius is significantly lower for these regions.

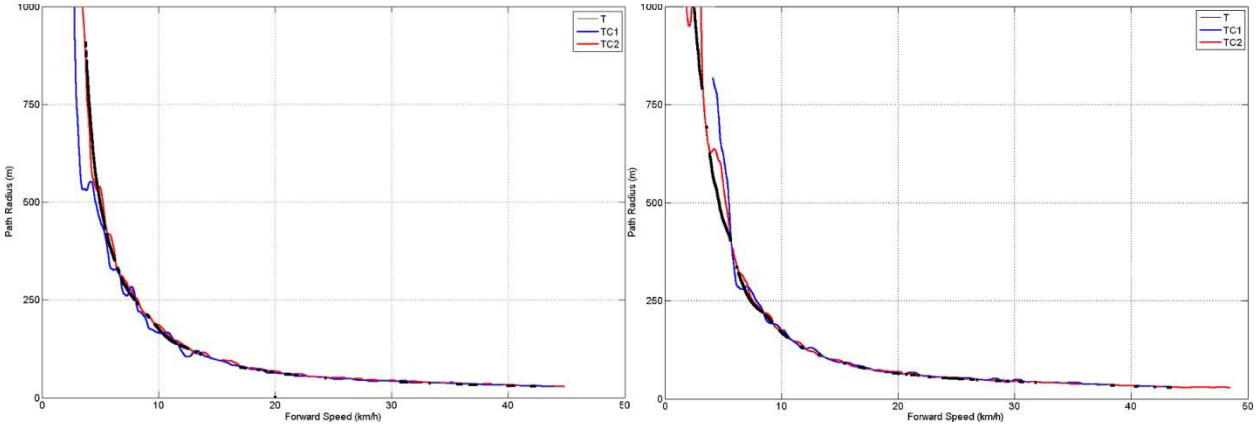

Figure 7-3. Graph. Speed vs. radius (clockwise) (left) and counter-clockwise (right)

Analysis of the tractor's path for the three vehicle configurations did not indicate any significant difference in the observed radius of curvature between the suspensions for the clockwise (Figure 7-4) and counter-clockwise directions (Figure 7-5). In these figures, the radius is plotted against the observed lateral acceleration, because lateral acceleration is generally used as the reference variable in discussing handling performance.

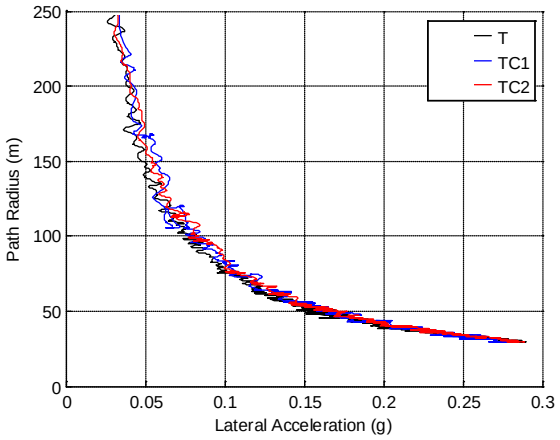

Figure 7-4. Graph. Clockwise path radius

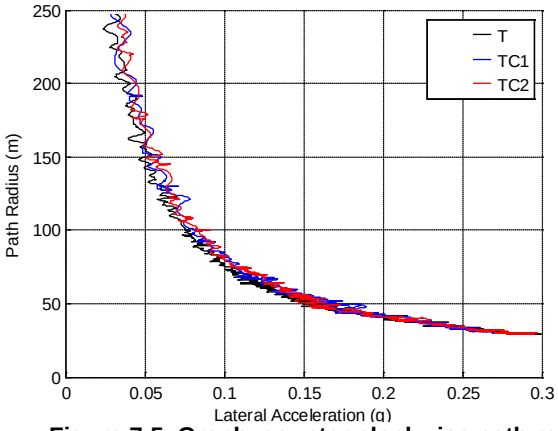

Figure 7-5. Graph. counter-clockwise path radius

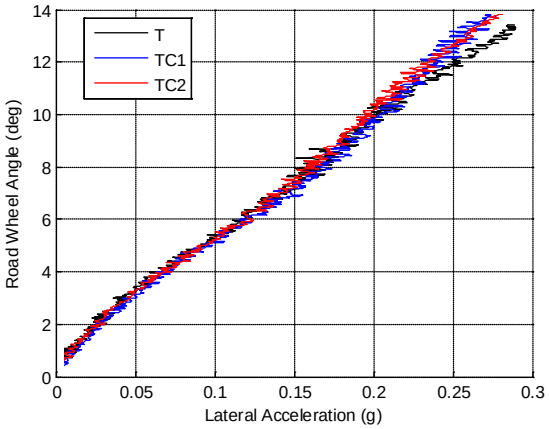

Figure 7-6. Graph. Clockwise steering input

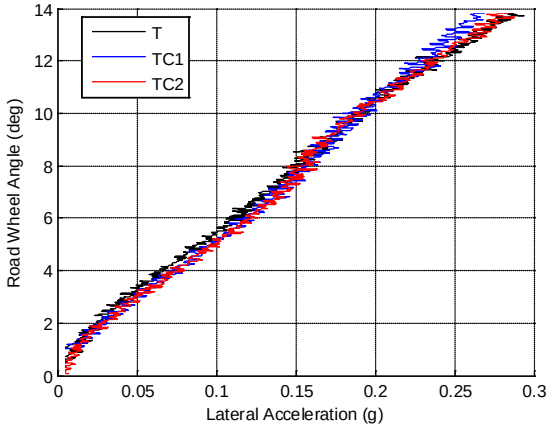

Figure 7-7. Graph. counter-clockwise steering input

Analysis of the road wheel steering angles for the three trailer configurations showed a nearly linear relationship with the measured lateral acceleration for all test cases. Noticeable deviations in the road wheel steering angle occurred for only the highest lateral accelerations, and these regions are above the linear response range of the tractor (Figure 7-6 and Figure 7-7).

Using the effective wheel base of the tractor (6.75 m), the Ackerman steering angle for the tractor could be evaluated for the measured radii. The Ackerman steering angle is defined as:

$$\delta_A = \frac{180}{\pi} * \frac{L}{R}$$

Equation 24

where L is the tractor wheel base and R is the path radius. Taking the difference between the observed steering angle and the Ackerman angle gives the Ackerman corrected steering angle:

$$\delta_c = \delta_A - \delta_r$$

Equation 25

where δ_A is the Ackerman steering angle, δ_r is the actual steering input (road wheel angle), and δ_c is the correction or Ackerman steering error. Generally, the Ackerman correction should be positive, which indicates that the driver is supplying a greater steering input than dictated by the Ackerman steering. It is also desirable to have an Ackerman correction that increases with lateral acceleration, to mitigate the potential for the driver to accidently input more steering than needed in a maneuver. For illustration, consider an increasing speed constant radius maneuver. With a positive Ackerman correction gradient, the driver must continue to add steering to maintain the course with increasing speed. For a negative Ackerman correction gradient, the driver must remove steering input. Although a positive Ackerman correction gradient is always stable, a

negative Ackerman correction gradient can lead to instability (e.g., a jackknife in the case of a combination vehicle) if the driver fails to correct the steering.

Analysis of the Ackerman corrected steering for the three cases suggests that the wider trailer axle did affect the tractor understeer properties (Figure 7-8 and Figure 7-9). Because the noise in the measurement of the lateral acceleration and the steering input yield a noisy Ackerman correction, Figure 7-8 and Figure 7-9 were re-evaluated with a fifth order polynomial. The fitted Ackerman plots are shown in Figure 7-10 and Figure 7-11.

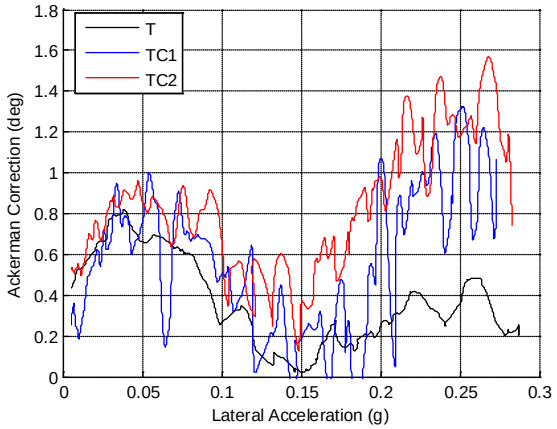

Figure 7-8. Graph. Clockwise Ackerman correction

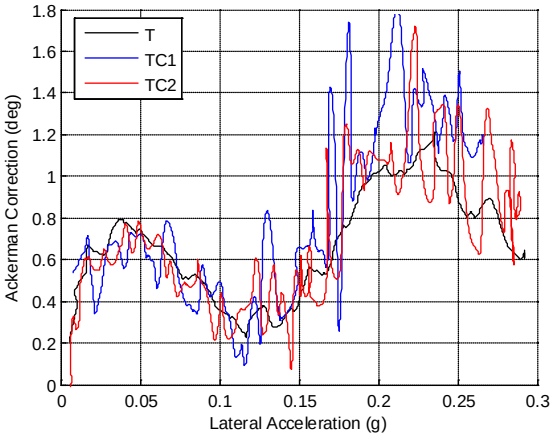

Figure 7-9. Graph. counter-clockwise Ackerman correction

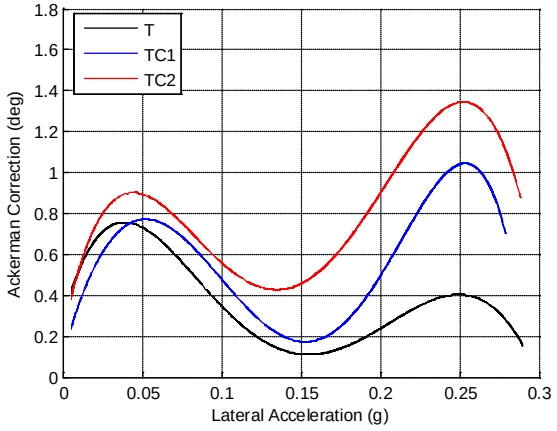

Figure 7-10. Graph. Clockwise Ackerman correction fit

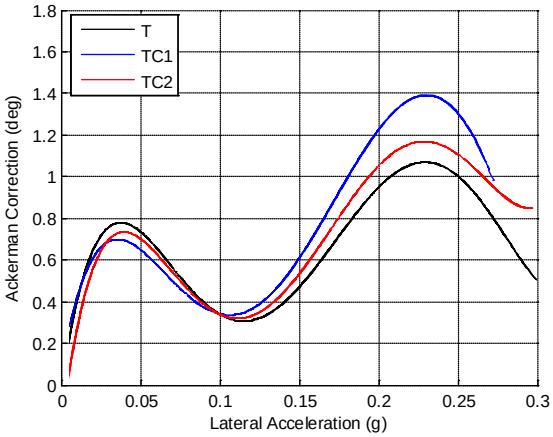

Figure 7-11. Graph. counter-clockwise Ackerman correction fit

At low lateral accelerations (i.e., low overturning moments), the effect of the trailer axle changes is minimal. As the lateral acceleration levels increase, the wider trailer axles appear to increase the understeer seen in the tractor, but because the test was not repeated, the differences cannot be assessed for statistical significance. The best conclusion allowable is that the configuration of the trailer axle does not qualitatively affect the tractor's understeer behavior in the linear (below 0.2 g) range.

Since considerable effort was focused on determining characteristics that differed between the TC1 and TC2 suspensions, the steer characteristics of the trailer were determined with each suspension. Understeer analysis of the trailer was performed using the articulation angle between the tractor and trailer as the steer angle for the trailer. Using this, the calculated effective wheelbase of the trailer and the trailer turn radius are used to establish the steer characteristics of the trailer as shown in Equation 26:

$$\textit{Articulation angle} = \text{Trailer Ackermann angle} + \text{understeer angle}$$

$$\textit{Articulation angle} = ATAN\left(\frac{\text{effective wheel base}}{\text{Turn radius}}\right) * 57.3 + k\left(\frac{velocity^2}{\text{Turn radius} \times g}\right)$$

Equation 26

Trailer understeer increases the articulation angle between the tractor and the trailer. Oversteer decreases the articulation angle and the off-tracking up to the point where the articulation angle changes sign and the potential for jackknifing or spin is present.

Plots of lateral acceleration and road wheel angle for the TC1 suspension in the low-speed clockwise and counter-clockwise ramp steer maneuvers appear in Figure 7-12 through Figure 7-15. Although the tractor's behavior is consistent in both the clockwise and counter-clockwise maneuvers, the trailer had a steer bias or asymmetry that differed between the clockwise and counter-clockwise directions.

Figure 7-12 and Figure 7-13 show the roll steer behavior of the TC1 suspension in a clockwise, low-speed ramp steer, while Figure 7-14 and Figure 7-15 show similar plots for the counter-clockwise maneuver. All plots consistently show the understeer of the tractor and the "oversteer" of the trailer. This slight oversteer reduces the articulation angle slightly and reduces the off tracking at higher lateral accelerations. The trailer oversteer is slightly asymmetric, producing greater oversteer in the clockwise direction than in the counter-clockwise direction. There should be no reason for the asymmetric steer other than zeroing or gain errors in the data system. The average understeer gradient is approximately -7 deg per g of lateral acceleration, with the negative value implying that oversteer is present. The tractor steer is consistent with that which was measured in the Phase B testing, confirming the procedure.

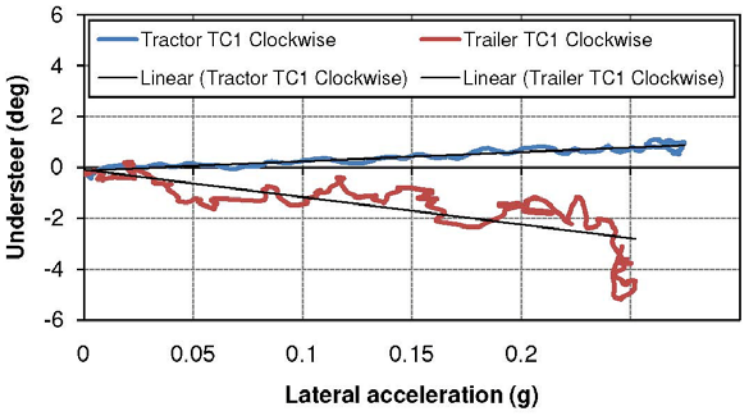

Figure 7-12. Graph. Understeer vs. lateral acceleration for Tanker TC1 in the clockwise direction

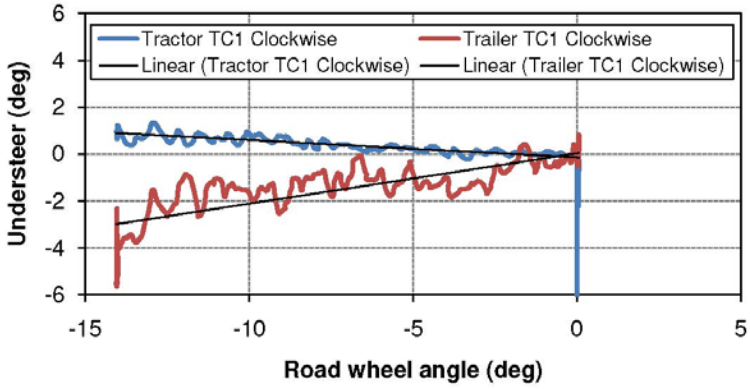

Figure 7-13. Graph. Understeer vs. road wheel angle for Tanker TC1 in the clockwise direction

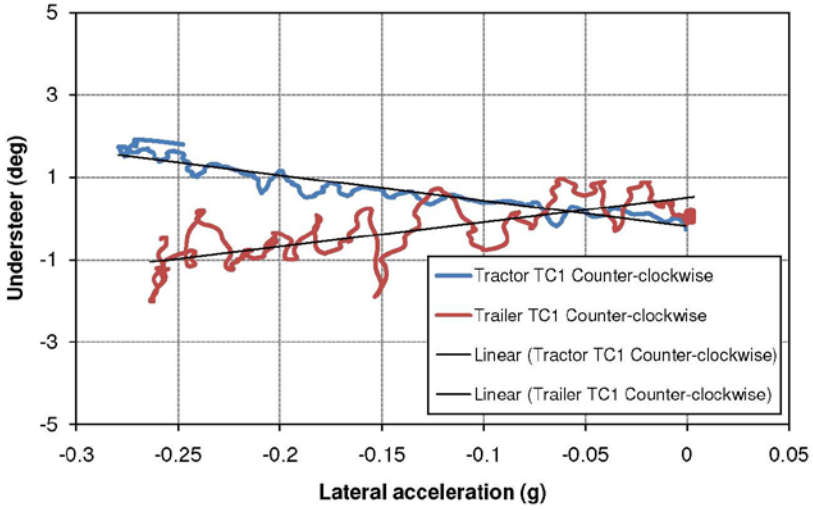

Figure 7-14. Graph. Understeer vs. lateral acceleration for Tanker TC1 in the counter-clockwise direction

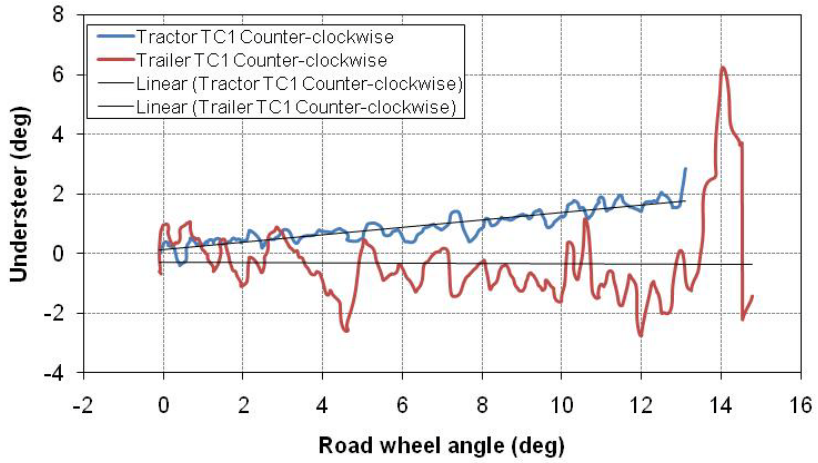

Figure 7-15. Graph. Understeer vs. road wheel angle for Tanker TC1 in the counter-clockwise direction

Figure 7-16 and Figure 7-17 present the understeer behavior for the low-speed clockwise ramp steer maneuver for the TC2 suspension, while Figure 7-18 and Figure 7-19 present analogous understeer behavior for the counter-clockwise maneuver. The roll understeer for the TC2 suspension is approximately -5 deg per g of lateral acceleration.

It was anticipated that the TC2 suspension should produce a greater roll steer, which is shown in the counter-clockwise data, but the reason for the large asymmetry between clockwise and counter-clockwise tests is not understood. Low speed testing of axle configuration TC2 was performed with tires that had experienced two days of testing which may have introduced some bias to their behavior due to asymmetrical wear. Additionally, the axle change itself, and any misalignment introduced with said change, could have produced a steer offset. Any combination of these could account for the asymmetry between the clockwise and counter-clockwise and as a result conclusions on the cause of the understeer bias are difficult to draw.

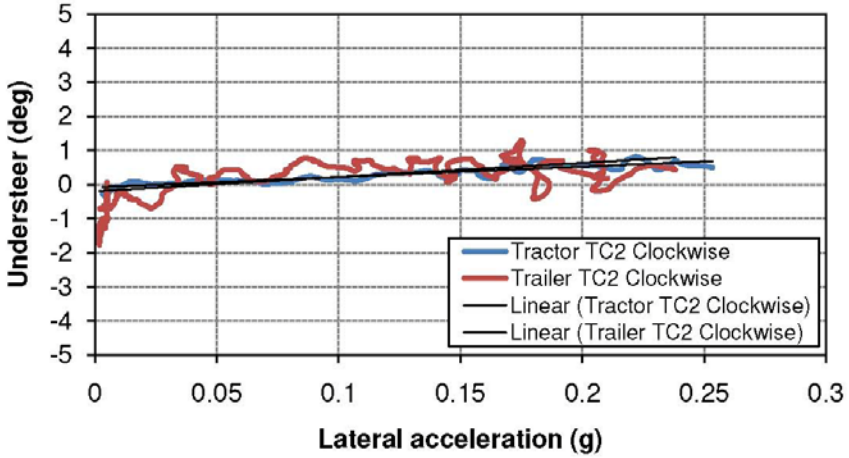

Figure 7-16. Graph. Understeer vs. lateral acceleration for Tanker TC2 in the clockwise direction

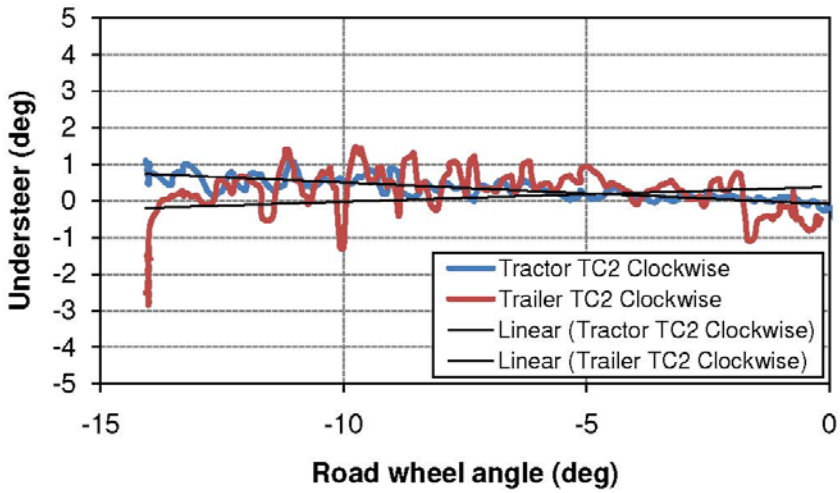

Figure 7-17. Graph. Understeer vs. road wheel angle TC2 CW maneuver

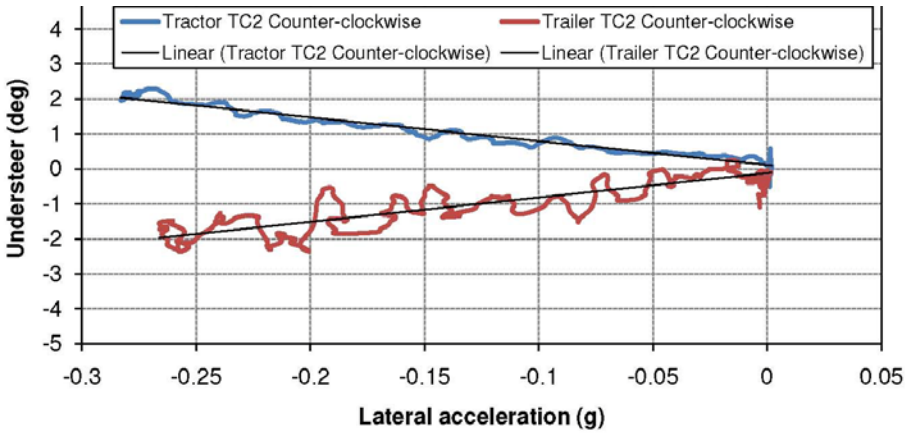

Figure 7-18. Graph. Understeer vs. lateral acceleration for Tanker TC2 in the counter-clockwise direction

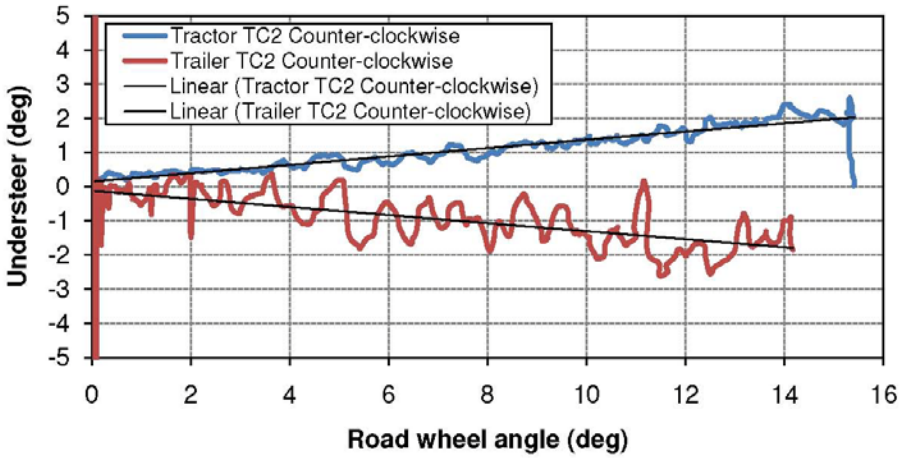

Figure 7-19. Graph. Understeer vs. road wheel angle for Tanker TC2 in the counter-clockwise direction

Figure 7-20 through Figure 7-23 compare the steer characteristics of the TC1 and TC2 suspensions. Figure 7-20 displays the trailer understeer as a function of lateral acceleration and Figure 7-21 displays trailer understeer as a function of articulation angle, both for the clockwise maneuver. Figure 7-22 and Figure 7-23 display the same information for the counter-clockwise maneuver.

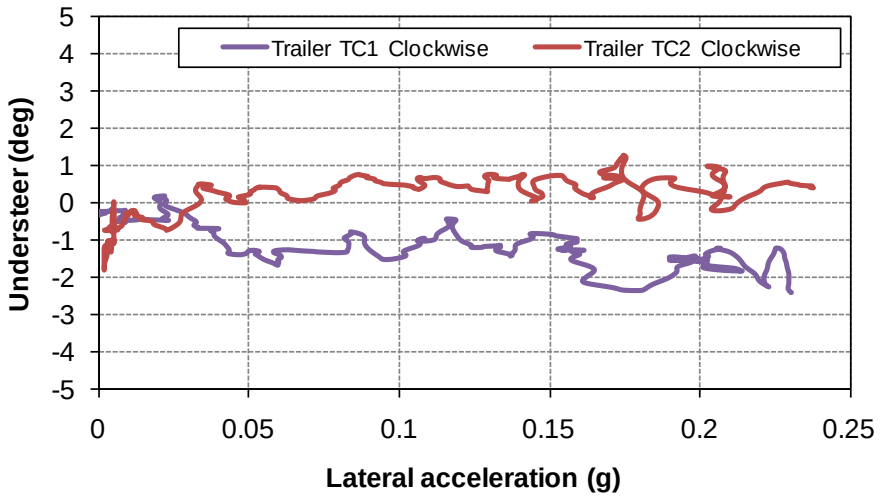

Figure 7-20. Graph. Comparison of the trailer understeer vs. lateral acceleration between Tankers TC1 and TC2 in the clockwise direction

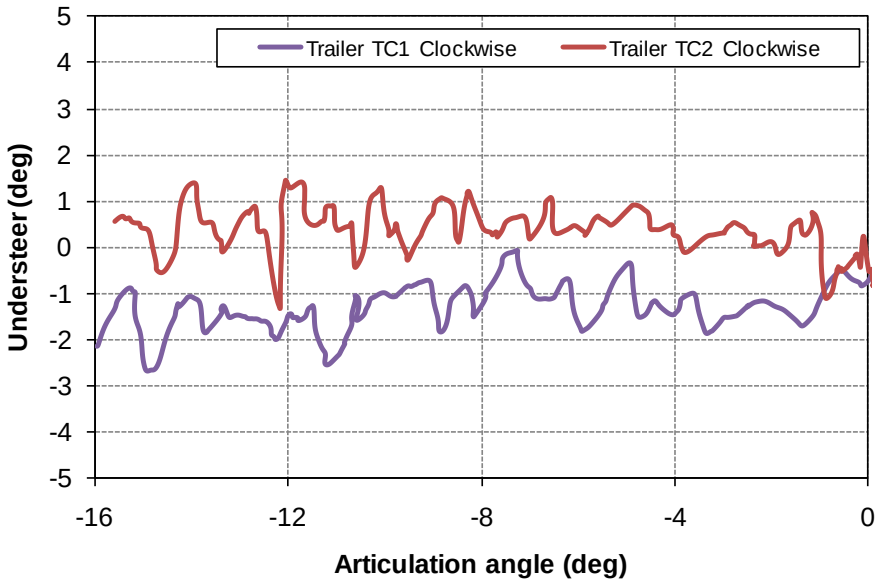

Figure 7-21. Graph. Comparison of trailer understeer vs. articulation angle between Tankers TC1 and TC2 in the clockwise direction

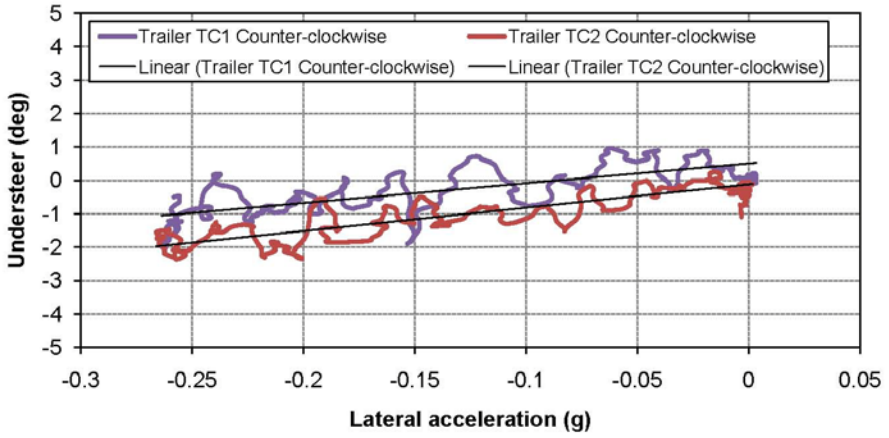

Figure 7-22. Graph. Comparison of trailer understeer vs. lateral acceleration between Tankers TC1 and TC2 in the counter-clockwise direction

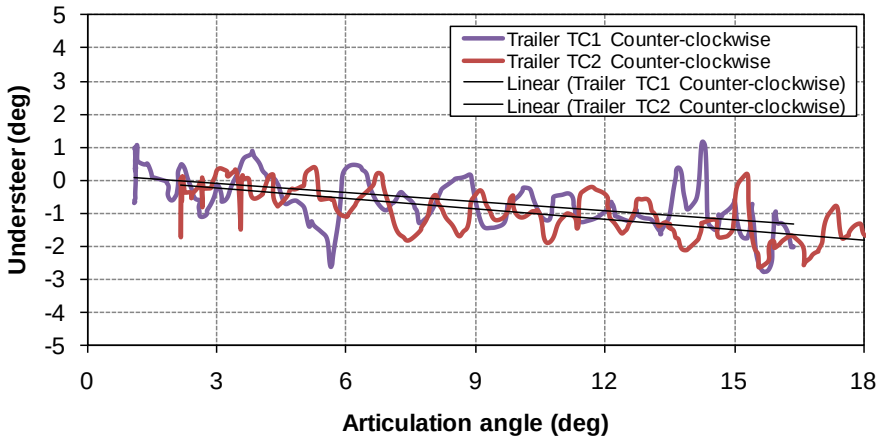

Figure 7-23. Graph. Comparison of trailer understeer vs. articulation angle between Tankers TC1 and TC2 in the counter-clockwise direction

Conclusions related to understeer and axle selection

Suspension configurations appeared to have a minimal effect on the understeer gradient. One important finding is that the steer characteristics of the trailer produce an oversteer tendency. This oversteer does not appear to be detrimental because the off tracking of the trailer is not overcome by the small amount of oversteer attained even in the limiting behavior. Further studies in the simulation environment should be conducted to identify the potential for optimization of this parameter. The roll oversteer is related to tire slip angles and the trailer suspension geometry.

7.2.3 Roll Stiffness

The difference between the TC1 and TC2 suspensions was the spacing between the beams, as illustrated in Figure 6-2. These suspensions were constructed so they not only support the weight of the trailer in the vertical direction, but they also act as an anti-sway bar or an anti-roll bar. That is, if the trailer body begins to roll, it will lift up the end of the axle beam on one side and

push down the beam on the other side. The beams are welded to the axle tube, and the torsional stress (the “twist”) in the tube resists the rolling of the body and helps to prevent it from rolling over. Strain gages were mounted on the axle tube of a TC1 axle and a TC2 axle to measure the torsional deflection of the tube for studying the anti-roll properties of the axles, and for measuring the bending load in the axles during the maneuvers. The axles in Phases A and B were not instrumented in this manner.

Rosette gages were mounted to the top and bottom of both trailer axle sets, at a mid-span position, with the diagonal gages of the rosette configured into a full bridge with a Wheatstone bridge layout that uncoupled the lateral and flexural loads from the torsional loads. These center mounted gages, in a full bridge configuration (torsional bridges), were then sensitive only to axle tube torque. Due to the welded beams that locate the axles under the trailer chassis, axle roll resisting torque was produced whenever the trailer rolled. This torque was assumed to produce a high percentage of the roll stiffness for the suspension.

The center linear gages of the rosettes were configured into a half bridge for each axle and configured to measure bending loads (aligned with the tube axis) at the axle center. These gages could be used to determine the effect of beam spacing on axle bending deflection in the vertical plane.

Calibrating the torque of an axle mounted on the trailer was not possible, so axle 5 of the unmounted TC2 set was used. To perform the calibration, the cables and smart modules were disconnected from the trailer axles and, with an extension wire, were connected to the remote TC2 calibration axle. The axle was then loaded with the same weights as were used to calibrate the axle on the ground. This provided input to the eDAQ system, as configured, with the appropriate smart modules being used on the trailer. When calibrated, the system was switched back to the system installed in the trailer with the TC1 axles and re-zeroed to account for any offset differences. Since all gage factors were equal, the system gain was equal for all bridges on the other axles..

When the TC1 axles were removed from the trailer, they were verified to assure correlation with the calibration axle. This methodology provided accurate assessment of the actual axle torques, from which the contribution to roll stiffness could be determined. To determine the relationship between axle torque measured from the torsional gages and the roll resisting moment provided by the trailer, a geometric relationship was established (Equation 27).

$$\text{Axle antiroll moment} = \frac{\text{eDAQ torque measured} \times \text{beam spacing}}{\text{beam length to axle centerline}}$$

Equation 27

String potentiometers were connected between the tank trailer chassis and axle 5 on both sides of the tank trailer. Axle 4 was not instrumented with either string potentiometers or axle height gages.

Roll stiffness contribution from axle torsion

The following plots and tables show the values obtained from the axle torsion gages for the TC1 and TC2 configurations during track testing. Figure 7-24 shows the axle contribution to anti-roll moment of axle 5 for both the TC1 and TC2 configurations during the high-speed ramp steer maneuver.

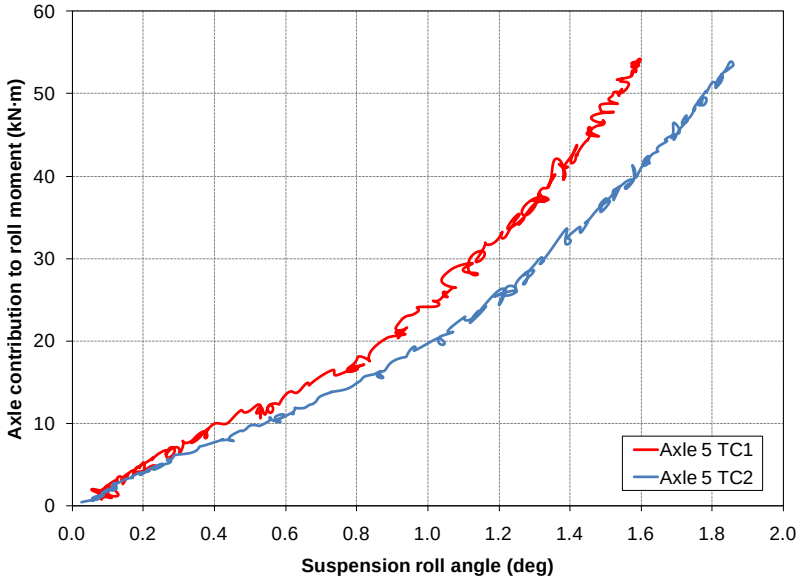

Figure 7-24. Graph. Axle contribution to roll moment vs. suspension roll angle in the high-speed ramp steer maneuver

Figure 7-25 shows the axle contribution to anti-roll moment of axle 5 for both the TC1 and TC2 configurations during the low-speed ramp steer maneuver. Unlike the high-speed ramp steer, which was only performed counter-clockwise, the low-speed ramp steer maneuver was performed in both counter-clockwise and clockwise directions.

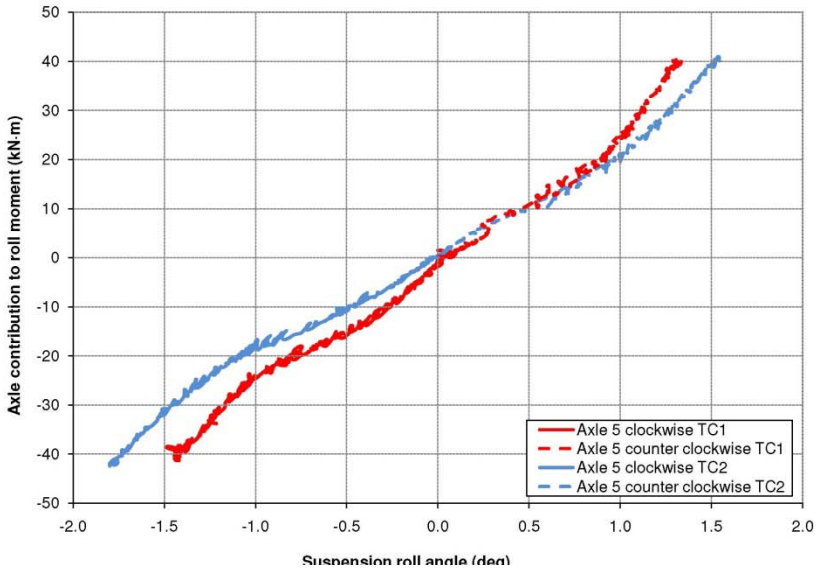

Figure 7-25. Graph. Axle contribution to roll moment vs. suspension roll angle – low-speed ramp steer maneuver

Table 7-1 and Table 7-2 summarize the axle contribution to anti-roll moment of axle 5 at 1 deg of roll during the low-speed and high-speed ramp steer maneuvers. The tables also compare the experimentally determined differences between the TC1 and TC2 suspensions, and differences that exist between the maneuvers performed in the clockwise and counter-clockwise directions. All data points in Table 7-1 and Table 7-2 are for 1 deg of roll in a range in which the roll moment is primarily linear with respect to the roll angle.

Table 7-1. Axle torsion contribution to roll moment (low-speed ramp steer)

Tanker	Direction	Axle 5 roll moment at 1 deg suspension roll (experimental)	Axle 5 roll moment at 1 deg suspension roll (comparison to lab evaluated)
		N·m	N·m
TC1	counter-clockwise	24237	
	clockwise	-24903	
TC2	counter-clockwise	20576	
	clockwise	-17831	
Percent difference TC1 and TC2 counter-clockwise		17.8%	17.5%
Percent difference TC1 and TC2 clockwise		39.7%	28.8%
Average difference between TC1 and TC2		28.7%	23.1%

Table 7-2. Axle torsion contribution to roll moment (high-speed ramp steer)

Tanker	Direction	Axle 5 roll moment at 1 deg suspension roll (experimental)	Axle 5 roll moment at 1 deg suspension roll (lab testing)
		N·m	N·m
TC1	counter-clockwise	24123	
TC2	counter-clockwise	19687	
Percent difference between TC1 and TC2		22.5%	17.5%
Percent difference between lab testing and field testing (TC1)		23.71%	
Percent difference between lab testing and field testing (TC2)		18.60%	

The difference between the roll stiffnesses of TC1 and TC2 measured in the low-speed ramp steer was approximately 28.7%. Differences existed between clockwise and counter-clockwise directions, and some difference existed between the laboratory-evaluated roll stiffness and the field-evaluated roll stiffness. The differences between the field and laboratory testing can be attributed to the fact that the field testing did not include the flexural contribution of the axle from the beam center out to the wheel center. Field results from the gages were thus higher than experimentally determined in the laboratory. Additionally, some non-linear string potentiometer movement existed due to the longitudinal changes in the axle position, which could not be accounted for in the calculations. Overall, the differences between the TC1 and TC2 configurations were verified and were within 5.6%.

Before the experiments began, the suspensions were simulated in a ramp steer in an Adams model of a vehicle different from that used in the experiments. The TC1 suspension was predicted to have a roll stiffness 22 to 23 % higher than that of the T suspension. The K&C measurements (Section 7.2.1) showed Tanker TC1 having a roll stiffness 8 to 10 % higher than that of Tanker T. These three measurements of three related but distinct properties were not resolved.

Figure 7-26 shows the axle contribution to the roll moment as a function of the suspension roll angle during the lane change maneuver. As noted above for the ramp steer maneuver, and as can be seen in Figure 7-26 for the lane change, the contribution to the roll moment provided by the axles is linear only until approximately 1 deg of roll, after which the roll stiffness begins to increase. The stated roll angle is the roll between the tank trailer chassis and the axles, so therefore, tire effects on the roll stiffness are not included.

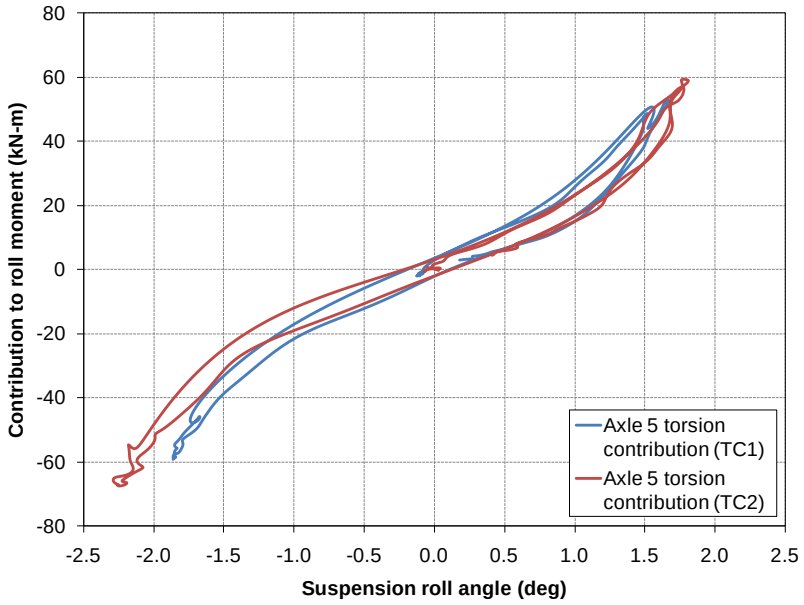

Figure 7-26. Graph. Axle contribution to roll moment vs. suspension roll angle in the lane change maneuver

Figure 7-27 shows the axle contribution to the anti-roll moment versus time during the lane change maneuver. The "dips" observed in Figure 7-27 at around 4.8 s for TC1 and TC2, and 5.5 s for TC1 are due to the lifted wheel returning to the ground.

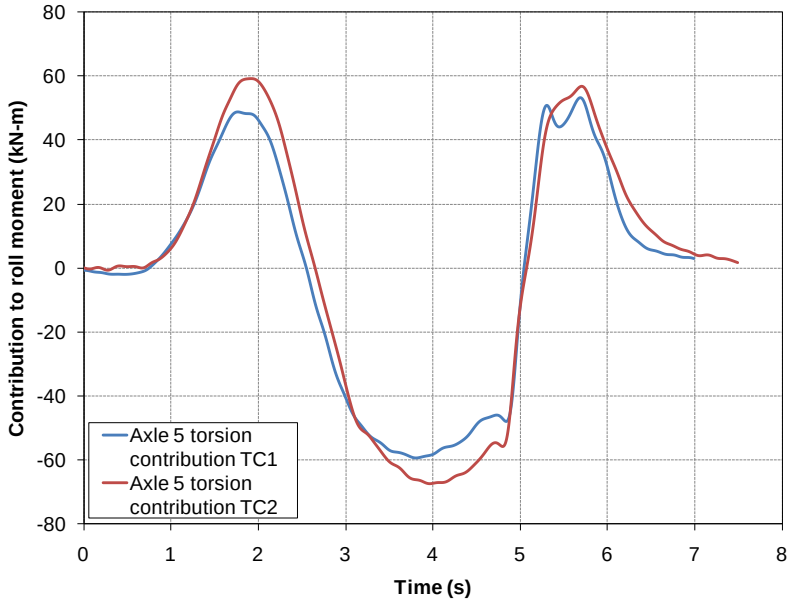

Figure 7-27. Graph. Axle contribution to roll moment vs. time in the lane change maneuver

Summary of axle gaging

Instrumented axles helped assess the contribution of the suspensions to the roll resistance. The outer end gages provided accurate assessment of wheel lift, and the torsional gages were excellent predictors of the axle torque contributing to roll stiffness. In future tests, string potentiometers should be installed on both trailer axles. Wheel lift occurs at different roll angles for axles 4 and 5, so the data from the one set of string potentiometers did not allow accurate assessment of the contribution of each separate axle at each time. Attempts were made to use the body roll angle measured by the RT unit and to subtract the axle roll, but the axle roll sensors at wheel lift could go out of range and produce discontinuous results. The results were quite predictable, and this predictability might translate to useable information for active stability systems or for roll margin warnings systems.

7.2.4 Auxiliary Roll Damping

The simulation of the lane change maneuver did not match the experimental results of Phase B in that the roll oscillation of the trailer following the maneuver was much more damped in the experiment than in the simulation. Providing substantial auxiliary roll damping (i.e., damping not from the shock absorbers) in the model reduced the post-maneuver oscillation to match the experiment. This led to the special experiment, described here, to measure the auxiliary roll damping in the trailer. The experiment showed that only about 10 percent of the trailer's total roll damping comes from the shock absorber. The model's prediction was confirmed.

The maneuver was a modified step steer that would lift the trailer tires on one side. The maneuver was exited by rapidly straightening the road wheels, bringing the tires back into contact with the road surface. This "drop test" produced roll oscillations that would subsequently be damped by the suspension system, dampers, and any damping inherent in the system. The drop testing was performed with the TC1 suspension with conventional shock absorbers; with the TC2 suspension with conventional shock absorbers; and with the TC2 suspension with the shock absorbers removed. A typical plot of roll angle vs. time for the trailer in the maneuver is shown in Figure 7-28. An approximate 10 deg of roll angle, relative to the ground, was held for roughly 0.5 to 1.5 s. The wheels lifted during this time, with the outriggers maintaining the tank trailer roll angle. Subsequently, the steering wheels of the tractor were straightened, rapidly bringing the trailer wheels in contact with the road surface. The period of interest is from the time of tire contact to the end of any oscillation.

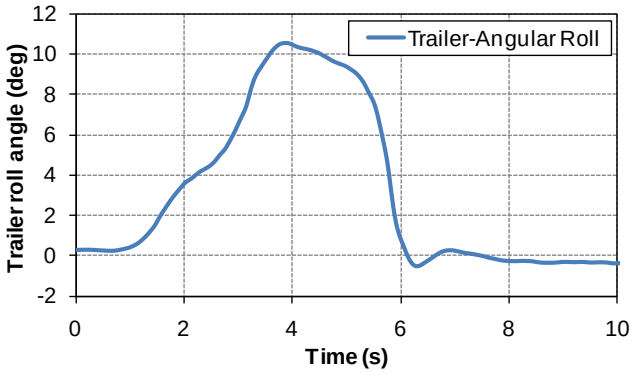

Figure 7-28. Graph. Typical roll in the modified step steer maneuver for evaluating roll damping

The roll angle evaluation conducted during the Phase C testing included string potentiometers connected between the trailer chassis and axle 5. The string potentiometer data, taking into consideration their span, was used to calculate a roll angle between the axles and the trailer chassis. The string potentiometers were used to assess the oscillatory behavior of the trailer chassis. Axle height sensors on axle 5 allowed for measuring the axle roll angle relative to the road surface, and the trailer body roll was measured with the RT unit.

During the time that one side's tires are off the pavement, air moves from the air bag on the low side to the air bag on the high side. When the tires return to the pavement, there is a difference in pressure generated between the two sides as the bag with the higher volume is rapidly compressed, but the line between the left and right bags prevents air from flowing quickly to equalize the pressure differential. This side-to-side pressure differential opposes the roll motion of the trailer and can be termed an "air bag damping moment." The instantaneous air bag damping moment was calculated from the air bag pressures and their separation.

Figure 7-29 shows a plot of the air bag damping moment and the roll rate vs. time. The plots of Figure 7-28 and Figure 7-29 demonstrate how there is a slight overshoot when contact is re-established that is quickly damped. The peak differential pressures in the bags, and consequently the peak damping moment is achieved shortly after the trailer tires first come back in contact with the ground at just beyond 6 s.

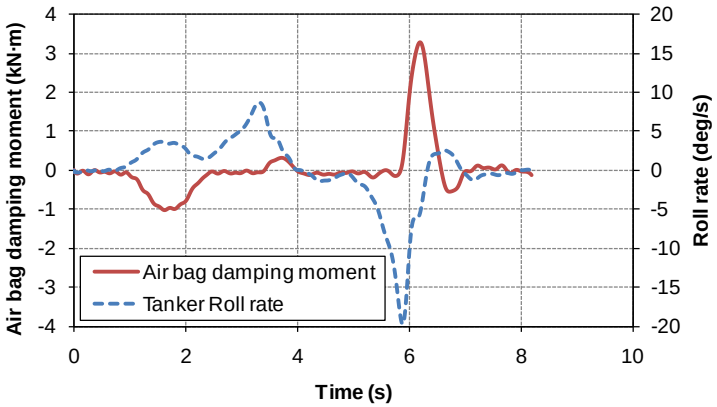

Figure 7-29. Graph. Air bag damping moment in Tanker TC1

The TC2 axle results, shown in Figure 7-30, can be compared with the results of the TC1 axle of Figure 7-29 to identify that the TC2 axle generated lower instantaneous air bag damping moments than the TC1 axle. The TC1 axle, which had a 16% greater beam center spacing, produced approximately 25% greater air bag damping in the drop test than the TC2 axle. The air bag contribution to roll moment was significantly higher when the roll rate at the time of tire contact was higher, for the TC1 configuration. Although the roll rates for the two cases appear to be similar, there are slight differences between them, which may be seen in Table 7-3 below. This phenomenon is consistent with the air bag contribution being related to the flow between the air bags on opposite sides of the trailer.

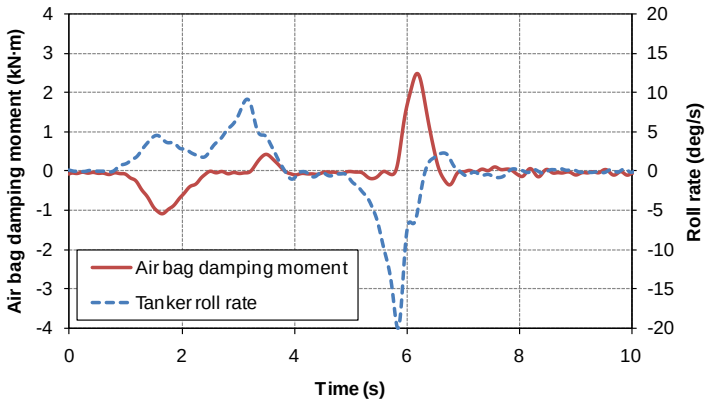

Figure 7-30. Graph. Air bag damping moment in Tanker TC2

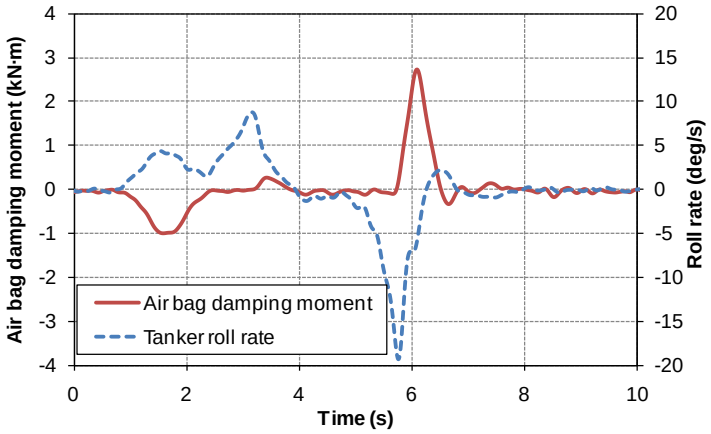

Figure 7-31. Graph. Air bag damping moment in Tanker TC2 with the shock absorbers removed

When comparing the air bag contribution to roll damping, with (Figure 7-30) and without (Figure 7-31) shock absorbers (dampers) attached, the air bag contribution and the roll rate are largely unaffected by the removal of the dampers. The direct comparison in Figure 7-32 shows the roll angle vs. time for the dampers-installed and dampers-removed cases. The roll angles were measured with the string potentiometers; they are axle-to-body roll angles. This indicates that for this particular suspension design, the roll damping from the shock absorbers was minimal compared to the auxiliary damping provided by the suspension components; any suspension air related plumbing; the fifth wheel coupling to the tractor; and the structure.

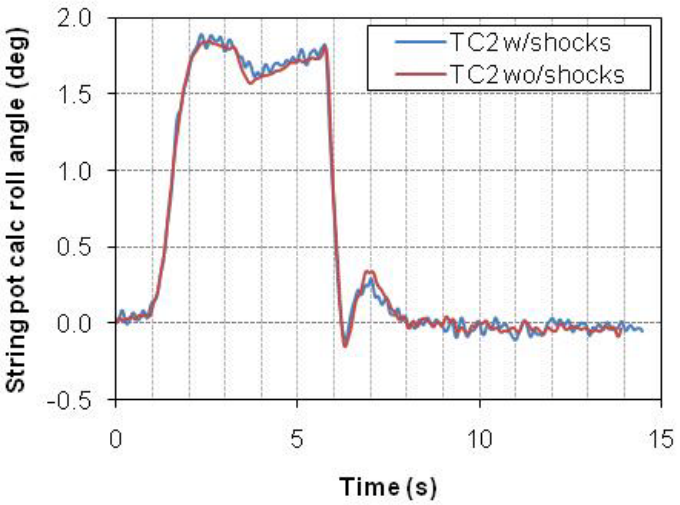

Figure 7-32. Graph. Roll angle in the modified step steer maneuver for Tanker TC2 with and without shock absorbers

Table 7-3 shows the data collected during the damping tests and clearly indicates the difference between suspension configurations TC1 and TC2. The roll rate is the roll rate at the time the

lifted tires re-established contact with the ground resulting in a pressure difference in the air bags. The product of the pressure difference and the air bag cross sectional area, with consideration for air bag spacing and motion ratio (i.e., the ratio of the air bag compression to the axle displacement) established the air bag roll moment. The air bag damping coefficient is defined as the ratio of the maximum damping moment to the roll rate at the time of peak pressure difference between the air bags.

The average equivalent air bag damping coefficient measured with the TC1 suspension installed was 603 N•m•s/deg, and the average damping coefficient measured with TC2 installed was 450 N•m•s/deg. The change in the beam and air bag spacing clearly makes a difference in the damping. (The 95-percent confidence interval for the difference between the means is 111 to 194 N•m•s/deg, well above zero.) When the shock absorbers were removed from the TC2 suspension, the average damping coefficient dropped by only 5 N•m•s/deg. The 95-percent confidence interval for the difference is -18.65 to 28.65 N•m•s/deg. The range includes zero, and the upper end of the range is less than ten percent of the mean, so the shock absorbers contribute, at most, ten percent of the total roll damping of the TC2 suspension.

Table 7-3. Air bag effects from the modified step steer

	Auxiliary damping test Calculated air bag effects from differential pressures				
	Tanker -run number	**Time**	**Roll velocity**	**Air bag damping moment**	**Air bag damping coefficient**
		s	deg/s	N•m	N•m-s/deg
TC1	TC1-2	6.00	-6.34	3379	533
	TC1-3	6.10	-5.70	3227	566
	TC1-4	6.18	-6.27	3274	587
	TC1-5	6.15	-6.32	3842	608
	TC1-6	6.10	-6.22	3784	632
	TC1-7	6.23	-6.10	3761	656
	TC1-8	6.20	-6.05	3806	639
	Average TC1		-6.14	3582	603
	Standard deviation		0.2	275	44
TC2	TC2-1	6.19	-5.46	2487	455
	TC2-2	6.12	-5.86	2598	443
	TC2-3	6.23	-6.52	3026	464
	TC2-4	6.13	-5.45	2435	446
	TC2-5	6.12	-5.61	2490	444
	Average TC2		-5.78	2607	450
	Standard deviation		0.4	241.5	9.0
TC2 without shock absorbers	TC2-wo-1	6.10	-5.75	2737	476
	TC2-wo-2	6.10	-5.52	2474	448
	TC2-wo-3	6.10	-5.76	2478	437
	TC2-wo-4	6.13	-5.99	2562	428
	TC2-wo-5	6.15	-5.72	2508	438
	Average TC2 (without)		-5.75	2552	445
	Standard deviation		0.2	109.3	18.5

The logarithmic decrement (δ) is a technique used to determine the percentage of critical damping or damping ratio (ξ) for a system. If two successive peaks in roll amplitude are known, and a logarithmic decaying behavior is assumed, the damping ratio can be determined as shown in Equations 28 and 29. Although it is difficult to obtain precise peaks in the data, this method was applied to the measured values from the string potentiometers measuring the frame-to-axle spacing and the roll of the body relative to the axles.

$$\delta = \ln \frac{x_1}{x_2} = \ln \frac{e^{-\xi \omega_n t_1} \mathrm{Sin}\left(\sqrt{1-\xi^2}\ \omega_n t_1 + \phi\right)}{e^{-\xi \omega_n (t_1+\tau_d)} \mathrm{Sin}\left(\sqrt{1-\xi^2}\ \omega_n (t_1+\tau_d) + \phi\right)}$$

Equation 28

$$\delta = \frac{2\pi\xi}{\sqrt{1-\xi^2}}$$

Equation 29

When the identified successive peaks were analyzed the roll damping ratio was determined to be between 23% and 25%. These values represent a best effort calculation based on the collected data. The values obtained from the analysis represent an under-damped system, which is reasonable, because damping ratios used in automotive design commonly fall in the range of 25% to 30%. No discernable difference was found on this vehicle between the tests with the shock absorbers installed and the shock absorbers not installed, implying that the majority of the damping is system damping.

Summary of the auxiliary roll damping tests

With the shock absorbers not installed, post exit pitch/bounce oscillations were present which were not present when the shock absorbers were installed. Shock absorbers did therefore control oscillations in bounce and pitch.

In the modified step steer maneuver, roll oscillation behavior was the same in the damper and no-damper test configurations using the TC2 suspension. This indicated that in roll, the system damping far overshadowed the roll damping contribution of the axle dampers. The significance of this auxiliary roll damping was observed to be beam spacing dependent and is anticipated to be suspension design dependent with some suspension designs offering more auxiliary damping than other designs. A clear difference exists between the air bag damping provided between the TC1 and TC2 suspensions, with the TC1 configuration offering increased air bag roll damping over Tanker TC2.

7.3 Common Approach to Analyzing Maneuvers

As noted in the Phase C Test Plan (discussed in Chapter 6 and presented in Appendix A), the roll stability of the vehicle was tested in three maneuvers—a ramp steer, a step steer, and an open-loop double lane change. Three of the institutional HTRC team members analyzed the resulting data in detail, each analyzing two maneuvers. Thus, data from each of the three maneuvers was

analyzed by two groups. The groups followed a common basic approach but worked independently to achieve different perspectives on the results.

Each of the three groups used the strain gages mounted on the axle ends (described below) to identify when the tires lifted from the pavement. Each decided on its own methods of filtering and reducing the data. A single statistician supported all groups and analyzed the tabulated outputs. A statistical test was used to identify those differences that could be confidently attributed to the experiment. The statistical hypothesis tests were akin to a simple t-test, but they were actually a Smith/Welch/Satterthwaite test (Smith 1936, Davenport and Webster 1975, Satterthwaite 1946, and Welch 1938), because the standard deviations of the two treatments were usually different. Finally, all analysts met several weeks after the experiments to discuss their respective results and agree on a single set of conclusions. Analyses of the three maneuvers are in Sections 7.4 through 7.6. The single set of data analysis conclusions is in Section 7.7.

Axle Mounted Strain Gages

To objectively assess wheel lift of both the tractor and the trailer, axle tube mounted linear strain gages were located outboard of the Z-springs on the tractor and outboard of the beam centers on the trailer. These are the same wheel end gage configurations as used in Phases A and B of testing. Since the gages were mounted outboard of the load carrying suspension member, they could be used to accurately assess the point at which wheel lift occurred. Throughout the analysis, the measured quantity is referred to as “wheel load.” This is a misnomer because the combinations of vertical load, cornering forces and the resulting cornering bending moments did not allow measurement of the actual vertical wheel loads. However, it is sufficient for the purposes of the analyses because the primary issue of concern is determining whether the wheels have lifted from the ground. The presence of “wheel load” indicates that the wheels are in contact with the pavement, whereas a near-zero wheel load indicates that the wheel probably lifted. Each section of the respective analyses details how these measurements were used to determine if and when the wheels lifted.

7.4 Ramp Steer Maneuver

Ramp steer testing consisted of both low speed and high-speed tests. The low-speed ramp steer, conducted at 32 km/h entrance speed to the maneuver, included both clockwise and counter-clockwise maneuvers. The high-speed ramp steer maneuver was performed with a maneuver entrance speed of 48 km/h. The low-speed ramp steer was conducted to establish understeer / oversteer behavior. The high-speed ramp steer tests were used to determine the lift threshold under near steady-state test conditions. The high-speed ramp steer tests were conducted by establishing an entrance velocity and then increasing the steering wheel input by 10 deg/s to the point at which wheel lift occurred.

To determine the wheel lift of the tractor and trailer, the vertical wheel loads were monitored through the measurement of axle bending strain at the wheel ends. The strain gages were zeroed by lifting the vehicle off the ground in a garage. After the completion of a maneuver, the

measured strains at the wheel ends were then used to identify if wheel lift had occurred and, if so, when the lift occurred. Because there is no vertical load on the wheel when it has lifted off the ground, the measured wheel load will “flat line” when the wheel lifts, as illustrated in the wheel load measurement for axles 4 and 5 in Figure 7-33. Axles 2 and 3 would have illustrated a similar flat line after lifting had the data recording not been terminated at 23 s.

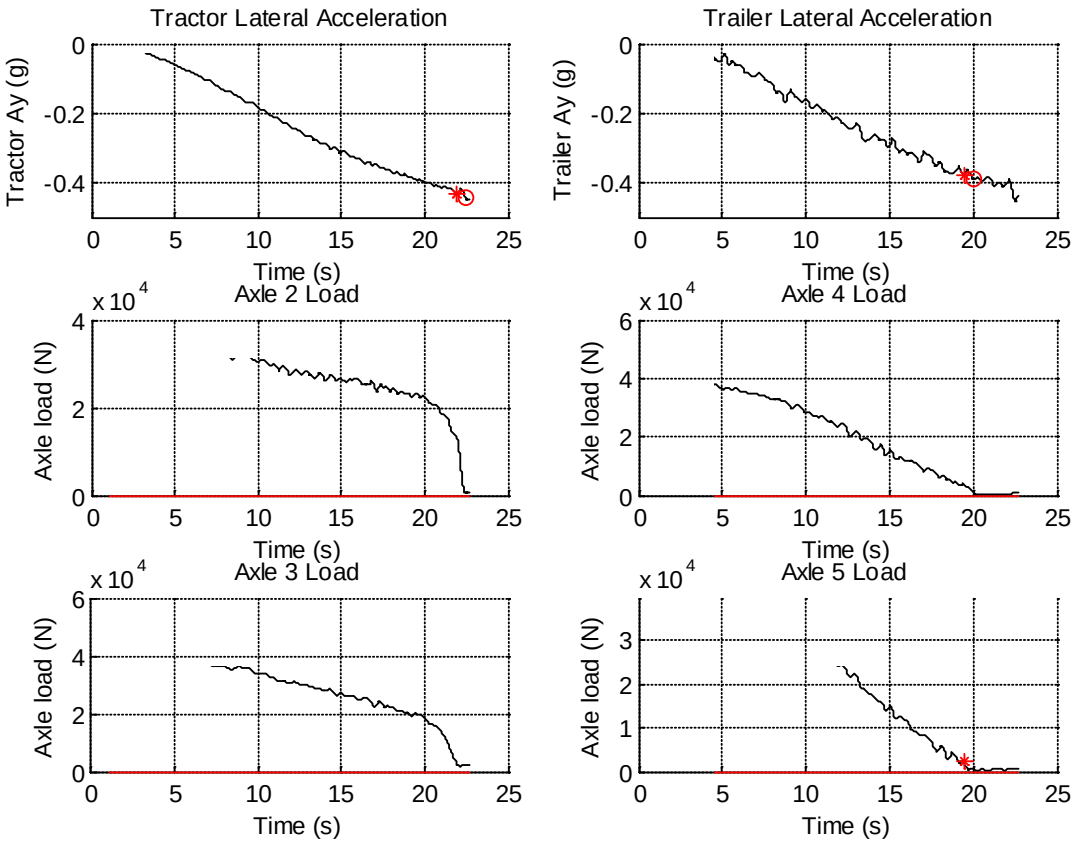

Figure 7-33. Graph. Time history of the lateral acceleration and measured wheel loads during a high-speed ramp steer maneuver that lifted both drive axles and both tank trailer axles

First Analysis of Maneuvers with the ESC System Disabled

For each test, wheel lift was identified by observing when the wheel load flattened out. In Figure 7-34, axles 4 and 5 indicate wheel lift occurred (flat sections in the wheel load curve) while axles 2 and 3 do not so indicate.

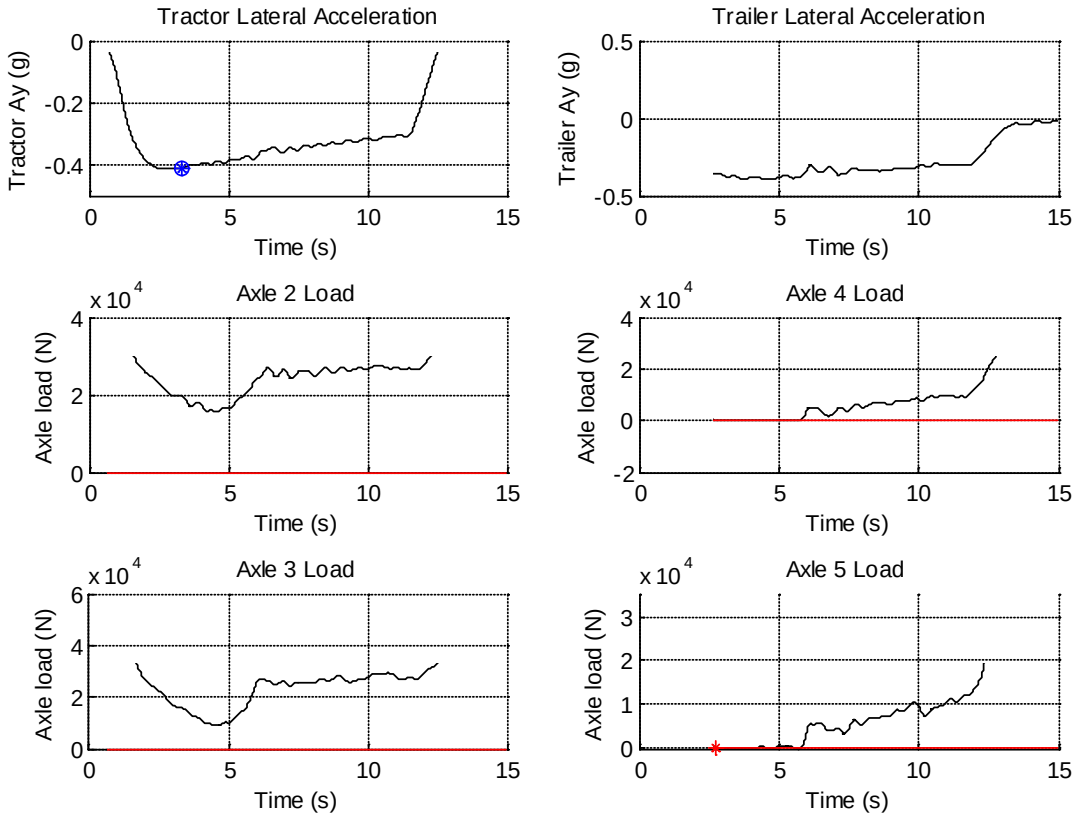

Figure 7-34. Graph. Time history of a ramp steer maneuver in which only the trailer axles lifted

When a wheel lift was observed, an algorithm was used to determine the lift threshold (i.e., the associated lateral acceleration) of the vehicle. The lateral acceleration for a wheel lift event was defined to be the peak lateral acceleration seen by the vehicle unit up to the moment of lift. For events without lift, the lateral acceleration reported for the maneuver was the peak lateral acceleration observed in the maneuver.

The ramp steer maneuver was repeated several times with each suspension. Due to the natural variation in the experiment, the lateral acceleration (a_y) measured for the wheel lift was different in the repeated runs. The average (the mean) of the lateral accelerations was calculated for the repeated runs. The run-to-run variation in the values was used to calculate the 95-percent confidence interval, which is a measure of the spread of the values. If the experiment were to be repeated 100 times, then 95 of the values would fall within the confidence interval. The means are tabulated in Table 7-4 and indicated by the locations of the circles in Figure 7-35. The figure indicates confidence intervals by the height of the bars. As noted in the bottom of the figure, the points are grouped first by axle (2 and 3 are the front and rear drive axles on the tractor, and 4 and 5 are the front and rear trailer axles), and then by experimental condition (T is the Phase B Tanker T data with the narrower track, and TC1 and TC2 are the newly taken data for the suspensions with the wider track and the narrower and wider beam spacing). The a_y values on the vertical axis are negative because the ramp was a left turn. A more negative lateral acceleration

at lift is a preferable condition—the vehicle can turn a corner harder without lifting a wheel off the ground. Looking first at Axle 5, the rearmost axle in the vehicle, the point for Tanker T is high and less negative, so the narrower axle permits the wheel to lift at a lower lateral acceleration. The two circles for TC1 and TC2 are at about the same height as each other but well below the circle for Tanker T.

Table 7-4. Means of the lateral acceleration (g) leading to wheel lift in the ramp steer maneuver

	Tanker		
	T	TC1	TC2
Axle 2	-0.430	-0.437	-0.441
Axle 3	-0.417	-0.435	-0.436
Axle 4	-0.370	-0.390	-0.394
Axle 5	-0.364	-0.389	-0.388

The significance of the differences was assessed with a Smith/Welch/Satterthwaite test, which is a special form of the more familiar t-test that does not assume equal variances in the groups being compared. The results of the statistical tests are presented in Table 7-5. The “p-value” is the probability of observing differences this large or larger if there were no true underlying difference. Small p-values are evidence of a difference. Generally statisticians declare a result to be significant if the p-value is below 0.05; that is, there is more than a 95 percent probability that the experiment is causing the means to be different. (Caution is necessary because there are many tests in the table and in the report; one would expect about 1 out of 20 to have a p-value below 0.05 purely by chance.) The results presented in Table 7-5 are the same as those in Figure 7-35; they are merely in a different format. Again, considering Axle 5 as the example, configurations TC1 and TC2 differed significantly in lift threshold from Tanker T, but not significantly from each other.

Table 7-5. Significance of differences in the lateral acceleration leading to wheel lift in the ramp steer maneuver

Context	Comparison	p-value
	TC1 vs. TC2	0.8185
Axle 5	T vs. TC2	0.0002
	T vs. TC1	<.0001
	TC1 vs. TC2	0.2630
Axle 4	T vs. TC2	<.0001
	T vs. TC1	<.0001
	TC1 vs. TC2	0.8809
Axle 3	T vs. TC2	<.0001
	T vs. TC1	<.0001
	TC1 vs. TC2	0.0968
Axle 2	T vs. TC2	<.0001
	T vs. TC1	0.0003
	Axles 4 vs. 5	0.3020
TC2	Axles 2 vs. 3	0.0422
	Axles 3 vs. 5	<.0001
	Axles 4 vs. 5	0.7738
TC1	Axles 2 vs. 3	0.3483
	Axles 3 vs. 5	<.0001
	Axles 4 vs. 5	0.0051
T	Axles 2 vs. 3	0.2326
	Axles 3 vs. 5	<.0001

Summarizing, the analysis of the ramp steer lift thresholds indicated that the two wider axles (TC1 and TC2) improved the trailer's rollover performance. However, the increased frame attachment spacing of axle TC1 over TC2 was not a statistically significant improvement. The improved trailer rollover performance for axles TC1 and TC2 also resulted in improved rollover performance of the tractor because the wider axles were more capable of countering the trailer's overturning moments, thereby reducing the overturning moment imparted to the tractor.

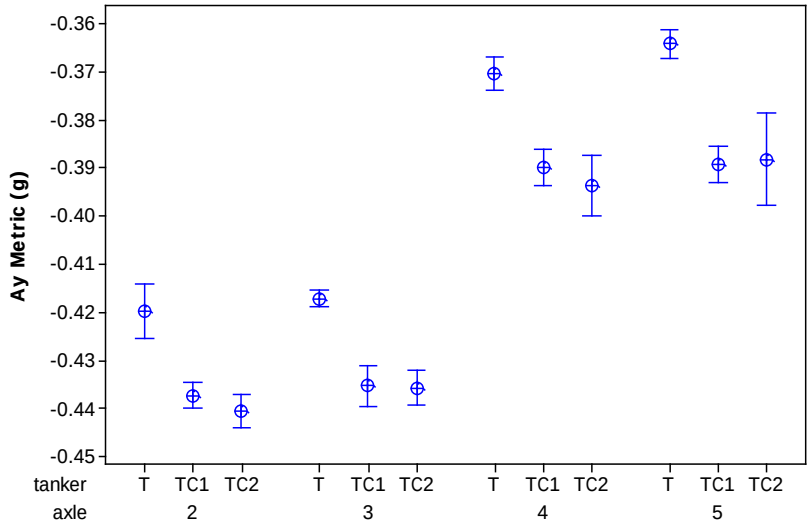

Figure 7-35. Graph. Means of the lateral acceleration leading to wheel lift in the ramp steer maneuver (with 95% confidence intervals of the means)

Second Ramp Steer Analysis

Table 7-6 presents a separate analysis of conditions at wheel lift for both the TC1 and TC2 suspensions, including the time at which lift occurred; the lateral acceleration of the tractor and trailer at the point of wheel lift for each axle; and the roll angle, roll velocity, yaw angle, yaw velocity, yaw acceleration and articulation angle. The data presented is the average for the runs for that particular maneuver along with their standard deviations. In the high-speed ramp steer maneuver, with the ESC system disabled, both trailer axles and tractor axles lifted. In the sequence, axle 5 lifted first and axle 2 (first drive axle) lifted last.

Table 7-6. Wheel lift summary (left wheels) for the high-speed ramp steer maneuver

Tanker		Axle	Entrance speed (km/h)	Values are recorded at the time of wheel lift														
				Time (s)	Lateral acceleration (g) at wheel lift		Roll angle (deg)		Roll velocity (deg/s)		Yaw angle (deg)		Yaw velocity (deg/s)		Yaw acceleration (deg/s^2)		Articulation angle (deg)
				Lift	Tractor	Trailer	Tractor	Trailer	Tractor	Trailer	Tractor	Trailer	Tractor	Trailer	Tractor	Trailer	
TC1	Average	2	48.69	21.21	-0.419	-0.397	4.623	9.249	2.264	3.616	-172.5	171.19	-19.474	-17.580	-5.614	-0.399	15.491
		3		20.93	-0.425	-0.392	4.025	7.724	1.876	5.767	-3.12	166.34	-18.360	-17.601	-1.273	-0.806	15.253
		4		18.91	-0.395	-0.380	2.767	3.377	0.282	0.516	145.53	132.60	-16.689	-16.175	-0.502	-0.844	14.099
		5		18.73	-0.394	-0.379	2.716	3.311	0.069	0.261	142.49	129.61	-16.543	-15.985	-0.617	-0.945	14.000
	Standard deviation	2	0.16	0.19	0.018	0.026	0.074	0.120	0.720	0.724	1.445	2.281	0.178	0.032	3.157	0.767	0.342
		3		0.21	0.006	0.007	0.114	0.105	0.239	0.440	158.082	2.375	0.081	0.105	0.997	0.623	0.393
		4		0.33	0.011	0.021	0.099	0.082	0.200	0.411	5.369	5.306	0.139	0.231	1.166	0.895	0.308
		5		0.30	0.006	0.021	0.064	0.029	0.337	0.243	4.488	4.454	0.152	0.195	1.158	0.931	0.322
TC2	Average	2	48.348	22.20	-0.438	-0.413	4.666	9.272	2.155	3.368	-167.4	184.3	-19.562	-17.629	-6.502	-0.545	16.095
		3		21.89	-0.427	-0.408	4.077	7.684	1.692	5.697	-171.7	171.7	-18.346	-17.545	-0.125	-0.492	15.889
		4		20.04	-0.397	-0.387	3.014	3.828	0.028	0.215	154.3	140.4	-16.894	-16.284	-1.047	-0.393	15.023
		5		19.67	-0.394	-0.372	2.946	3.698	0.076	0.315	148.3	134.6	-16.566	-16.000	-0.661	-1.072	14.673
	Standard deviation	2	0.277	0.31	0.005	0.020	0.084	0.073	0.231	0.318	2.689	11.414	0.130	0.116	1.511	0.696	0.086
		3		0.33	0.005	0.009	0.146	0.219	0.389	0.285	1.008	2.703	0.111	0.086	1.620	0.521	0.092
		4		0.27	0.007	0.008	0.052	0.090	0.247	0.227	1.899	1.861	0.177	0.042	1.002	0.575	0.193
		5		0.21	0.013	0.019	0.032	0.058	0.250	0.212	2.255	2.101	0.162	0.244	0.746	0.505	0.190

Figure 7-36 displays the body roll vs. time and Figure 7-37 displays roll angle vs. lateral acceleration for suspensions TC1 and TC2. Both plots indicate a lower roll angle prior to the point of wheel lift for suspension TC1. Although slight, this indicates the increased roll stiffness of the TC1 configuration. Lift is present when the body roll angle rapidly increases.

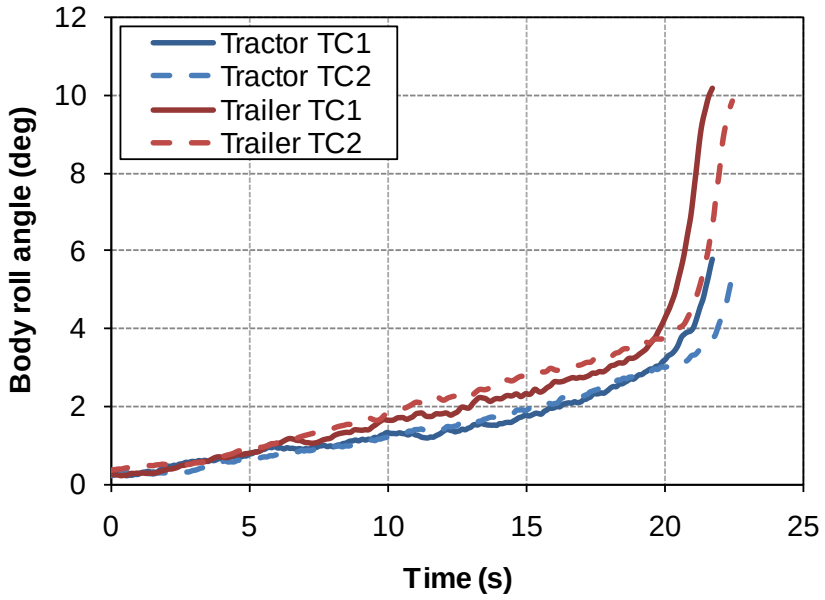

Figure 7-36. Graph. Roll angle vs. time for Tankers TC1 and . TC2

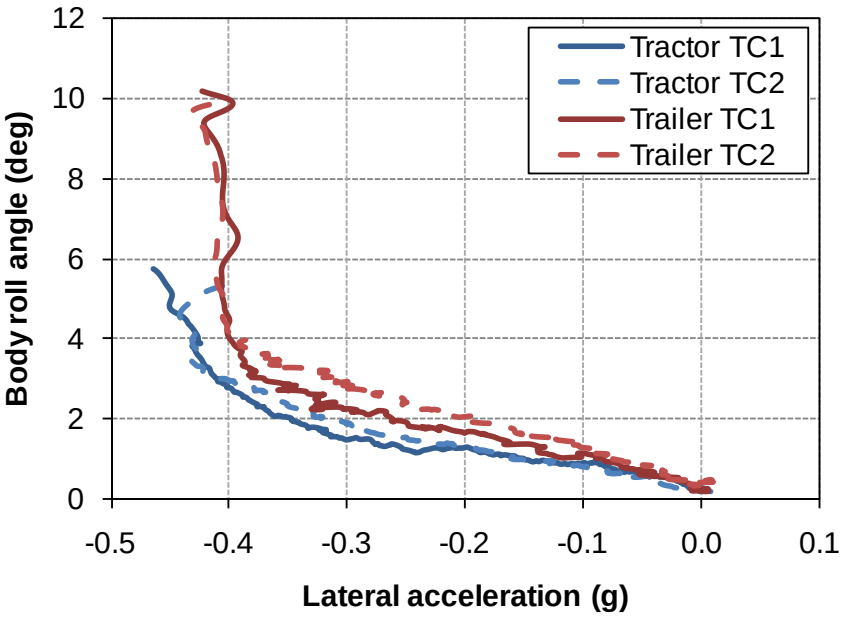

Figure 7-37. Graph. Roll angle vs. lateral acceleration for Tankers TC1 and . TC2

Figure 7-38 indicates that the TC1 suspension produces a slightly higher articulation angle than does the TC2 suspension. This could be due to the increased roll steer of the TC2 suspension, which results from the closer beam spacing and was measured in the K&C testing.

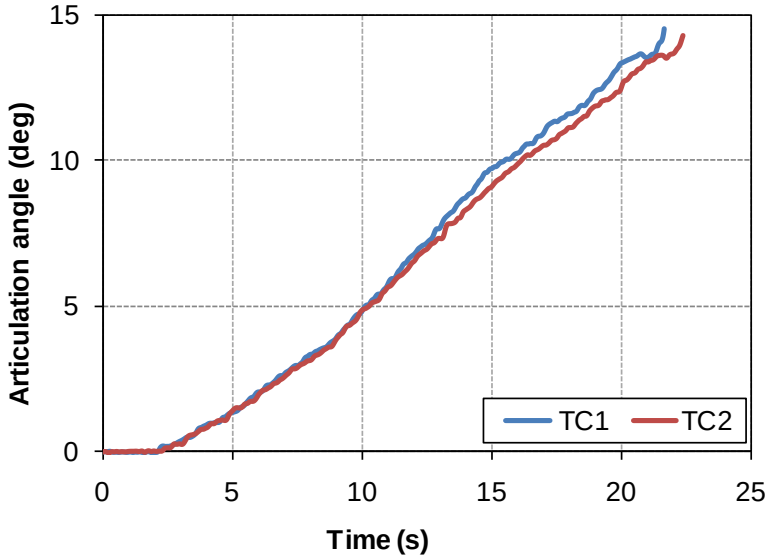

Figure 7-38. Graph. Articulation angle comparison for Tankers TC1 and TC2

Figure 7-39 and Figure 7-40 indicate that suspension has no discernable effect on either yaw angle or yaw velocity.

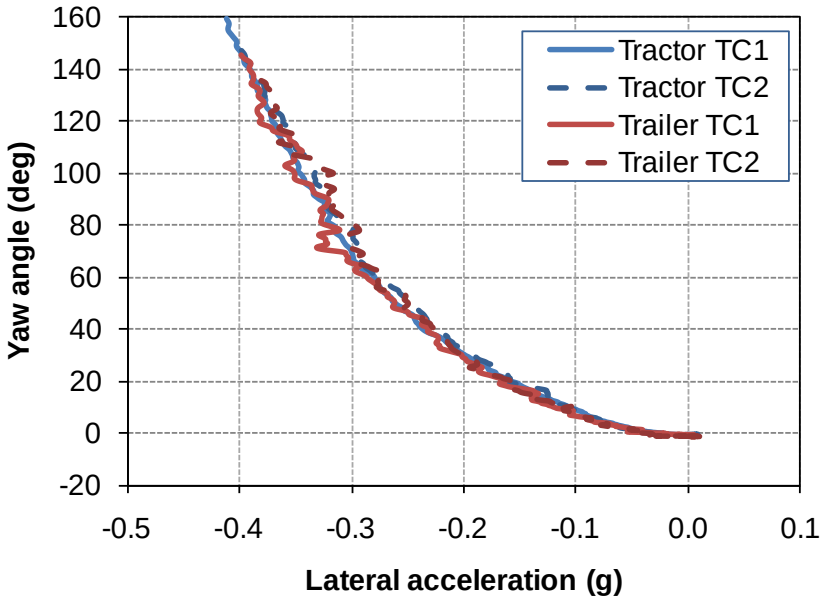

Figure 7-39. Graph. Yaw angle comparison for Tankers TC1 and TC2

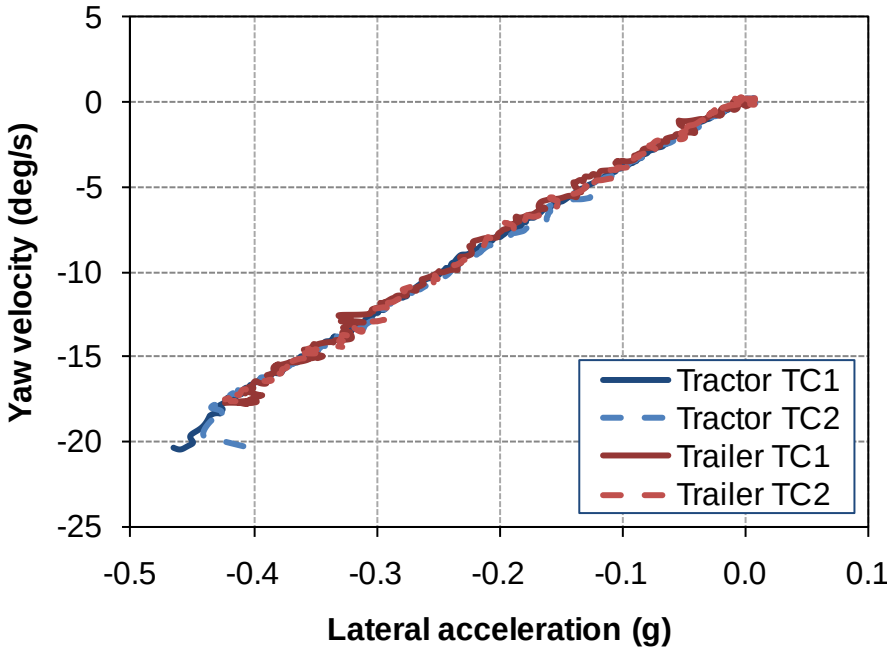

Figure 7-40. Graph. Yaw velocity comparison of for Tankers TC1 and TC2 in the ramp steer maneuver

Statistical analysis was performed on data that showed the potential for discerning differences between the suspensions. Data means, with confidence intervals, appear in Figure 7-41 through Figure 7-43. Figure 7-41 shows the time into the maneuver at which wheel lift occurred. The time for lift is delayed for all TC2 axle configuration maneuvers and the lateral acceleration at lift is also delayed yet the magnitude of the lateral acceleration at wheel lift is approximately the same. This would imply a delayed or slower lateral acceleration build for the TC2 axle configuration. The TC2 configuration also had a slower articulation angle build as shown in Figure 7-41. The significance of this time variable is uncertain until other attributes are examined.

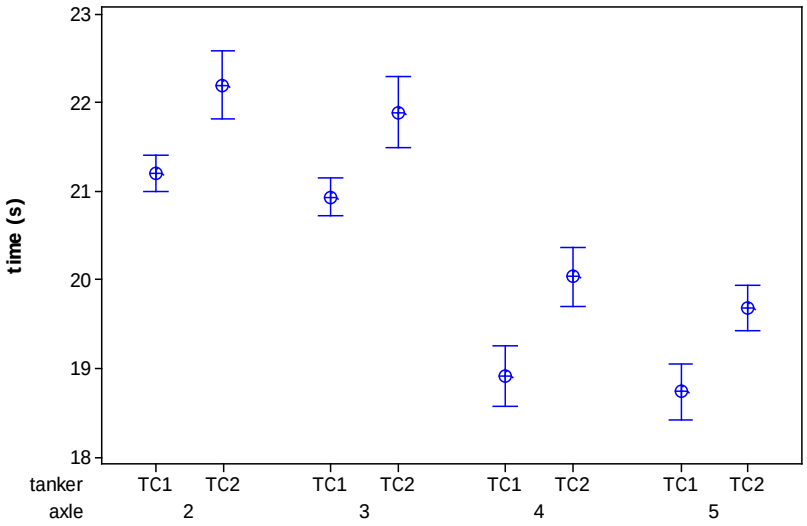

Figure 7-41. Graph. Wheel lift time from the start of the ramp steer maneuver

Figure 7-42 presents the lateral acceleration for the wheel lift of axle 2, the front drive axle on the tractor. Although there is an identifiable difference in the mean value the overlap of the confidence intervals would indicate that there may, or may not, be a statistically significant difference for axle 2 lift as related to trailer axle choice.

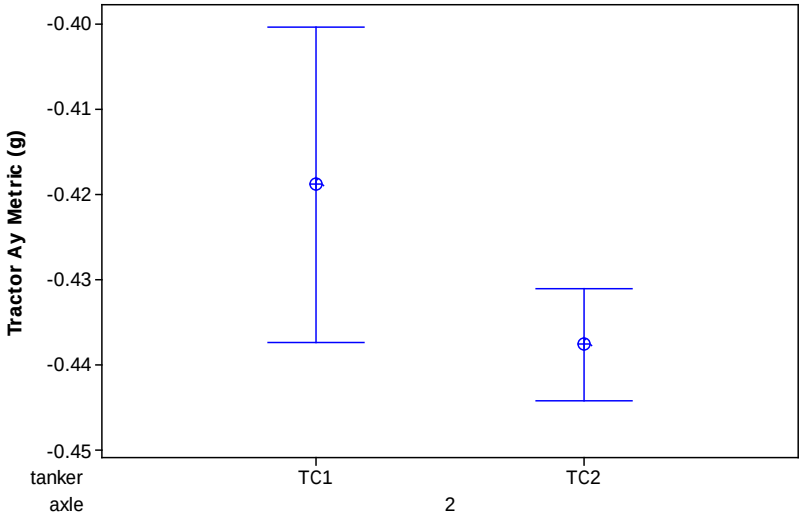

Figure 7-42. Graph. 95% confidence interval plot for the tractor lateral acceleration at wheel lift for axle 2

Figure 7-43 shows a statistically significant difference in the roll angle at wheel lift for axles 4 and 5 when comparing suspensions, with suspension TC2 having the larger roll angle at the point of axle 4 and axle 5 wheel lift. The lower roll stiffness of the TC2 suspension permits the trailer body to roll farther before the wheel lift.

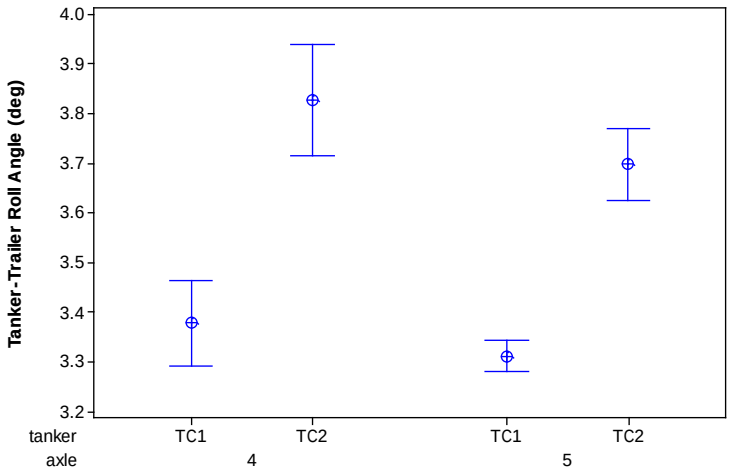

Figure 7-43. Graph. 95% confidence interval for the body roll angle of the trailer at wheel lift for axles 4 and 5

Figure 7-44 shows that the suspension does not significantly affect the yaw angle at wheel lift.

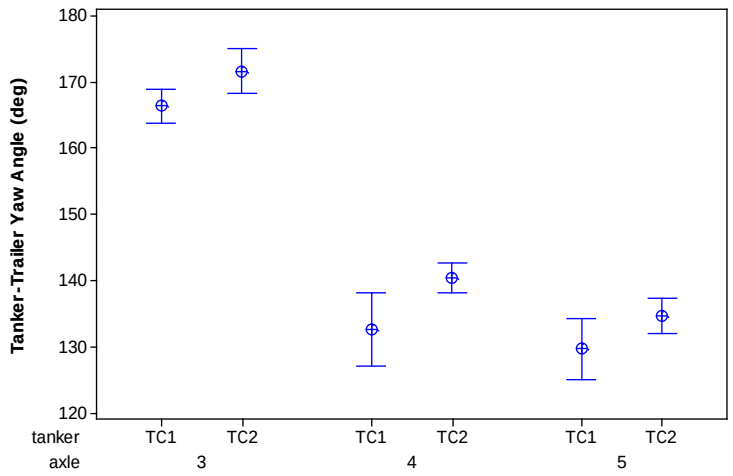

Figure 7-44. Graph. 95% confidence interval for the trailer yaw angle at wheel lift for axles 3, 4 and 5

Scatter in the roll velocity was so high that the data analysts considered it an unreliable measurement. The yaw velocity data was essentially the same for both suspensions and was therefore not statistically evaluated. The yaw acceleration at the time of wheel lift showed enough variation in the average values that it was also not considered to be an effective decision metric.

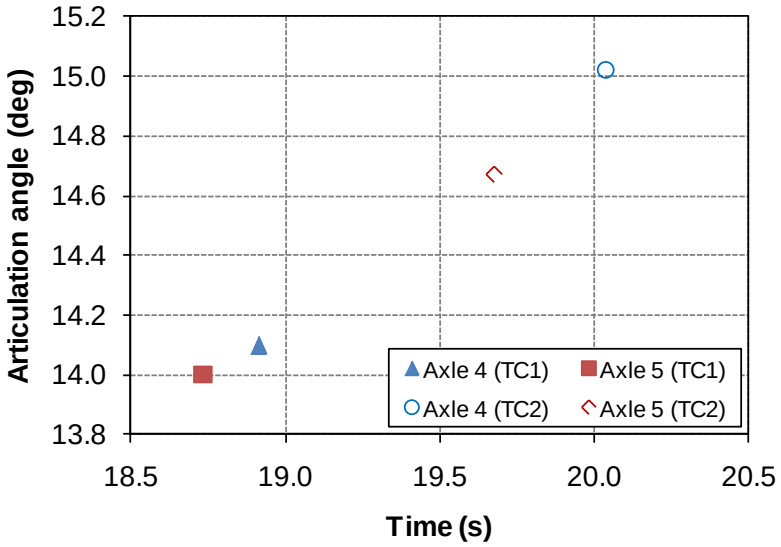

Figure 7-45. Graph. Articulation angle at wheel lift for Tankers TC1 and TC2

Conclusions regarding the high-speed ramp steer maneuver with the ESC system disabled
The TC1 configuration showed a significant difference in the roll angle at wheel lift for axles 4 and 5 when compared with TC2. The TC2 configuration had the larger roll angle at the point of axle 4 and axle 5 wheel lift. Tanker TC2 had a significantly lower roll stiffness which would typically allow a higher roll angle at wheel lift. TC1 would be the preferred suspension in a roll-controlled or roll-sensitive handling situation as a result of the reduced roll angles.

ESC system activation for the high-speed ramp steer maneuver
Separate high-speed ramp steer maneuvers were run with the tractor and trailer ESC systems both enabled. When the ramp steer maneuver path reaches a certain curvature, the ESC system is almost certain to activate.

Table 7-7 summarizes ESC system activation for the high-speed ramp steer. No wheel lift occurred on any axle during this testing. Values recorded were lateral acceleration, roll angle, roll velocity, yaw angle, yaw velocity, yaw acceleration and lateral or side slip velocity (all at the time the ESC system was activated).

Table 7-7. ESC system activation summary for the ramp steer maneuver

Tanker		Lift occurrence	Entrance speed (km/h)	Values are recorded at the time of ESC system activation															
				Time (s)	Lateral acceleration (g) at activation		Roll angle (deg)		Roll velocity (deg/s)		Yaw angle (deg)		Yaw velocity (deg/s)		Yaw acceleration (deg/s^2)		Articulation angle (deg.)	Lateral velocity (m/s)	
					Tractor	Trailer	Tractor	Trailer	Tractor	Trailer	Tractor	Trailer	Tractor	Trailer	Tractor	Trailer		Tractor	Trailer
TC1	Average	None	48.43	11.58	-0.229	-0.211	1.343	1.817	0.011	0.143	44.52	37.39	-9.727	-8.816	-1.073	-1.267	5.32	-0.042	-0.351
	Standard deviation	None	0.51	0.19	0.009	0.023	0.037	0.061	0.461	0.178	0.79	0.70	0.068	0.040	0.803	0.474	0.10	0.011	0.025
TC2	Average	None	48.21	12.26	-0.253	-0.237	1.594	2.066	0.419	0.357	51.85	43.50	-10.413	-9.488	-0.683	-0.961	6.86	0.056	-0.431
	Standard deviation	None	0.83	0.35	0.009	0.023	0.056	0.059	0.568	0.305	3.85	3.41	0.331	0.263	0.692	0.351	0.87	0.013	0.071

When pulling Tanker TC1, the tractor had a lower lateral acceleration and roll angle at the moment of ESC system activation than when pulling Tanker TC2 (Figure 7-46). Tanker TC1 also had a lower trailer roll angle when the ESC system activated (Figure 7-46). Most interesting is the fact that ESC system activation for the TC1 suspension occurred at a lower lateral acceleration, lower roll angle, lower yaw angle, lower yaw velocity, lower articulation angle and lower lateral velocity (Figure 7-46 through Figure 7-51). The only parameter that appears to have a higher value for the TC2 configuration at ESC system activation is the yaw acceleration of both the tractor and the trailer (Figure 7-51).

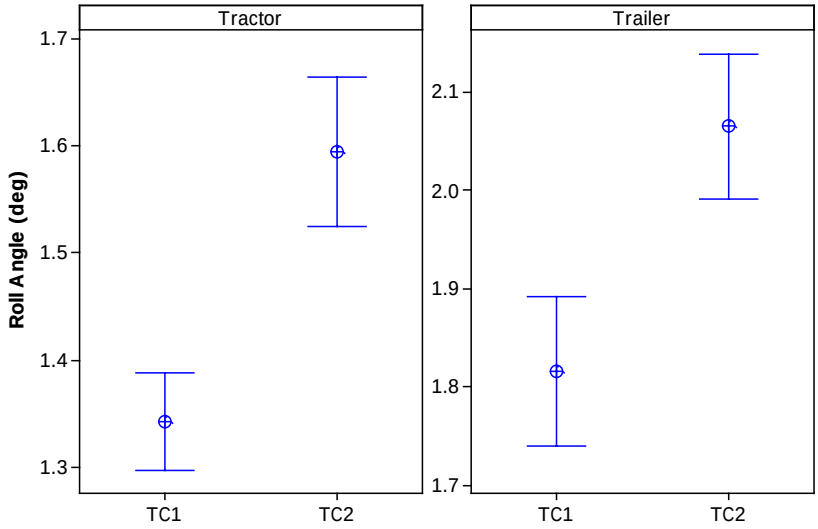

Figure 7-46. Graph. Roll angle at ESC system activation

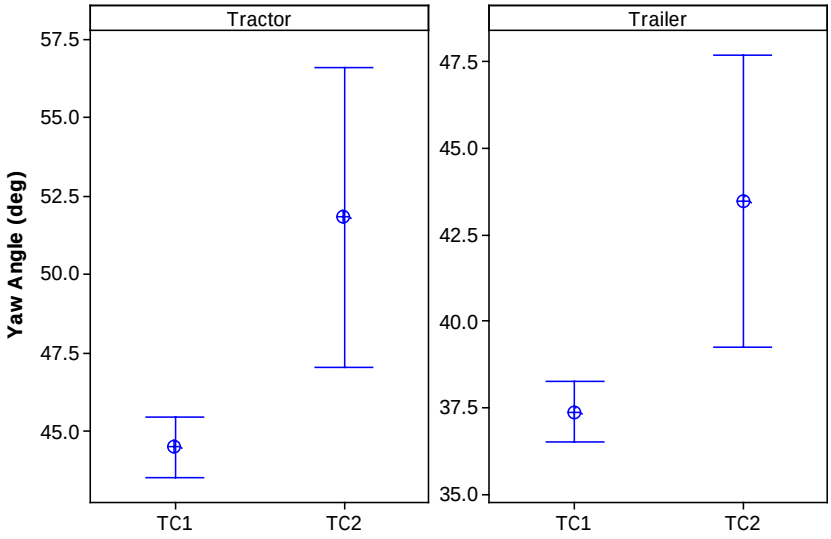

Figure 7-47. Graph. Yaw angle at ESC system activation

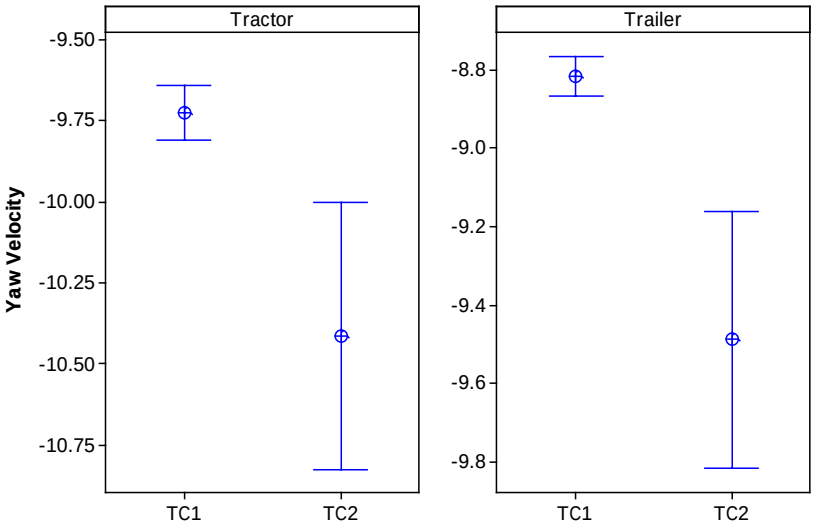

Figure 7-48. Graph. Yaw velocity at ESC system activation

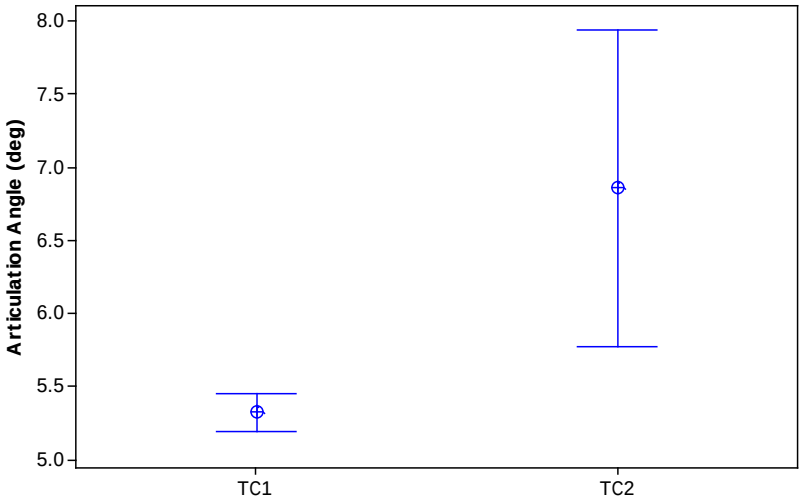

Figure 7-49. Graph. Articulation angle at ESC system activation

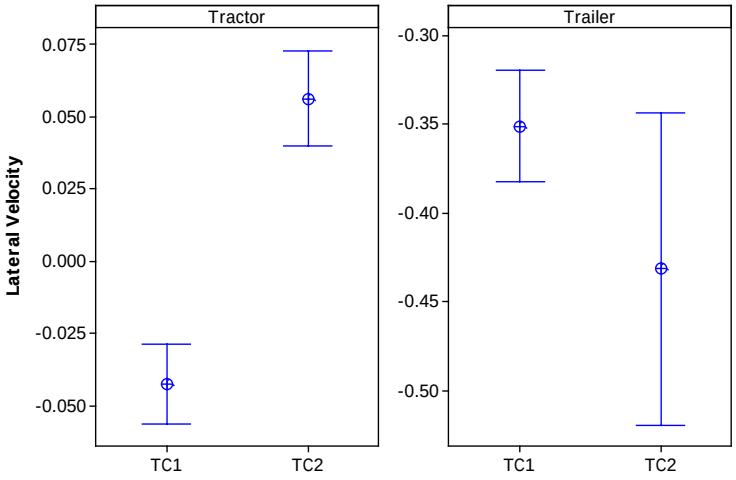

Figure 7-50. Graph. Lateral velocity at ESC system activation

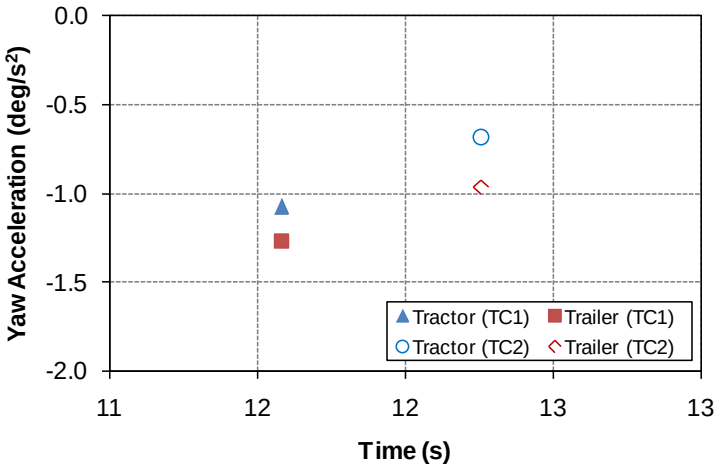

Figure 7-51. Graph. Yaw acceleration of the tractor and trailer with the TC1 and TC2 suspensions

Conclusions regarding suspension design and ESC system activation

Axle design had no significant effect on when the ESC system activated. The ESC system controlled wheel lift in the ramp steer maneuver, doing so with a substantial margin from wheel lift. The potential for increased lateral acceleration afforded by the wider axles did not translate into a higher ESC system activation threshold.

Fifth wheel separation

Fifth wheel separation was studied using a small infrared camera. In addition to the camera, markings were installed on the fifth wheel and a pointer was attached to the fifth wheel plate for reference angle identification. A simplified fifth wheel schematic is shown in Figure 7-52 to promote understanding of this behavior with the actual fifth wheel behavior during separation shown in Figure 7-53.

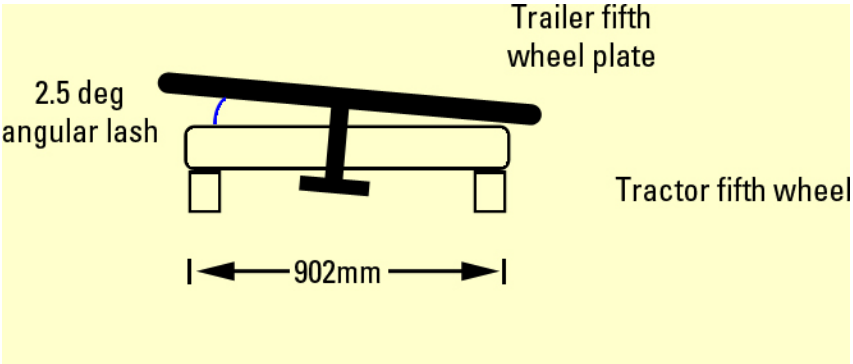

Figure 7-52. Sketch. Fifth wheel schematic

Figure 7-53. Photograph. Fifth wheel image during separation

Table 7-8 summarizes the fifth wheel separation data from the ramp steer maneuver. The fifth wheel maximum separation start is when the kingpin is extended through its lash in the fifth wheel and tops out. The lateral acceleration at separation for both the tractor and the tank trailer are included in this table, as are roll angle, roll velocity, yaw angle, yaw velocity, yaw acceleration and articulation angle, all at the moment the fifth wheel reaches maximum separation.

Table 7-8. Fifth wheel separation summary ramp steer maneuver

Tanker		Entrance speed	Time (s)		Lateral acceleration (g) at fifth wheel separation		Roll angle (deg)		Roll velocity (deg/s)		Yaw angle (deg)		Yaw velocity (deg/sec)		Yaw acceleration (deg/sec^2)		Articulation angle (deg)
			Fifth wheel separation start	Fifth wheel maximum separation start	Tractor	Trailer	Tractor	Trailer	Tractor	Trailer	Tractor	Trailer	Tractor	Trailer	Tractor	Trailer	
TC1	Average	48.69	19.91	21.13	-0.411	-0.402	3.220	4.246	0.549	1.584	162.04	148.39	-17.398	-16.709	-0.419	-0.085	15.11
	Standard deviation	0.141	0.39	0.57	0.009	0.005	0.149	0.312	0.219	0.589	5.67	5.48	0.209	0.249	0.741	0.245	0.25
TC2	Average	48.35	20.57	21.38	-0.418	-0.402	3.231	4.454	0.410	1.244	162.98	149.10	-17.282	-16.582	-1.227	-0.674	15.35
	Standard deviation	0.276	0.46	0.51	0.010	0.013	0.294	0.942	0.388	1.246	9.70	9.95	0.483	0.498	0.322	0.363	0.38

Confidence intervals were examined for some of the fifth wheel parameters at separation. Figure 7-54 shows the time of initial separation from the start of the maneuver. The overlapping intervals demonstrate that this specific parameter does not identify any differences between Tankers TC1 and TC2 in regard to fifth wheel separation. Similarly Figure 7-55, which plots yaw acceleration at lift, does not show any statistically significant relationship to the suspensions.

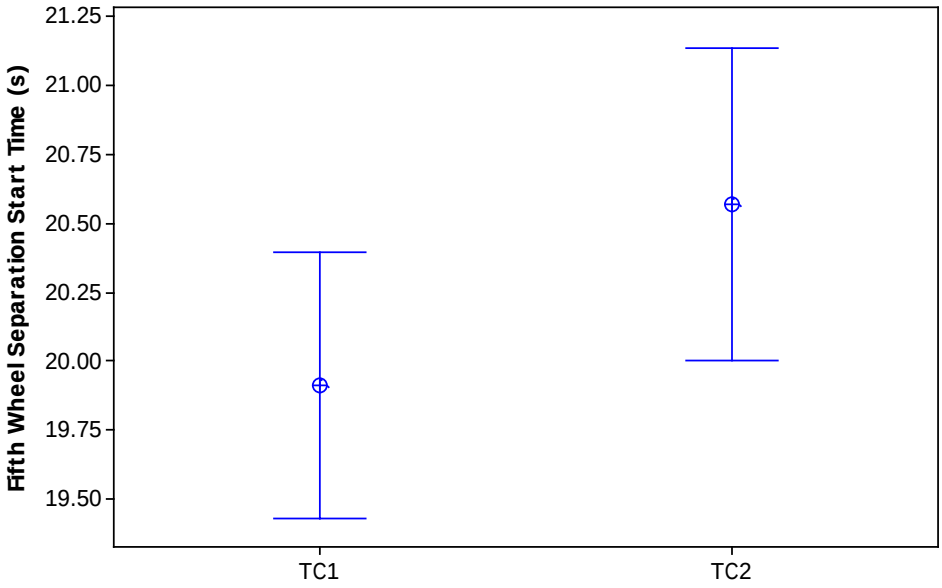

Figure 7-54. Graph. 95% confidence interval for the fifth wheel separation start time

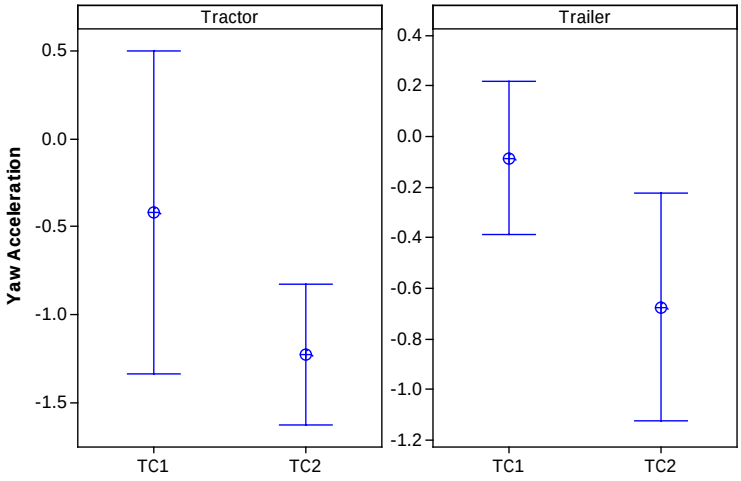

Figure 7-55. Graph. 95% confidence interval for the yaw acceleration at fifth wheel separation

Fifth wheel separation does not appear to be influenced by axle choice in any statistically significant way. Slight, but nearly imperceptible, differences exist in the roll angle at separation

as shown in Figure 7-56. The roll stiffness differences between the suspensions could account for this subtle difference.

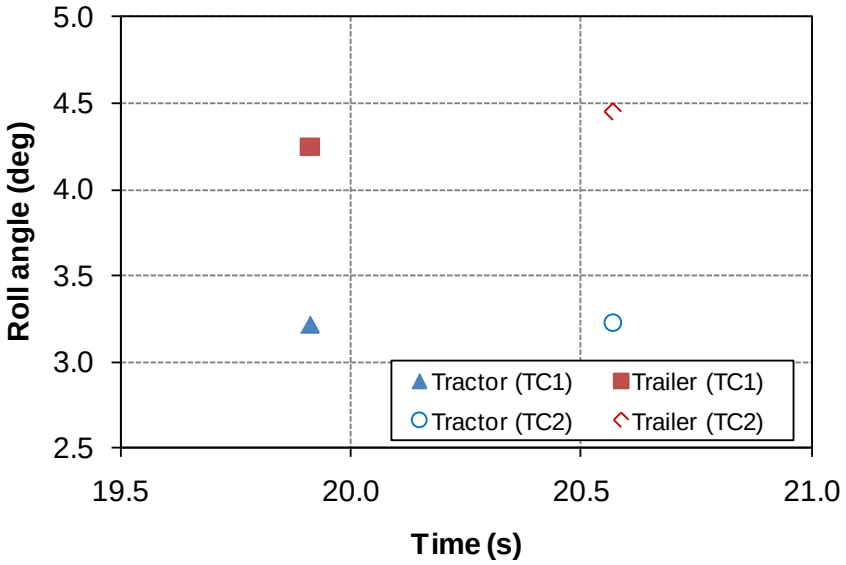

Figure 7-56. Graph. Roll angle at fifth wheel separation

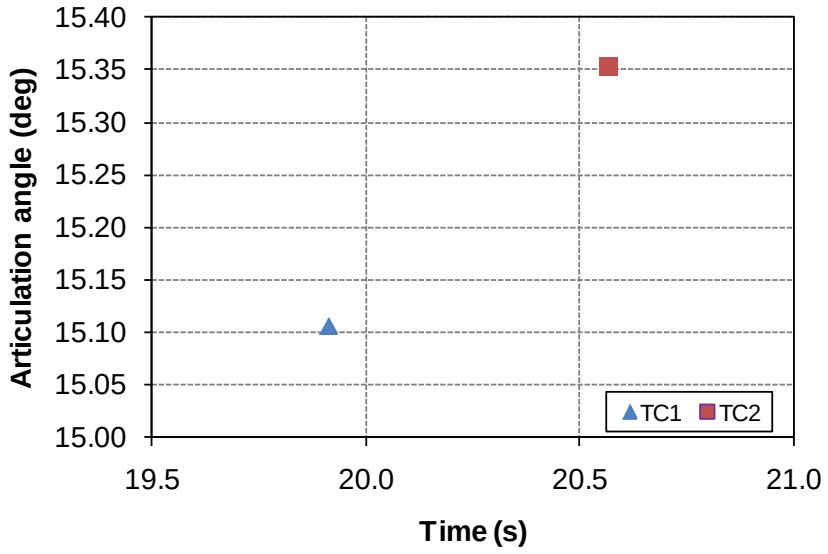

Figure 7-57. Graph. Articulation angle vs. time for Tankers TC1 and TC2

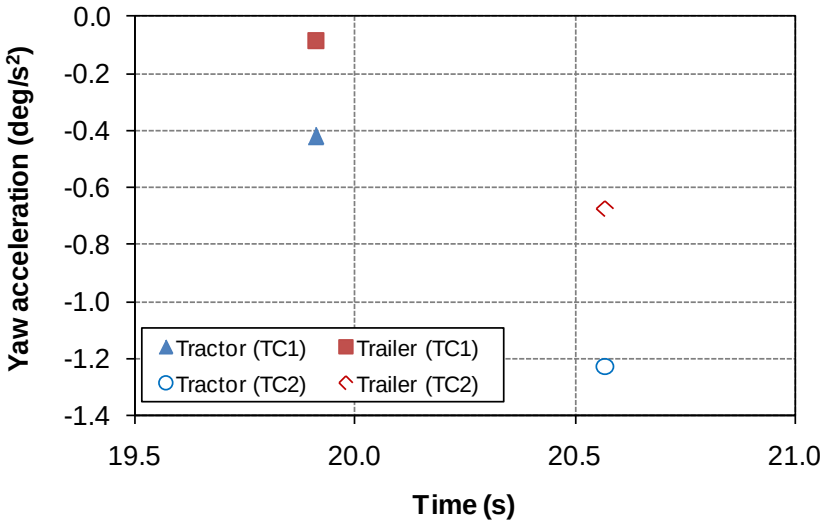

Figure 7-58. Graph. Yaw acceleration vs. time for Tankers TC1 and TC2

Concluding remarks regarding fifth wheel separation

Fifth wheel separation was not significantly influenced by axle design. Barely perceptible differences exist in roll angle at separation. These subtle differences may be attributable to the roll stiffness differences between the suspensions.

7.5 Step Steer Maneuver

The step steer maneuver tests were performed with the two vehicle configurations (TC1 and TC2), with the ESC system disabled, and at two distinct testing speed ranges. The low-speed step steer runs were performed at 32 km/h, while the high-speed tests were performed at three speeds: 51.5 km/h, 54.7 km/h, and 56.3 km/h. The tests were conducted by a steering robot with a protocol that called for the driver to accelerate the vehicle to a speed above the desired test speed, and then shifting into neutral, allowing the vehicle to gradually coast down. When the test speed was reached, the steering robot began the maneuver.

Fifteen runs were conducted with the TC1 configuration, with ten of them showing wheel lift. The initial speed of the maneuver ranged between 53 km/h and 57.8 km/h and between 48.1 km/h and 51.4 km/h for runs with and without wheel lift events, respectively. For the TC2 configuration, wheel lift occurred on ten out of the fourteen runs conducted with this suspension. For configuration TC2, the initial speed of the maneuver ranged between 54.4 km/h and 56.3 km/h and 51.3 km/h and 51.4 km/h for runs with and without wheel lift events, respectively.

Information collected through fourteen data channels was used in the analysis of the step steer maneuver. The variables included the wheel loads at each wheel end for axles 2 and 3 (tractor) and axles 4 and 5 (trailer), lateral accelerations for the tractor and trailer, vehicle speed, and time. Figure 7-59 shows these variables for a Tanker TC2 run.

First Step Steer Analysis

Figure 7-59 shows data a step steer maneuver test and illustrates the reason for selecting the peak lateral acceleration rather than the lateral acceleration at the point of actual wheel lift. For this maneuver, the hand wheel was turned such that the road wheel angle was approximately 8.5 deg. This large road wheel angle resulted in the tractor losing speed during the maneuver which, in turn, caused the lateral acceleration experienced by the vehicle to drop with time after reaching an initial peak with the initial steering input. Because the tractor was still rolling when the lateral acceleration began to drop (the roll lags the lateral acceleration), the actual wheel lift occurred, in some cases, after the peak lateral acceleration was reached. Had the vehicle maintained a constant velocity, the lateral acceleration at the point of wheel lift would have been at or very near the peak lateral acceleration. The upper left plot in Figure 7-59 shows this lateral acceleration decay for the tractor in a step steer maneuver.

In all cases, the difference between the lateral acceleration at the point of wheel lift and the peak lateral acceleration up to the point of wheel lift was relatively small. Finally, the few differences between the lateral accelerations at wheel lift and at peak did not result in a significant change to the reported lift threshold except for the tractor in the step steer maneuver. For the remaining cases (i.e., all of the tank trailer analyses and the ramp steer tractor results), the peak lateral acceleration and the lateral acceleration at the wheel lift point were the same.

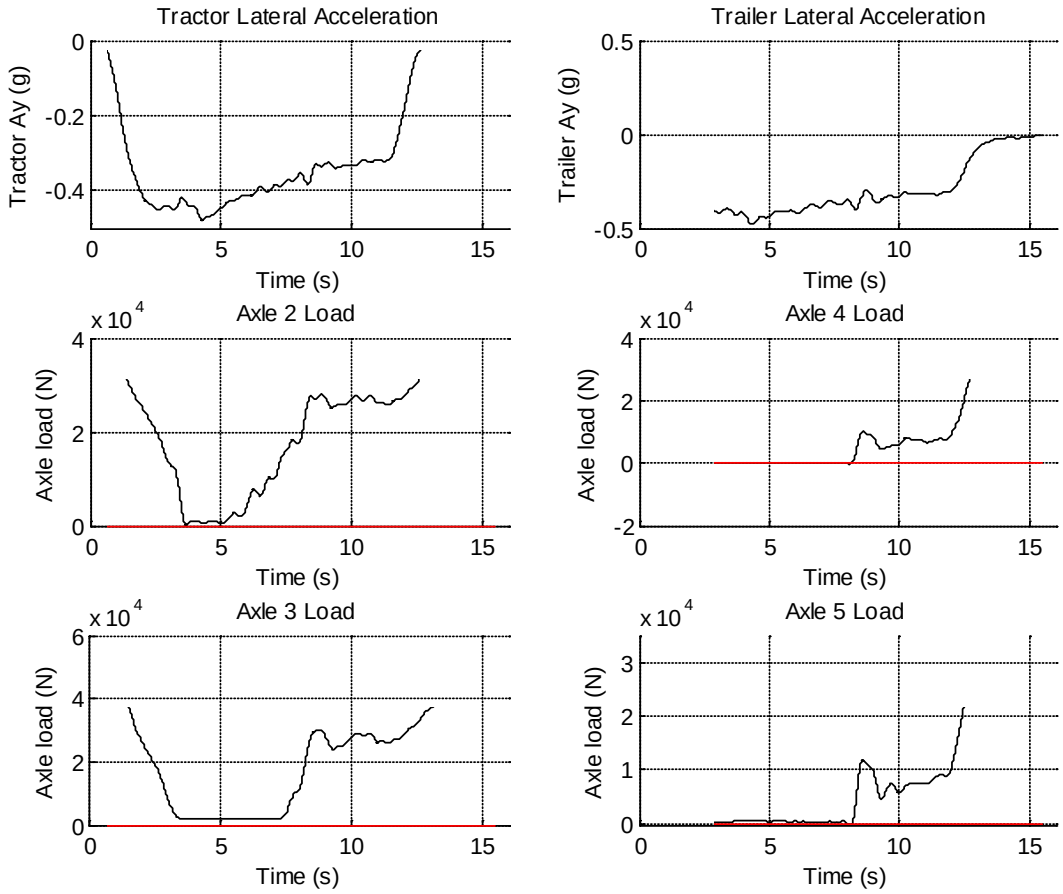

Figure 7-59. Graph. Yaw acceleration vs. time for suspensions TC1 and TC2 in a step steer maneuver

Similar results were obtained for the trailer in the step steer maneuver (Figure 7-60) in which the wider axles improved the rollover performance of the trailer with the exception that the results of Tanker TC1 were not statistically separable from Tanker T, though the TC1 suspension does appear to improve rollover performance. In a similar manner, only Tanker TC2 indicated a statistically significant improvement to the tractor's rollover performance relative to the original Tanker T axle design. However, the wider suspensions yielded a lesser increase in a_y at tractor wheel lift than those seen in the ramp steer test (Figure 7-35). Because the tractor experiences roll moments much earlier than the trailer for the step steer maneuver, the reduced impact of a trailer change on tractor stability is probably due to the fact that the improved trailer stability comes into play much later, thereby limiting the influence of the trailer stability change on the tractor's stability.

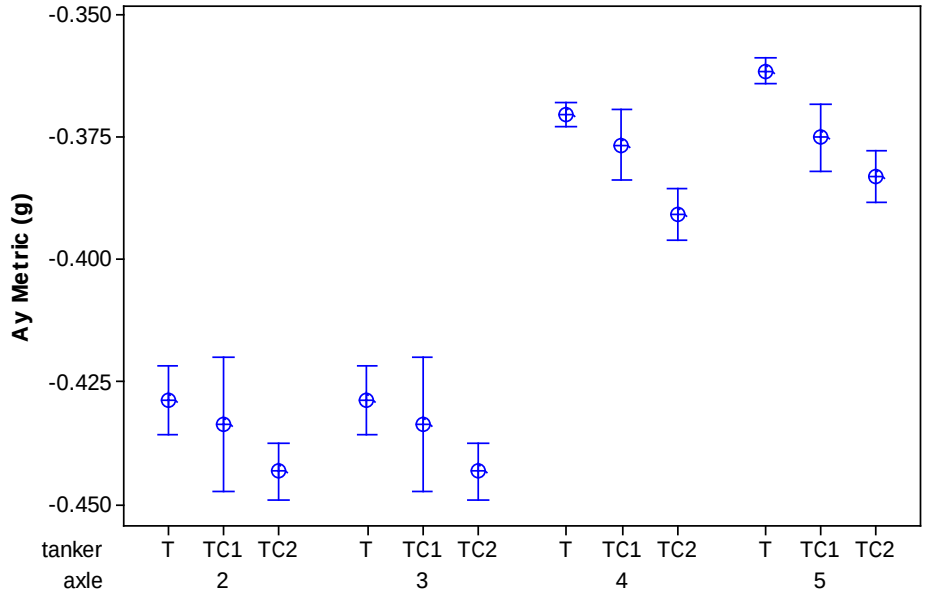

Figure 7-60. Graph. Means of the lateral acceleration leading to wheel lift in the step steer maneuver, and 95% confidence intervals of the means

Second Step Steer Analysis

A second step steer analysis approach used a 500 N threshold to determine wheel lift. If a "flattening" of the wheel load was registered by an axle end and the force was less than the 500 N threshold for a duration of at least 0.2s (which was in all cases considerably shorter than the actual duration of the wheel lift), it was deemed that a wheel lift event had occurred. For example, Figure 7-62 shows the data for wheel lift for axles 4 (left) and 5 (left). No other axle presented wheel lift for that particular run.

This procedure was used to minimize subjective judgment in the determination of wheel lift events and the lateral accelerations that produced these events. The procedure is, however, sensitive to the selection of the threshold.

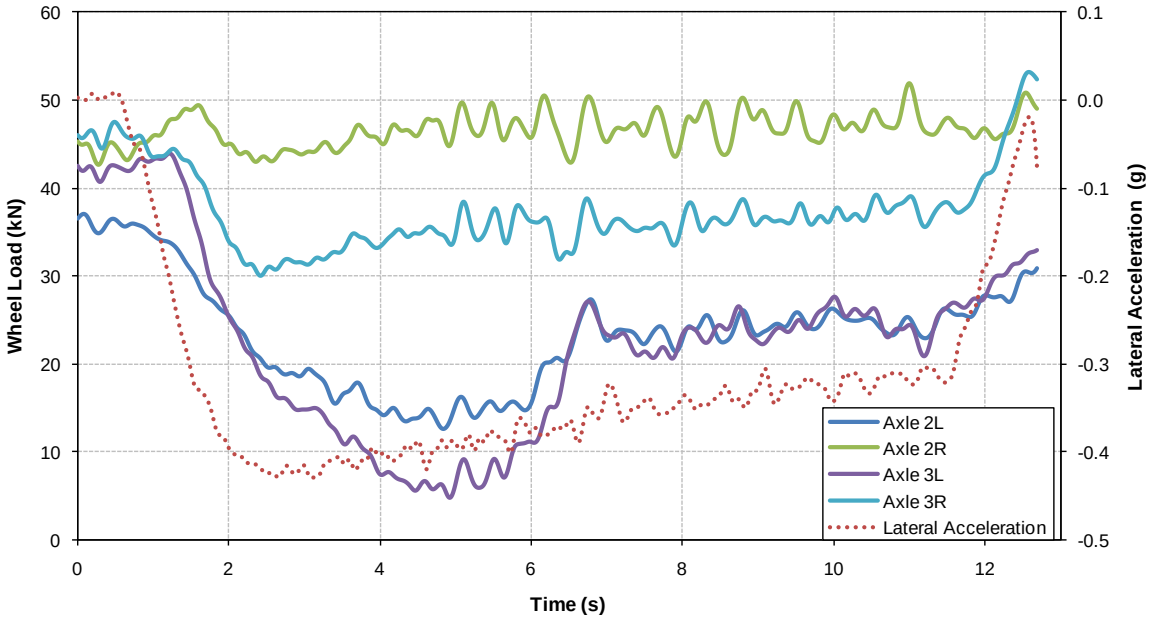

Figure 7-61. Graph. Step steer – tractor wheel loads and lateral acceleration (No wheel lift)

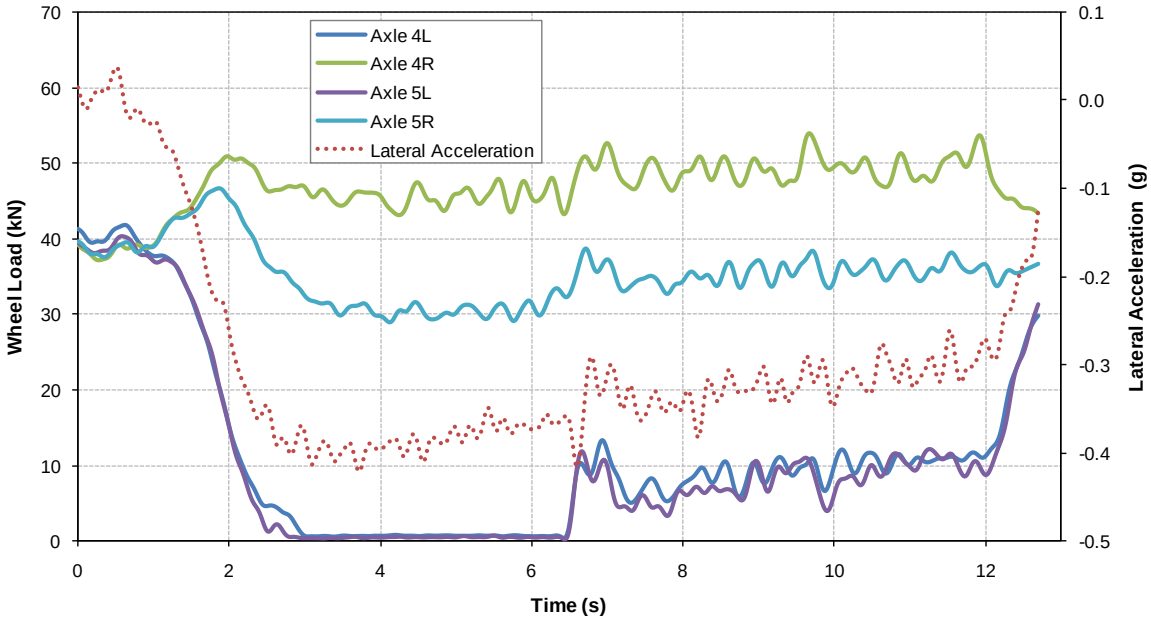

Figure 7-62. Graph. Step steer – trailer wheel loads and lateral acceleration (wheel lift)

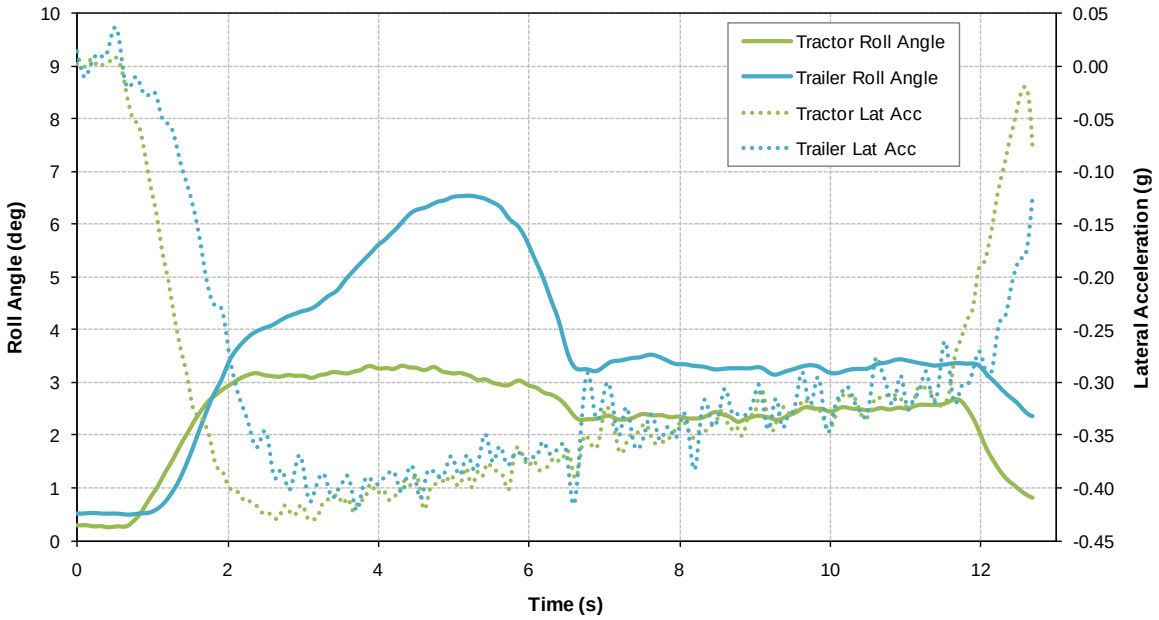

Figure 7-63. Graph. Step steer – lateral acceleration and roll angle

Figure 7-64 presents the wheel loads for axles 2 and 3 as well as the tractor lateral acceleration for a Tanker TC1 run. The graph shows a "flattening" of the wheel loads registered by axles 2 and 3 (left side for both) as would be expected when both of the axles lift. However, axle 3 flattens at a value of about 2,000 N, well above the established threshold for wheel lift. Therefore, axle 3 was not considered to have experienced a wheel lift during this run. Axle 3 never showed values below 1,500 N during any run, likely indicating a measurement bias of 1,500 N. To prevent this measurement bias from influencing the results and conclusions of this analysis, axle 3 was disregarded and only axle 2 was considered. Axle 3 data is presented in Appendix E for completeness.

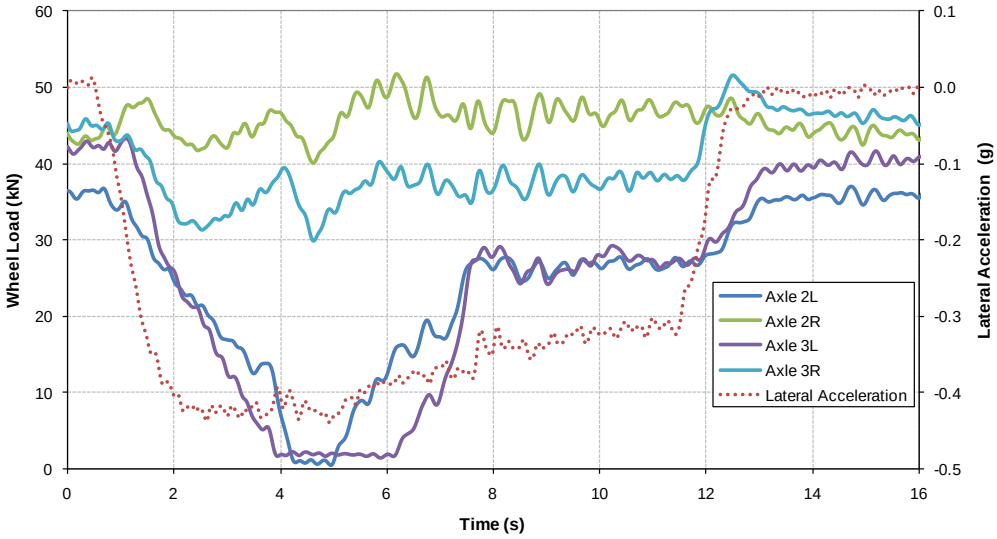

Figure 7-64. Graph. Step steer – tractor wheel loads and lateral acceleration (Axle 2 left wheel lift)

In the runs in which a wheel on axle 2 lifted, the wheel load registered by the left end of axle 3 showed a "flat" region that was always between three and four times the selected threshold. This was probably a calibration issue with the axle 3L strain gage, which introduced a systematic bias in the wheel load data. If this bias were corrected (e.g., by subtracting 1,500 N from the observed wheel load) the wheel lift lateral accelerations for axle 3L would have been similar to those shown by axle 2L.

In addition, there were three other cases for Tanker TC1 and one for Tanker TC2 in which axles 2 and 3 showed a "flattening" of the respective wheel loads, but the minimum achieved was above the selected threshold.

For the axle ends that presented wheel lift, the time at which the corresponding wheel load crossed the established threshold was registered and was used to find a local maximum (in absolute value) in the corresponding tractor or tank trailer lateral acceleration that occurred immediately before the start of the wheel lift event (Figure 7-64). The value of that lateral acceleration was assigned as the one that produced the wheel lift. Appendix E shows these values for all of the runs used in this analysis. The tables also show the lateral accelerations that corresponded to cases in which the selected threshold was not crossed, but which presented "flattening" areas in the wheel load vs. time diagram (axles 2 and 3). Those lateral accelerations were not used in the analysis that follows. Other tables included in the appendix show, in absolute value, the maximum lateral acceleration and the maximum roll angle registered for each run for both the tractor and the trailer.

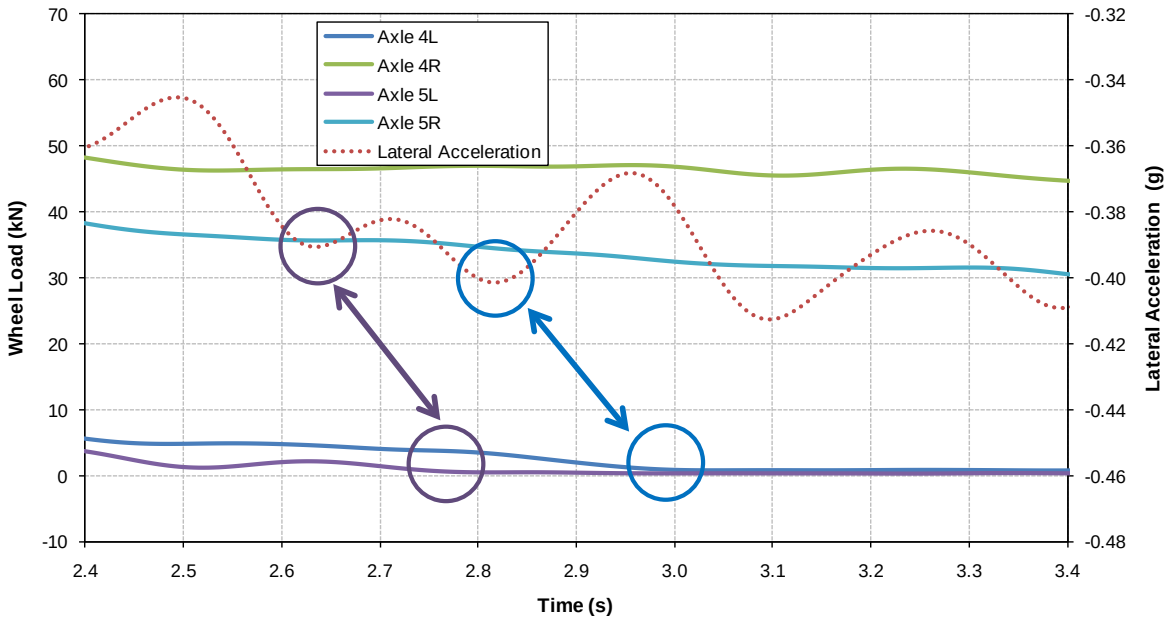

Figure 7-65. Graph. Step steer – determining lateral acceleration corresponding to wheel lift

The data generated for the step steer wheel lift analysis is presented graphically in Figure 7-66. For each vehicle configuration and axle end, the figure shows the distribution of lateral accelerations observed at the time of wheel lift computed as described previously. In this figure, the absolute value of the lateral acceleration (vertical axis) increases downwards.

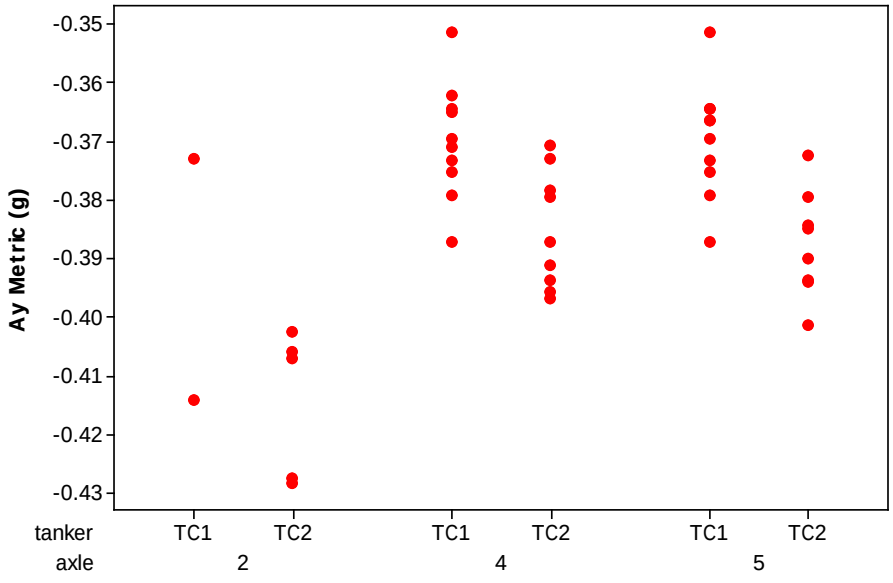

Figure 7-66. Graph. Step steer – lateral acceleration at wheel lift for Tankers TC1 and TC2

In all of the cases (i.e., axles 2, 4 and 5) Figure 7-66 shows that, on average, Tanker TC2 required higher lateral accelerations for wheel lift than Tanker TC1. This can be better appreciated in Figure 7-67, which shows the 95% confidence interval of the mean of the distribution of wheel lift lateral accelerations. In each case, the center of the confidence interval for Tanker TC2 is below (i.e., its higher lateral acceleration is higher) than that for Tanker TC1. The size of the confidence intervals are similar for Tanker TC1 and Tanker TC2 for axles 4 and 5, indicating that there was the same dispersion in the values of the wheel lift lateral accelerations for these two configurations. For axle 2, the large size of the confidence intervals is mostly due to the small number of observations (two for Tanker TC1 and five for Tanker TC2).

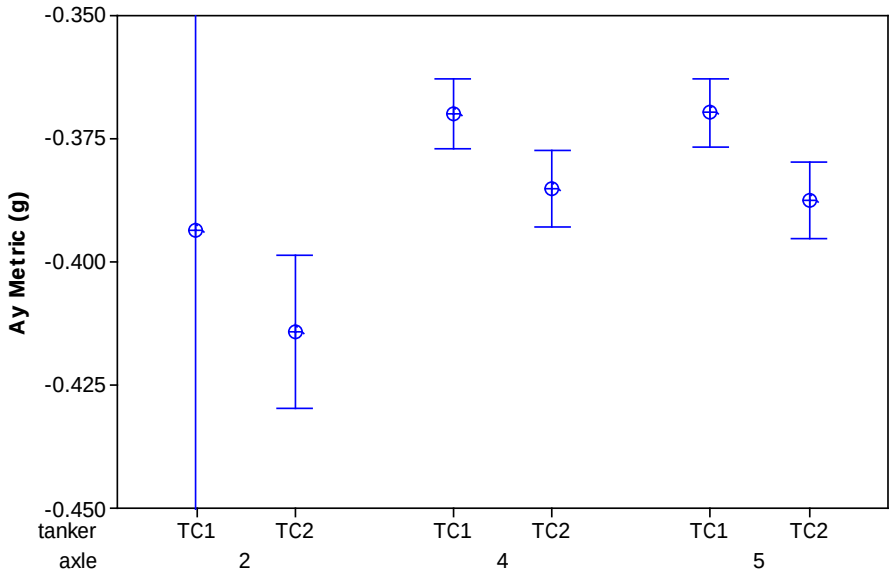

Figure 7-67. Graph. Step Steer – 95% confidence interval for the mean lateral acceleration at wheel lift for suspensions TC1 and TC2

More detailed summary statistics of the distributions of the observed wheel lift lateral accelerations are presented in Appendix E. Table 7-9 and Table 7-10 show the number of observations (N), the mean and standard deviation of the distributions of lateral acceleration, the standard error (SE) of the mean, as well as the minimum, median, and maximum of the observed values. As discussed above, on average, Tanker TC2 required 0.02g larger lateral acceleration to produce wheel lift than Tanker TC1.

Table 7-9. Step steer – summary statistics for the lateral acceleration for Tanker TC1

Variable	Axle	N	Mean	SE Mean	Std Dev	Minimum	Median	Maximum
Lateral acceleration	2L	2	-0.39350	0.02050	0.02910	-0.41410	-0.39350	-0.37300
	4L	10	-0.36980	0.00312	0.00987	-0.38712	-0.37024	-0.35138
	5L	10	-0.36968	0.00307	0.00970	-0.38712	-0.36789	-0.35138

Table 7-10. Step steer – summary statistics for the lateral acceleration for Tanker TC2

Variable	Axle	N	Mean	SE Mean	Std Dev	Minimum	Median	Maximum
Lateral acceleration	2L	5	-0.41423	0.00562	0.01257	-0.42832	-0.40700	-0.40248
	4L	9	-0.38512	0.00333	0.01000	-0.39687	-0.38728	-0.37074
	5L	8	-0.38746	0.00325	0.00919	-0.40142	-0.38737	-0.37231

The information presented in Table 7-9 and Table 7-10 can also be used to test the hypothesis of equality in the mean values of the lateral acceleration distribution at wheel lift between Tankers TC1 and TC2. To do that, a Smith-Satterthwaite Test (i.e., a t-test in which the equality of the variances in the groups being compared is not assumed) was used to test whether the means of the lateral acceleration distributions for Tankers TC1 and TC2 were equal or different. The results of these statistical tests are presented in Table 7-11.

Table 7-11. Step steer – test of hypothesis for equality in the means of the wheel lift lateral acceleration

Context	Comparison	p-value
Axle 5L	TC1 vs. TC2	0.0011
Axle 4L	TC1 vs. TC2	0.0038
Axle 2L	TC1 vs. TC2	0.4909
TC2	Axles: 4L vs. 5L	0.6223
TC1	Axles: 4L vs. 5L	0.9790

In Table 7-11 the first column indicates the context in which the test of hypothesis was conducted (e.g., distribution of lateral accelerations for axle 5L wheel lift, shown as axle 5L in the table), The second column shows the comparison made, and the last column presents the result of the test of hypothesis. Small p-values indicate a statistically significant difference between the mean of the two distributions compared. The table shows that for axles 4L and 5L, the mean of the distribution of the lateral acceleration that produced wheel lift for Tanker TC2 was larger (in absolute value) than that of Tanker TC1. The differences were statistically significant at higher than a 95% confidence level. For the other comparisons shown in Table 7-11, there were no statistically significant differences in the mean of the lateral acceleration distributions. The low number of test cases that produced wheel lift on Axle 2 prevented a finding of statistical significance between Tankers TC1 and TC2.

As in previous phases, comparisons were made using the roll compliance parameter (RC) computed as the ratio between the maximum roll angle and the maximum lateral acceleration. The values of RC appear in Appendix E for all of the step steer runs that presented wheel lift.

With this information, a test of hypothesis similar to the one presented above was conducted for the means of the distribution of the maximum lateral accelerations. This test showed that there were no statistically significant differences in the means of the maximum acceleration observed in the tests. The test of hypothesis involving the RC parameter showed no statistically significant differences between the TC1 and TC2 suspensions.

Comparing the data between Tanker TC1 and Tanker T (tested in Phase B) with similar load and tire conditions, there were no statistically significant differences between the means of the maximum lateral acceleration distributions—that is, the maneuvers were performed identically for Tanker TC1 and Tanker T. However, Tanker TC1 showed a lower absolute value of RC (that is, an indication of higher roll stability) than Tanker T, which was statistically significant for the axles on the trailer.

The same results were obtained when comparing Tanker TC2 and Tanker T using the means of the trailer RC distributions. In this case the mean of the distribution of the maximum lateral acceleration was slightly larger for the Tanker TC2 runs than for the Tanker T runs, indicating a disadvantage for the TC2 configuration. Regarding the tractor, in both cases (comparisons between Tanker TC1 vs. Tanker T and between Tanker TC2 vs. Tanker T) the Tanker T configuration showed, on average, a larger RC (that is, greater roll angles), but this difference was not statistically significant.

Tanker TC2 was better able to keep the tires on the pavement in the step steer maneuver than was Tanker TC1. Statistical tests showed that there was a difference in the mean of the distribution of the lateral acceleration at wheel lift between Tanker TC1 and Tanker TC2, with the TC2 configuration requiring higher lateral accelerations (on average) to lift a wheel from the pavement.

As measured by the RC parameter, both Tanker TC1 and Tanker TC2 rolled less than Tanker T. For the trailer, this observation was statistically significant at the 95% confidence level. For the tractor, Tankers TC1 and TC2 displayed lower absolute value mean RCs than Tanker T, although the difference was not statistically significant.

7.6 Open-Loop Double Lane Change Maneuver

The open-loop double lane change maneuver tests were conducted with both vehicle configurations (i.e., Tankers TC1 and TC2), and with the ESC system disabled and enabled. The test protocol called for a speed of 54.7 km/h at the beginning of the maneuver. As with the ramp and step steer tests, a steering robot was used to perform the maneuver, but for the lane change

maneuver the driver controlled the speed of the vehicle. This resulted in a greater variation in the initial speed of the lane change maneuver than for the ramp and steep steer runs.

Five runs were performed in the TC1 tanker with the ESC system disabled, and all showed wheel lift. The initial speed of the maneuver ranged between 54.5 km/h and 55.6 km/h. The TC1 tanker was also tested with the ESC system enabled (four runs). In this case, the initial speed varied between 54.8 km/h and 55.7 km/h.

For the TC2 tanker, thirteen lane change maneuver tests were conducted with the ESC system disabled (all with wheel lift events) and five were conducted with the ESC system enabled. The initial speed of the maneuver ranged between 54.5 km/h and 56.0 km/h and between 54.6 km/h and 55.5 km/h for the ESC system disabled and enabled runs, respectively.

The responses of the tractor and trailer in the lane change maneuver essentially reduce to three segments, according to the direction of the trailer's roll (Figure 7-68). The steer input always leads the roll angle; that is, the trailer rolls a short time after the steer input begins.

The maneuver begins with the tractor steering left (positive hand wheel angle), as if to avoid an obstacle directly in its path. The hand wheel turns rapidly to the right as the tractor reaches the imaginary adjacent lane, just as the tank trailer roll angle is beginning to build, as shown in the figure. This hand wheel motion is followed by a slower rate of steer right as the tractor heads back into the original lane of travel. When the tank trailer roll angle crosses zero and the tank trailer begins leaning to the right, segment 2 begins. While the tank trailer continues rolling right, the tractor approaches the center of its original lane, so the hand wheel angle comes rapidly to the left (positive) again to align the tractor in the original lane. The hand wheel angle returns to zero to straighten the tractor's path. As this occurs, the tank trailer's roll direction is again to the right, and segment 3 begins.

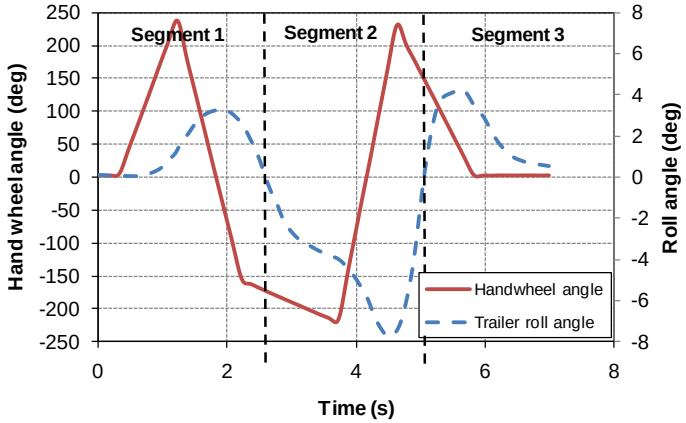

Figure 7-68. Graph. Hand wheel angle and trailer roll angle vs. time, showing the three segments of the lane change maneuver

Segment one produces a positive roll angle (a roll to the right, or clockwise if the tank trailer is viewed from the rear). If wheel lift occurs in segment one, it would occur on the inside (left) wheels in the turn. Segment two produces a negative roll angle, with the possibility of lifting the right side tires, which are on the inside of that turn. Segment three occurs as the vehicle returns to a parallel direction to its original path. If wheel lift occurred during the lane change maneuver, it was present in either segment two or segments two and three. If the ESC system activates, it does so in segment one, preventing any wheel lift in segments two and three.

Similar to the step steer maneuver, information gathered through fourteen data channels was used in the analysis of the lane change maneuver. These variables included the wheel loads at each wheel end for axles 2 and 3 (tractor) and axles 4 and 5 (trailer), lateral accelerations for the tractor and trailer, vehicle speed, and time. Figure 7-69 and Figure 7-70 show the wheel loads and lateral accelerations for a Tanker TC1 run, for the tractor and trailer, respectively.

First Lane Change Analysis

In order to determine wheel lift for a given axle end, the corresponding wheel load was again compared to a 500 N threshold. If the wheel load stayed below that threshold for more than 0.2 s, a wheel lift event was deemed to have occurred. For example, Figure 7-69 shows wheel lift for axles 4R and 5R during the second segment of the maneuver, and wheel lift for axles 4L and 5L during the third segment of the maneuver, with the latter wheel lift event showing a considerably shorter duration (i.e., 1.2 s vs. 0.25 s). Axles 2 and 3 did not present wheel lift for that particular run (Figure 7-70) or any other run of the lane change maneuver tests. On the other hand, axles 4 and 5 showed wheel lift in all of the ESC system disabled runs for both Tankers TC1 and TC2, with all of these runs showing wheel loads that were negative.

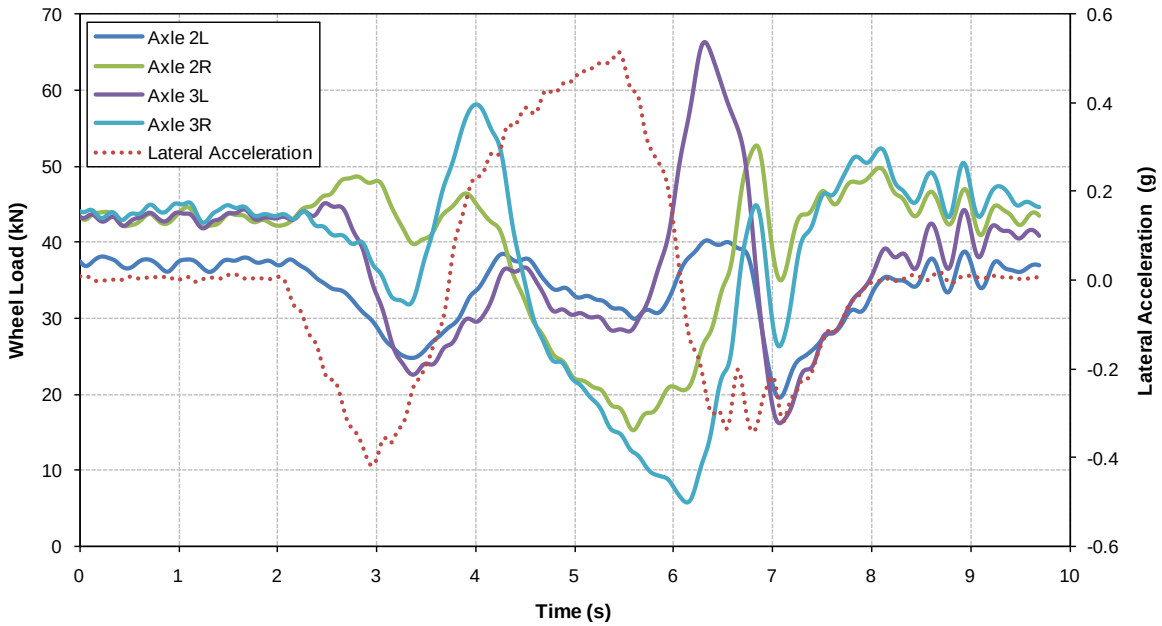

Figure 7-69. Graph. Lane change/ESC system disabled – tractor wheel loads and lateral acceleration (no wheel lift)

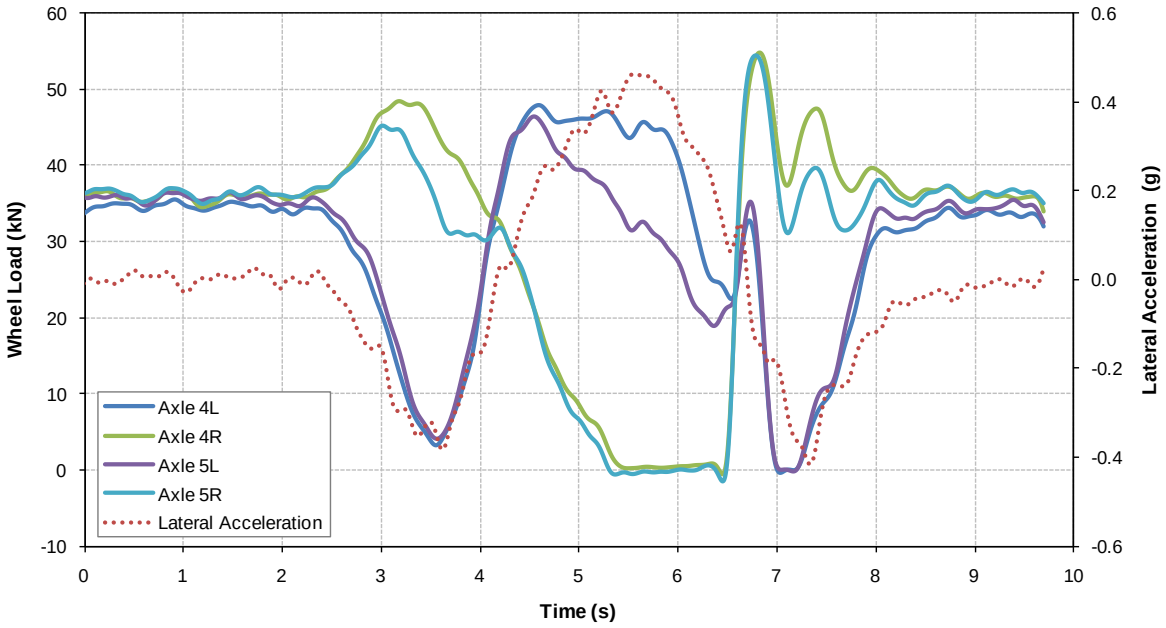

Figure 7-70. Graph. Lane change/ESC system disabled – Trailer wheel loads and lateral acceleration (Axles 4L, 4R, 5L and 5R wheel lift)

Figure 7-71 shows lateral acceleration and roll angle for both the tractor and trailer for the same Tanker TC1 run. As in the previous phases in which the lane change maneuver was analyzed, there was a time delay between the occurrence of the maximum lateral acceleration and the

maximum roll angle (in absolute value) in all three segments of the maneuver. For example, in the case shown in Figure 7-71, the time lags between the maximum lateral acceleration and the maximum roll angle were 0.17s, 0.10s, and 0.23s for the tractor during the first, second, and third segment of the maneuver, respectively. For the trailer, the lags were 0.22 s, 0.61 s, and -0.06 s, respectively. (The negative value indicates a reverse in the sequence of the events, with the maximum roll angle occurring before the maximum lateral acceleration was registered. The difference is very small compared to the other two time lags and could be attributed to an artifact of the filtering algorithm.) The maximum absolute values for the lateral acceleration and roll angle in each segment of the lane change maneuver were used to compute the RC parameter.

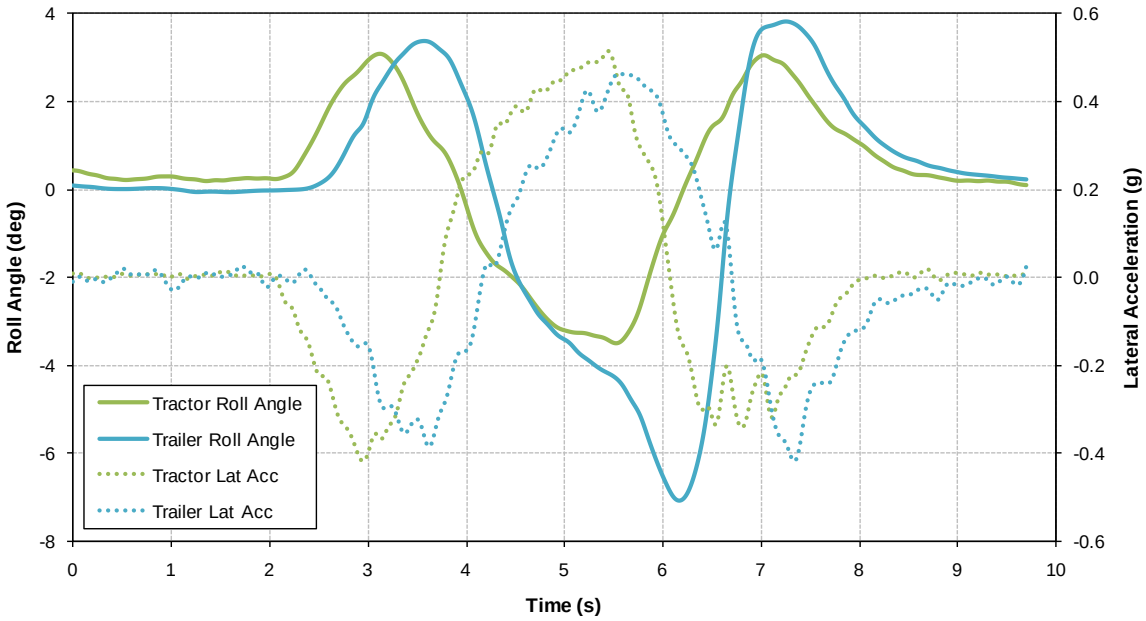

Figure 7-71. Graph. Lane change/ESC system disabled – lateral acceleration and roll angle

Nine runs of the lane change maneuver (four for Tanker TC1 and five for Tanker TC2) were performed with the ESC system enabled for both the tractor and the trailer. As discussed elsewhere in this report, the maneuvers were performed using a steering robot and the information was collected by a DAS that was triggered by the driver of the vehicle to start and finish the data gathering process for each run. In the case of the nine ESC system enabled runs, the driver stopped the DAS before the run was completed when the ESC system slowed the vehicle significantly.

An example of an ESC system enabled run for Tanker TC1 is shown in Figure 7-72 and Figure 7-73. Figure 7-72 shows the wheel loads for axles 4 and 5 and the trailer lateral acceleration for the entire first segment and half of the second segment of the lane change maneuver, while Figure 7-73 presents the speed of the vehicle and tractor and trailer lateral accelerations. Comparing Figure 7-70 to Figure 7-72 it is possible to see that the ESC system intervened early (i.e., in the first segment of the maneuver) decreasing the lateral accelerations and thereby

decreasing the speed of the vehicle. Notice that during the first segment of the maneuver the wheel loads on axles 4L and 5L (Figure 7-70) were smaller than those registered in the ESC system disabled case (Figure 7-72). This was due to the higher initial speeds with which the ESC system enabled runs were conducted compared to the tests with the ESC system disabled. Nevertheless, no wheel lift event was registered since axle 5L (the worst case) presented a minimum wheel load of 659 N (which is greater than 500 N, the defined wheel lift threshold) for an interval of about 0.1 s (Figure 7-72).

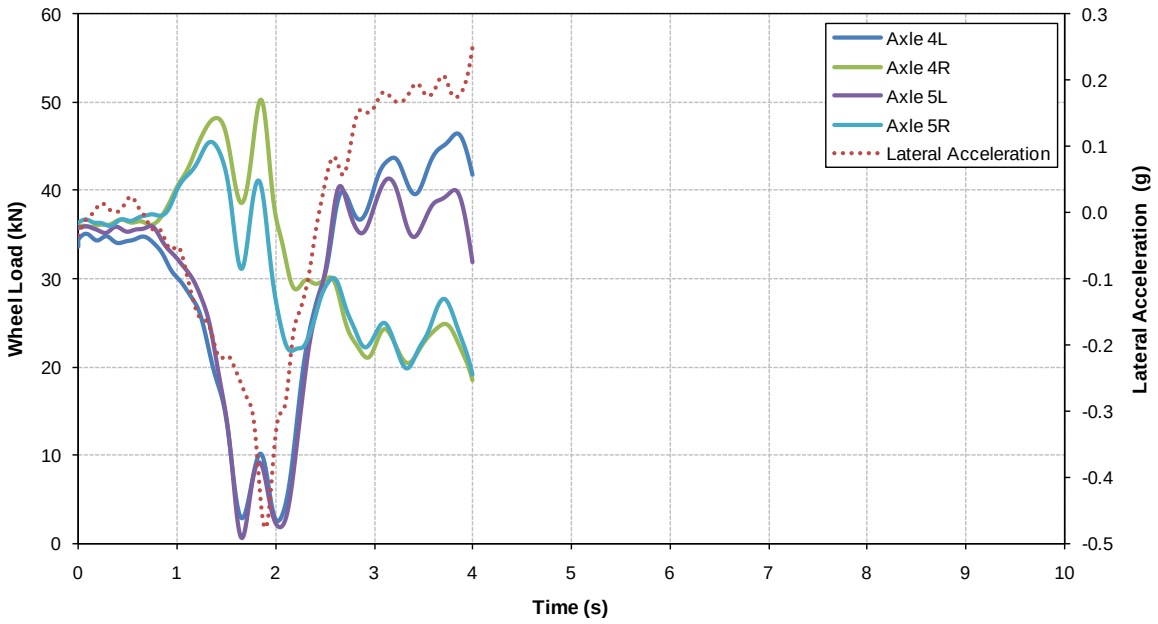

Figure 7-72. Graph. Lane change/ESC system enabled – tank trailer wheel loads and lateral acceleration (Tanker TC1 configuration)

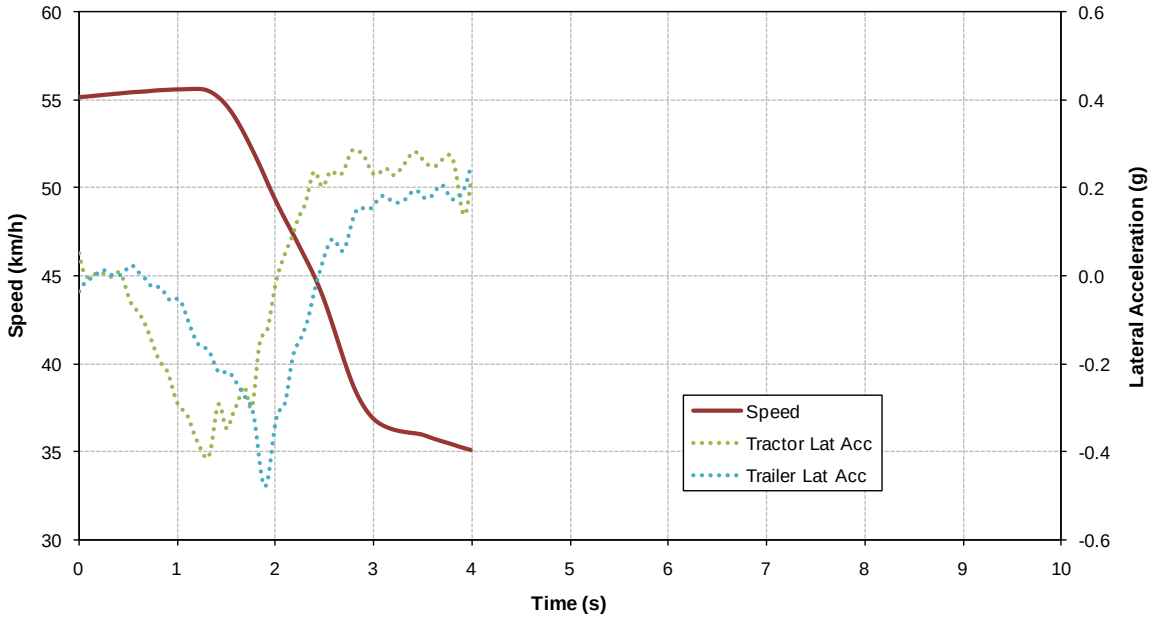

Figure 7-73. Graph. Lane change/ESC system enabled – vehicle speed and tractor and trailer lateral accelerations (Tanker TC1)

The information generated for the lane change wheel lift analysis is presented graphically in Figure 7-74. The figure shows the distribution of lateral accelerations observed at the time of wheel lift for each vehicle configuration and axle end. The vertical axis represents the lateral acceleration at wheel lift and increases (in absolute value) downwards. In the figure, a negative sign convention was used to represent the lateral accelerations for all the axle ends that were analyzed, even though at wheel lift in this maneuver the right ends of axles 4R and 5R lifted under positive lateral accelerations. For the latter, the absolute value of the wheel lift lateral acceleration multiplied by -1 was used in the representation.

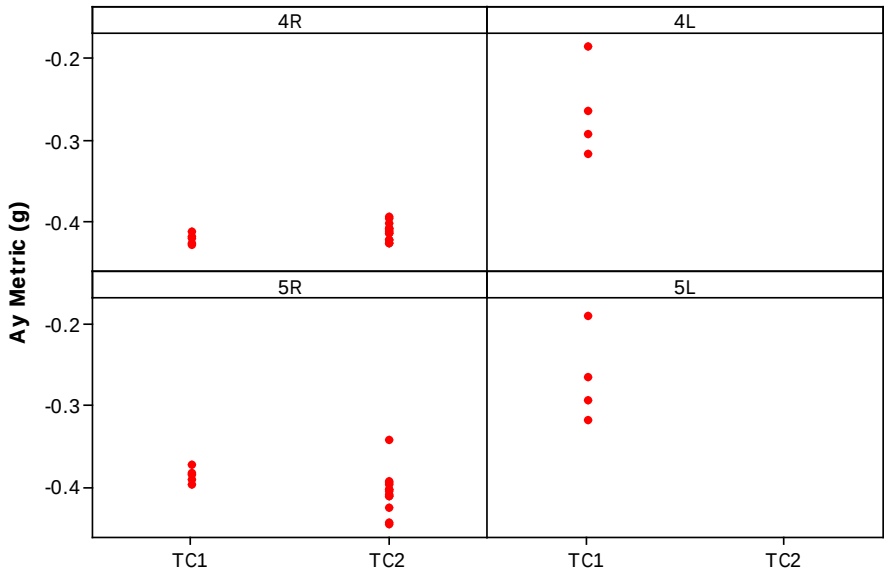

Figure 7-74. Graph. Lane change/ESC system disabled – lateral acceleration at wheel lift for specific axles for Tankers TC1 and TC2

The 95% confidence intervals for the mean of the lateral acceleration distributions are presented in Figure 7-75. The size of the confidence intervals are similar for Tanker TC1 and Tanker TC2 for axles 4R and 5R, indicating the same dispersion in the values of the wheel lift lateral accelerations for these two configurations. For axles 4L and 5L (Tanker TC1 only), the dispersion was greater.

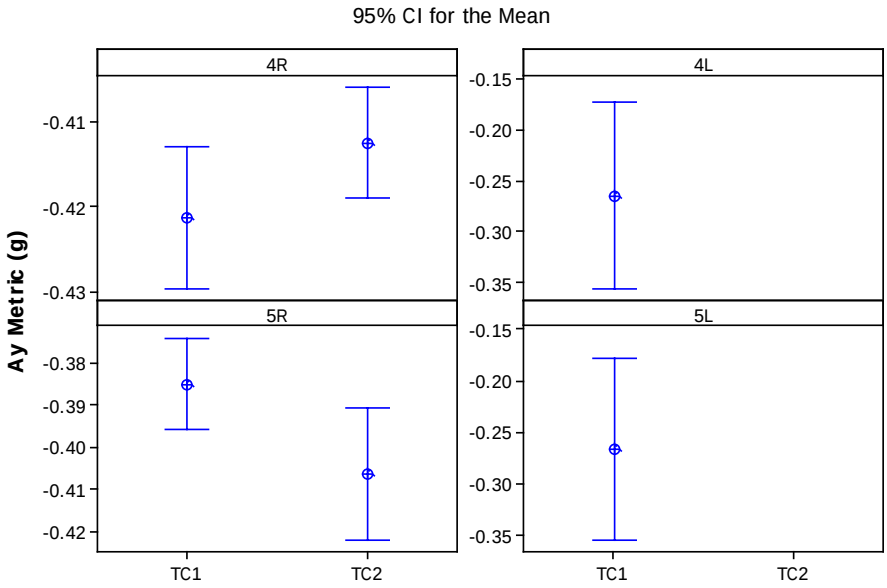

Figure 7-75. Graph. Lane change/ESC system disabled – 95% confidence interval for the mean lateral acceleration at wheel lift for specific axles for Tankers TC1 and TC2

Figure 7-74 and Figure 7-75 show that for the lane change maneuver, only the trailer axles lifted and there were no instances of axles 2 and 3 lifting during this maneuver. Axle-end lift data is also shown in Figure 7-76 and Figure 7-77, but in those figures, the data are presented as a function of the initial speed of the maneuver, which was computed as the average vehicle speed over the first 0.5s after data collection began. Except for one run at about 55.4 km/h, Tanker TC1 always shows wheel lift for both the left and right ends of axles 4 and 5. It is noteworthy that Tanker TC2 never shows wheel lift for axles 4L or 5L, even at speeds that were about 0.6 km/h higher than the maximum initial speed of the fastest Tanker TC1 lane change test.

Regarding the order in which the events occurred, for Tanker TC1, axle 5R lifted first in all runs followed by axle 4R (both 5 and 4 lifted during the second segment of the maneuver), and by axles 4L and 5L which lifted almost simultaneously in the third segment of the maneuver. The same pattern was observed for Tanker TC2 in ten of the thirteen runs for axles 5R and 4R in the second segment of the maneuver. In the remaining three runs, the order was reversed; that is, axle 4R lifted earlier than axle 5R. Axles 4L and 5L never lifted under this vehicle configuration.

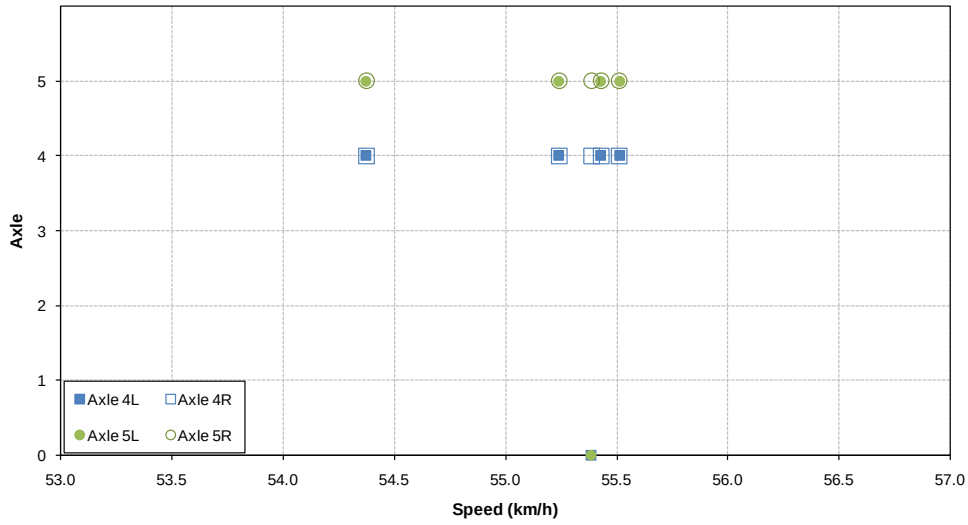

Figure 7-76. Graph. Lane change/ESC system disabled/Tanker TC1 – axles that lifted by initial speed

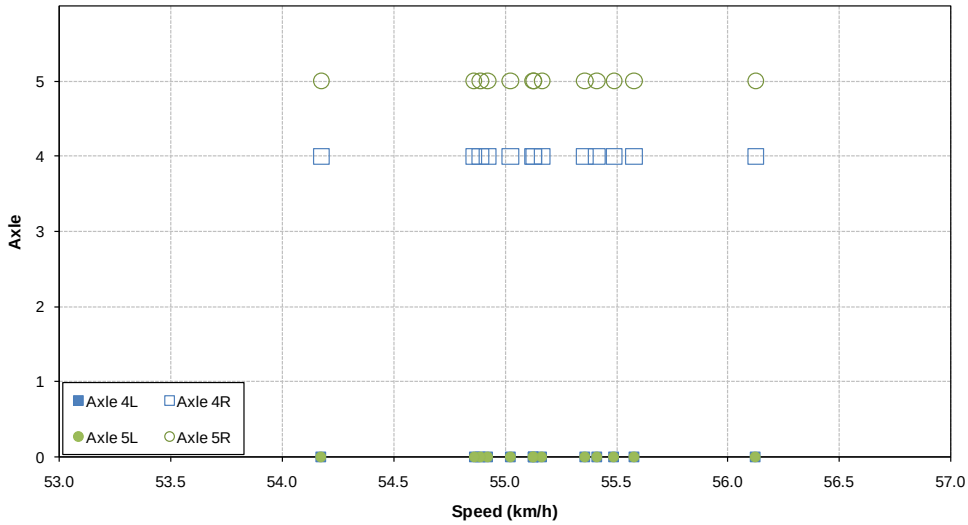

Figure 7-77. Graph. Lane change/ESC system disabled/Tanker TC2 – axles that lifted by initial speed

Table 7-12 and Table 7-13 summarize the distribution of the observed lateral accelerations at wheel lift for tankers TC1 and TC2, respectively. The tables show the mean and standard deviation of the distributions, as well as the maximum and minimum observed values among other statistics.

Table 7-12. Lane change/ESC system disabled – summary statistics for Tanker TC1

Variable	Axle	N	Mean	SE Mean	Std Dev	Minimum	Median	Maximum
a_y	4L	4	-0.26440	0.02900	0.05790	-0.31680	-0.27850	-0.18390
	4R	5	0.42123	0.00301	0.00673	0.41231	0.42053	0.42936
	5L	4	-0.26540	0.02800	0.05610	-0.31680	-0.27850	-0.18800
	5R	5	0.38487	0.00388	0.00867	0.37281	0.38436	0.39602

Table 7-13. Lane Change/ESC system disabled – summary statistics for Tanker TC2

Variable	Axle	N	Mean	SE Mean	Std Dev	Minimum	Median	Maximum
a_y	4R	13	0.41242	0.00297	0.01070	0.39379	0.41173	0.42681
	5R	13	0.40618	0.00714	0.02573	0.34183	0.40417	0.44583

The data in Table 7-12 and Table 7-13 could be used to test whether the lateral accelerations at wheel lift are different for Tanker TC1 than Tanker TC2. The test would not be meaningful, however, because Axles 4R and 5R showed opposite trends between Tankers TC1 and TC2.

Comparisons between the two tankers tested in Phase C and the vehicle configuration tested in Phase B (Tanker T) were also made using the RC parameter, computed as the ratio between the maximum roll angle and the maximum lateral acceleration. The calculated values of the RC parameter used in the analysis are presented in Appendix F for the Tanker TC1 and Tanker TC2 lane change runs.

First, a test of hypothesis similar to the one presented above was conducted for the means of the distribution of the maximum lateral accelerations. This test showed that there were no statistically significant differences in the means of the maximum lateral accelerations. A test of hypothesis involving the RC parameter subsequently showed no statistically significant differences between Tanker TC1 and Tanker TC2, although Tanker TC2 presented a lower average RC for the trailer during the second segment of the maneuver (i.e., the part of the maneuver where wheel lift was always observed).

Comparing Tanker TC1 vs. Tanker T (Phase B), and Tanker TC2 vs. Tanker T, the mean of the maximum lateral accelerations observed in Phase B was lower than those of Tanker TC1 and Tanker TC2. Wheel lift occurred at a lower speed for the Phase B configuration, indicating less stability, but the lower speed is the cause of the lower lateral accelerations. The differences in the maximum lateral accelerations, which were statistically significant at higher than a 95% confidence level, were about 8% and 13% lower, respectively, for the tractor and the tank trailer relative to Tanker TC1, and 10% and 12% lower with respect to Tanker TC2. Because of the lower test speed for Tanker T, it was not possible to make relevant comparisons between Tanker T and Tanker TC1 or between Tanker T and Tanker TC2. Nevertheless, even under these unfavorable conditions, Tanker TC1 showed a statistically significant lower mean in the RC

parameter than Tanker T for the tank trailer in the first segment of the maneuver, and for the tractor in the second segment. The same was true for Tanker TC2, although the differences were not statistically significant in this case.

Regarding the lane change tests with the ESC system enabled, Table 7-14 and Table 7-15 present the minimum wheel loads registered by the left ends of axles 4 and 5 (first segment of the lane change maneuver), as well as the initial speed of the maneuver, and the maximum longitudinal deceleration that the vehicle experienced as a consequence of the ESC intervention.

Table 7-14. Lane change/ESC system enabled – axles 4 and 5 minimum wheel loads and vehicle deceleration (Tanker TC1) in the first segment of the maneuver

Run	Initial speed (km/h)	Minimum wheel load (N)		Maximum deceleration (m/s^2)
		Axle 4L	Axle 5L	
34 LANE CHANGE SYS ON_040910_175246_RN_001_filt.csv	54.9	3,362	1,009	2.80
34 LANE CHANGE SYS ON_040910_175246_RN_002_filt.csv	54.8	3,705	1,653	2.99
34 LANE CHANGE SYS ON_040910_175246_RN_003_filt.csv	55.7	2,505	659	3.52
34 LANE CHANGE SYS ON_040910_175246_RN_004_filt.csv	54.9	3,234	1,766	3.27

Table 7-15. Lane change/ESC system enabled – axles 4 and 5 minimum wheel loads and vehicle deceleration (Tanker TC2) in the first segment of the maneuver

Run	Initial speed (km/h)	Minimum wheel load (N)		Maximum deceleration (m/s^2)
		Axle 4L	Axle 5L	
TC2 SYS ON LANE CHANGE_041210_183619_RN_001_filt.csv	55.5	4,273	2,398	2.69
TC2 SYS ON LANE CHANGE_041210_183619_RN_002_filt.csv	54.9	5,451	2,316	2.82
TC2 SYS ON LANE CHANGE_041210_183619_RN_003_filt.csv	55.5	4,912	413	2.89
TC2 SYS ON LANE CHANGE_041210_183619_RN_004_filt.csv	54.7	4,883	1,673	2.95
TC2 SYS ON LANE CHANGE_041210_183619_RN_005_filt.csv	54.6	3,591	1,072	3.17

Under the conditions defined in this analysis regarding wheel load thresholds and event duration, none of the nine ESC system enabled runs presented wheel lift events in the first part of the maneuver (but neither did the eighteen ESC system disabled runs). One ESC system enabled run, however, seems to show that axle 5L (and perhaps 4L as well) were heading towards wheel lift (see Figure 7-78). As discussed previously, data collection was stopped as soon as the vehicle slowed down, which prevented verification of whether there was a wheel lift event in this case.

Table 7-14 and Table 7-15 also show the maximum deceleration that the vehicle experienced as a result of the ESC system intervention. Deceleration rates were higher for Tanker TC1 than for the Tanker TC2 (3.15 m/s^2 vs. 2.91 m/s^2 respectively), even though the initial speed of the maneuver was, on average, the same for the two configurations (i.e., 55.08 km/h vs. 55.04 km/h respectively). The effect of these high rates and their difference needs to be further investigated.

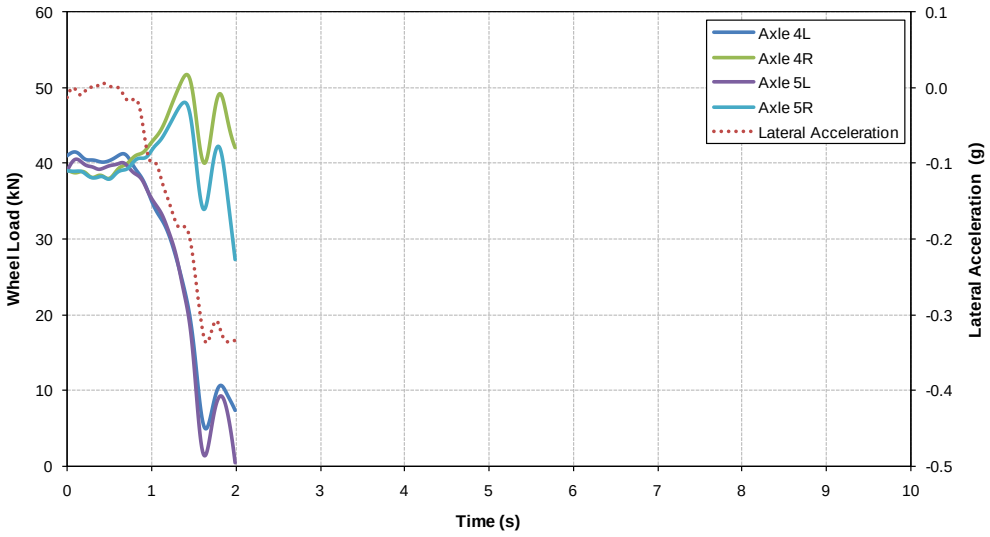

Figure 7-78. Graph. Lane change/ESC system enabled – trailer wheel loads and lateral acceleration (Tanker TC2)

The analysis of the lane change maneuver with the ESC system disabled indicates that Tanker TC2 is less likely to lift a wheel than Tanker TC1. Statistical tests showed that there was a difference in the mean of the distribution of the lateral acceleration at wheel lift between Tanker TC1 and Tanker TC2 for axle 5R, with the latter requiring higher lateral accelerations (on average) to produce wheel lift. This observation was also supported by the fact that out of the five TC1 runs with wheel lift, in four cases the right and left end of axles 4 and 5 lifted (second and third segments of the maneuver), while for the thirteen Tanker TC2 runs, only axles 4R and 5R lifted (second segment of the maneuver).

The test of hypothesis involving the RC parameter showed no statistically significant differences between tankers TC1 and TC2, although Tanker TC2 presented a lower average RC for the trailer during the second segment of the maneuver (i.e., the segment of the maneuver in which wheel lift was always observed under both configurations). Because the lane change maneuver in this phase of the project presented statistically significant higher lateral accelerations than in Phase B (due to higher test speeds), it was not possible to make relevant comparisons between Tanker T and Tanker TC1 and between Tanker T and Tanker TC2. Nevertheless, Tanker TC1 showed a statistically significant lower mean in the RC parameter than Tanker T for the trailer in the first segment of the maneuver, and for the tractor in the second segment. The same was true for Tanker TC2, although the differences were not statistically significant in this case.

Tanker TC2 required less intervention on the part of the ESC system than Tanker TC1.

Second Lane Change Analysis

To identify the point at which lift occurred in the data, a threshold value for the wheel load was established for each of the three segments of the maneuver shown in Figure 7-68. The runs for

each test maneuver, with each suspension, were analyzed to establish the wheel lift threshold. This wheel lift threshold, due to variations in gage zeroing, did not always reflect a true zero, in which case a true horizontal asymptote of the wheel lift, near zero, would be used. This threshold allowed wheel lift to be identified when present. Care was taken to assure the "knee" of the rapidly decreasing strain gage load curve, as it transitioned to a horizontal asymptote, was identified as shown in Figure 7-79.

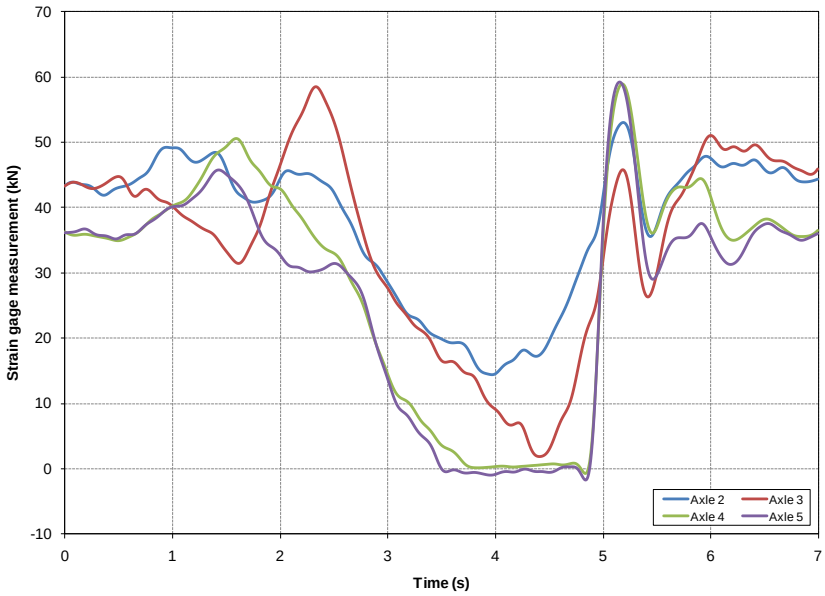

Figure 7-79. Graph. Typical wheel end gage output indicating wheel lift on axles 4 and 5

The time, lift duration, lateral acceleration, roll angle, roll velocity, yaw angle, yaw velocity, yaw acceleration, and articulation angle were all recorded for both tractor and trailer at the instant of wheel lift for each axle (Table 7-16). Although a limited number of runs was used in each maneuver, the average of the data in each of the categories and the standard deviations were assessed. If the standard deviation compared to the average value was determined to be large, the variable being assessed was not analyzed further.

Table 7-16 contains information obtained on segment two of the lane change maneuver. In segment two, the vehicle rolls counter-clockwise and attempts to lift the inside or right side tires. The average lift values for axle 5 were recorded as 0.406 g for Tanker TC1 and 0.388 g for Tanker TC2. Axle 4 lifted subsequent to axle 5 and run values were averaged to be 0.433 g for Tanker TC1 and 0.414 for Tanker TC2.

Table 7-17 contains selected information for segment three of the maneuver. In segment three, the vehicle rolls to the right and tends to lift the left side wheels. The average lateral acceleration value for axle lift was 0.315 g. Axle 4 and axle 5 lifted at approximately the same lateral

accelerations and at approximately the same times for Tanker TC1. No wheel lift was observed for either axle of Tanker TC2 tanker during segment three of the maneuver.

The data that showed promise for identifying differences between Tankers TC1 and TC2 were analyzed further. Figure 7-80 displays the lateral acceleration of the tank trailer at wheel lift, for axles 4 and 5, for both TC1 and TC2 tankers. To compare the behavior of Tankers TC1 and TC2 in the third segment of the lane change maneuver, Figure 7-81, shows lateral accelerations measured during individual runs. The two solid red circles for Tanker TC1 are the trailer lateral accelerations measured at the moment the left wheel on Axle 5 lifted. The higher value was 0.358 g. The three empty green circles for Tanker TC2 are the peak trailer lateral accelerations measured during the third segment of the maneuver, for the three runs. Because the wheels did not lift in these runs, the values can be taken as a lower bound on the lateral acceleration required to lift a trailer wheel on Tanker TC2 in the third segment of the lane change maneuver. As was observed in the step steer, the other transient maneuver, the wheels of Tanker TC2 are more difficult to lift than those of Tanker TC1.

Table 7-16. Wheel lift summary (right wheels) for the lane change maneuver with the ESC system disabled

Wheel lift summary (right wheels-segment 2 of the maneuver)													
Tanker		Axle	Entrance speed (km/h)	Values recorded at the time of wheel lift									
				Time (s)			Lateral acceleration (g)		Roll angle (deg)		Roll velocity (deg/s)	
				Lift	Settle	Duration	Tractor	Trailer	Tractor	Trailer	Tractor	Trailer
TC1	Average	4	55.11	3.767	4.863	1.097	0.504	0.433	-3.413	-4.045	-1.039	-1.562
		5		3.640	4.870	1.230	0.483	0.406	-3.343	-3.877	-0.175	-1.463
	Standard deviation	4	0.544	0.055	0.057	0.102	0.015	0.056	0.121	0.085	0.630	0.327
		5		0.137	0.056	0.171	0.008	0.030	0.075	0.168	0.173	0.076
TC2	Average	4	55.50	3.860	4.788	0.928	0.462	0.414	-3.587	-4.337	-0.181	-1.629
		5		3.733	4.795	1.063	0.488	0.388	-3.527	-4.162	-0.488	-1.228
	Standard deviation	4	0.366	0.042	0.039	0.010	0.015	0.006	0.061	0.070	0.395	0.293
		5		0.036	0.034	0.033	0.007	0.008	0.068	0.057	0.410	0.211

Tanker		Axle	Entrance speed (km/h)	Yaw angle (deg)		Yaw velocity (deg/s)		Yaw acceleration (deg/s^2)		Articulation angle (deg)
				Tractor	Trailer	Tractor	Trailer	Tractor	Trailer	
TC1	Average	4	55.11	-9.292	3.341	19.210	14.654	4.644	7.130	-15.358
		5		-6.889	5.091	18.625	13.721	3.697	7.906	-14.732
	Standard deviation	4	0.544	1.925	1.604	0.420	0.215	0.799	0.952	0.308
		5		1.146	0.849	0.202	0.554	0.378	1.511	0.369
TC2	Average	4	55.50	-8.721	3.213	18.713	15.010	-0.064	6.038	-15.522
		5		-6.330	5.121	18.560	14.214	3.154	7.358	-15.033
	Standard deviation	4	0.366	0.861	0.736	0.129	0.123	2.243	0.195	0.123
		5		1.117	0.997	0.106	0.221	0.971	0.296	0.156

Table 7-17. Wheel lift summary (left wheels) for the lane change maneuver with the ESC system disabled

Wheel lift summary (left wheels-segment 3 of the lane change maneuver)													
Tanker		Axle	Entrance speed (km/hr)	Values recorded at time of wheel lift									
				Time (s)			Lateral acceleration (g)		Roll angle (deg)		Roll velocity (deg/s)	
				Lift	Settle	Duration	Tractor	Trailer	Tractor	Trailer	Tractor	Trailer
TC1	Average	4	55.11	5.360	5.745	0.385	-0.214	-0.315	3.048	3.680	0.945	5.079
		5		5.360	5.740	0.380	-0.214	-0.315	3.048	3.680	0.945	5.079
	Standard deviation	4	0.180	0.042	0.078	0.035	0.028	0.062	0.102	0.176	0.217	0.515
		5		0.042	0.071	0.028	0.028	0.062	0.102	0.176	0.217	0.515
TC2	Average	4	55.50	No Lift			No Lift		No Lift		No Lift	
		5										
	Standard deviation	4	0.198									
		5										

Tanker		Axle	Entrance speed (km/hr)	Values recorded at the time of wheel lift						
				Yaw angle (deg)		Yaw velocity (deg/s)		Yaw acceleration (deg/s^2)		Articulation angle (deg)
				Tractor	Tank trailer	Tractor	Tank trailer	Tractor	Tank trailer	
TC1	Average	4	55.11	-7.253	-13.018	-14.641	-7.492	-1.221	-17.590	9.325
		5		-7.253	-13.018	-14.641	-7.492	-1.221	-17.590	9.325
	Standard deviation	4	0.180	3.356	2.956	0.721	0.547	2.410	2.964	0.310
		5		3.356	2.956	0.721	0.547	2.410	2.964	0.310
TC2	Average	4	55.50	No Lift		No Lift		No Lift		No Lift
		5								
	Standard deviation	4	0.198							
		5								

Table 7-18. Right wheel lift statistical analysis P-value summary during the lane change maneuver, segment 2

Right wheel lift summary, lane change maneuver, segment 2													
Tanker	Axle	Values recorded at the time of wheel lift											
		Time (s)			Lateral acceleration (g)		Roll angle (deg)		Yaw angle (deg)		Yaw velocity (deg/s)		Articulation angle (deg)
		Lift	Settle	Duration	Tractor	Trailer	Tractor	Trailer	Tractor	Trailer	Tractor	Trailer	
TC1 vs. TC2	4	0.499	0.291	0.015	0.003	0.406	0.036	0.002	0.670	0.783	0.018	0.025	0.389
TC1 vs. TC2	5	0.512	0.289	0.048	0.525	0.362	0.010	0.011	0.775	0.877	0.298	0.087	0.125
		Pink shading indicates p-value ≤ 0.05											

Figure 7-82 displays the 95% confidence intervals for the tractor lateral acceleration at the time of wheel lift. When examining the p-values for the lateral acceleration of the tractor at the time of lift of axle 4, a significant statistical difference was observed, with a p-value of 0.018.

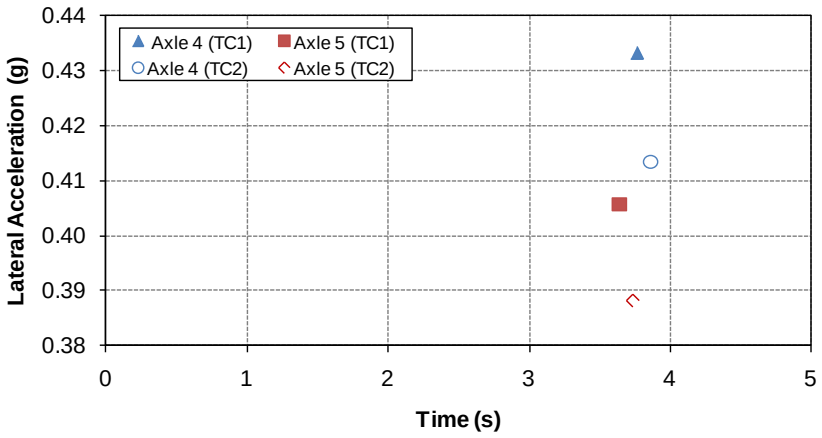

Figure 7-80. Graph. Wheel lift summary (right wheels) tank trailer lateral acceleration vs. time for the lane change maneuver for Tankers TC1 and TC2

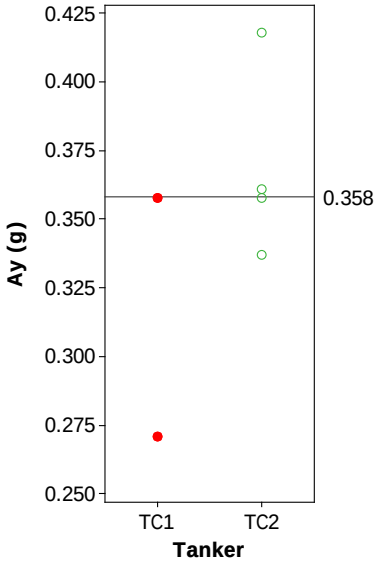

Figure 7-81. Graph. Lateral acceleration at wheel lift in the third segment of the lane change for Tanker TC1 (solid circles) and peak accelerations in the same segment for Tanker TC2, where wheels did not lift (empty circles)

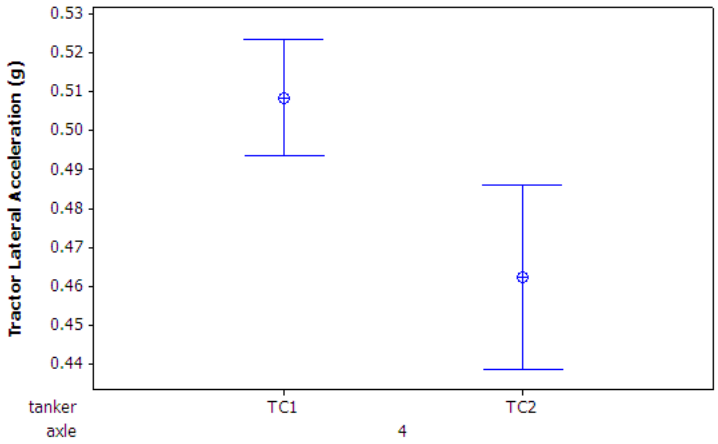

Figure 7-82. Graph. 95% confidence interval for the tractor lateral acceleration at right wheel lift axle 4 lane change maneuver segment 2 for Tankers TC1 and TC2

Figure 7-83 displays the body roll angle of the trailer at lift for axles 4 and 5 for both TC1 and TC2 configurations and Figure 7-84 displays the value with their 95% confidence levels. When examining the lift of axle 4, a significant statistical difference was observed with a p-value of 0.009. Axle 5, however, has a marginal statistical difference with a p-value of 0.089. Also, it would be reasonable to expect lower roll angles for TC1 as it has higher roll stiffness. Figure 7-85 displays the roll angle plotted against lateral accelerations for axle 4 and axle 5 lift. For similar lateral acceleration values, a higher body roll angle was experienced by the trailer for the TC2 tanker.

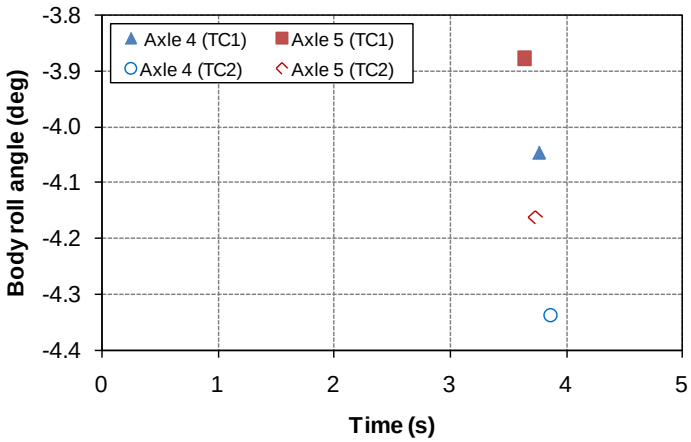

Figure 7-83. Graph. Wheel lift summary (right wheels) trailer body roll angle vs. time for the lane change maneuver

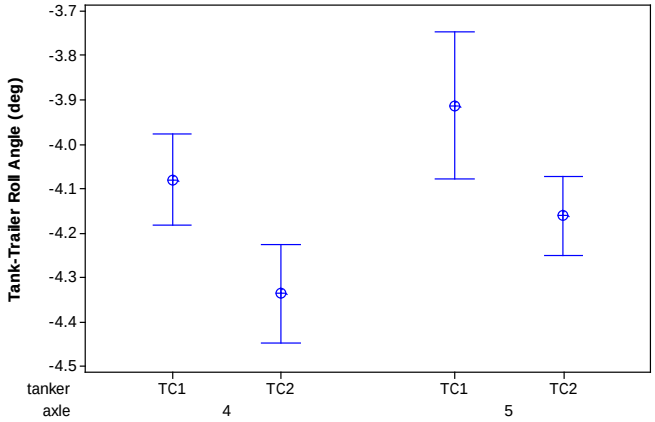

Figure 7-84. Graph. 95% confidence interval for the trailer body roll angle at right wheel lift axle 4 lane change maneuver segment 2 for Tankers TC1 and TC2

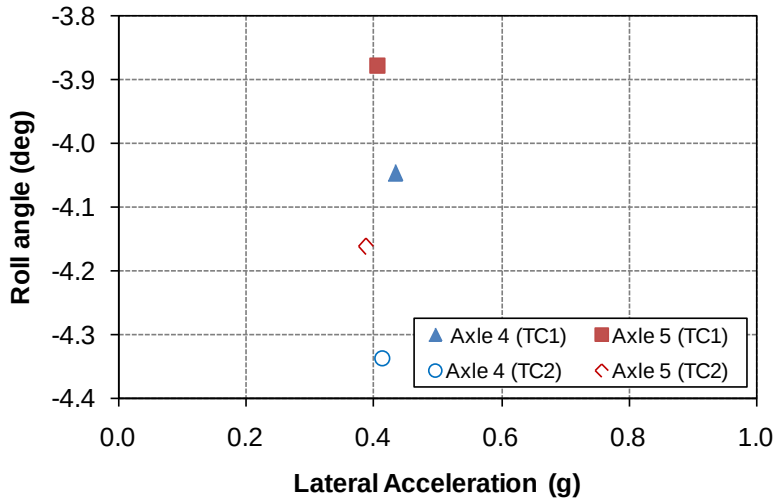

Figure 7-85. Graph. Wheel lift summary (right wheels) roll angle vs. lateral acceleration for the lane change maneuver

Suspension TC1 shows a lower trailer yaw velocity at the time of wheel lift for both axles 4 and 5. However, the difference for axle 4 was marginal, with a p-value of 0.082, shown in Figure 7-86, and axle 5 did not show a statistically significant difference.

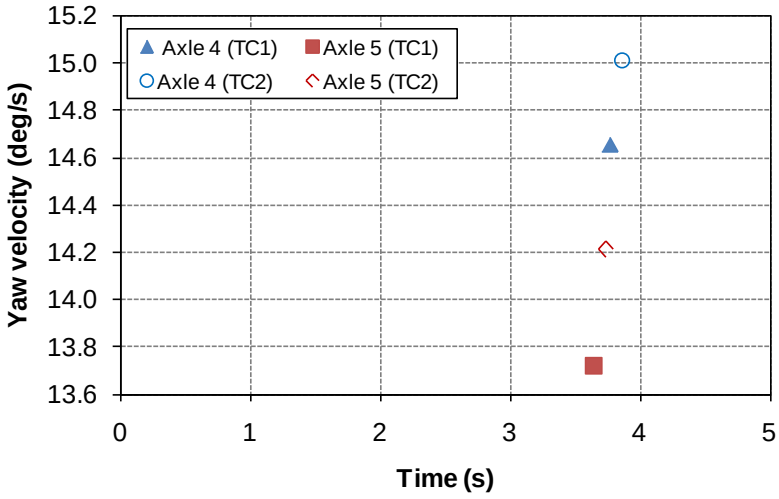

Figure 7-86. Graph. Wheel lift summary (right wheels) yaw velocity vs. time for the lane change maneuver

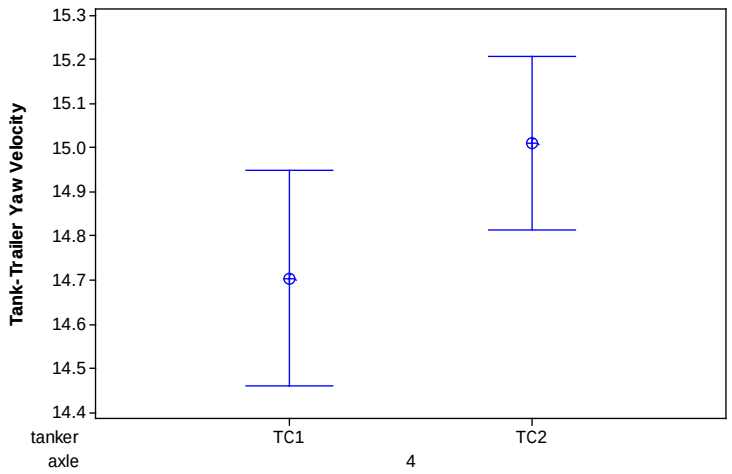

Figure 7-87. Graph. 95% confidence interval for trailer yaw velocity at right wheel lift axle 4 during the lane change maneuver, segment 2

The values of yaw acceleration (Figure 7-88) differ for the two tankers, with Tanker TC1 showing a higher value at the time of both axle 4 and 5 wheel lift.

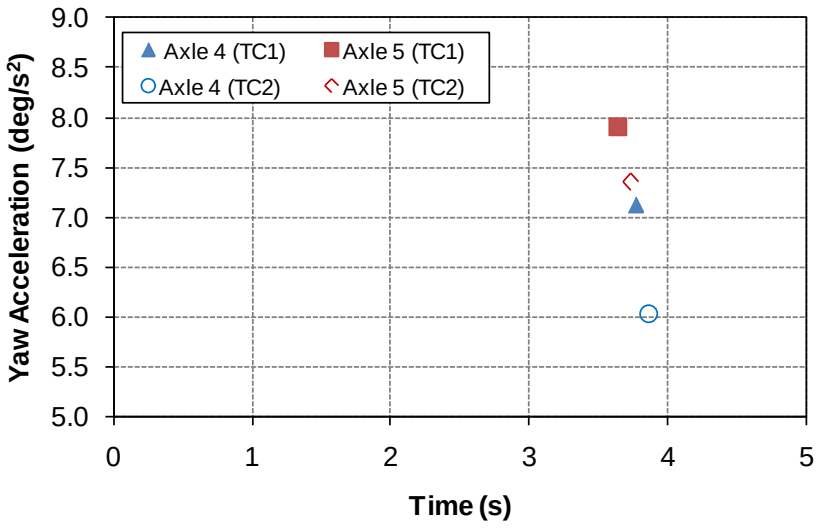

Figure 7-88. Graph. Wheel lift summary (right wheels) yaw acceleration vs. time for the lane change maneuver

Figure 7-89 presents the articulation angle versus time. A lower articulation angle for Tanker TC1 is consistent with the yaw acceleration shown in Figure 7-88. This value was not analyzed for statistical significance.

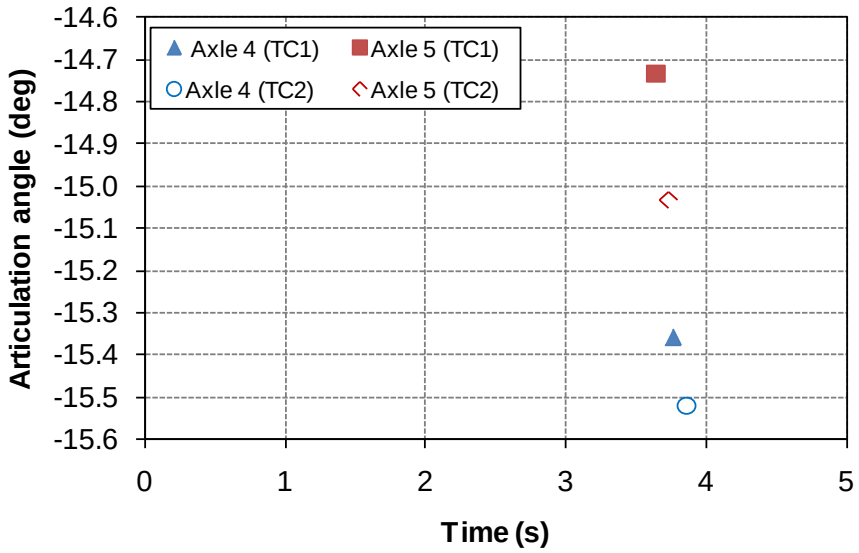

Figure 7-89. Graph. Wheel lift summary (right wheels) articulation angle vs. time for the lane change maneuver

The peak values of six quantities in each segment of the maneuver were recorded. They are listed in Table 7-19. The peak values are the highest value achieved in each segment of the test, which did not necessarily correspond to the point of wheel lift. Table 7-20 lists the p-values for the comparisons between Tankers TC1 and TC2.

Table 7-19. Peak value summary for the lane change maneuver by segments (1, 2, and 3)

Tanker		Maneuver segment	Entrance speed (km/hr)	Lateral acceleration (g)		Lateral velocity (m/s)		Roll angle (deg)	
				Tractor	Trailer	Tractor	Trailer	Tractor	Trailer
TC1	Average	1	55.11	-0.417	-0.352	0.404	-0.077	3.084	3.484
		2		0.507	0.453	-0.424	0.895	-3.509	-7.047
		3		-0.364	-0.383	0.422	-0.077	2.973	4.110
	Standard deviation	1	0.544	0.009	0.025	0.017	0.009	0.113	0.188
		2		0.017	0.003	0.065	0.049	0.154	0.971
		3		0.007	0.010	0.050	0.027	0.181	0.417
TC2	Average	1	55.50	-0.432	-0.360	0.567	-0.224	3.115	3.918
		2		0.493	0.442	-0.353	0.664	-3.598	-6.373
		3		-0.371	-0.369	0.509	-0.250	2.409	3.727
	Standard deviation	1	0.366	0.007	0.011	0.005	0.031	0.009	0.043
		2		0.005	0.006	0.012	0.025	0.051	0.216
		3		0.006	0.035	0.025	0.026	0.087	0.052

Tanker		Maneuver segment	Entrance speed (km/hr)	Yaw angle (deg)		Axle torsion (N·m)		Articulation angle
				Tractor	Trailer	Axle 4	Axle 5	(deg)
TC1	Average	1	55.11	14.974	12.979	24558.667	23947.333	10.808
		2		-17.838	-13.747	-29770.000	-27661.000	-16.137
		3		No Peak	No Peak	25046.667	24442.667	9.581
	Standard deviation	1	0.544	1.489	1.413	1027.922	1106.194	0.396
		2		2.321	2.314	234.774	323.116	0.373
		3		No Peak	No Peak	2163.087	2198.634	0.292
TC2	Average	1	55.50	4.025	3.515	6396.781	6263.326	3.425
		2		-5.170	-3.807	-9845.073	-9112.618	-5.252
		3		No Peak	No Peak	9069.922	8880.442	3.308
	Standard deviation	1	0.366	7.344	6.356	12117.612	11800.868	5.029
		2		11.031	8.685	17255.892	16064.183	9.429
		3		No Peak	No Peak	13878.473	13522.041	5.434

Table 7-20. P-values for comparing peaks of quantities recorded during the lane change maneuver

Tanker	Maneuver segment	Lateral acceleration (g)		Lateral velocity (m/s)		Roll angle (deg)		Yaw angle (deg)		Measured axle torsion (N·m)		Articulation angle
		Tractor	Trailer	Tractor	Trailer	Tractor	Trailer	Tractor	Trailer	Axle 4	Axle 5	(deg)
TC1 vs. TC2	1	0.074	0.669	0.002	0.001	0.68	0.052	0.122	0.310	0.019	0.021	0.133
TC1 vs. TC2	2	0.273	0.023	0.198	0.006	0.426	0.352	0.157	0.265	0.000	0.002	0.275
TC1 vs. TC2	3	0.195	0.486	0.078	0.001	0.020	0.252	No Peak	No Peak	0.510	0.346	0.179
		Pink shading indicates p-value ≤ 0.05										

First, the lateral acceleration peaks were examined (Figure 7-90). The p-value of 0.074 for the tractor during segment one showed a marginal statistical difference in lateral acceleration with Tanker TC1 being 0.015 g greater than Tanker TC2. The p-value of 0.023 for the tank trailer during segment two showed a strong statistical difference in lateral acceleration with Tanker TC1 being 0.011 g greater than Tanker TC2 (Figure 7-91).

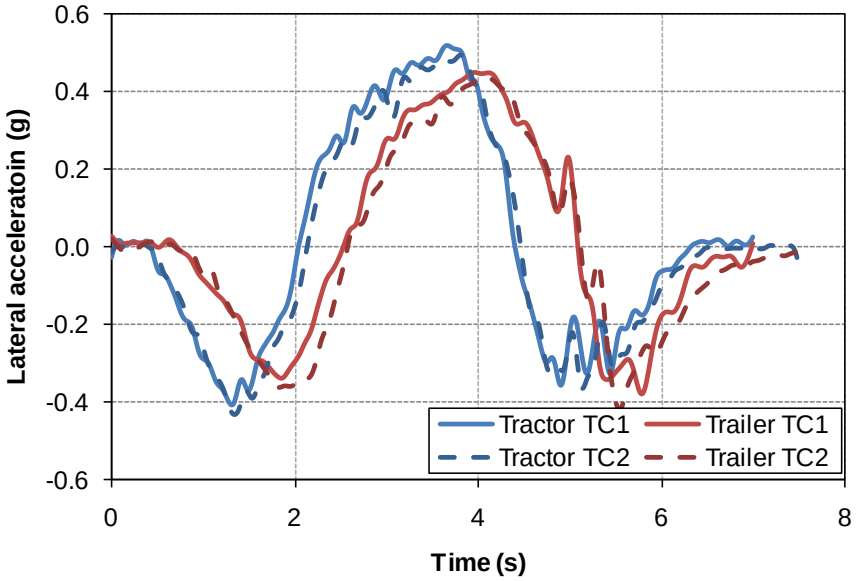

Figure 7-90. Graph. Example lateral acceleration vs. time during the lane change maneuver

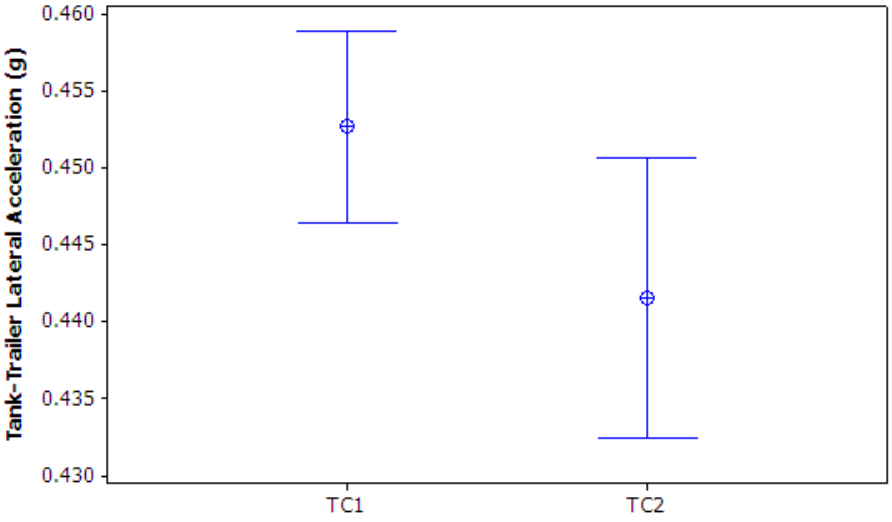

Figure 7-91. Graph. 95% confidence interval for peak trailer lateral acceleration during the lane change maneuver, segment 2

The body roll angle for the tractor and trailer (Figure 7-73) throughout the maneuver was analyzed. The tank trailer shows a lag in the body roll angle compared to the body roll angle of the tractor. Tanker TC1 shows a lower trailer body roll angle in segment one but shows a higher body roll angle in segments two and three. This difference in segment one shows a marginal statistical benefit for Tanker TC1 based on a p-value of 0.052 (Figure 7-93).

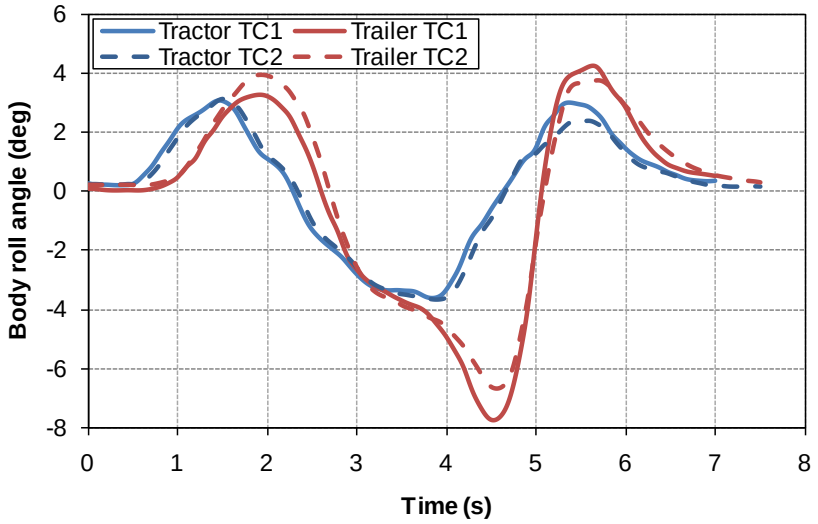

Figure 7-92. Graph. Example body roll angle vs. time during the lane change maneuver

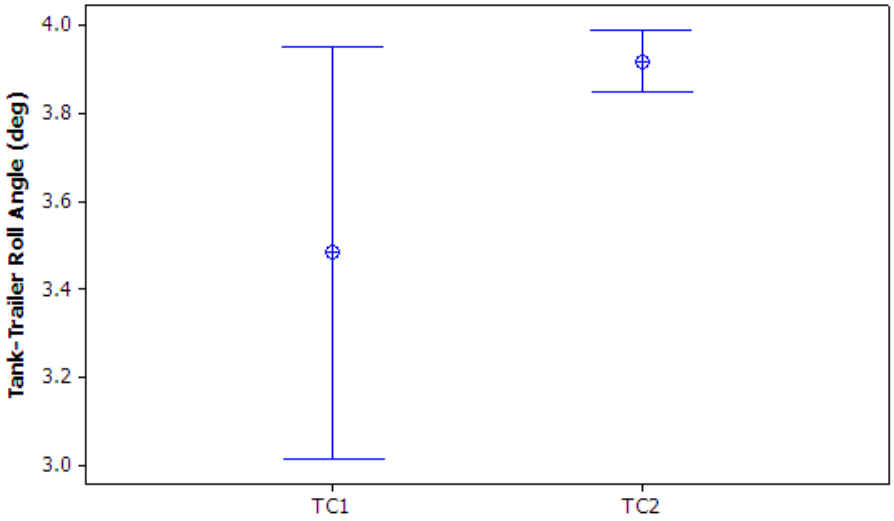

Figure 7-93. Graph. 95% confidence interval for peak trailer body roll angle lane change maneuver segment 1

Lateral velocity was examined in Figure 7-94 and articulation angle in Figure 7-95. While there was a difference in average values for articulation angle, no statistical difference was found.

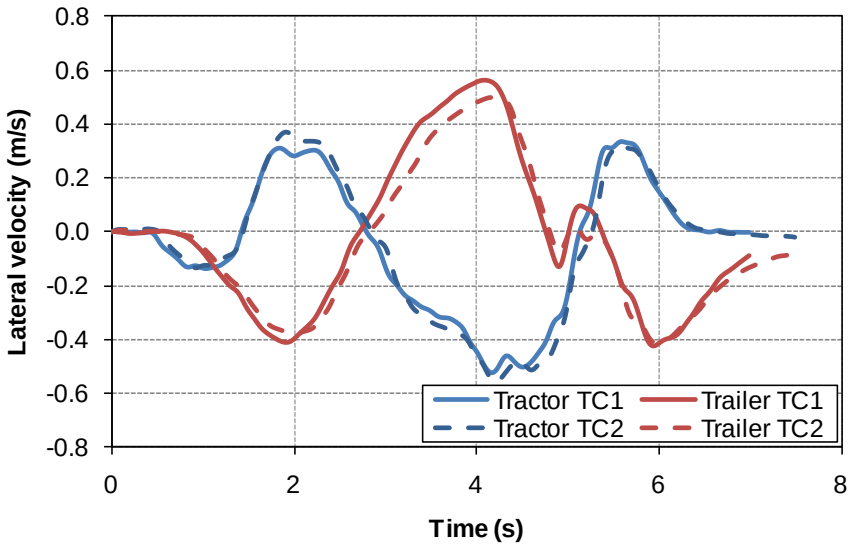

Figure 7-94. Graph. Example lateral velocity vs. time lane change maneuver

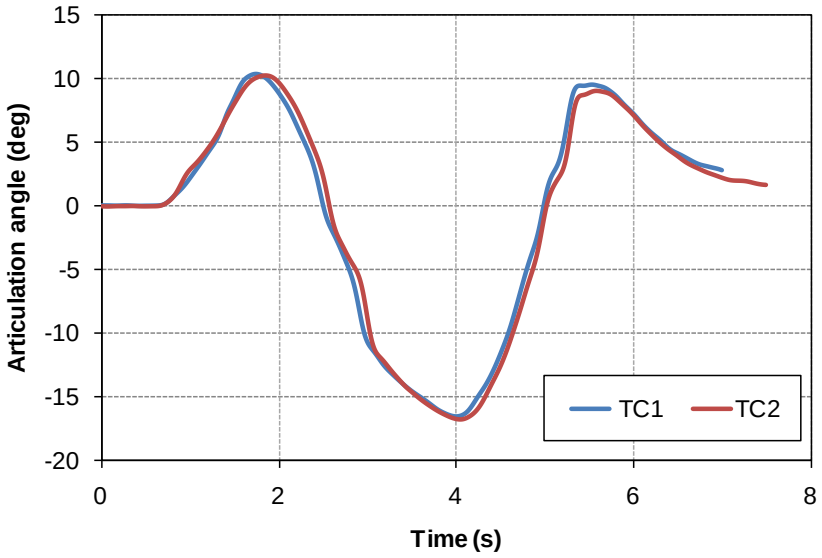

Figure 7-95. Graph. Example articulation angle vs. time lane change maneuver

The strain gage-measured axle torque is shown in Figure 7-96. This shows a consistency with the roll angle of the trailer for Tanker TC1. The statistical significance of the measured axle torsion is shown in Figure 7-97.

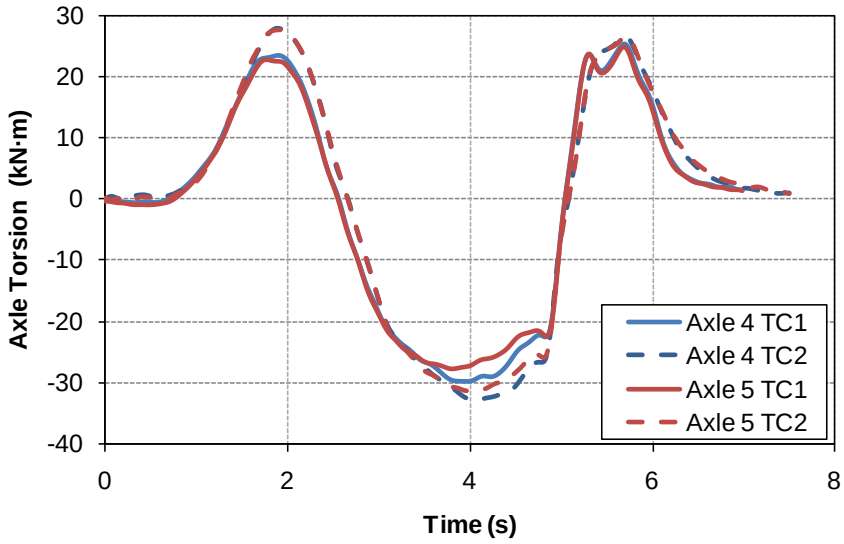

Figure 7-96. Graph. Example measured trailer axle torsion vs. time lane change maneuver

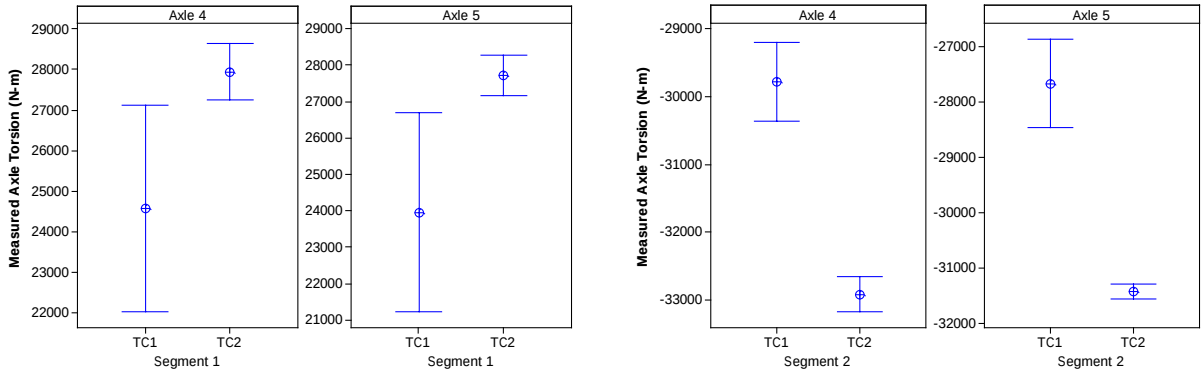

Figure 7-97. Graph. 95% confidence interval for peak measured trailer axle torsion lane change maneuver segments 1 and 2

Fifth wheel separation

To understand the decoupling of the tractor and the trailer during the lane change maneuver, the separation of the fifth wheel was examined. To indicate fifth wheel separation, video data was analyzed for the start of the maneuver to correlate with the data recorded through the eDAQ system, the time of separation, the time at which the fifth wheel separation was at a maximum or "topped out," the time at which the maximum separation ended, and the time at which the fifth wheel reconnected. At the time of separation, the values of lateral acceleration, roll angle, roll velocity, yaw angle, yaw velocity, yaw acceleration, and articulation angle were recorded and are shown in Table 7-21.

Table 7-21. Fifth wheel separation summary for the lane change maneuver with the ESC system disabled

Tanker		Entrance speed (km/hr)	Values recorded at the time of fifth wheel separation									
			Time (s)						Lateral acceleration (g)		Roll angle (deg)	
			Lift	Reconnect	Duration	Maximum Separation Start	Maximum Separation End	Duration	Tractor	Trailer	Tractor	Trailer
TC1	Average	55.11	3.60	4.57	0.97	3.81	4.13	0.31	0.478	0.409	-3.327	-3.823
	Standard deviation	0.544	0.07	0.09	0.15	0.10	0.10	0.05	0.008	0.038	0.066	0.070
TC2	Average	55.50	3.658	4.605	0.948	3.888	4.133	0.245	0.479	0.372	-3.497	-3.988
	Standard deviation	0.366	0.071	0.161	0.173	0.089	0.076	0.068	0.009	0.022	0.072	0.161

Tanker		Entrance speed (km/hr)	Values recorded at the time of fifth wheel separation								
			Roll velocity (deg/s)		Yaw angle (deg)		Yaw velocity (deg/s)		Yaw Acceleration (deg/s^2)		Articulation Angle (deg)
			Tractor	Trailer	Tractor	Trailer	Tractor	Trailer	Tractor	Trailer	
TC1	Average	55.11	-0.392	-1.390	-6.213	5.666	18.474	13.395	2.951	8.074	-14.546
	Standard deviation	0.544	0.355	0.168	1.848	1.577	0.326	0.294	1.198	0.704	0.372
TC2	Average	55.50	0.049	-1.262	-4.001	6.831	18.195	13.252	1.798	9.020	-14.427
	Standard deviation	0.366	0.455	0.334	2.466	1.876	0.357	0.886	0.465	0.983	0.593

Table 7-22. Fifth wheel separation statistical analysis p-value summary during the lane change maneuver

Tanker	Time (s)	Values recorded at the time of fifth wheel separation						
		Lateral acceleration (g)		Roll angle (deg)		Yaw acceleration (deg/s^2)		Articulation angle (deg)
	Duration	Tractor	Trailer	Tractor	Trailer	Tractor	Trailer	
TC1 vs. TC2	0.8603	0.8209	0.2333	0.0256	0.1363	N/A	0.1979	0.7591
	Pink shading indicates p-value ≤ 0.05							

A strong difference was observed for the tractor body roll angle with Tanker TC2 having a 0.170 deg higher roll angle at fifth wheel separation with a p-value of 0.0256. The two means, with their respective 95% confidences, are shown in Figure 7-98.

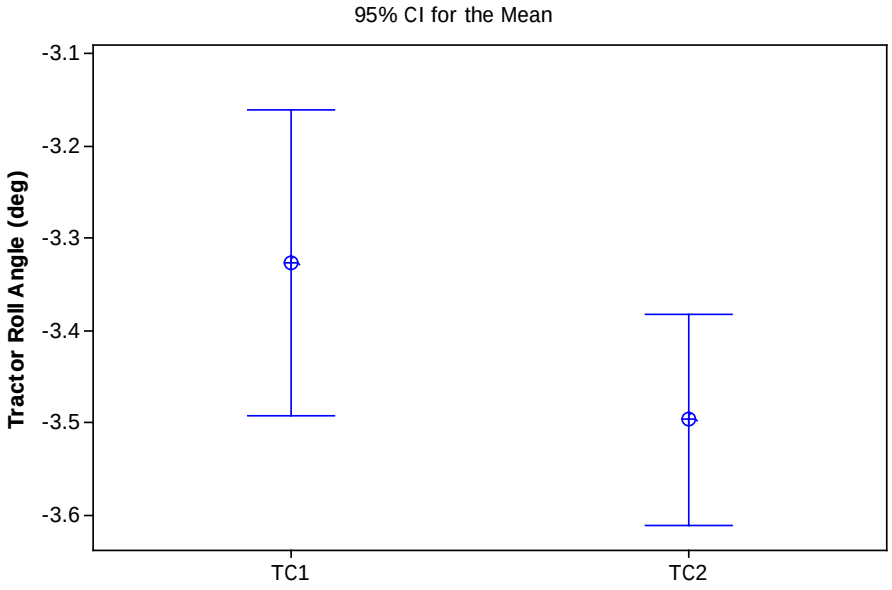

Figure 7-98. Graph. 95% confidence interval for the tractor body roll angle at fifth wheel separation during the lane change maneuver

The body roll angles for the tractor and tank trailer at fifth wheel separation show differences between Tankers TC1 and TC2, with Tanker TC1 having lower roll angles as shown in Figure 7-99 and Figure 7-100. Figure 7-101 shows the articulation angle at fifth wheel separation with Tanker TC1 having the greater articulation angle.

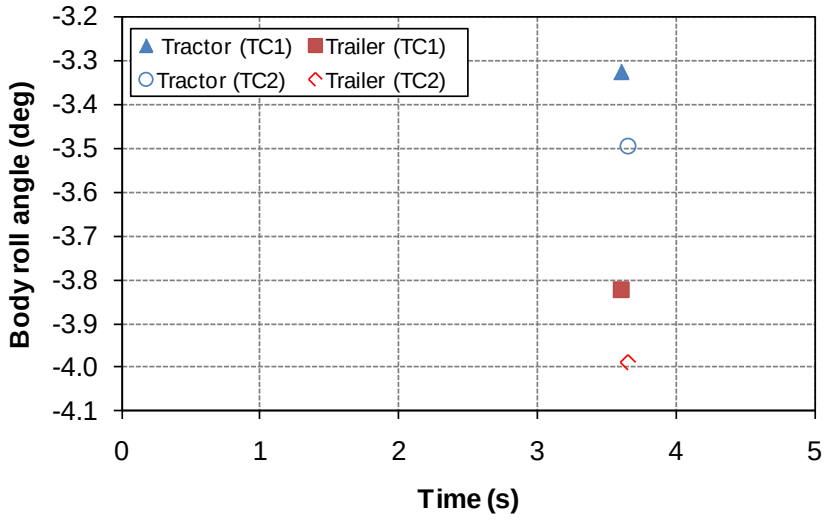

Figure 7-99. Graph. Fifth wheel separation body roll angles vs. time during the lane change maneuver

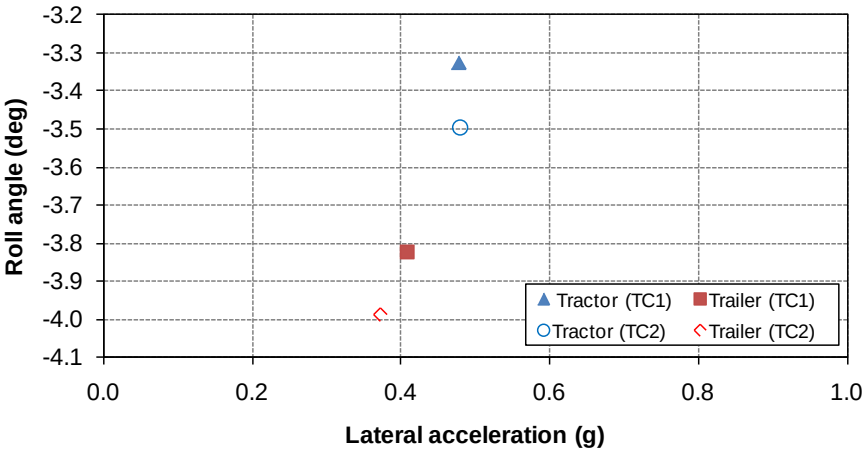

Figure 7-100. Graph. Fifth wheel separation roll angle vs. lateral acceleration during the lane change maneuver

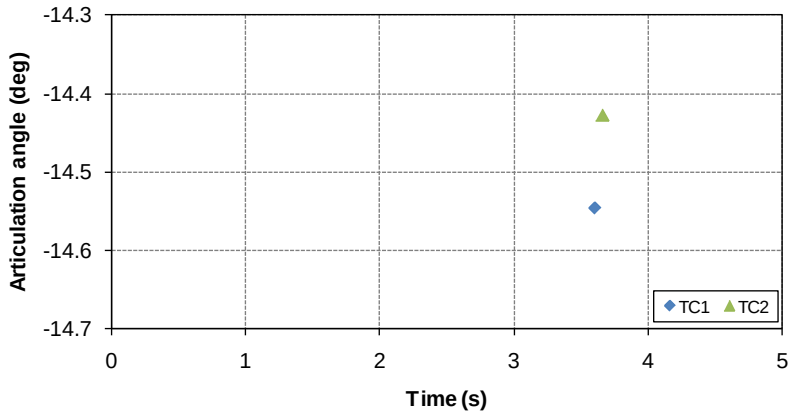

Figure 7-101. Graph. Fifth wheel separation articulation angle vs. time during the lane change maneuver

ESC system activation

To determine the point at which the ESC system activated during the lane change maneuver, the roll stability system Brake Control Activation Indicator within the tractor's CAN bus data was monitored. As shown in Figure 7-102, activation was confirmed by the increase in the Axle 2 brake pressure. Activation always occurred in the first segment of the lane change maneuver. The time of activation, as well as the lateral acceleration, roll angle, roll velocity, yaw angle, yaw velocity, and yaw acceleration were recorded (see Table 7-23). The tractor always experiences the lateral acceleration before the trailer in a maneuver. As a result the delay in lateral acceleration of the trailer would always result in a tractor ESC activating first, given the same activation threshold for tractor and trailer. The list was narrowed to what was deemed appropriate for statistical analysis to determine if there were a difference in ESC system activation between Tankers TC1 and TC2. The p-values are shown in Table 7-24.

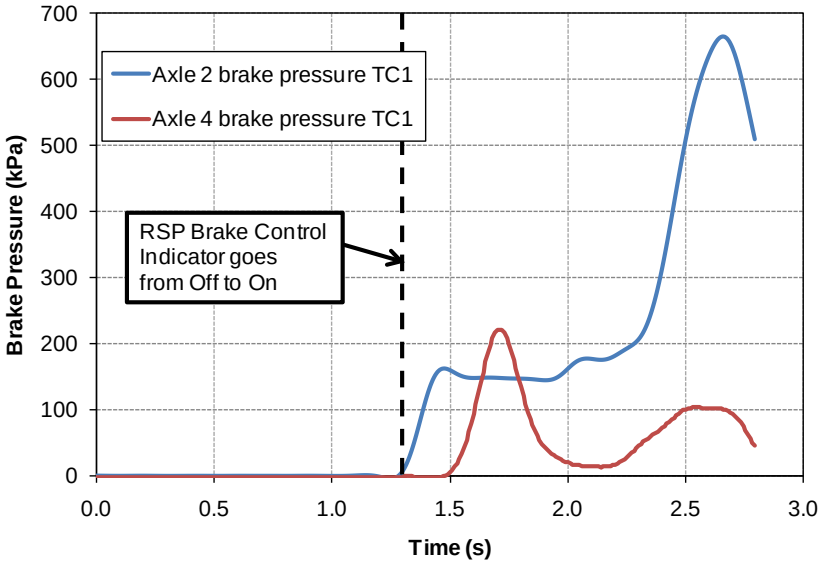

Figure 7-102. Graph. Example of ESC system activation indication during the lane change maneuver

Table 7-23. ESC system activation summary for the lane change maneuver

Tanker		Entrance speed (km/hr)	Time (s)	Lateral acceleration (g)		Roll angle (deg)		Roll velocity (deg/s)	
				Tractor	Tank trailer	Tractor	Tank trailer	Tractor	Tank trailer
TC1	Average	55.052	1.278	-0.399	-0.162	2.648	1.426	1.821	4.654
	Standard deviation	0.225	0.056	0.023	0.010	0.006	0.153	0.525	0.251
TC2	Average	55.066	1.224	-0.400	-0.149	2.497	1.361	2.192	5.218
	Standard deviation	0.439	0.023	0.014	0.016	0.163	0.190	0.294	0.357

Tanker		Entrance speed (km/hr)	Time (s)	Yaw angle (deg)		Yaw velocity (deg/s)		Yaw acceleration (deg/s^2)		Articulation angle (deg)
				Tractor	Tank trailer	Tractor	Tank trailer	Tractor	Tank trailer	
TC1	Average	55.052	1.278	5.313	1.091	-15.465	-4.433	-20.348	-13.512	3.860
	Standard deviation	0.225	0.056	0.657	0.679	1.193	0.557	3.049	0.856	0.520
TC2	Average	55.066	1.224	6.469	1.770	-15.450	-4.295	-20.392	-12.945	4.729
	Standard deviation	0.439	0.023	0.623	0.487	0.504	0.401	2.672	1.052	0.564

Table 7-24. ESC system activation statistical analysis p-value summary during the lane change maneuver

Tanker	Values are recorded at the time of ESC system activation								
	Lateral acceleration (g)		Roll Angle (deg)		Roll Velocity (deg/s)		Yaw Angle (deg)		Articulation Angle (deg)
	Tractor	Tank trailer	Tractor	Tank trailer	Tractor	Tank trailer	Tractor	Tank trailer	
TC1 vs. TC2	0.9562	0.1670	0.1067	0.5919	0.2682	0.0275	0.0341	0.1497	0.0485
	Pink shading indicates p-value ≤ 0.05								

The trailer roll velocity at the time of ESC system activation was higher for Tanker TC2 than for Tanker TC1 by 0.565 deg/s. The p-value of the difference is 0.0275, which is marginal. The average values of tractor and tank trailer roll velocity at the time of ESC system activation are shown in Figure 7-104. While not statistically significant, the tractor roll velocity at the time of activation shows a similar trend.

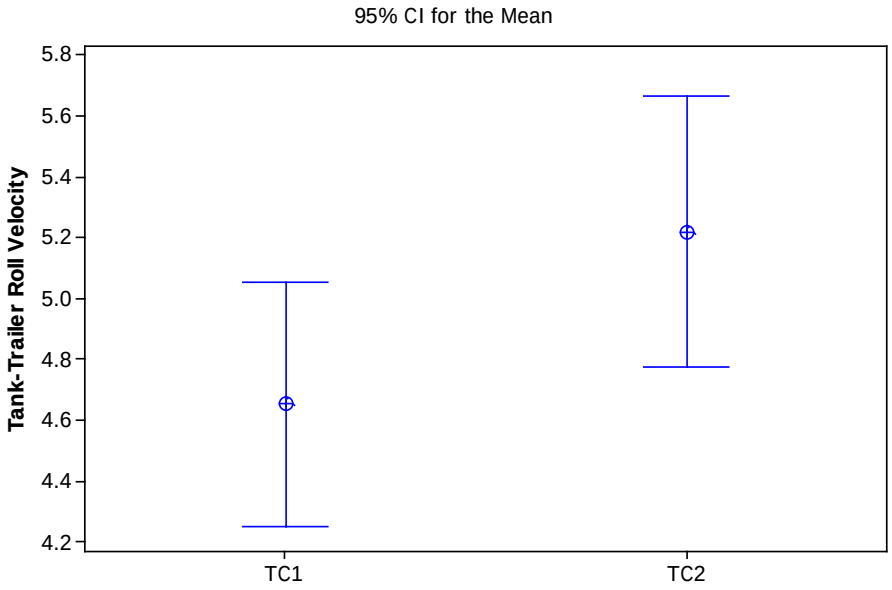

Figure 7-103. Graph. 95% confidence interval for tank trailer body roll velocity at ESC system activation for the lane change maneuver for Tankers TC1 and TC2

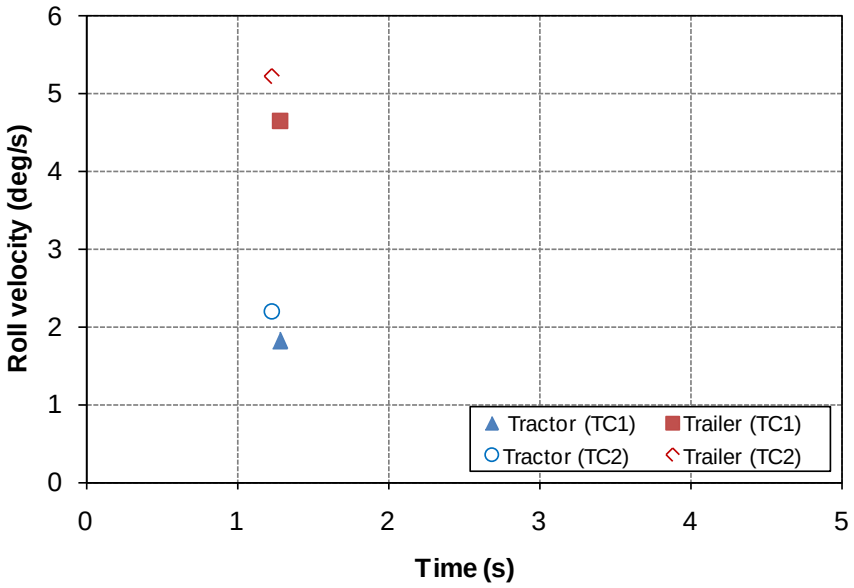

Figure 7-104. Graph. ESC system activation summary roll velocity vs. time for the lane change maneuver

The articulation angle at the time of ESC system activation was higher with Tanker TC2 than with Tanker TC1 by 0.869 deg (Figure 7-105). The difference was significant with a p-value of 0.0485.

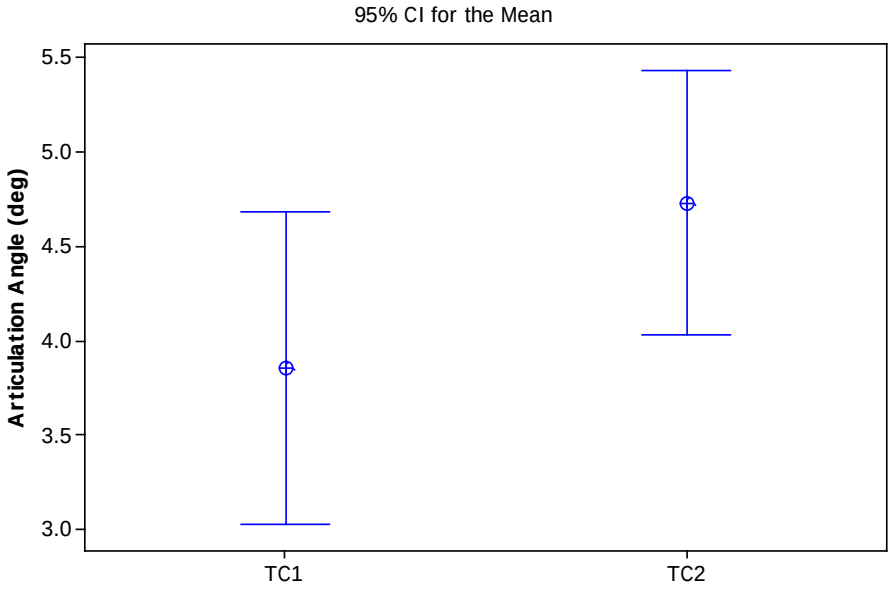

Figure 7-105. Graph. 95% confidence interval for trailer body roll velocity at ESC system activation for the lane change maneuver

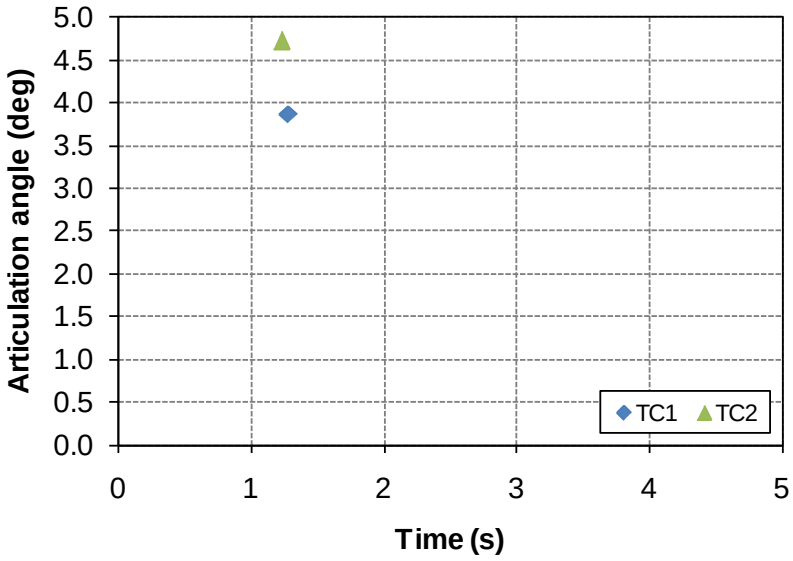

Figure 7-106. Graph. ESC system activation summary articulation angle vs. time for the lane change maneuver

As shown in Figure 7-107 and Figure 7-108, the lateral acceleration and body roll angle for the trailer at the time of ESC system activation are similar for both Tankers TC1 and TC2. This behavior is expected and noteworthy.

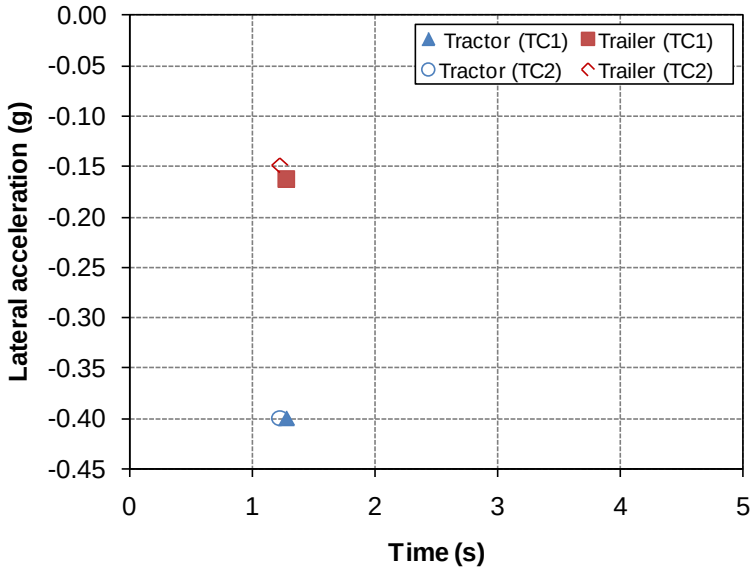

Figure 7-107. Graph. ESC system activation summary lateral acceleration vs. time for the lane change maneuver

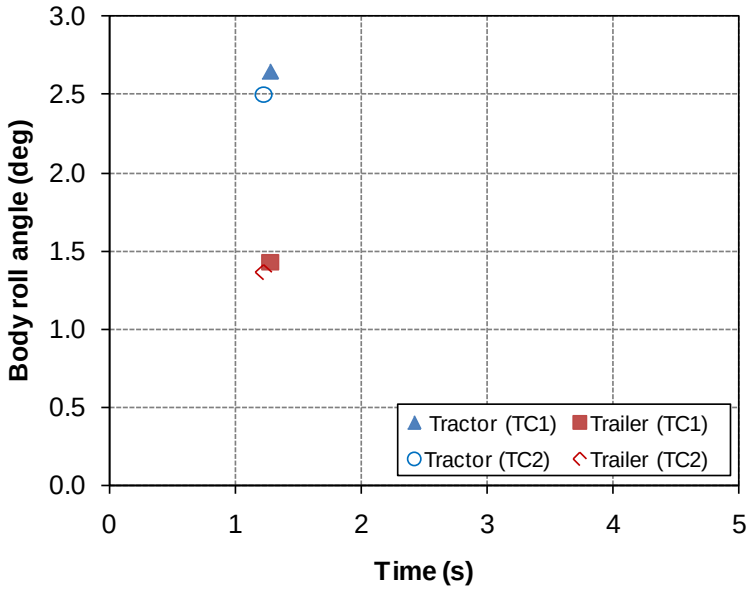

Figure 7-108. Graph. ESC system activation summary body roll angle vs. time for the lane change maneuver

Summary conclusions for the TC1 and TC2 suspension configurations

Consistent throughout the lane change maneuver were slight advantages to Tanker TC1 over Tanker TC2. While not always shown in the statistical analysis for the chosen p-value data, the average values showed an advantage of Tanker TC1 over Tanker TC2. These advantages were shown in roll angle reductions, in slight lateral acceleration advantages, and in some of the transient response characteristics.

The discovery of the air bag contribution to roll damping, although only considered as a part of the total roll damping, was considered significant enough to examine its potential contribution in the lane change maneuver.

Shown in Figure 7-109 for the TC1 suspension and in Figure 7-110 for the TC2 suspension are the air bag damping moments plotted with the roll angular velocity of the trailer, obtained from the RT unit, for the lane change maneuver. The differences between the two suspensions are quite visible in the plots. The plotted damping moments are the sum of both axles of the tandem.

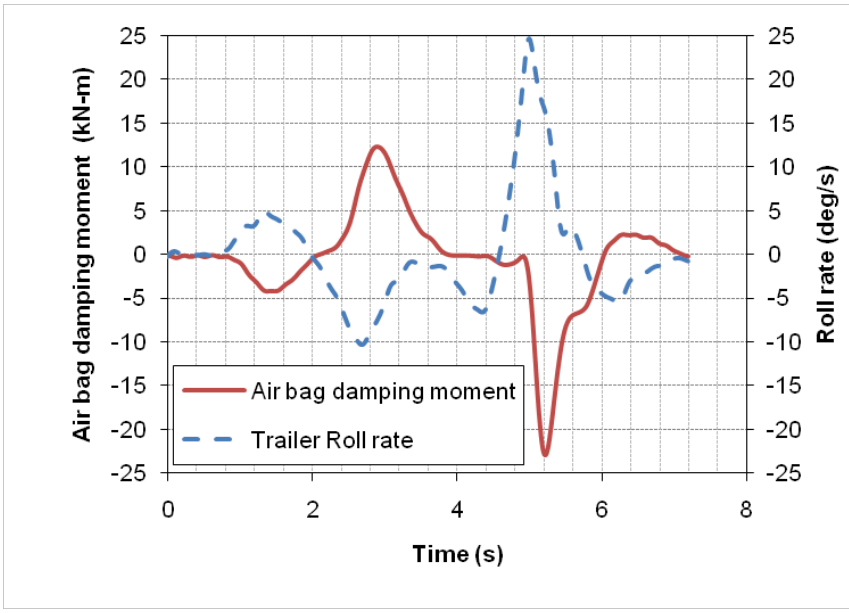

Figure 7-109. Graph. Air bag damping in the lane change maneuver for Tanker TC1

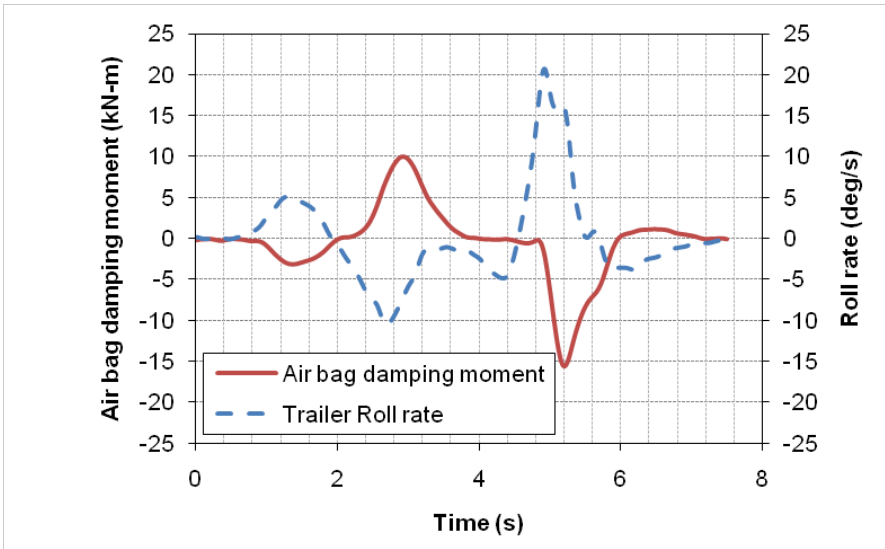

Figure 7-110. Graph. Air bag damping in the lane change maneuver for Tanker TC2

Table 7-25 presents the peak air bag moment recorded during each segment of the lane change maneuver. The roll rates are the values at the time when the peak air bag moment was recorded.

Table 7-25. Calculated air bag effects during the lane change maneuver

Lane change maneuver Calculated air bag effects from differential pressures						
Tanker	Axle run number	Segment number	Time	Roll rate at the instant of peak air bag moment	Peak air bag moment	Air bag damping coefficient.
			s	deg/s	N•m	N•m-s/deg
TC1	TC1-1	1	1.4	4.38	-3622	-828
	TC1-2	1	1.39	4.44	-3376	-760
	TC1-3	1	1.38	4.77	-3489	-731
	Average	TC1 seg 1	1.39	4.53	-3496	-773
	Std dev.	TC1 seg 1	0.008	0.171	101	41
	TC1-1	2	2.81	-6.8	9669	-1421
	TC1-2	2	2.85	-6.88	10012	-1456
	TC1-3	2	2.9	-7.51	10024	-1362
	Average	TC1 seg 2	2.853	-7.06	9902	-1413
	Std dev.	TC1 seg 2	0.037	0.32	165	39
	TC1-1	3	5.17	16.18	-20204	-1249
	TC1-2	3	5.18	13.66	-14900	-1090
	TC1-3	3	5.22	15.9	-19026	-1197
	Average	TC1 seg 3	5.19	15.2	-18043	-1179
	Std dev.	TC1 seg 3	0.022	1.128	2274	66
TC2	TC2-1	1	1.39	4.94	-2646	-535
	TC2-2	1	1.37	5.08	-2614	-514
	TC2-3	1	1.31	4.98	-2508	-504
	TC2-4	1	1.29	5.1	-2680	-526
	Average	TC2 seg 1	1.34	5.03	-2612	-520
	Std dev.	TC2 seg 1	0.04	0.07	64	12
	TC2-1	2	2.85	-7.76	8646	-1114
	TC2-2	2	2.93	-7.23	8338	-1154
	TC2-3	2	2.88	-7.83	7841	-1002
	TC2-4	2	2.86	-7.1	7960	-1121
	Average	TC2 seg 2	2.88	-7.48	8196	-1098
	Std dev.	TC2 seg 2	0.03	0.32	318	57
	TC2-1	3	5.14	14.32	-12435	-868
	TC2-2	3	5.2	15.47	-12984	-839
	TC2-3	3	5.17	14.7	-12495	-850
	TC2-4	3	5.14	14.87	-12866	-865
	Average	TC2 seg 3	5.16	14.84	-12695	-856
	Std dev.	TC2 seg 3	0.02	0.41	235	12

Figure 7-111 demonstrates the difference in the air bag damping coefficient between Tanker TC1 and Tanker TC2. Conclusive is the fact that Tanker TC1, with the greater beam spacing, provides a greater roll damping coefficient. Figure 7-112 plots the effective moment due to the air bag differential pressures for Tankers TC1 and TC2. The three clusters of points in the figure are from the three segments of the lane change maneuver. The benefits of beam center spacing are diminished as the roll velocity of the trailer decreases.

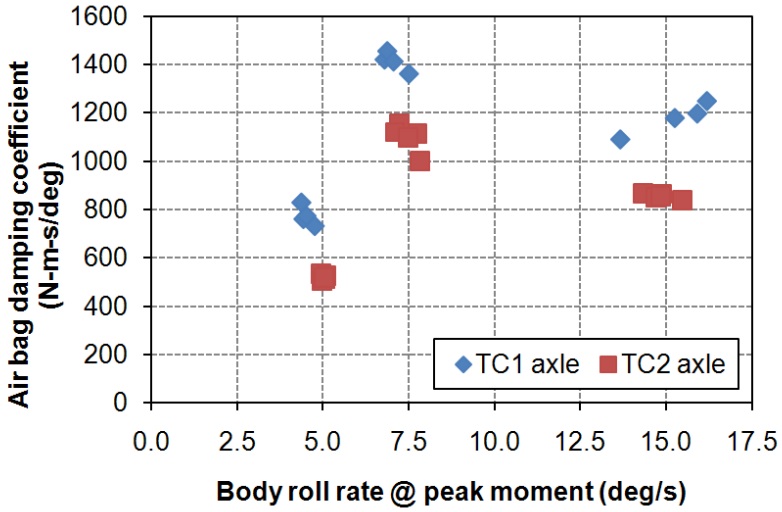

Figure 7-111. Graph. Air bag damping coefficients as a function of body roll rate

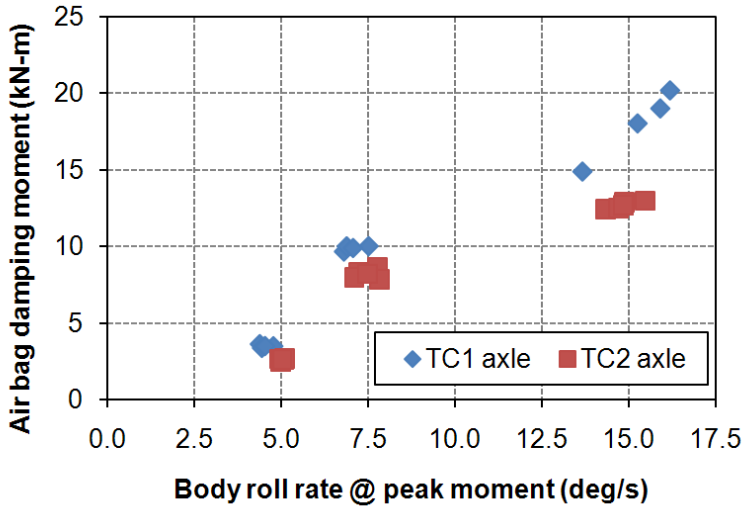

Figure 7-112. Graph. Axle moments, which add damping, as a function of body roll rates

7.7 Comparison of Modeling Predictions with Test Track Behavior

The TruckSim® rigid body model that was developed in earlier phases and discussed in Section 4.1 of this report performed well in predicting the test vehicle's behavior. The wheel loading and accelerations predicted by the model matched the data recorded on the test track. Results of the ramp steer, step steer, and open-loop double lane change maneuvers are compared.

7.7.1 Ramp Steer Maneuver

The experimental data agreed with the model's values, both as to control inputs and to the vehicle's response.

Steering Input

The road wheel angle, which is directly related to the hand wheel angle through the steering box ratio and any compliance which is present in the system, is shown in Figure 7-113.

The hand wheel angle for steering and the speed for the model were compared with the experimental data from Phase C. The steering rates (hand wheel angle per unit time) were input into TruckSim® as an open loop steer control.

Figure 7-113 shows the robot steer input in dark red, and the steering input used in TruckSim® in dashed red (major axis). The steering wheel potentiometer angle was used in the simulation as it provided the most accurate input to the road wheels, showing a slight sinusoidal shaped input. The road wheel angle (minor axis) is also shown, with the left front road wheel angle from Phase C plotted in dark blue and the left front road wheel angle from TruckSim® plotted in medium blue.

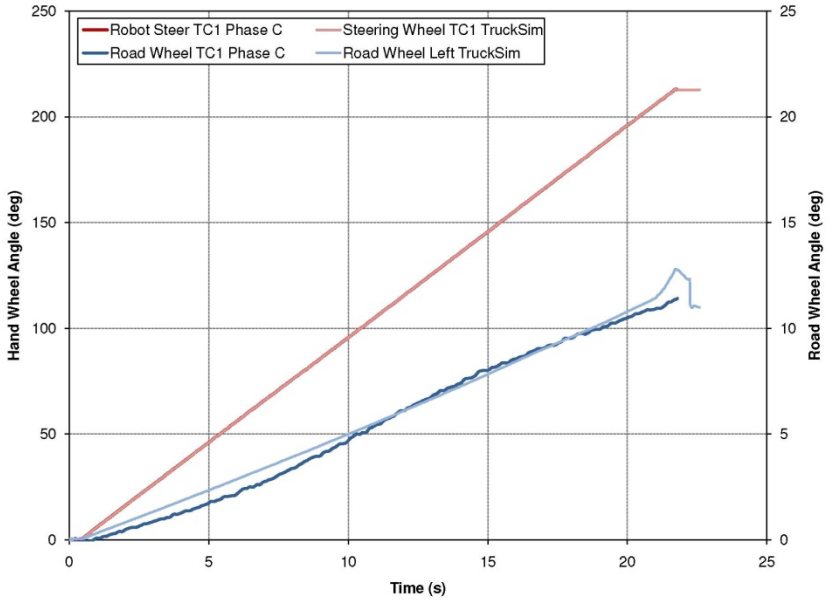

Figure 7-113. Graph. Model confirmation: Steering vs. time

The positions of the tractor and tank trailer were compared with the model to determine the accuracy of the path followed by both units. This characteristic is highly sensitive to tire cornering stiffness and any roll and compliance steer. The model comparison was deemed to be acceptable.

With the maneuver verified, the vehicle behavior and response could then be compared. First, the vehicles steering performance was evaluated by comparing hand wheel input and road wheel angle versus lateral acceleration, shown in Figure 7-114 and Figure 7-115. The final model responded nearly perfectly to the steering input as to the lateral accelerations achieved. The parameter that is being assessed is referred to as lateral acceleration gain, which is a fundamental property in vehicle handling and is the lateral acceleration increase per unit steer angle increase as shown in Equation 30. Equation 30 compares the lateral acceleration (a_y) to road wheel steer angle (δ_{RW}) with consideration of wheelbase length (L), speed (v) and under steer gradient (K_{us}).

$$\frac{a_y}{\delta_{Rw}} = \frac{1}{57.3\left(\frac{L\,g}{v^2}\right) + K_{US}}$$

Equation 30

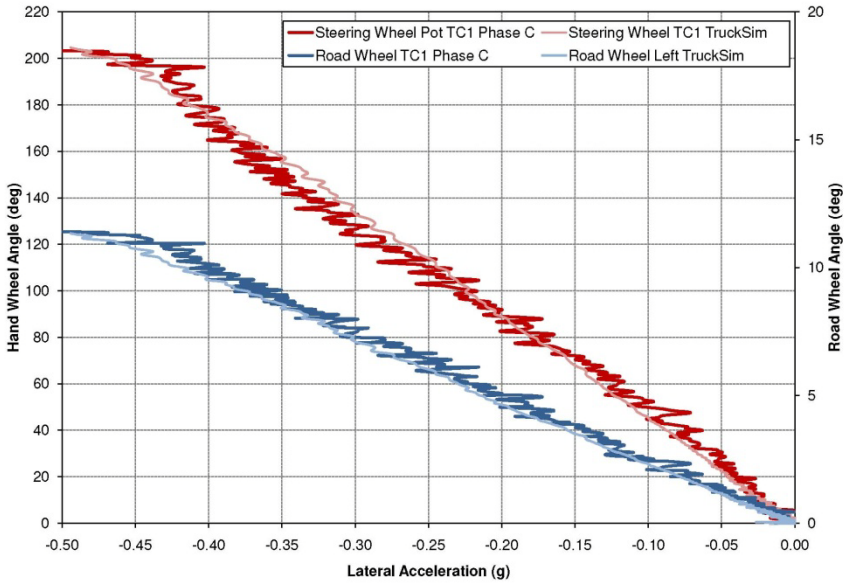

Figure 7-114. Graph. Model confirmation: TC1 steering vs. lateral acceleration

Speed

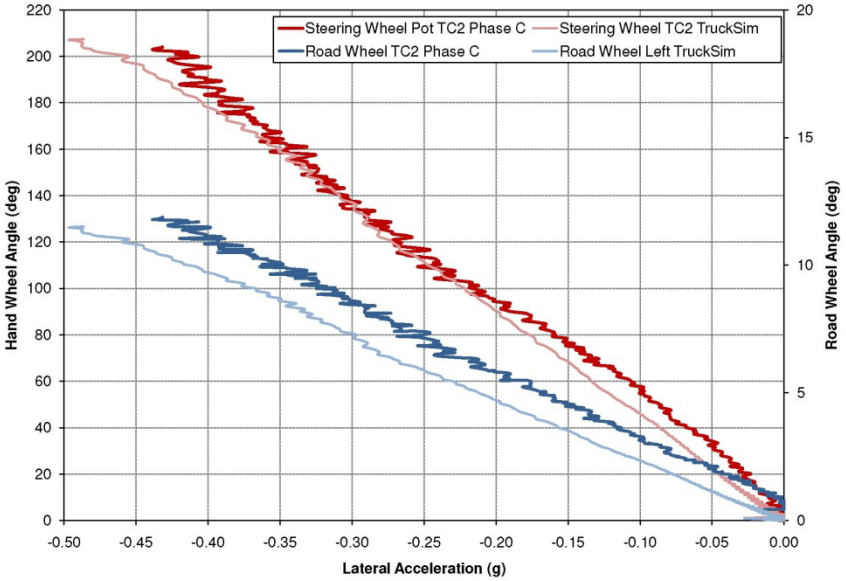

Figure 7-115, Graph. Model confirmation: Steering vs. lateral acceleration

The model confirmation also included a speed validation. Figure 7-116 shows a plot of the measured vehicle speed and the TruckSim® model speed. The plots only confirm that TruckSim® is following the experimental data. The TruckSim® data would characteristically have a slight response delay; however, this is shown to be largely insignificant in the plots.

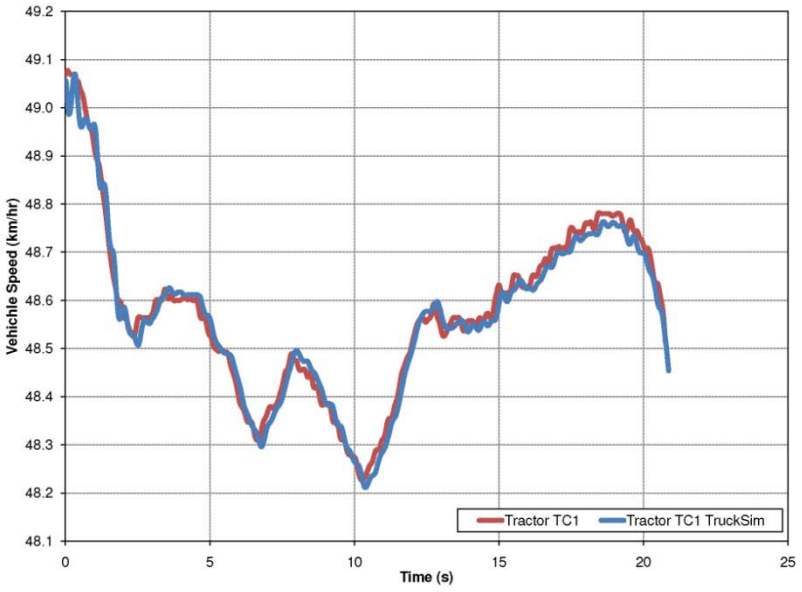

Figure 7-116. Graph. Model confirmation: Vehicle speed vs. time

Lateral Acceleration

The measured lateral acceleration of both the tractor and the trailer were plotted alongside the Phase C TruckSim® model predictions in Figure 7-117.

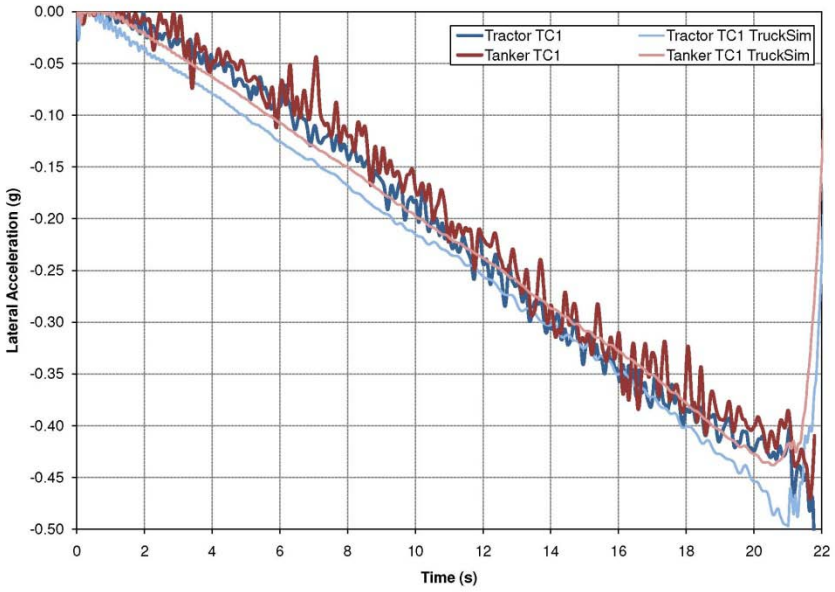

Figure 7-117. Graph. Model Confirmation: Lateral acceleration vs. time Tanker TC1

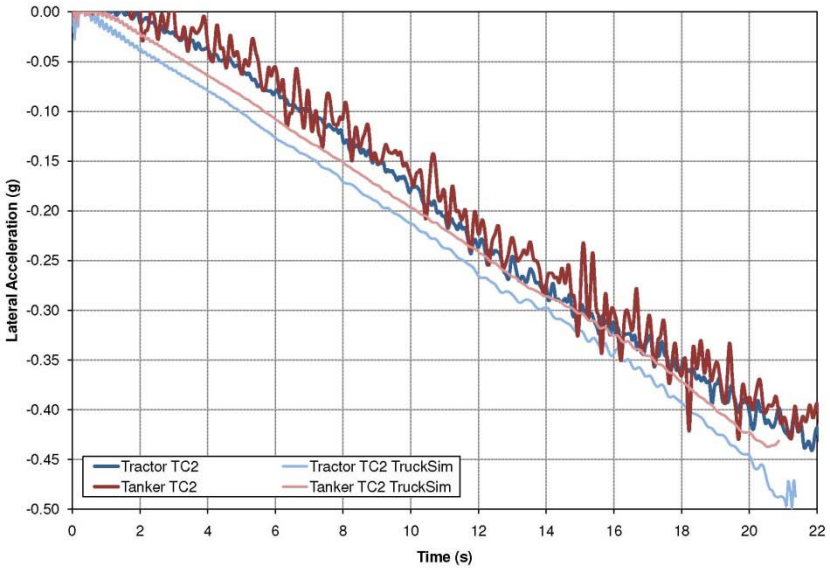

Figure 7-118. Graph. Model Confirmation: Lateral acceleration vs. time Tanker TC2

Wheel Load

The moments of wheel lift for both the tractor and trailer were compared using the wheel loads versus time and wheel loads versus lateral acceleration. The measured and predicted results are presented for the left hand (driver) side wheels. Figure 7-119 shows the wheel loads as a function of time for both the tractor drive axles and trailer axles. TruckSim® produced results that compared well with the actual lift point and more accurately represented actual wheel loads leading to wheel lift.

Once again, the strain gage data was intended to provide only an indication of when wheel lift occurs. The measured strain gage data is presented with predicted wheel load, and it was calibrated based on static wheel loads, but it does not accurately represent the wheel load except when wheel lift occurs. A fuller discussion appears in the Open-Loop Double Lane Change discussion in Section 7.7.3.

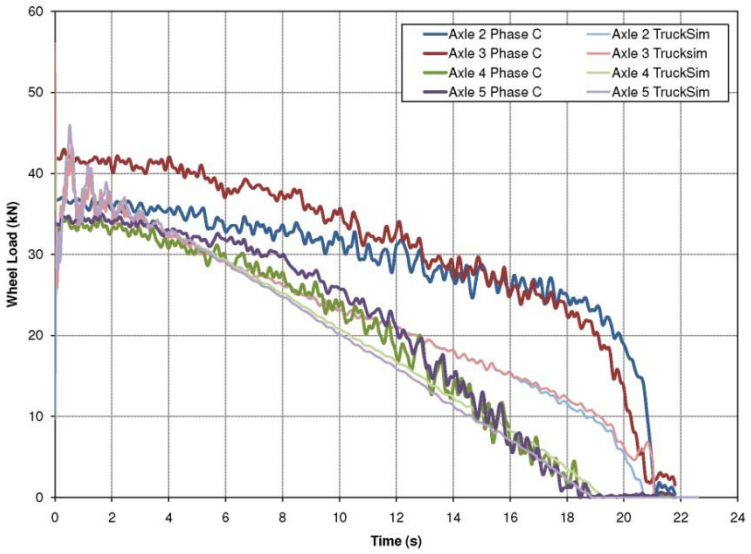

Figure 7-119. Graph. Wheel loads versus time for TC1 suspension

The ability of TruckSim® to accurately predict lift is further confirmed in Figure 7-120 and Figure 7-121 comparing wheel loads versus lateral acceleration, again showing lift off convergence for axles 3, 4, 5. This demonstrates the ability of the model to simulate and predict wheel lift characteristics.

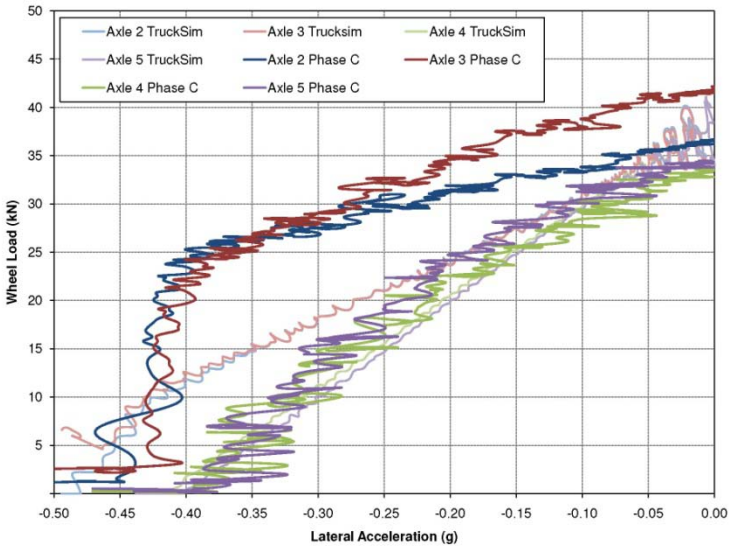

Figure 7-120. Graph. Model confirmation: Left wheel loads vs. lateral acceleration Tanker TC1

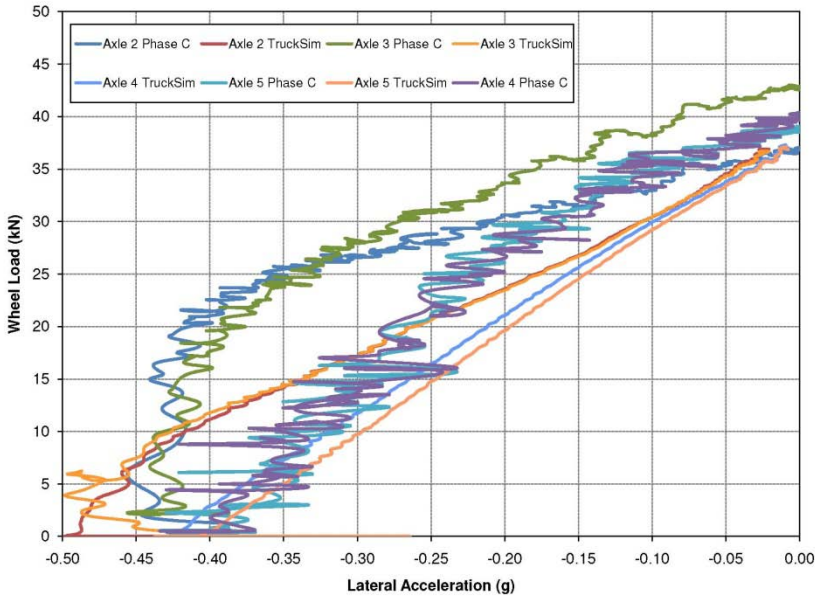

Figure 7-121. Graph. Model confirmation: Left wheel loads vs. lateral acceleration Tank Trailer TC2

Roll Angle

The roll angle of the sprung mass of both the tractor and tank trailer for TC1 and TC2 configurations are shown in Figure 7-122 and Figure 7-123 respectively and plotted against lateral acceleration. The RT unit measured body roll angle and showed a non-linear relationship with lateral acceleration while TruckSim® predicts a fairly linear relationship. Suspension contributed roll angle is the difference between the body roll angle and the axle roll angle. Slight deviations between RT unit and the TruckSim® prediction are shown. The tractor indicates greater deviations in roll angle between the TruckSim® models and the experimental data; however, fifth wheel stiffness and lash properties greatly alter these relationships.

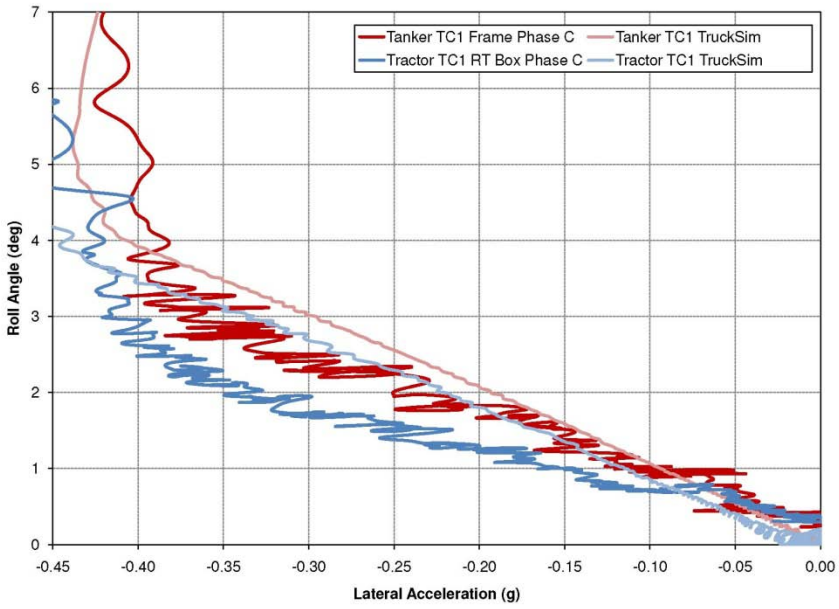

Figure 7-122. Graph. Model confirmation (Tanker TC1): Roll angle vs. lateral acceleration

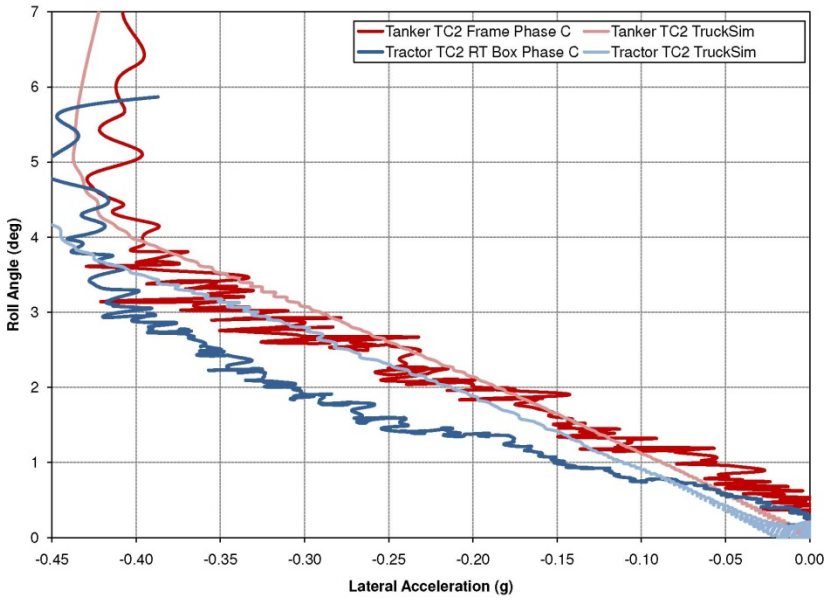

Figure 7-123. Graph. Model confirmation (Tanker TC2): Roll angle vs. lateral acceleration

7.7.2 Step Steer Maneuver

Figure 7-124 through Figure 7-127 compare model predictions with track measurements for the step steer maneuver. Figure 7-124 shows the correlation between roll angle versus lateral acceleration for Tankers TC1 and TC2. Figure 7-125 shows the lateral acceleration versus time for the models versus the experimental data. Figure 7-126 and Figure 7-127 show measured wheel end strain gage loads as compared to TruckSim® wheel loads.

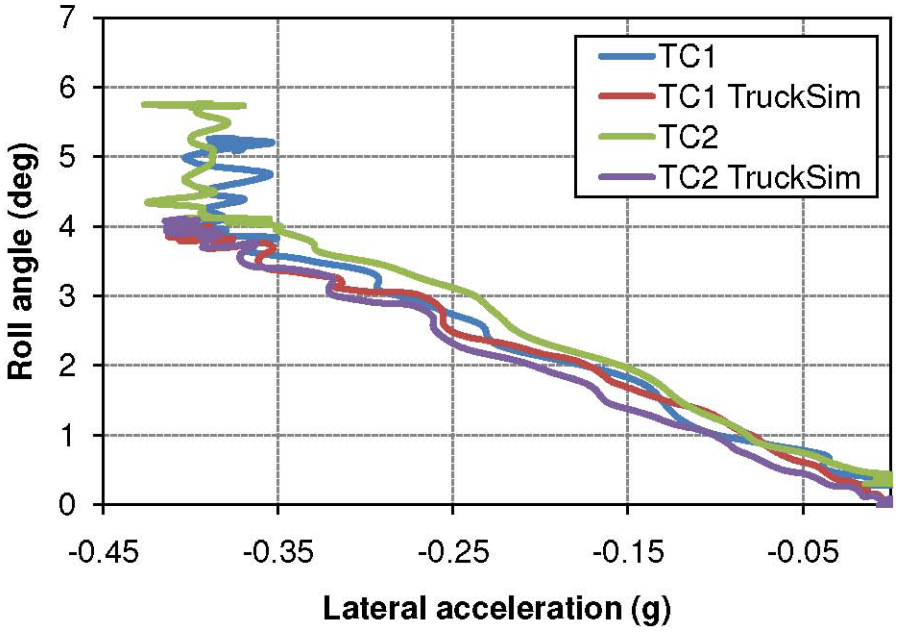

Figure 7-124. Graph. Tank trailer roll angle vs. lateral acceleration

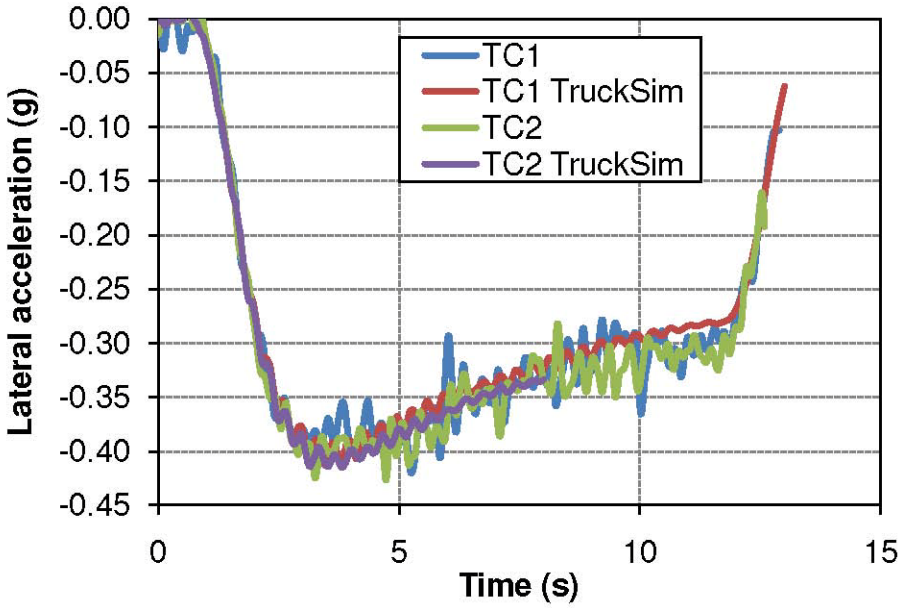

Figure 7-125. Graph. Tank trailer lateral acceleration vs. time

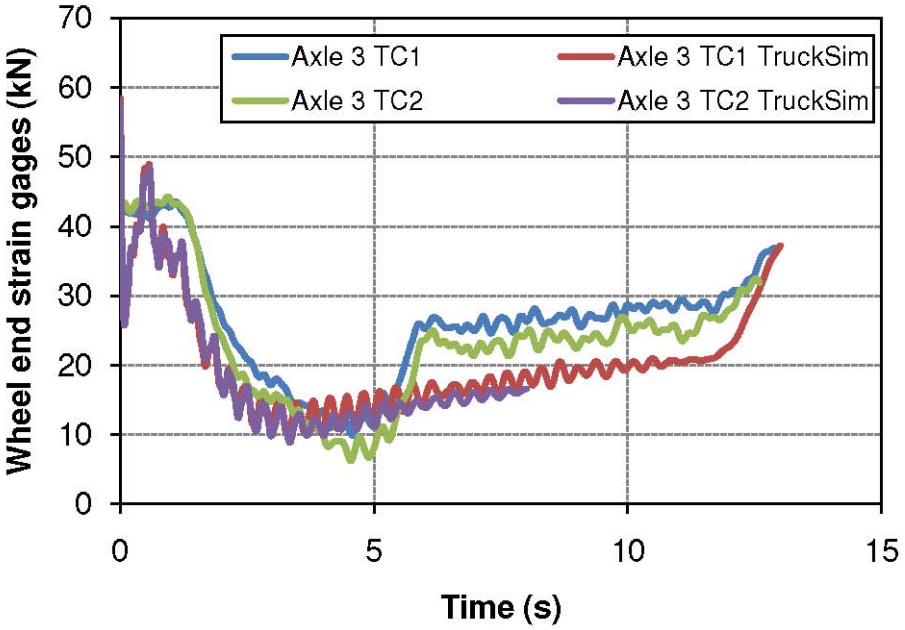

Figure 7-126. Graph. Axle 3 wheel end strain gage measurements vs. time

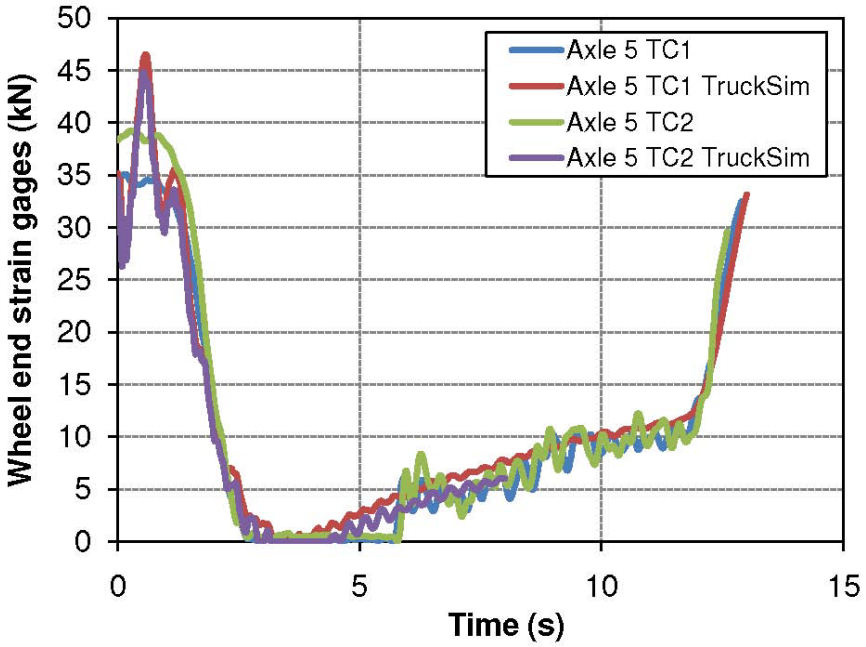

Figure 7-127. Graph. Axle 5 wheel end strain gage measurements vs. time

7.7.3 Open-Loop Double Lane Change Maneuver

On-track testing in Phase C using the designed steering robot profile resulted in a maneuver that closely approximated a double lane change maneuver.

Steering Input

The left side road wheel angle was measured with an angle potentiometer mounted on the wheel spindle assembly above the left kingpin. This angle potentiometer measured the road wheel angle relative to the steer axle. The output from this sensor, along with the hand wheel angle, is shown in Figure 7-128. The road wheel angle was only measured on the left front wheel.

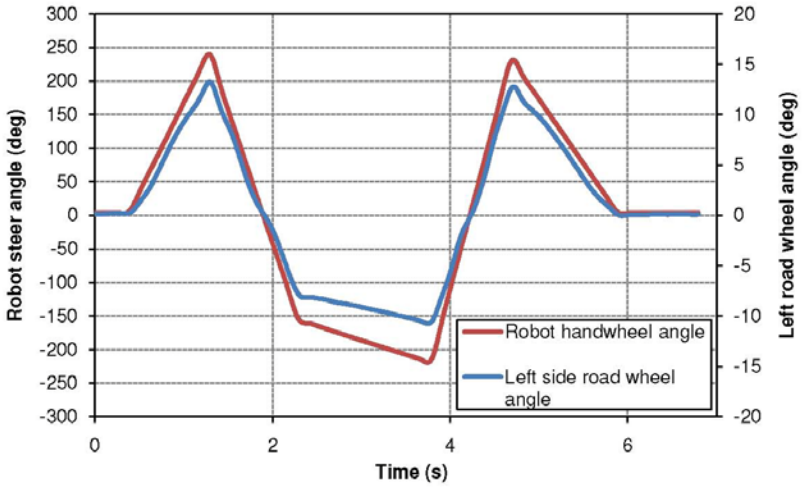

Figure 7-128. Graph. Robot input vs. left side road wheel angle

Lateral Acceleration

Model comparison plots for the tractor lateral acceleration with TC1 and TC2 suspensions are shown in Figure 7-129 and Figure 7-130 respectively.

Comparison plots for lateral acceleration for the tank trailer for the two suspensions are shown in Figure 7-131 and Figure 7-132 for the lane change maneuver. Suspension TC1, although showing a slight time offset which is merely a model timing issue, also shows an interesting correlation on each of the left steer segments of the maneuvers (clockwise roll). The model is predicting the lower value found between two adjacent higher values of lateral acceleration which may in fact be the proper value if noise in the experimental data is removed. The TC2 plots correlate well for peak values and time.

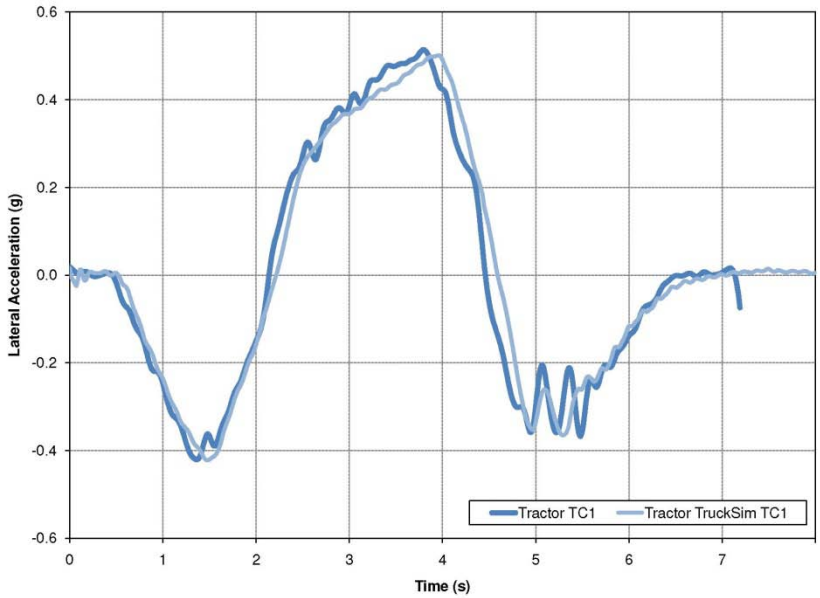

Figure 7-129. Graph. Comparison of tractor lateral acceleration and TruckSim® predicted lateral acceleration for the TC1 suspension

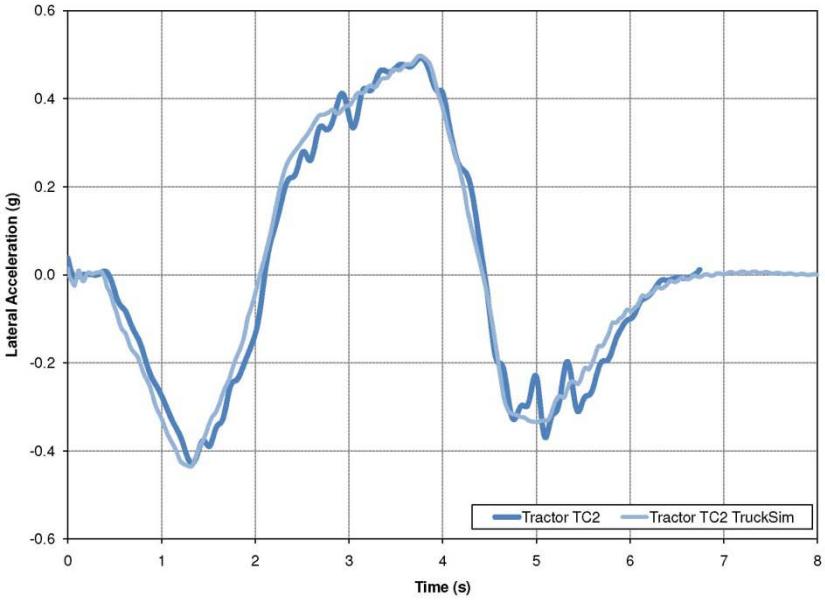

Figure 7-130. Graph. Comparison of tractor lateral acceleration and TruckSim® predicted lateral acceleration for the TC2 suspension

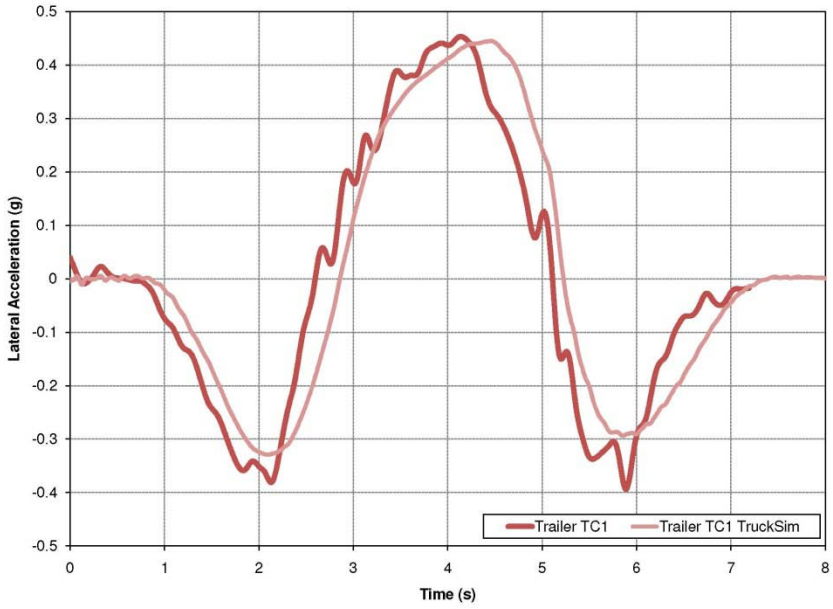

Figure 7-131. Graph. Comparison of tank trailer lateral acceleration and TruckSim® predicted lateral acceleration for the TC1 suspension

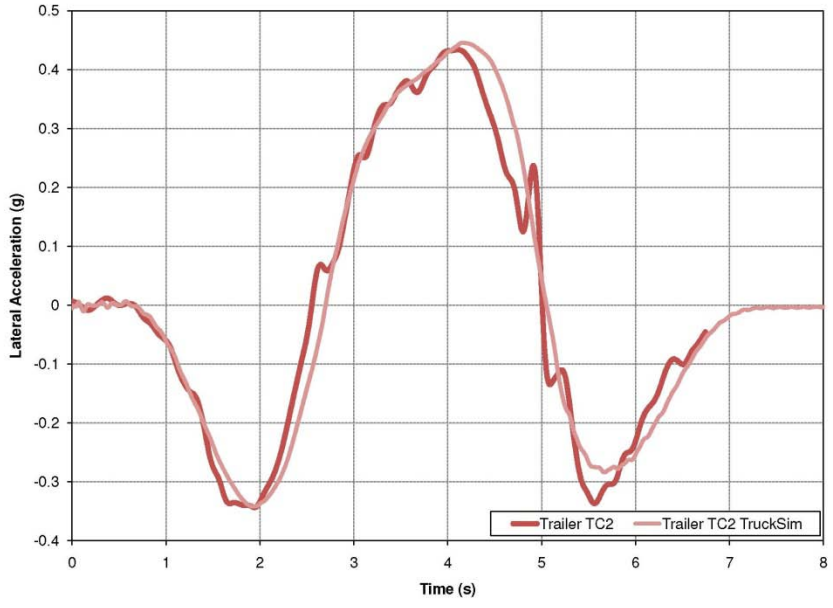

Figure 7-132. Graph. Comparison of tank trailer lateral acceleration and TruckSim® predicted lateral acceleration for the TC2 suspension

Challenges with Model Validation: Differences between Simulated Wheel Loads and Measured Strain Gage Data

In some cases the models do not accurately predict the physical parameters that were measured during testing. One such value is the strain data measured from the wheel end gages. Wheel loads from TruckSim® are not comparable with the test-track-measured strain gage data. The strain gages, whose locations are shown in Figure 7-133, measured a combination of moments, which match the instantaneous wheel loads only in a zero lateral acceleration steady-state component of the maneuver. On the other hand, when a lateral load is present, the situation is more complex with other bending moments and torsion. Therefore, although the output of these gages is labeled "wheel load", the gages serve only as a switch, indicating the moment when the tire lifts off the pavement and the vertical load goes to zero. Shown below are schematics showing the combinations which result in strain gage measurement changes.

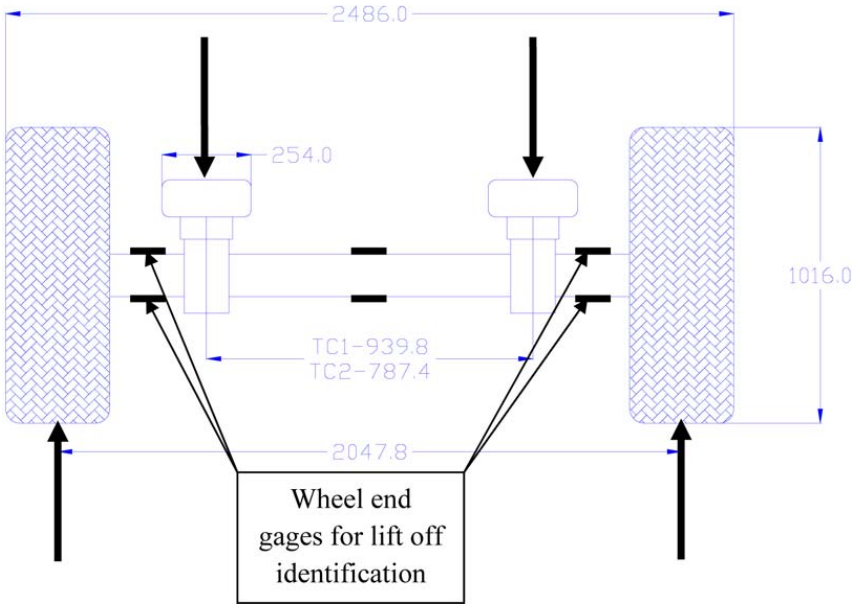

Figure 7-133. Diagram . Bending loads during zero lateral acceleration

Complementary moments from the inside wheel loads and opposite moments from the outside wheel loads are shown in Figure 7-134. As the vehicle enters the turn, the outside wheel vertical load increases, which in turn increases the wheel load bending moment (WLM in the figure). Simultaneously, on the outside wheel, the cornering moment (CM) increases. The two moments are of opposite sign and therefore the output of the axle end gages on the outside of the turn are primarily reflecting the relationship between bending moment and cornering moment, not the actual wheel load. The gage output therefore reads less than the actual wheel load.

Conversely on the wheel on the inside of the turn, the wheel load moment and the cornering moment are of the same sign. Thus, the output is higher than the actual load until the wheel actually lifts.

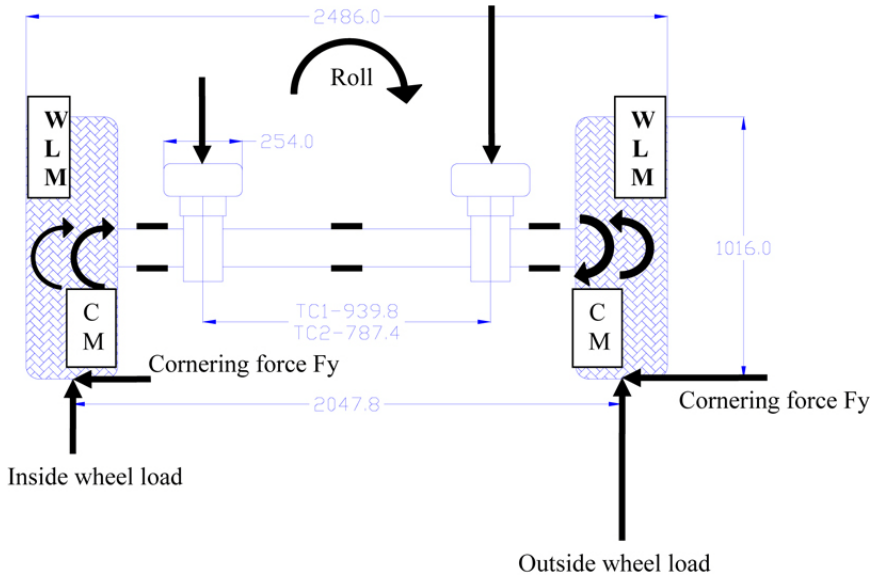

Figure 7-134. Graph. Axle loading and moments in maneuver segment 1 (left) of lane change

As the vehicle transitions into segment 2 of the maneuver, the above situation is reversed, as shown in Figure 7-135.

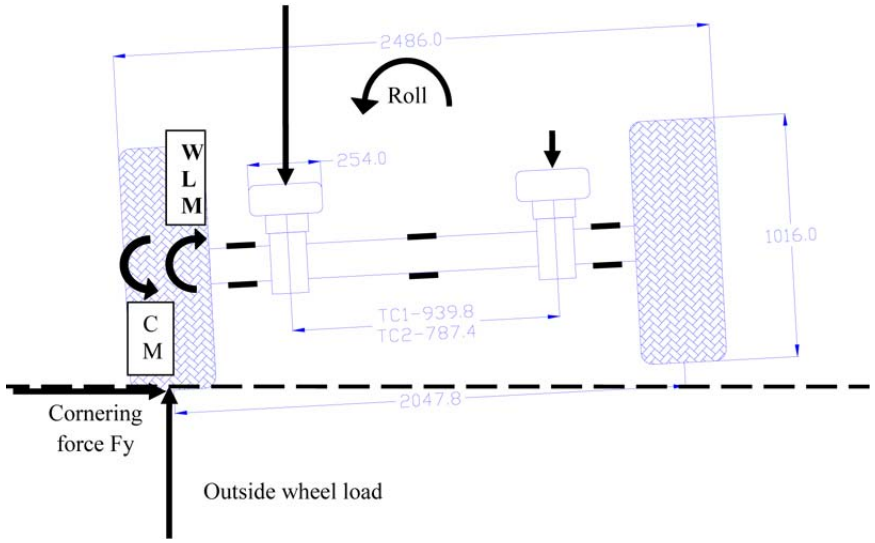

Figure 7-135. Diagram . Axle loading and moments in maneuver segment 2 (right) of lane change showing lift

The TruckSim® simulation and the track-measured wheel end gage data are shown in Figure 7-136 for the tractor and Figure 7-137 for the trailer. Deviation of the simulated wheel load from the measured strain gage data in the plots is due to the combining of lateral acceleration and wheel load strain as shown in Figure 7-135. The differences should be ignored as the axle end mounted gages were intended as lift indicators, not as wheel load indicators.

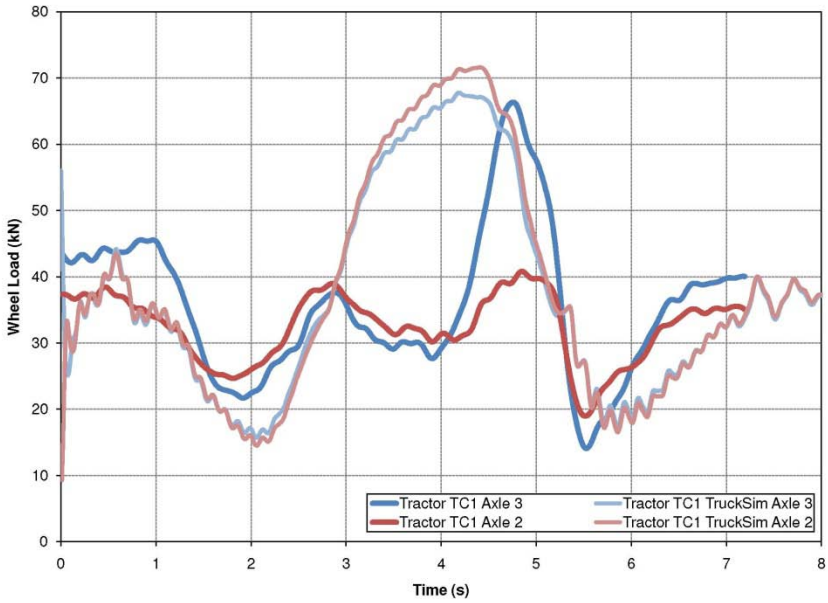

Figure 7-136. Graph. Plot showing the differences between TruckSim® and strain data from the tractor left side lift indicating axle end gages

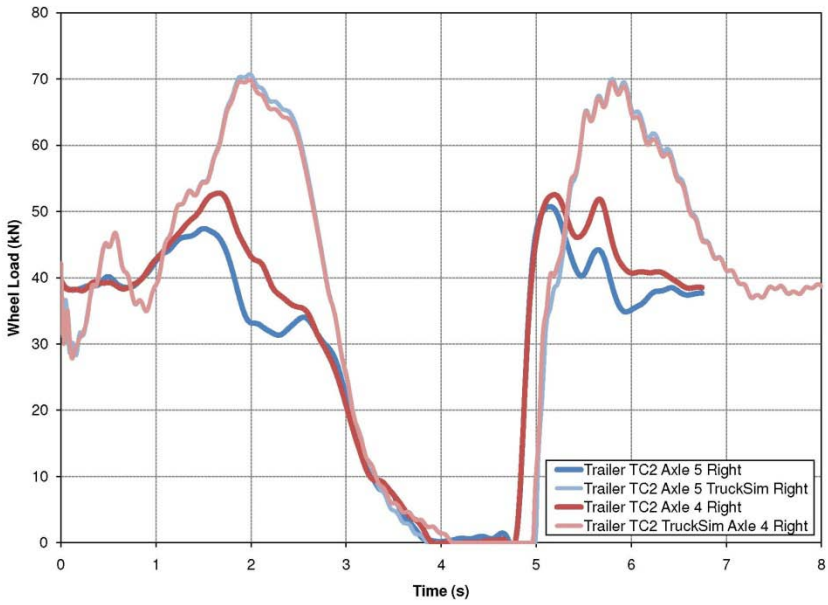

Figure 7-137. Graph. Plot showing the differences between TruckSim® and strain data from the tank trailer right side lift indicating axle end gages

Wheel load comparisons are shown in Figure 7-138 through Figure 7-140. All figures show the differences between the strain gage bending loads and the experimentally measured bending loads from axle mounted strain gages. The models are predicting wheel loads while the strain gages measure a combined loading. Intersections should occur at values close to the static loads when the lateral accelerations near zero value as shown in Figure 7-138.

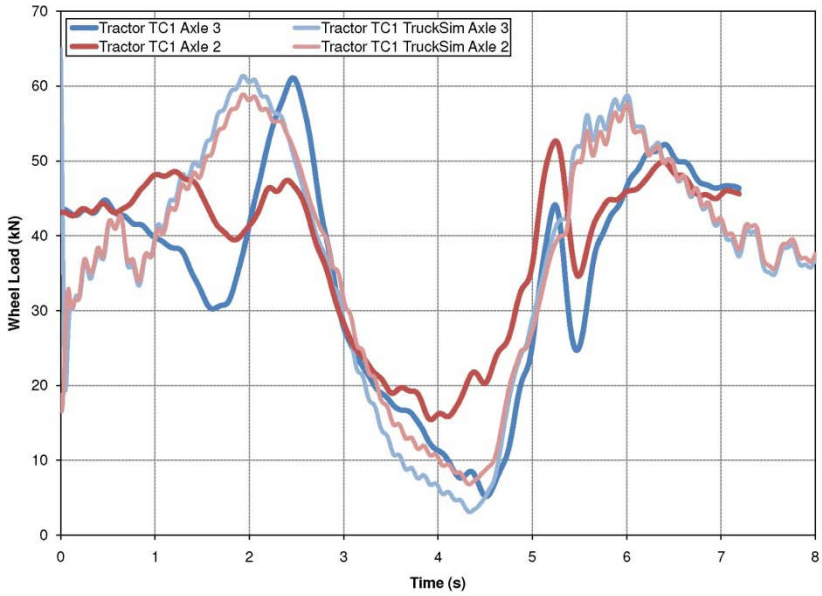

Figure 7-138. Graph. TC1 axle comparison; Left side tractor wheel loads compared to strain gage bending loads (differences are not errors)

Prediction of wheel loads in Figure 7-139 show a short duration lift for axle 5 in the third segment of the maneuver. The horizontal asymptote achieved in the same segments shows agreement of potential wheel lift in that same segment even though the strain gage data indicates a positive load. Figure 7-140 shows the accuracy of the wheel lift in the model in comparison to the experimental data for the second segment of the maneuver. Once again the differences in segment one and segment three are due to the combination of bending moments which the strain gages present. An interesting observation can be made about the strain gage data which indicates that at high cornering loads the most heavily loaded tires, due to the combination of bending moments do not appear to lead to damaging events from axle bending; however, existing the maneuver does lead to high bending loads.

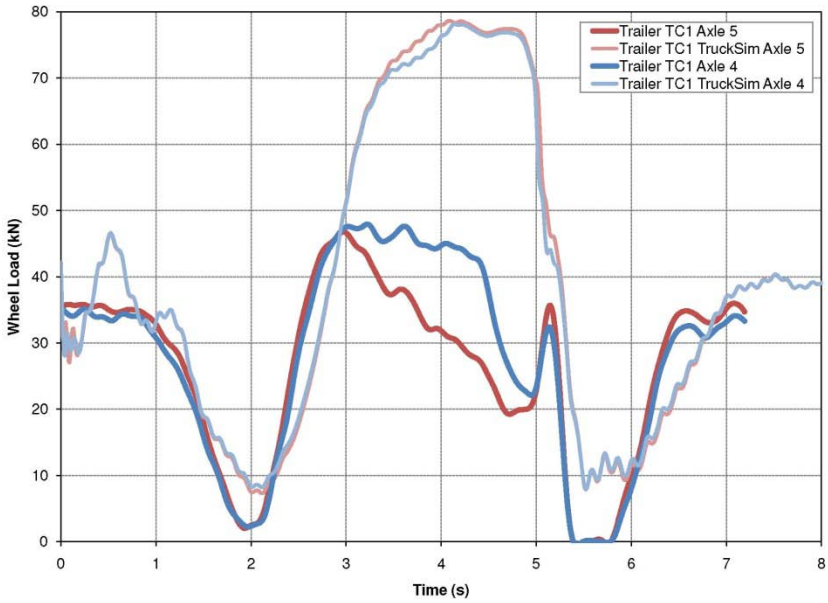

Figure 7-139. Graph. TC1 Axle comparison; Tank trailer left wheel loads comparing the model to experimental strain gage data (differences are not model errors)

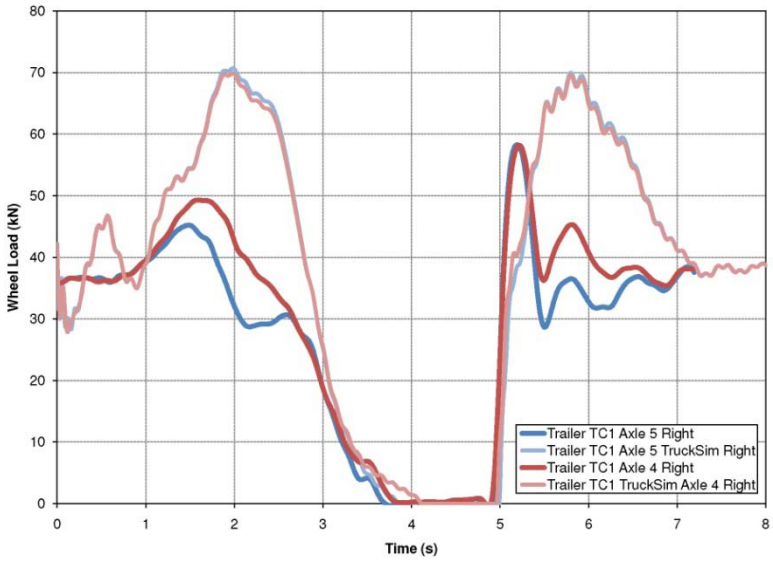

Figure 7-140. Graph. TC1 Axle comparison; Right wheel loads comparing the model to experimental strain gage data (differences are not model errors)

7.7.4 Concluding remarks on predictive modeling

Considerable efforts were made to first progress toward a suitable model that accurately predicted the vehicle's behavior. A number of parameters were adjusted to make the model behave as was shown by the experimental data. Care was taken to document the sensitivity to these parameters.

The TruckSim® models produced reliable predictions, albeit with high sensitivity to certain input parameters. Care will needed in assuring the high-sensitivity parameters are properly addressed in future modeling.

7.8 Data Analysis Conclusions

The Phase C testing provided new information that advances our understanding of tractor trailer stability, particularly with respect to parameters of the suspension design. The data from the ramp steer, step steer, and lane change maneuvers were analyzed statistically to develop an understanding of the differences in performance between the two tankers, TC1 and TC2, tested in Phase C. These tankers were also compared with the high center of gravity (CG) configuration with NGWBS tires used during the Phase B testing (Tanker T), which was most similar to the Phase C configurations. In addition to the comparisons between the different trailer configurations, a detailed analysis of the pressure difference across the suspension air bags of the trailer shed new light as to how the air bags provide a stabilizing moment during complex transient maneuvers. This analysis of results has yielded a better understanding of several suspension properties that are important for heavy truck stability and provides a rich data set for comparison with modeling results. Further research is needed to determine the damping contribution from the various components of the air suspension and how to optimize the benefits resulting from them.

The lateral acceleration at wheel lift from all of the foregoing analysis is summarized in Figure 7-141. The three large headings across the top of the figure indicate the three maneuvers—ramp steer, step steer, and open-loop double lane change. Within the black box for each maneuver are gray boxes identified in the row along the bottom of the figure as to which axle's data is being plotted. Axles 2, 3, 4, and 5 are the two drive and two trailer axles for the ramp and step maneuvers. Only the trailer axles were analyzed for the lane change; 4R and 5R indicate the right-side wheels lifting during the second segment of the maneuver (Figure 7-69) and 4L and 5L indicate the left-side wheels lifting during the third segment. The gray boxes are separated by a dotted gray line; on the left side of the gray line are the points for the "first" analysis in Sections 7.4 through 7.6, and on the right side are the points for the "second" analysis. The colors and shapes of the markers indicate the tanker, T, TC1, or TC2, as defined in Figure 6-2 and Table 6-1. The blue diamonds for Tanker T show data from Phase B (Arant et al. 2009), which was included in only some of the comparisons. The markers indicate the mean of the lateral acceleration (a_y) at wheel lift. The vertical lines extending from the markers denote the range of the 95% confidence interval of the mean. The "Ay metric" is the lateral acceleration at lift, which

was defined in subtly different manners for the different analyses. A higher lateral acceleration indicates a vehicle's greater ability to keep its tires on the pavement during the particular maneuver.

The figure shows how the wider track of Tankers TC1 and TC2 improves the roll performance over Tanker T, in the cases where they were compared in the ramp and step steer maneuvers. The difference between Tankers TC1 and TC2 in the ramp steer is small and inconsistent. In the step steer, the wheel lift for the trailer axles (4 and 5) was at consistently higher lateral accelerations for Tanker TC1 than Tanker T and for Tanker TC2 than Tanker TC1. Axles 4R and 5R (the 'R' indicating Segment 2) of the lane change showed no consistently discernible difference between Tankers TC1 and TC2. In the third segment of the lane change, the wheels on the trailer axles (4L and 5L) of Tanker TC1 lifted, but the low number of repeated runs led to a wide confidence interval. When the TC2 suspension was on the trailer, the trailer wheels never lifted during the third segment of the lane change.

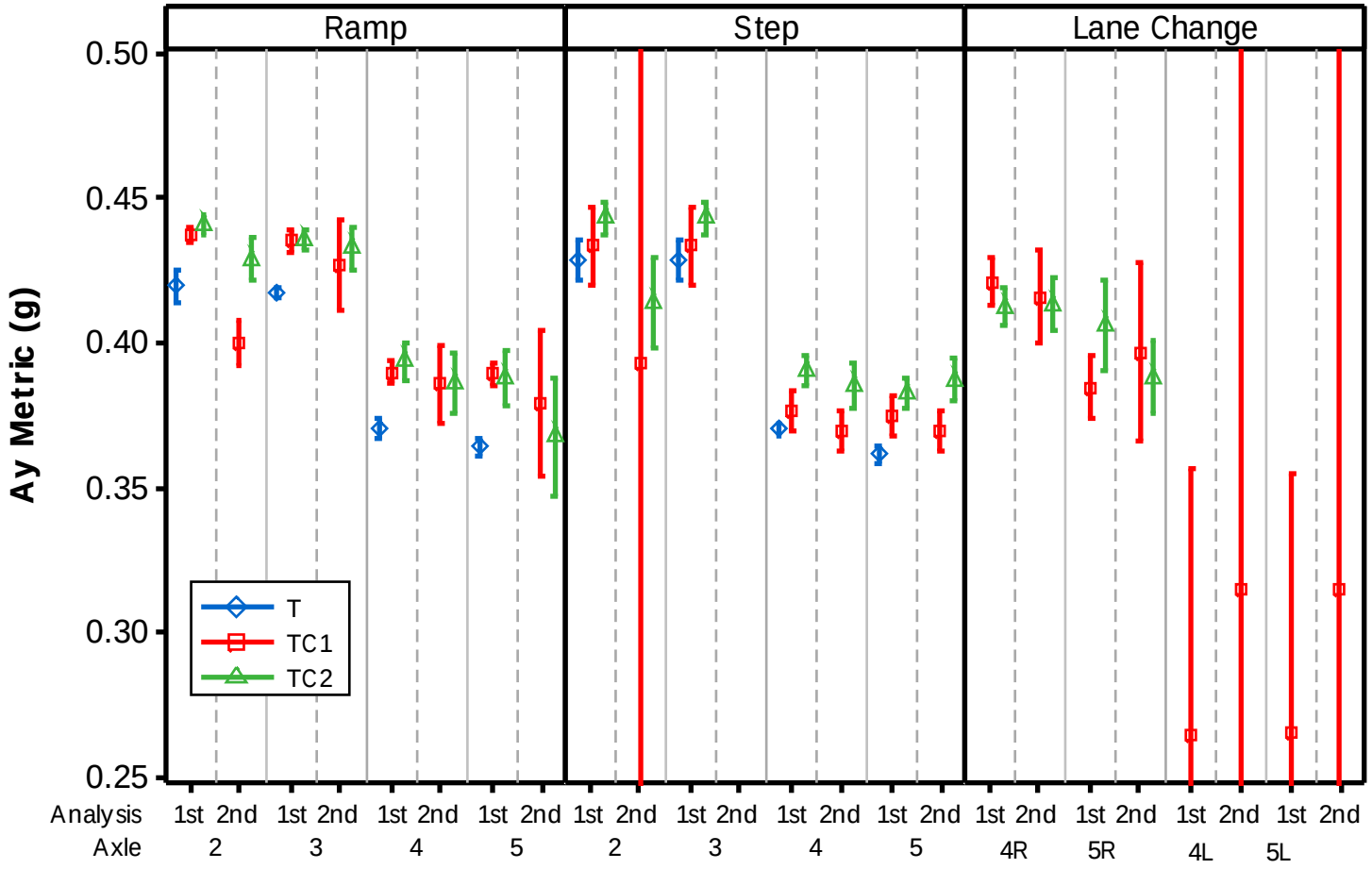

Figure 7-141. Graph. Summary of analysis of lateral acceleration at wheel lift

7.8.1 Ramp Steer Conclusions

Analysis of the low-speed ramp steer maneuver test data confirmed that the tractor trailer exhibits an understeer characteristic qualitatively similar to that observed with Tanker T of Phase B testing. This is significant because it confirms that the wider trailer axles used in tankers TC1 and TC2 did not adversely affect the understeer performance of the tractor trailer. Comparable steady state handling performance provides confidence that differences observed in high speed maneuvers are not a result of vehicle yaw instability accompanying a roll instability). Small differences in the understeer behavior, as indicated by the Ackerman correction, were observed between Tanker T and tankers TC1 and TC2, but the understeer behaviors are qualitatively quite similar in all three tankers. The understeer behavior was different between the clockwise and counterclockwise directions, which could be indicative of misalignment of the axles. This may have resulted, in part, from field mounting the TC2 suspension, and this may have influenced some of the wheel lift results between the TC1 and TC2 configurations. The understeer tests were not repeated for statistical assessment to save track time for other tests. The tests were executed once only to provide a general assessment of the steering behavior of the vehicle in the as-tested configuration.

The results for the high-speed ramp steer maneuver showed a minute difference in roll performance between the TC1 and TC2 tankers, with the tendency usually towards a slightly increased roll threshold (maximum lateral acceleration experienced prior to wheel lift) for TC2. The difference in lift threshold between the TC1 and TC2 tankers was not statistically significant. The difference between Tanker T and either Tanker TC1 or TC2, however, was statistically significant, with the wider axles used in both configurations of Phase C providing increased values of roll threshold, as expected.

7.8.2 Step Steer Conclusions

The results of the step steer maneuver were stronger and more consistent than those of the ramp steer maneuver. A general ranking of wheel lift threshold among the three configurations was consistent for all axles: Tanker T had the lowest roll threshold, followed by Tanker TC1, and Tanker TC2 showed the highest threshold. The wheel lift threshold rankings were not statistically significant consistently among the different axle positions of the tractor-trailer, but for specific axles, the results were statistically significant for some of the comparisons. Even though the roll threshold for the Tanker T tests was found to be similar to the roll threshold of both of the Tanker TC1 and TC2 tests, the test speed at which wheel lift first occurred was about 3.2 km/hr faster for the TC1 and TC2 tankers than for Tanker T. The higher speed to generate wheel lift (and the same lateral accelerations) does indicate a clear improvement in roll performance in this maneuver.

7.8.3 Open-Loop Double Lane Change Conclusions

The lane change maneuver is more complicated than other maneuvers tested in that it incorporates three distinct turns during which wheel lift could potentially occur. Wheels did not

lift in the first segment, when the vehicle was first turning away from its original travel lane. Trailer wheels did lift during the second segment, when the vehicle turns from the left lane back toward the right. The differences in lateral acceleration at wheel lift were either inconsistent or not statistically significant. In the third segment of the maneuver, when the vehicle turns back toward its original travel direction, the Tanker TC1's trailer wheels lifted, but Tanker TC2's did not. The maneuver was at least as severe for Tanker TC2 as for TC1, so there was a benefit to the narrower beam spacing in this particular instance. Direct comparisons of roll threshold between either Tanker TC1 or TC2 and Tanker T from Phase B testing are not meaningful, because the test speeds that generated initial lift during the Phase B testing were lower.

7.8.4 The Contribution of Air Bag Differential Pressures and Auxiliary Roll Damping

Two observations were made during the Phase C testing with respect to the effect that the trailer air bags for this particular trailer suspension design had on the tractor-trailer roll stability. The differential pressure across the air bags was measured during testing, and for transient maneuvers, the pressure between left and right air bags resulted in calculated roll moments of over 20,000 N·m, acting in a manner that helped to damp the roll of the trailer (stabilizing effect). This effect was most significant during the lane change maneuver, where the vehicle turned left, right and back to the left again.

This air bag effect takes place when the bag on one side of the vehicle is extended while the other is compressed. The tubing that connects the air bags and the rest of the suspension leveling system allows air to flow from the compressed bag to the extended bag, so that more air is present in the extended bag. The tubing has a time constant for the air pressure to equalize that is longer than the duration of the rapid turns of the lane change maneuver. When the vehicle turns quickly in the direction opposite to the initial turn, an increased load is applied to the air bag that was initially extended and the air mass differential that had previously developed between the bags generates a pressure differential. This pressure differential opposes the roll of the trailer and helps to stabilize the roll event.

The second observation of interest concerns the roll damping provided by the trailer shock absorbers. During Phase B, it became evident that modeling the shock absorbers as the only damping element in the trailer suspension did not provide sufficient damping to account for the observed damping of oscillations during testing. The TruckSim® modeling results could be made to match the experimental measurements only if "auxiliary roll damping" was included in the model to account for the damping provided by bushings, the air bags, and other components in the suspension other than the "normal" roll damping provided by the shock absorbers.

Phase C testing was designed to better quantify this effect, and the results were unexpected. When the shock absorbers were removed from the trailer with the TC2 suspension in place, there was no observable difference in the roll damping of the tractor trailer (although pitch and bounce damping were very clearly reduced), which implies that the shock absorbers have negligible effect on roll damping. This result suggests the conclusion that other elements of the trailer

suspension are entirely responsible for the roll damping. Analysis of the air bag contribution to roll damping, as a result of a differential pressure that develops across the left and right sides of the trailer, suggests that this is an important part of the total roll moment. While the relative contribution of air bags to the total auxiliary roll damping is not fully characterized, it is clear that they play a significant role.

7.8.5 Results with the ESC Enabled

When the ESC systems were activated, they prevented wheel lift in the for the ramp steer and lane change maneuvers. Although the tests performed with the ESC system activated were not comprehensive for evaluating the ESC performance in all maneuvers and possible combinations of ESC system activation (of the tractor and trailer ESC systems), the systems intervened at appropriate times without presenting any irregular behavior. The ESC system performed as expected with both suspensions.

7.8.6 General Conclusions of Phase C Testing

The Phase C testing gave some results that were not anticipated from simple arguments of the trailer roll stiffness. The wider beam spacing of the TC1 suspension was expected to provide higher roll stiffness than the TC2 suspension, and it did, as was shown in Section 7.2.3. Higher roll stiffness, if it were the only change, would be expected to lead to improved roll stability. However, the maneuver results actually showed similar or even a slightly better performance in roll stability of Tanker TC2. This is because widening the beam spacing changes more than just the roll stiffness—roll center height and a host of more subtle properties are also affected by this one design dimension. The implication is that tractor-semitrailer stability depends on interactions among many design variables. A detailed analysis of the complete tractor-semitrailer is needed to give an accurate assessment of the benefits that may be achieved with particular design changes.

Chapter 8 – Design and Technology Options, Selections, and Recommendations

Options for designs and technologies having the possibility of preventing a tractor-semitrailer rollovers are listed in this chapter. Changes in vehicle components are examined first, and then novel technologies are presented in the second section. In the interest of "casting a wide net," a number of approaches are presented in this chapter. These ideas can be carried forward for further research or perhaps they will spark new ideas. The HTRC team has not thoroughly analyzed all of the options named, and it is not necessarily recommending that any particular one of these options be adopted.

8.1 Vehicle Components Potentially Affecting Roll Stability

A vast number of vehicle components can conceivably be redesigned to improve a vehicle's roll stability. Taxonomy of those components is presented first, and then a few are analyzed for the contribution they could provide if they are implemented individually.

8.1.1 Categorized List of Components on a Tractor-Semitrailer

Figure 8-1 shows a flow chart of potential areas for examination regarding lowering the CG of the tractor, trailer, or both. This could be accomplished either with a semitrailer redesign, or the potential exists to modify the current air bag system to allow an active system to lower the vehicle a defined amount at a given speed. Since CG height is in direct relation to improvement in roll threshold this is always a beneficial choice of options. Some of the compounding effects are also indicated such as increasing the beam centers; in turn this could increase the frame rail spacing which in turn could allow the container to be lowered further into the frame structure.

Presented in Figure 8-2 are wheel and tire options. Although tires provide viable design options, the team feels confident in the choice of NGWBS tires for both tractor drive and trailer axles. One area that should not be overlooked is tire sensing technology to assure continuous inflation pressure and detection of impending failures due to either higher temperatures or reduced pressures. Details of tire construction, compounds or other tire related specifics were not addressed. Wheel offsets are important from both a design and loading perspective. Axle manufacturers provide limits as to maximum wheel offsets since bearing loadings and/or axle bending loads may be increased. Wheel offset may be a straight forward way to achieve track width goals; however, high offsets may not be supported by axle manufacturers.

Figure 8-3 is a flow chart for the tractor front suspension for a solid axle and in Figure 8-4 for an independent suspension. The flow charts bring some fundamental choices beginning with the choice of solid axle (conventional design) or an independent front suspension. The independent front suspension shown in Figure 8-4 offers greater flexibility in design choices and allows greater control over variables that influence the fundamental steer properties. Although the independent suspension is a viable design option, it is recognized that great reliability and

satisfactory tire life is accomplished with the conventional design and there is considerable confidence in its characteristics. The flexibility offered in design, and the potential for improved ride and handling with the independent option should not be totally overlooked, however.

Displayed in Figure 8-5 are steer axle component options and in Figure 8-6 are the geometry and related characteristics of the steer axle. These options focus primarily on the steering system components and choices. Some of the options presented are “cross-linked” with tractor front suspension options since the choice of either solid axle or independent front suspension may limit the applicability. The options presented provide the opportunity to either assist the driver in control or provide more reliable road wheel feedback to the driver. Further expansion into “smart” systems for driver assist or enhanced stability is also possible. The characteristics shown relate to steady-state stability, tire wear and fundamental steer characteristics. The displayed characteristics are closely aligned with the selected steer axle component options.

Tractor drive axle options are presented for rigid axles (Figure 8-7) and independent suspension systems (Figure 8-8). Although independent drive axle systems for class 8 trucks do not appear to be commercially viable in the near future, they are presented for comparison.

Shown in Figure 8-9 are design options related to choices in the fifth wheel. The fifth wheel is the main coupling point between the tractor and trailer and as such influences how suspension roll stiffness is developed and shared. Among the options explored were an actively positionable fifth wheel in the horizontal plane with both lateral and longitudinal control. Other considerations could include active lash elimination systems and active anti-jackknifing systems as well as key fundamental properties such as torsional stiffness and lash. Modeling has shown that fifth wheel properties have a significant influence on wheel lift for certain trailers and the magnitude of that influence is related to trailer torsional stiffness and payload distribution.

Figure 8-10 presents the tractor frame design parameters. Bending stiffness is critical to load capacity and torsional stiffness determines, to a large degree, how the roll behavior at the drive axles is shared with the steer axle. The tractor frames evaluated in Phases A and B have shown relatively low torsional stiffness values in comparison to the suspension roll stiffness. As a result of the low frame torsional stiffness, little weight transfer occurs between the steer axle suspension and the drive axle suspensions.

Figure 8-11 shows trailer axle suspension and axle options and Figure 8-12 shows some of the characteristics which may be desirable and can be limited by the choice of basic design. Beyond track width, parameters such as suspension roll stiffness, axle steer in roll and beam center spacing have all shown to influence the trailer’s roll stability. The roll stiffness and roll stiffness proportioning can affect the roll moment sharing between the trailer and the tractor. The beam center spacing has demonstrated an effect on auxiliary damping during transient maneuvers. Additionally, the beam center spacing influences, for an axle using the axle tube as a torsional

member, the roll stiffness of the axle. A wide variety of trailer axle designs are present in the marketplace; however, only one Hendrickson design was tested as a part of this study.

Phase C testing confirmed the obvious choice of increased track width. Preferably, the wider axles will be followed with an increase in the span of the beams. Measured in Phase C were the flexural loads at the axle center. With the wider track and the narrower beam centers used in TC2, the flexural loads were higher in all maneuvers than with the TC1 configuration. It has also been shown that the wider beam centers provide an increased transient damping from the air bags. Many other design choices exist, most of which add additional roll stiffness or add additional roll damping. It had been demonstrated in Phase B modeling that options could include active damper control, or active air bag control. In Phase C, the actual testing of the roll damping was performed, and it was determined that the suspension system, which was present on the tank trailer in Phase B and Phase C, provides adequate roll damping even with the individual axle shock absorbers removed. Auxiliary roll damping is present in the existing suspension design.

Figure 8-13 displays some of the considerations in the basic trailer frame design. The trailer frame bending stiffness has a significant influence on load capacity and the torsional stiffness influences the roll behavior of the vehicle. The flatbed trailer tested in Phase A had a much lower torsional stiffness than the tank trailer tested in Phases B and C. The higher torsional stiffness of the tank trailer allowed for a higher percentage of the roll moment produced by the tank trailer to be shared between the trailer suspension and the tractor drive axle suspension, when compared to the flatbed trailer. Advantages such as increasing the frame rail spacing, which may provide improvements which may allow for lowering the payload height, should be considered for all trailer configurations that employ lengthwise running frame rails. The increased frame rail spacing would allow easier implementation of wider suspension beams centers and air bag spacing. The wider frame rail spacing has the potential to also increase torsional stiffness properties for the trailer which could lead to stability improvements. Figure 8-14 and Figure 8-15 present options for electronic control of systems to reduce the possibility of wheel lift by either controlling the vehicle or warning the driver. The vehicle controls could include ESC systems which have proven in testing to be a reliable means to limit wheel lift in all but extreme cases.

Further enhancements and integration of the tractor and trailer sensing would provide benefits to moving the system control points to where control is closer to the “critical point.” A variety of stability enhancing systems could also provide improvements and move the system application closer to the critical point as well. Further work in roll and yaw stability systems should be completed as these can provide for more realistic control points unique to trailer loading and properties.

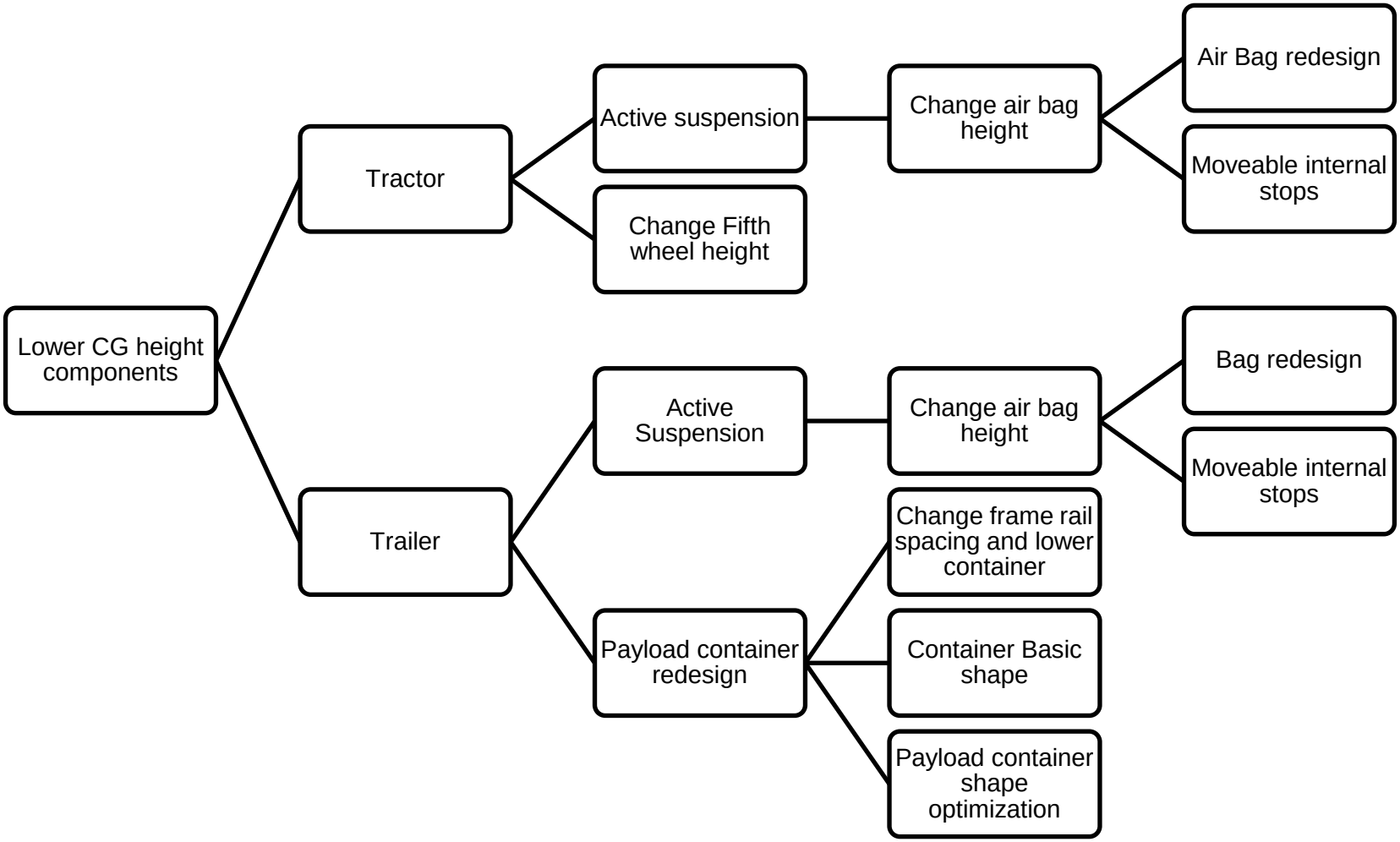

Figure 8-1. Graphic. Center of gravity height technology options for both tractor and trailer

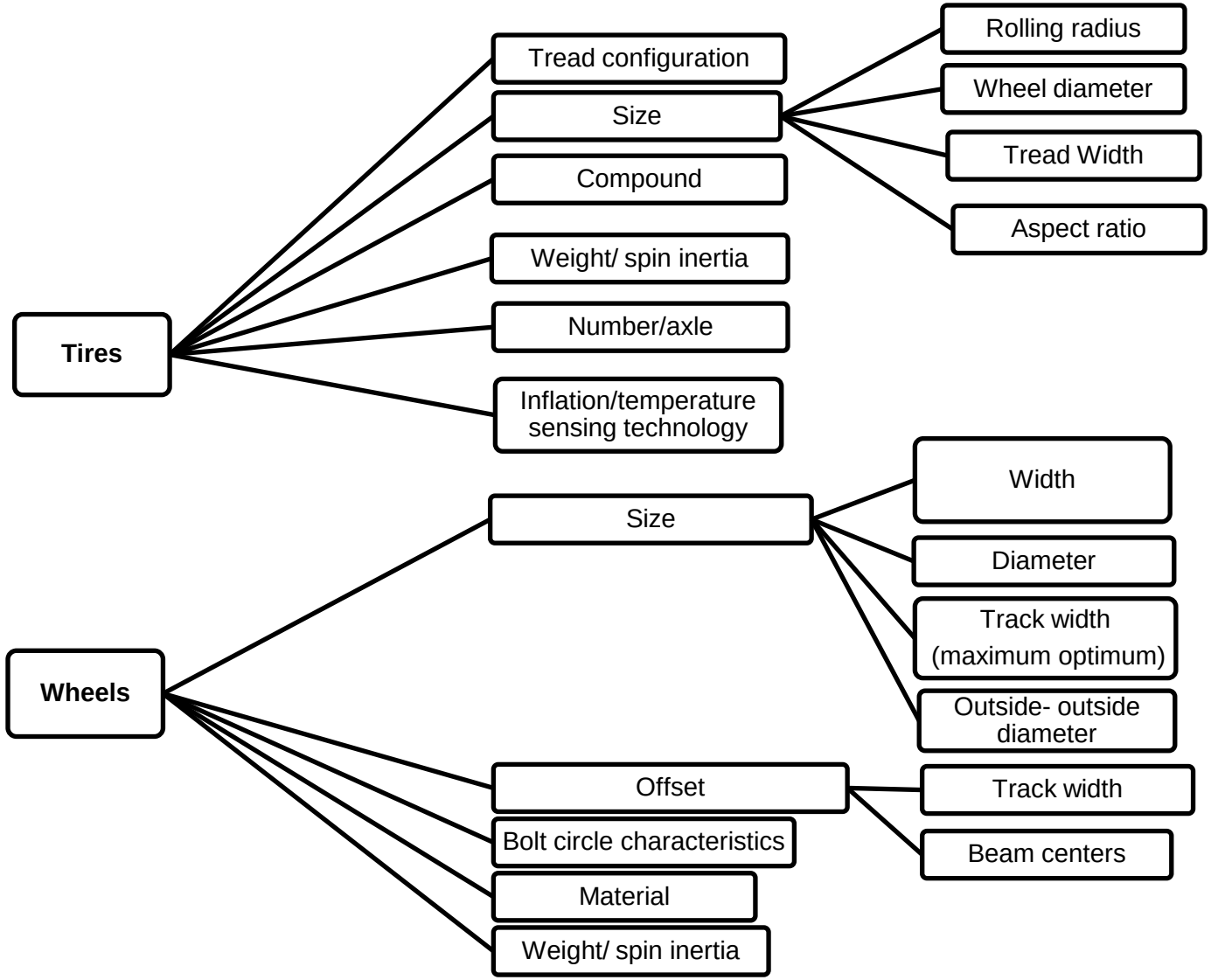

Figure 8-2. Graphic. Wheel and tire component options

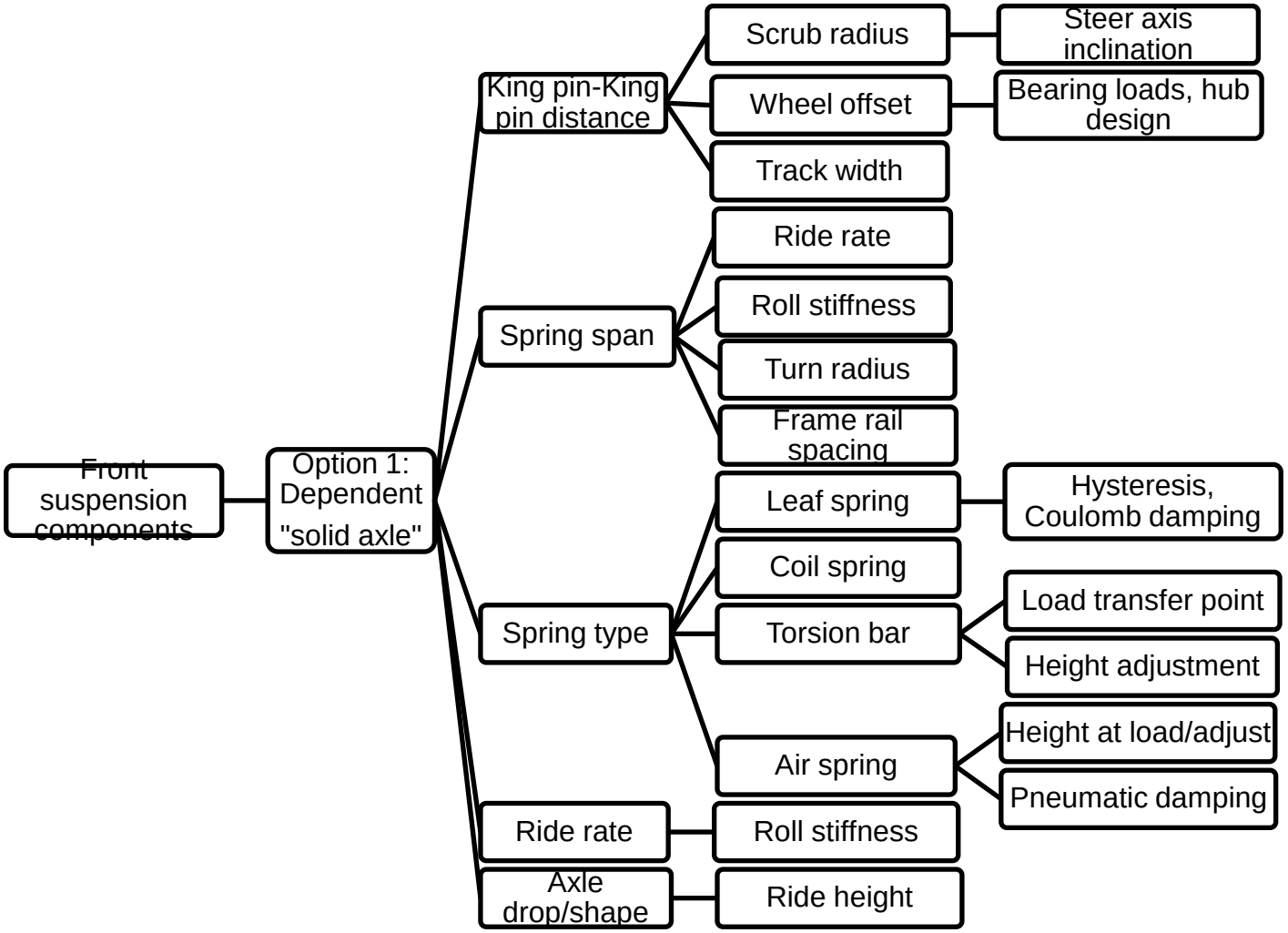

Figure 8-3. Graphic. Tractor front suspension component options with a solid axle

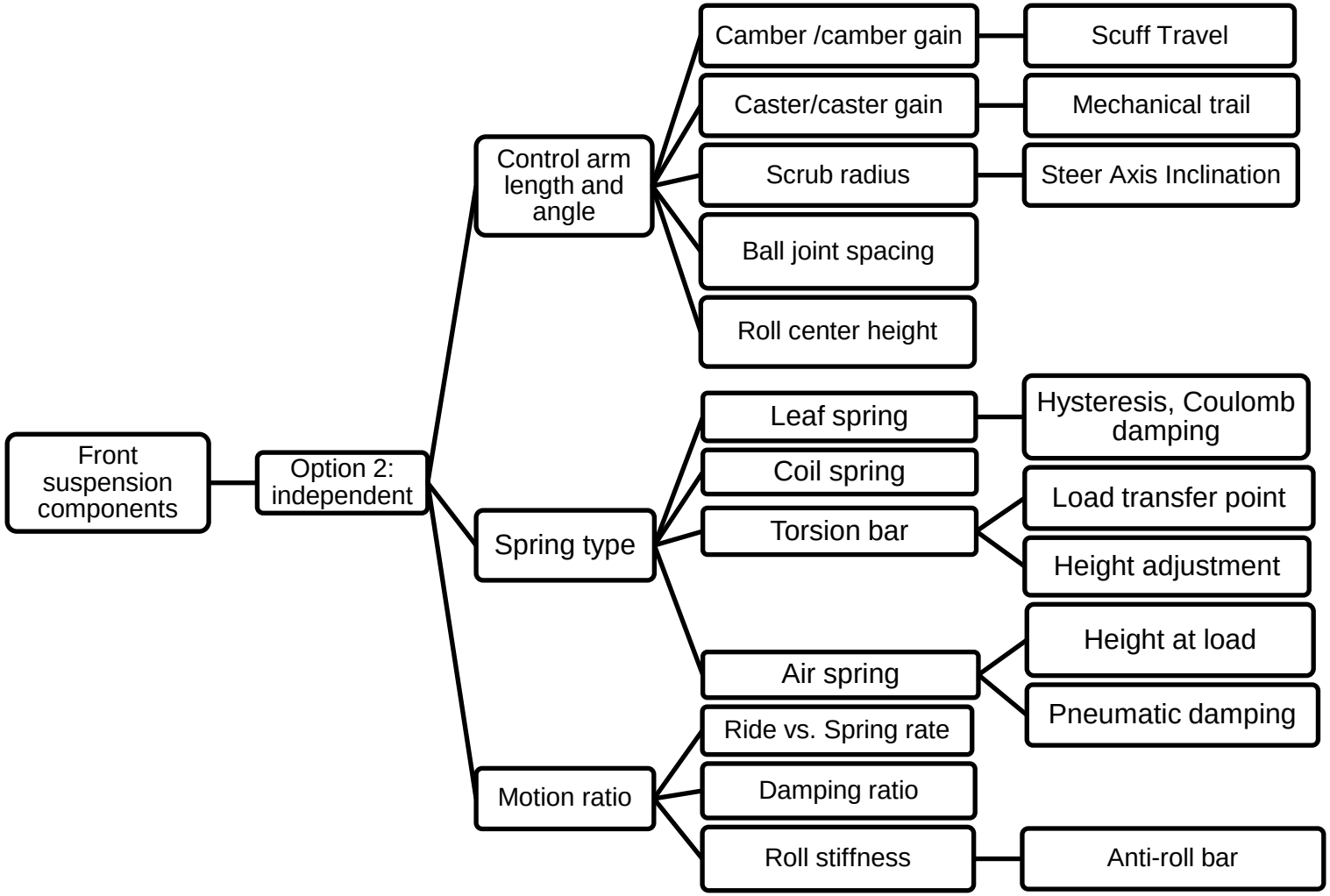

Figure 8-4. Graphic. Tractor front suspension component options with independent suspension

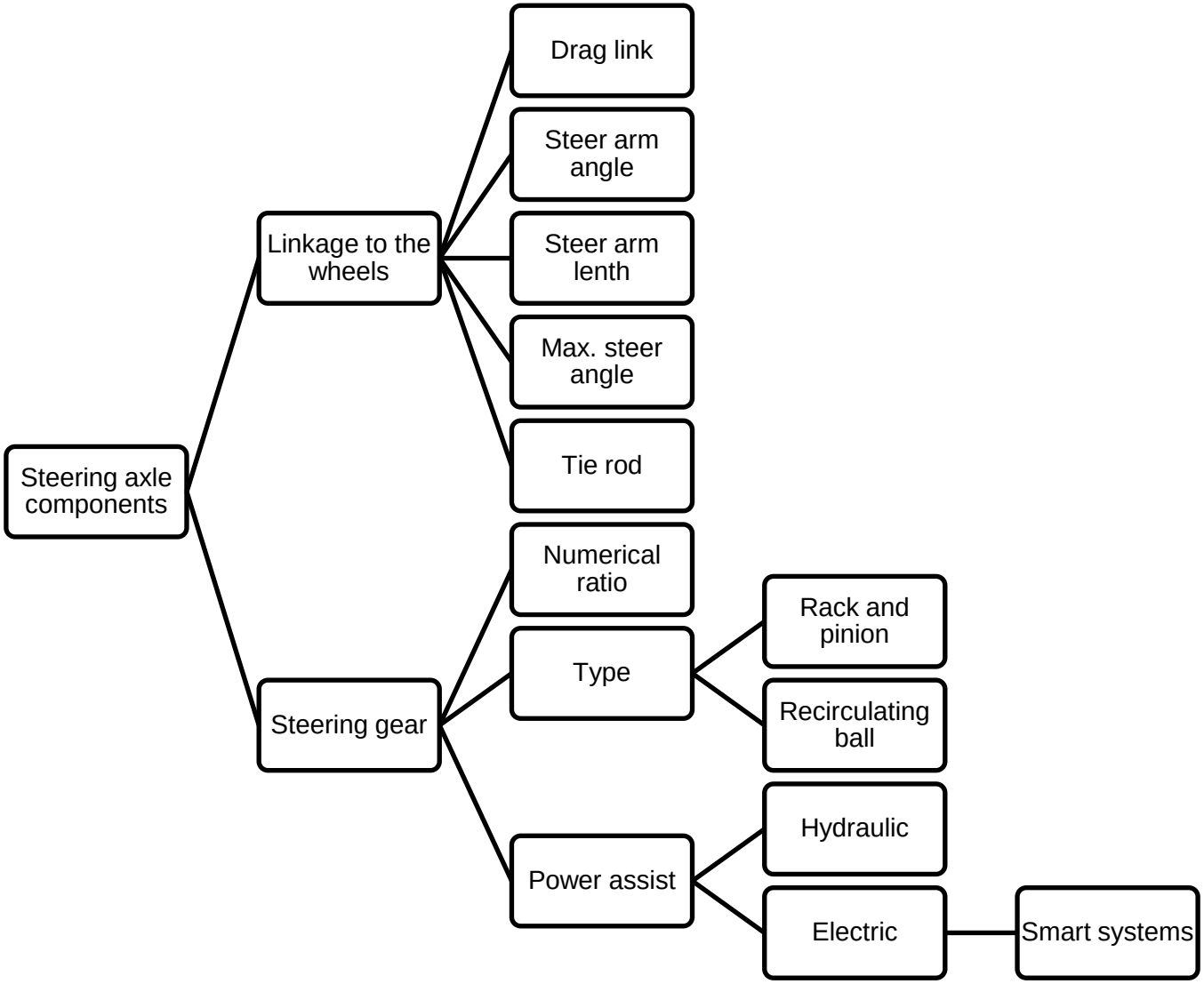

Figure 8-5. Graphic. Steer axle component options (1 of 2)

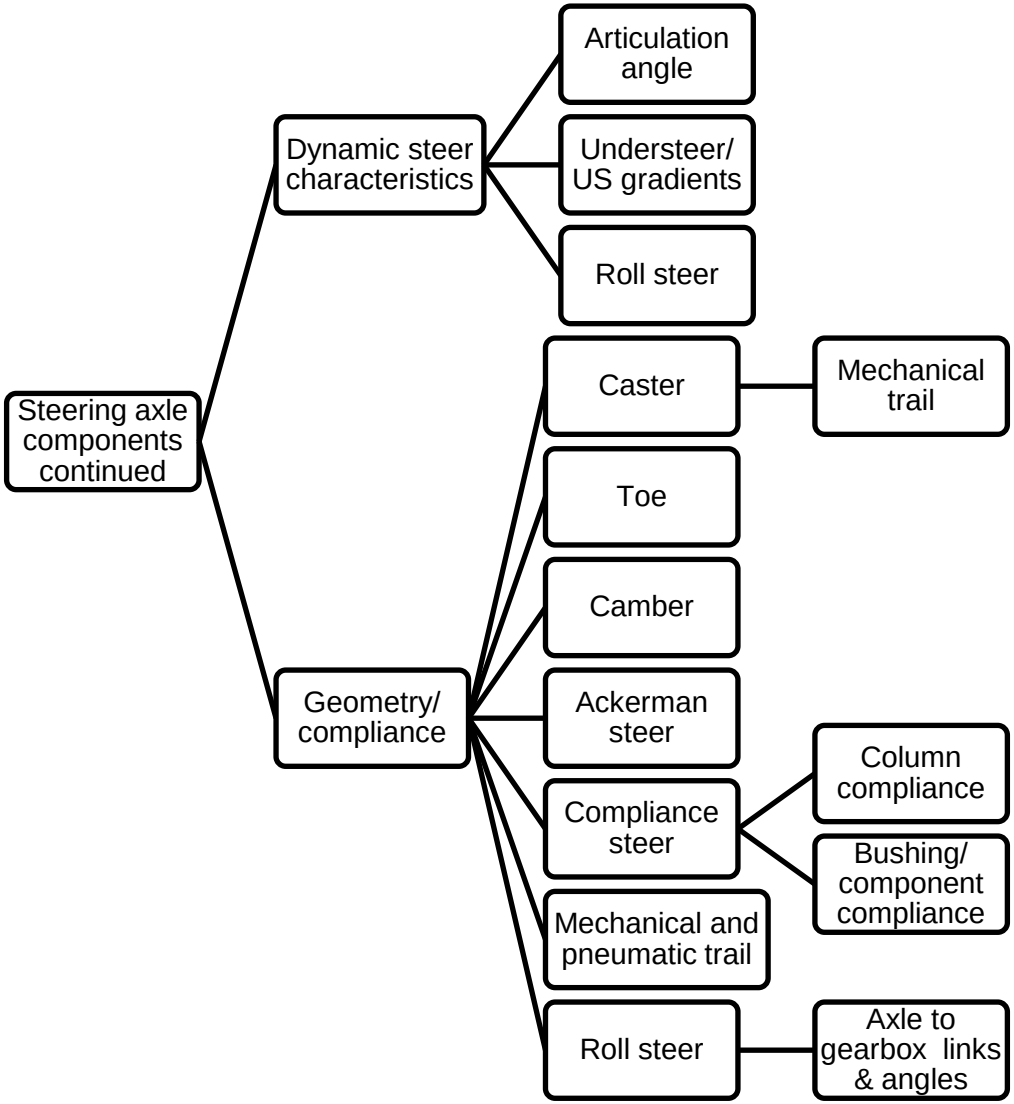

Figure 8-6. Graphic. Steer axle component options (2 of 2)

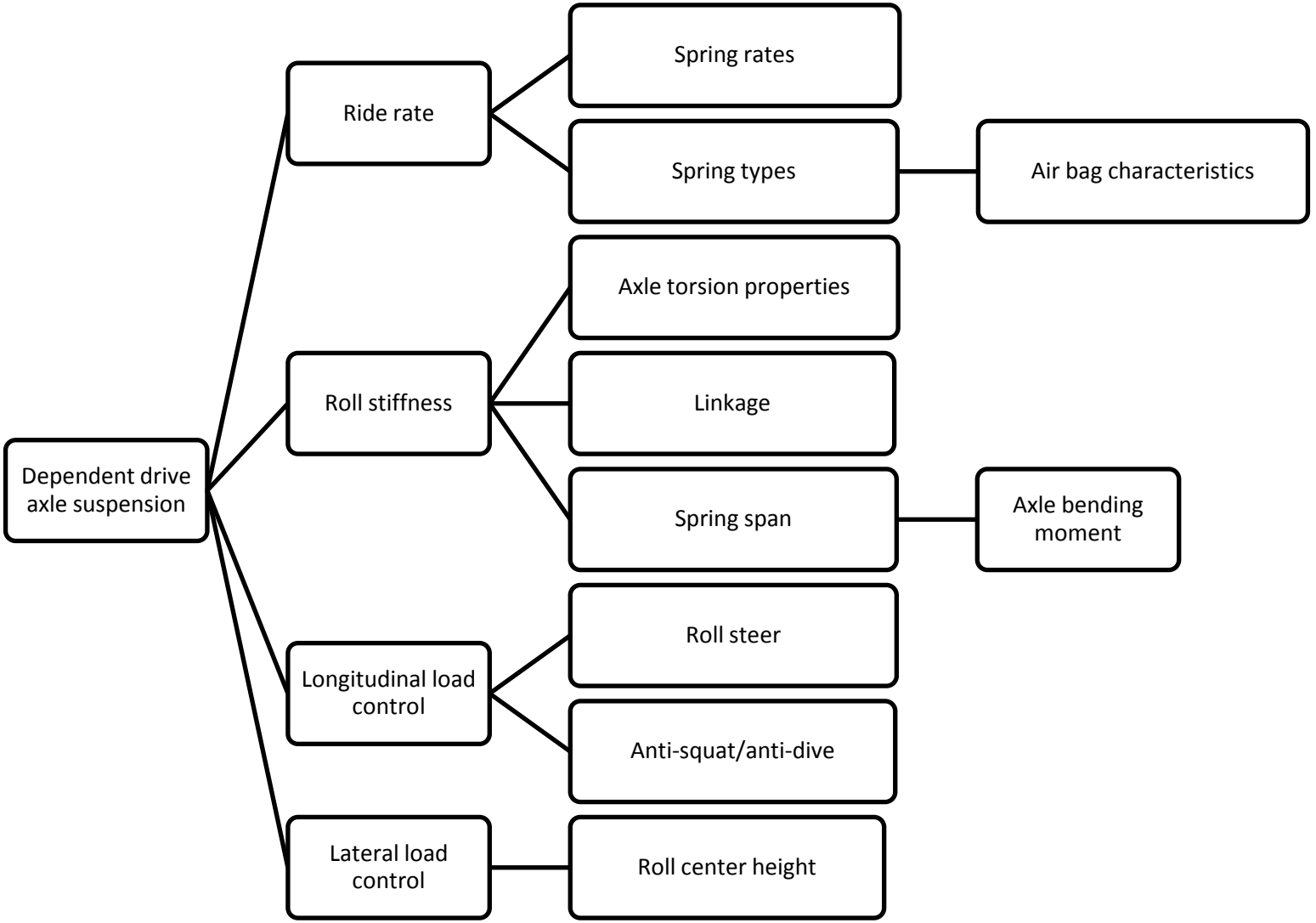

Figure 8-7. Graphic. Rigid drive axle suspension

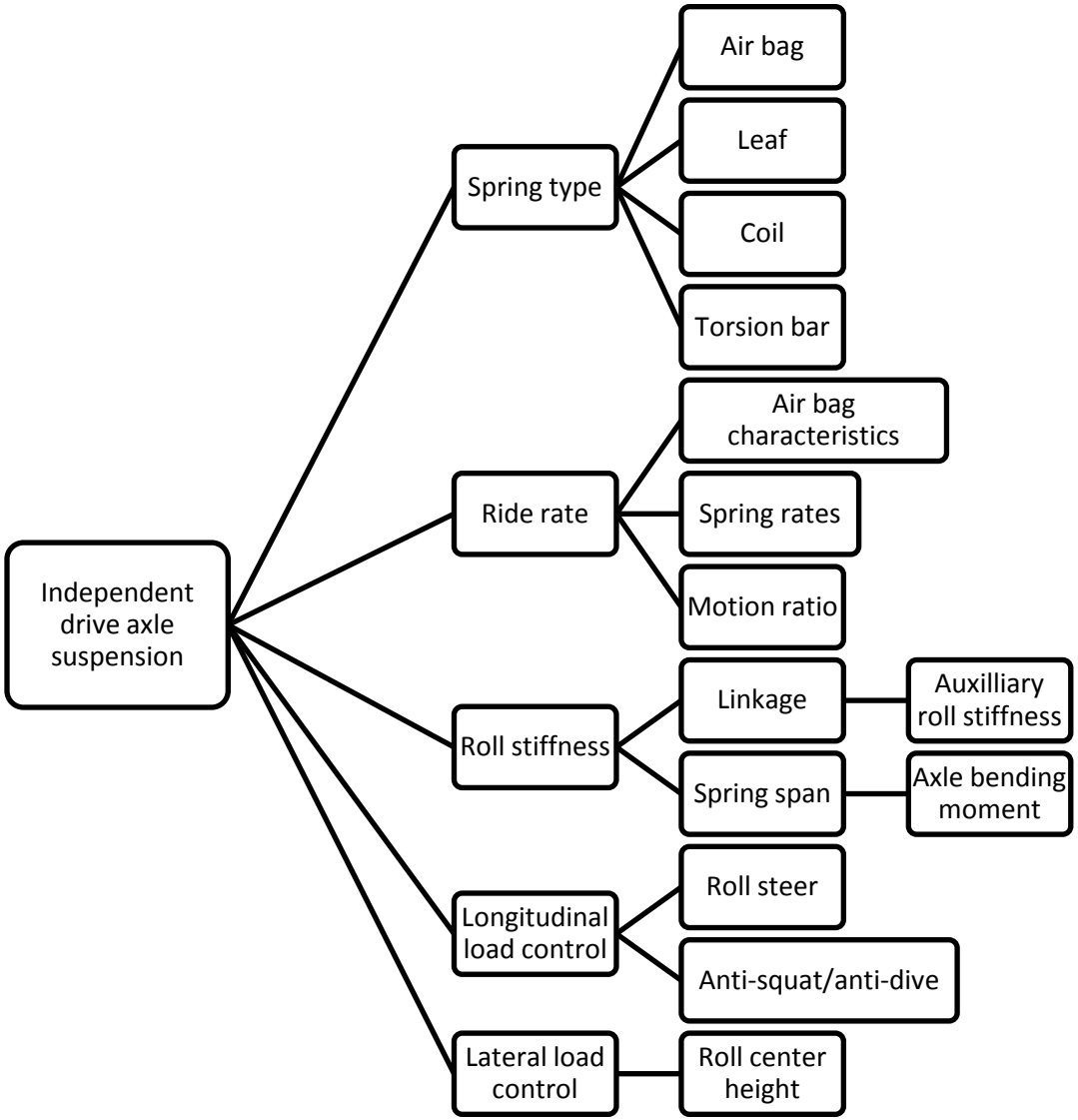

Figure 8-8. Graphic. Independent drive axle suspension

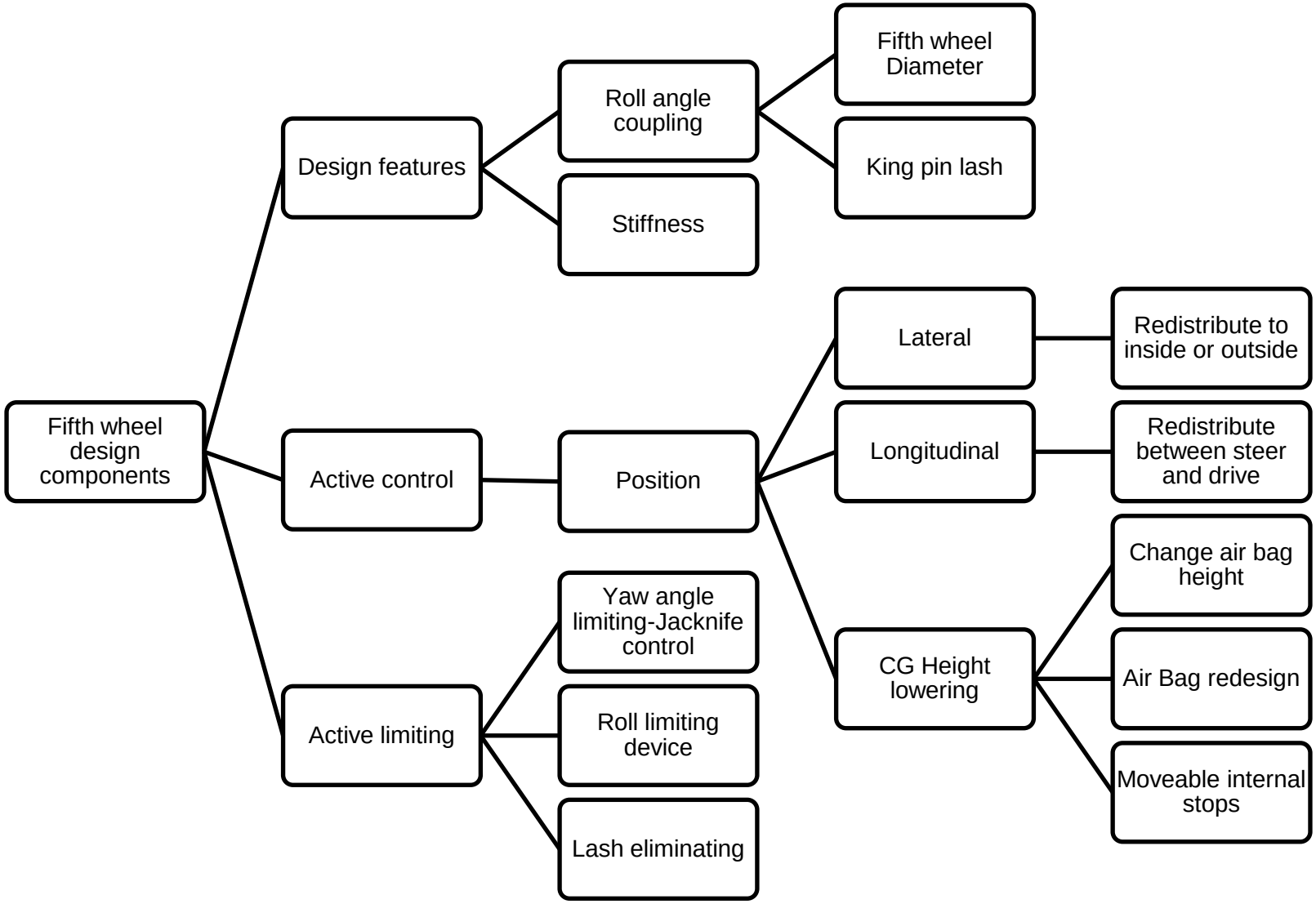

Figure 8-9. Graphic. Fifth wheel design component options

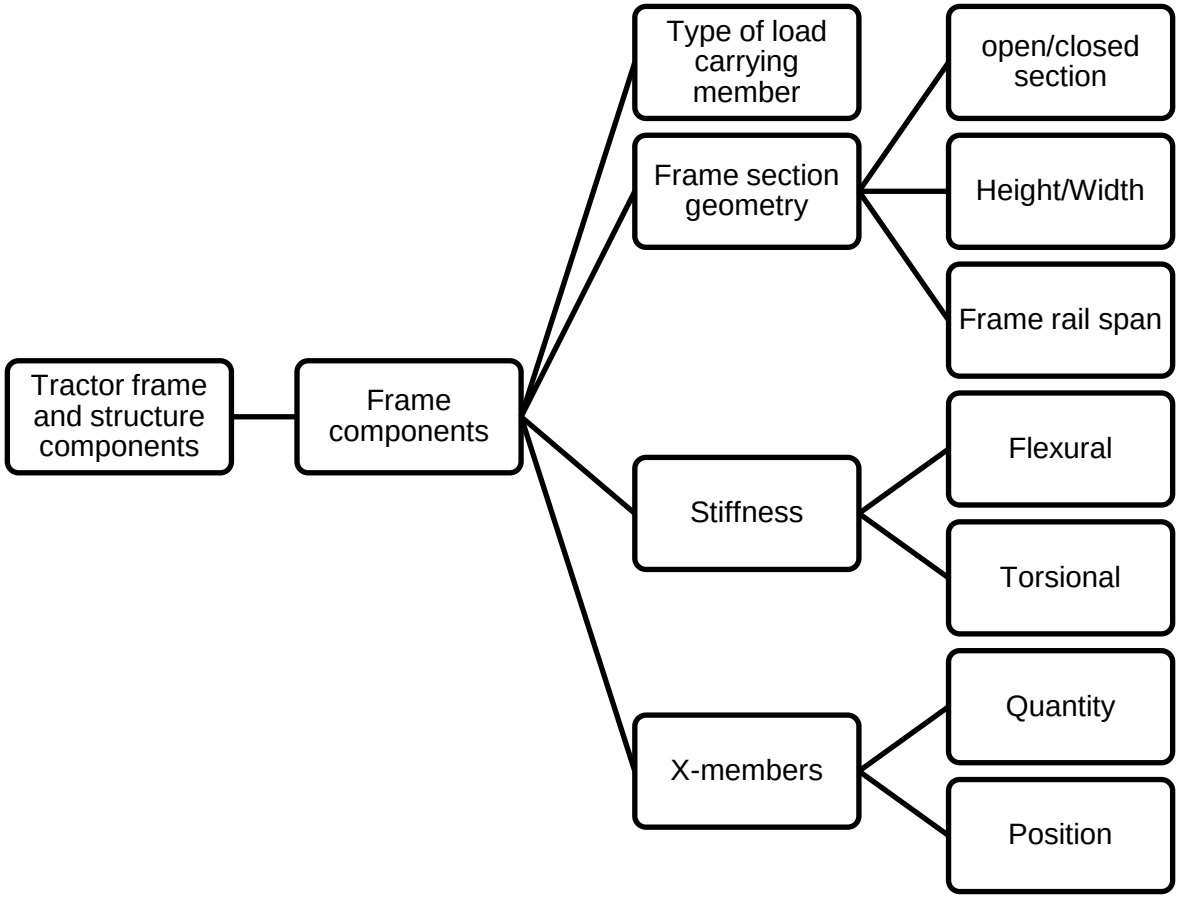

Figure 8-10. Graphic. Tractor frame and structure component options

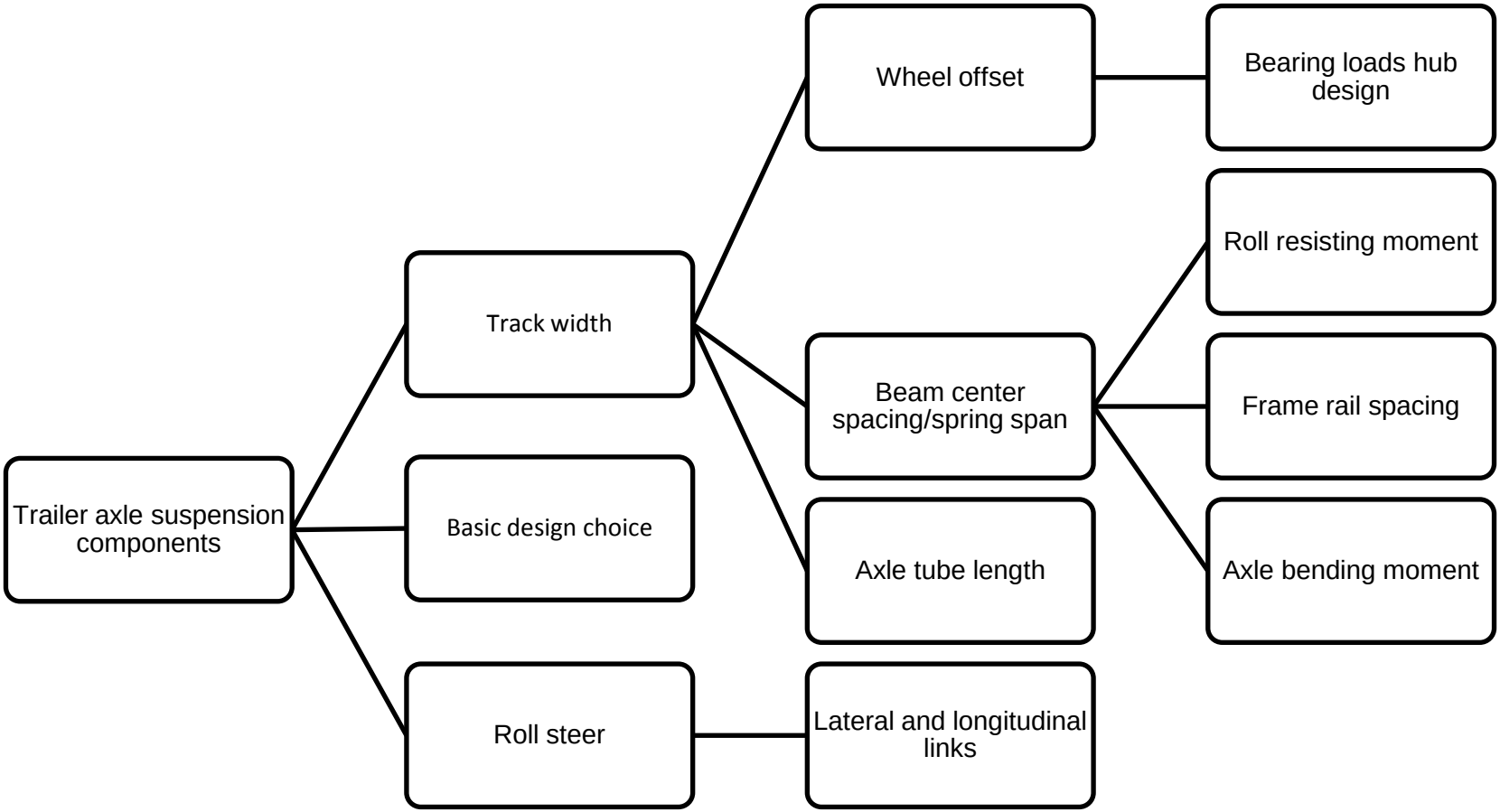

Figure 8-11. Graphic. Trailer axle suspension component options

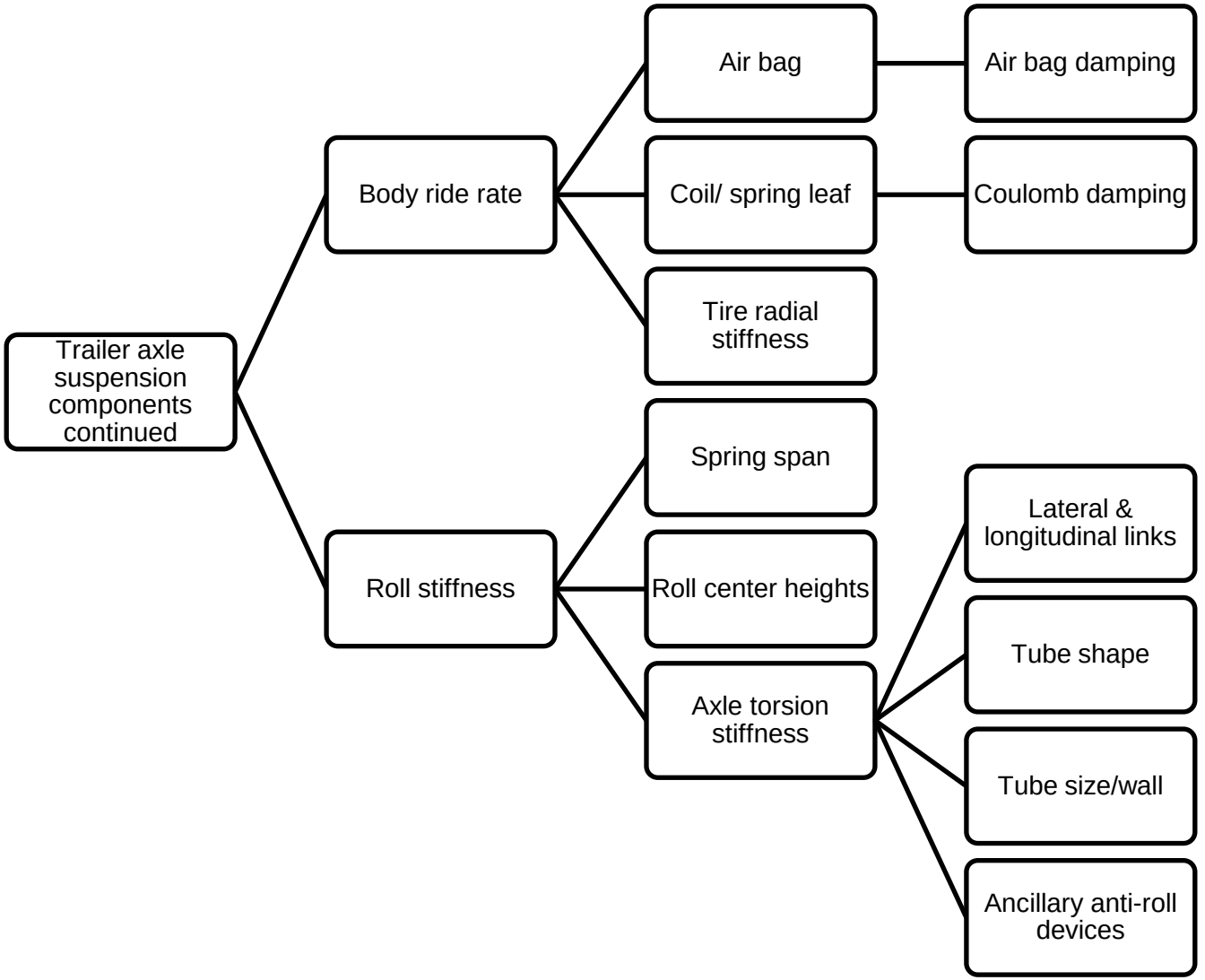

Figure 8-12. Graphic. Trailer axle suspension characteristics options

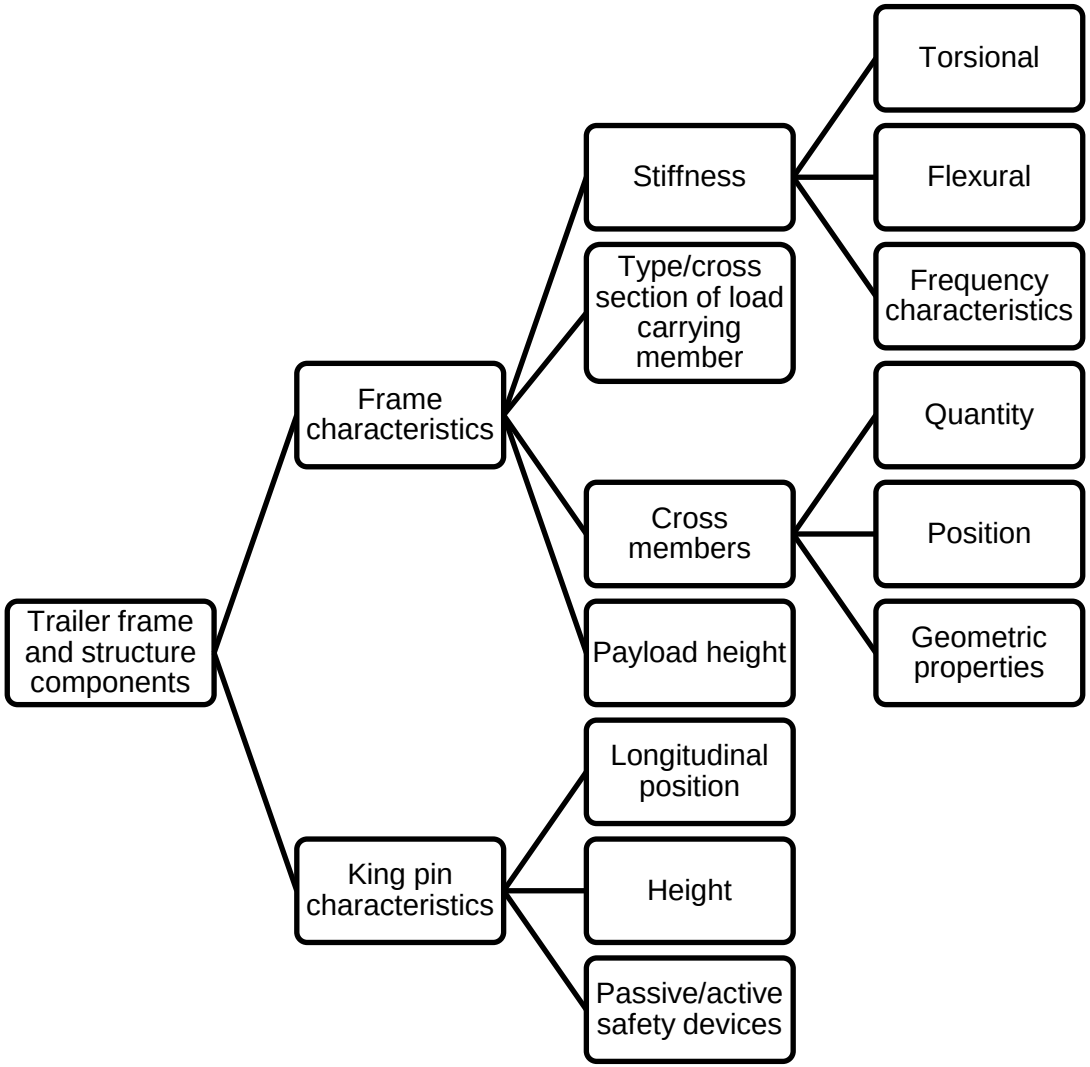

Figure 8-13. Graphic. Trailer frame and structure component options

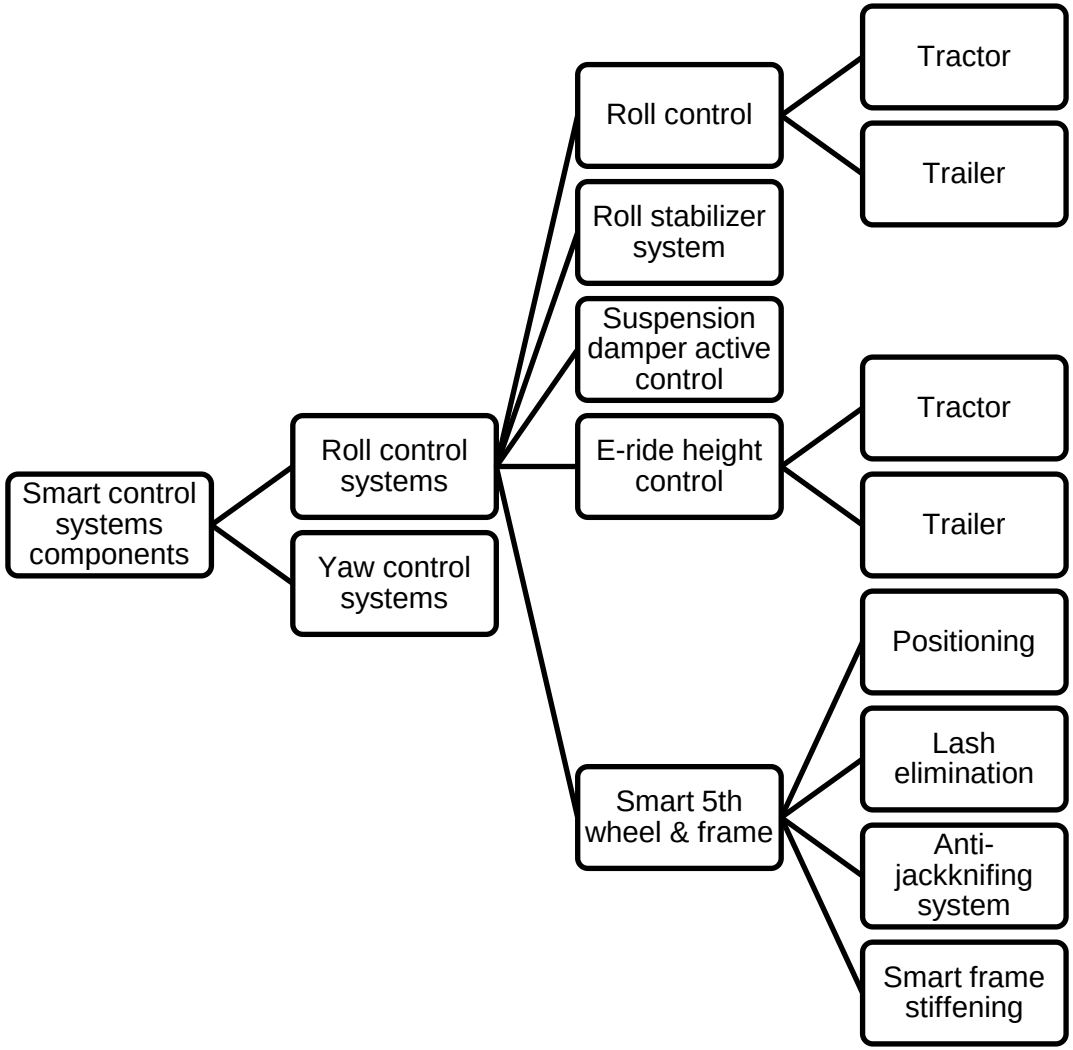

Figure 8-14. Graphic. Electronic system component options for stability control (1 of 2)

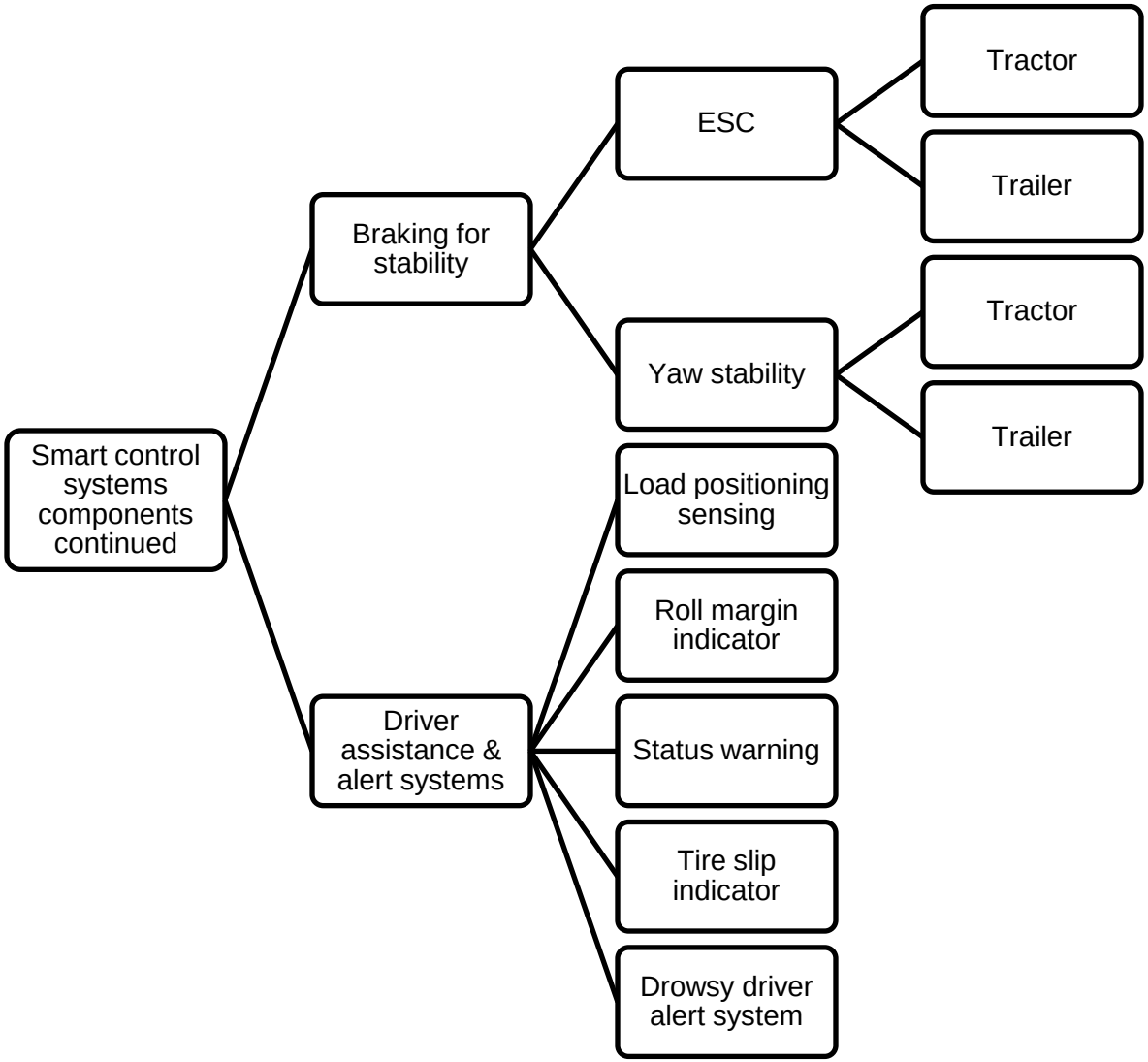

Figure 8-15. Graphic. Electronic system component options for stability control (2 of 2)

8.1.2 Estimates of Improvement in Wheel Lift Threshold

The potential benefits of some of the more straightforward design changes were explored in modeling. In addition to those shown below considerable work was done on identifying the effects of fifth wheel characteristics and has been addressed earlier in section 4.1.3.

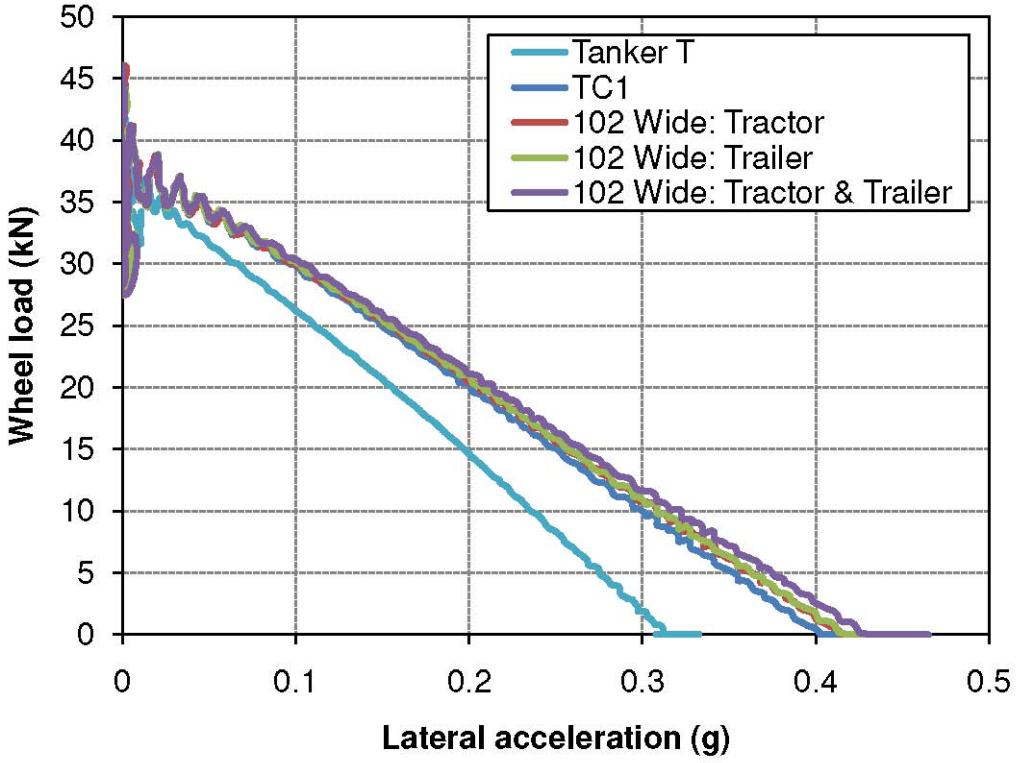

Figure 8-16. Graph. Axle 5 inside wheel load vs. tank trailer lateral acceleration for TC1 (98 in. outside-outside) and maximum (102 in.) outside-to-outside widths

Figure 8-16 shows the load on the inside wheel of Axle 5 in a TruckSim® simulation of the ramp steer maneuver of the Tanker T and Tanker TC1 test vehicles. The outside-to-outside width of the tires on Axles 4 and 5 of Tanker TC1 tires was the same as on the vehicle at the test track (nominally 2487 mm or 97.875 in.). The maximum width of commercial motor vehicles on the National Network of highways is 2,600 mm (102.36 in.) The ramp steer was simulated again in TruckSim® for vehicles similar to Tanker TC1, but with an overall width at the nominal 102 in. The inside wheel on Axle 5 of Tanker TC1 lifts at a lateral acceleration of 0.403 g in the simulation, and it lifts at 0.430 g if the drive and trailer axles are widened, an improvement of 0.027 g or 6.7 %. The results of this simulation and others are summarized in Figure 8-17.

Figure 8-17 displays the results of modeling with a lower CG height. For modeling purposes it was assumed that a tank trailer CG could be lowered 100 mm (4 in.). This would lower the total

sprung mass, not just the payload mass. The CG of the tractor was left at its design height. The model predicted a gain in wheel lift threshold of approximately .04 g.

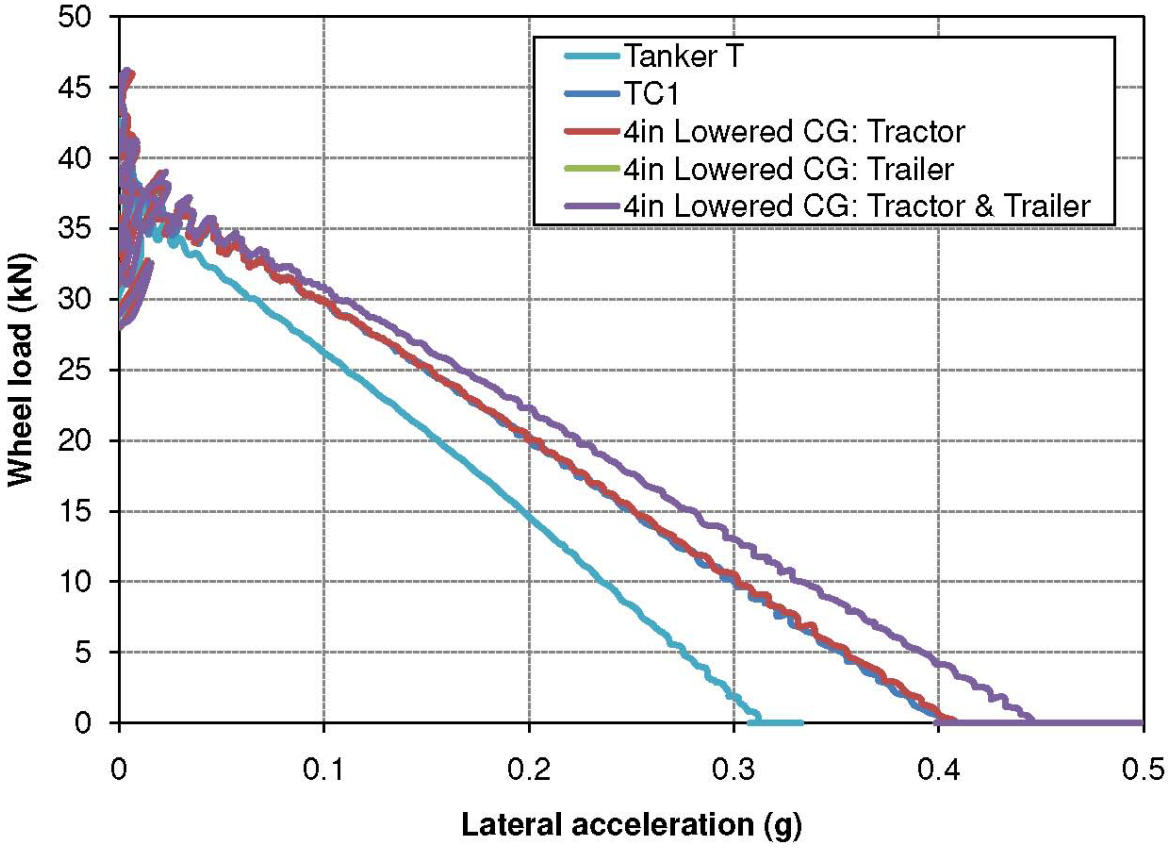

Figure 8-17. Graph. Axle 5 Inside wheel load vs. tank trailer lateral acceleration for TC1 (98 inch) with test height CG compared to CG lowered 100mm (4 inches)

Figure 8-18 displays the results of lowering both the CG height 100 mm and widening the track to the maximum allowable outside-to-outside dimension. The benefits of combining maximum width axles with lower CG height are obvious and all efforts to pursue changes of this nature are obviously beneficial. Approximately a 0.075 g (18.75%) can be gained through this arrangement.

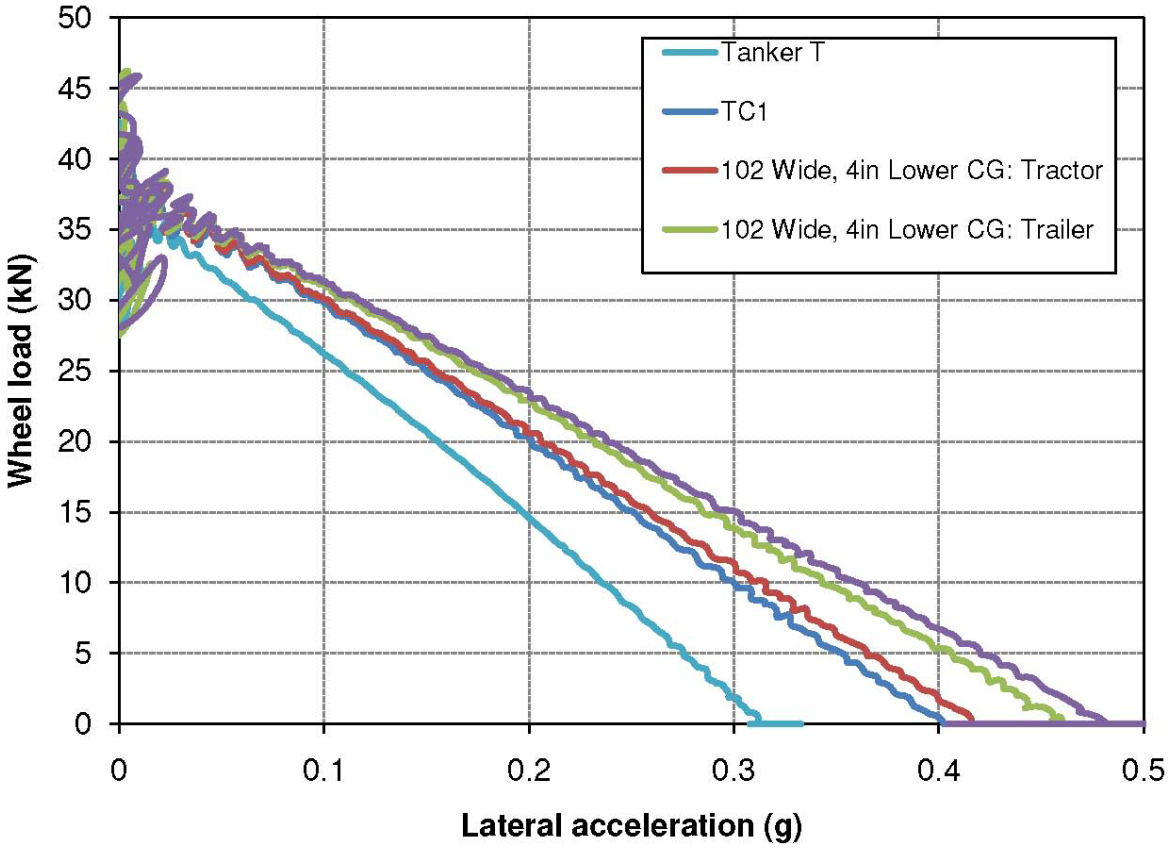

Figure 8-18. Graph. Axle 5 Inside wheel load vs. tank trailer lateral acceleration for TC1 (98 in. outside-outside) and maximum (102 in.) width axles in various configurations

To evaluate effects of roll stiffness and related roll angle benefits, the auxiliary roll stiffness was modified for both the tractor and the tank trailer. Figure 8-19 shows the result of the various configurations. When the tank trailer roll stiffness alone is increased, the graph shows the lateral acceleration for lift is reduced, producing earlier wheel lift. When the tractor auxiliary roll stiffness is increased the lateral acceleration of the tank trailer is increased above the baseline. However, when the tractor auxiliary roll stiffness is increased it lowers the lateral acceleration of the tractor, even though it increases the lateral acceleration for the tank trailer. The final comparison (intersecting at approximately 0.42 g) is when the tractor and trailer auxiliary roll stiffness are both increased. This reinforces the previously documented need to balance the roll stiffness of the axles of the entire vehicle.

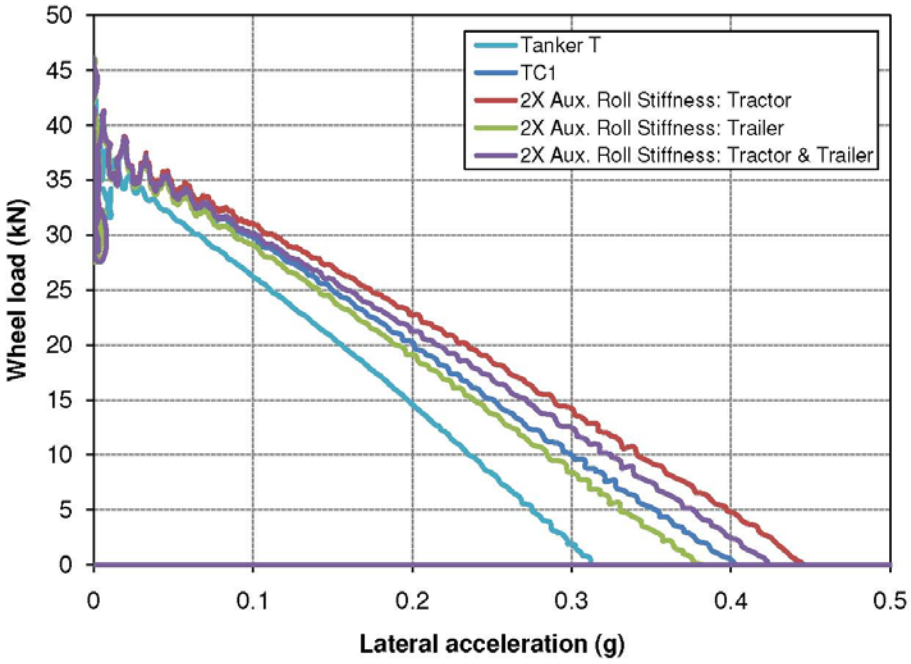

Figure 8-19. Graph. Axle 5 wheel load vs. lateral acceleration model comparison for increased auxiliary roll stiffness.

Table 8-1 shows comparisons of the wheel lift points for the various configurations tested. The time at the first wheel lift and the roll angle are also presented. Values are of lateral acceleration and body roll angle at the moment of each axle's wheel lift in a simulation of the ramp steer maneuver.

Table 8-1. Values at the moment of wheel lift in the ramp steer maneuver, as simulated in TruckSim®

Axle Configuration (all axle dimensions are outside tire to outside tire)	**Axle**	Values are at the moment of wheel lift				
		Time (s)	**a_y (g)**		**Roll Angle (deg)**	
		Lift	Tractor	Trailer	Tractor	Trailer
TC1 baseline (2349.5 mm drive axle , 2486 mm trailer axle, 919 mm tractor CG height, 1551 mm trailer CG height)	2	20.96	0.455	0.420	5.15	7.94
	3	20.99	0.456	0.423	5.43	8.15
	4	19.27	0.433	0.414	3.79	4.07
	5	18.87	0.425	0.403	3.68	3.94
2591 mm tractor drive axles (baseline trailer axle, baseline CG heights)	2	20.54	0.482	0.433	5.39	8.38
	3	20.61	0.480	0.441	5.86	8.96
	4	19.27	0.452	0.426	3.74	4.06
	5	18.88	0.440	0.415	3.63	3.93
2591 mm trailer axles (baseline tractor axle, baseline CG heights)	2	21.67	0.478	0.435	5.15	7.99
	3	21.68	0.474	0.435	5.29	8.06
	4	19.96	0.454	0.428	3.79	4.05

Axle Configuration (all axle dimensions are outside tire to outside tire)	**Axle**	Values are at the moment of wheel lift				
		Time (s)	**a_y (g)**		**Roll Angle (deg)**	
		Lift	Tractor	Trailer	Tractor	Trailer
	5	19.5	0.443	0.418	3.67	3.92
2591 mm tractor drive & trailer axles (baseline CG heights)	2	21.01	0.483	0.449	5.33	8.12
	3	21.11	0.495	0.451	5.88	9.07
	4	19.81	0.472	0.438	3.73	4.04
	5	19.52	0.466	0.430	3.63	3.91
817.4 mm tractor CG height (baseline trailer CG height, baseline axles)	2	20.01	0.508	0.426	4.57	7.65
	3	20.07	0.476	0.429	5.30	8.06
	4	18.57	0.441	0.416	3.75	4.05
	5	18.25	0.429	0.409	3.66	3.95
1449.6 mm trailer CG height (baseline tractor CG height, baseline axles)	2	23.63	0.513	0.491	4.76	5.24
	3	24.45	0.499	0.486	5.99	8.84
	4	21.35	0.492	0.459	3.72	3.97
	5	21.03	0.479	0.446	3.63	3.87
817.4 mm tractor CG height, 1449.6 mm trailer CG height (baseline axles)	2	23.63	0.513	0.491	4.76	5.24
	3	24.45	0.499	0.486	5.99	8.84
	4	21.35	0.492	0.459	3.72	3.97
	5	21.03	0.479	0.446	3.63	3.87
2591 mm tractor drive axles, 817.4 mm CG height tractor (baseline trailer axles and CG height trailer)	2	20.57	0.458	0.432	5.04	7.82
	3	20.67	0.478	0.439	5.54	8.66
	4	19.37	0.457	0.429	3.72	4.06
	5	18.97	0.445	0.417	3.60	3.92
2591 mm trailer axles, 1449.6 mm trailer CG height (baseline tractor axles, and CG height)	2	no lift				
	3	no lift				
	4	21.99	0.499	0.476	3.73	4.00
	5	21.71	0.499	0.460	3.62	3.87
2591 mm tractor drive axles & trailer axles, 817.4 mm tractor CG height & 1449.65 mm trailer CG height	2	24.25	0.642	0.506	4.49	8.25
	3	24.32	0.568	0.507	5.47	8.93
	4	21.85	0.536	0.489	3.62	3.96
	5	21.32	0.528	0.482	3.54	3.84
Double auxiliary tractor roll stiffness (baseline axles, CG height, and trailer roll stiffness)	2	20.01	0.516	0.451	3.63	6.73
	3	20.06	0.496	0.447	4.24	7.08
	4	19.36	0.486	0.453	3.46	4.02
	5	19.17	0.484	0.446	3.38	3.90
Double auxiliary trailer roll stiffness (baseline axles, CG height, and tractor roll stiffness)	2	21.05	0.451	0.415	5.15	7.94
	3	21.07	0.450	0.417	5.35	8.08
	4	18.35	0.403	0.384	3.01	3.18

Axle Configuration (all axle dimensions are outside tire to outside tire)	**Axle**	Values are at the moment of wheel lift				
		Time (s)	**a_y (g)**		**Roll Angle (deg)**	
		Lift	Tractor	Trailer	Tractor	Trailer
	5	18.2	0.397	0.382	2.99	3.17
Double auxiliary tractor and trailer roll stiffness (baseline axles, CG height)	2	20.57	0.514	0.448	3.74	6.79
	3	20.61	0.500	0.445	4.26	7.07
	4	19.12	0.455	0.430	2.90	3.18
	5	18.9	0.449	0.424	2.87	3.13

8.2 Review of Concepts for Technologies to Stabilize Vehicles

A number of technologies to limit vehicle rollovers have been proposed. Some of these ideas have been developed further than others and some have more merit than others. The topics discussed in this section have been reported in Phase A or Phase B and are presented here in summary form for completeness and for the possibility that they may spark more ideas.

8.2.1 Repositionable Fifth Wheel

A concept to reposition the fifth wheel within the tractor frame is shown in Figure 8-20. The objective is to optimally position the weight on the tractor chassis to add stability to the tractor itself. This concept has to be explored more fully in the future to understand all its implications, and should be modeled within a dynamic system to understand its potential for further development.

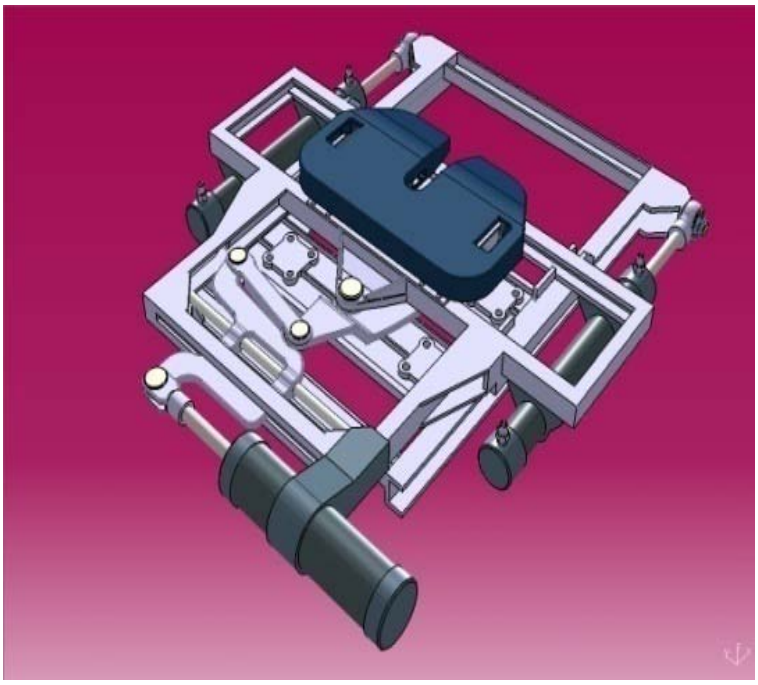

Figure 8-20. Drawing. Moveable fifth wheel (Courtesy of Ohio State University)

8.2.2 Active Suspension Control

Active suspension models have been developed for increasing rollover threshold. What makes this system an active suspension and not a reactive suspension is the way the system attempts to predict when roll will occur and prepares for it. It uses the roll angle, speed, and hand wheel angle to develop coefficients to multiply the original spring and damper forces to better control the roll angle of the tractor or trailer. If the vehicle is moving down the road with little to no roll, the system will effectively be off. When the hand wheel is turned rapidly, the system stiffens the suspension, preparing for a roll before the roll occurs. The system distinguishes between steady state and transient events and acts to reduce roll oscillations.

8.2.3 Active Roll Control

An experimental heavy vehicle with active roll control which tilts the vehicle into the turn to increase the rollover threshold has been developed by Miege and Cebon (2003) The active anti-roll system on the tractor and trailer is mounted on each axle with an anti-roll bar between the trailing arms of the suspension and has two hydraulic actuators which are controlled by two servo-valves. The hydraulic pressure is supplied to the servos by a high pressure radial piston hydraulic pump. The anti-roll bar is twisted and applies active roll moment to the vehicle by extending one actuator and retracting the other, thereby reducing the lateral load transfer. Approximately 70 sensors continually monitor suspension roll angle, active anti-roll moment, roll rate, yaw rate, lateral acceleration, etc.., constantly supplying the four local controllers and global controller with new data. As the controller receives and processes data, it operates the

hydraulic servos. A possible control strategy is to equalize the load transfer on all the critical axles and provide maximum roll inwards. The normalized lateral load peak can be reduced by as much as 40 % and roll-over accidents can be avoided by rolling the vehicle into the turn with this strategy.

8.2.4 Semi-Active Roll Control

A semi-active roll control was developed to improve heavy vehicle stability while having low power consumption (Stone and Cebon 2002, Stone and Cebon 2009). Highway vehicles typically have a trade-off between roll and ride: a soft suspension provides more comfortable ride, but a stiff suspension better resists roll. The Semi-active roll control works by altering the roll stiffness of the vehicle to soft (unlocked) during general driving or stiff (locked) during cornering maneuvers. This is accomplished by connecting and disconnecting an anti-roll bar on an independent trailing arm suspension with the use of hydraulic cylinders.

Further research is being currently done to increase the rollover threshold of the vehicle by using the semi-active roll control system with a changing roll stiffness and the addition of the ability to lock-in roll angle. For example, as the vehicle makes a slight left turn the roll angle is locked in as it rolls to the left before it makes a sharp right turn. To do this, it is essential to know the future path of the vehicle, which can be predicted by using a GPS unit and monitoring the steer angle. It was mentioned that the system's performance would reduce greatly if the vehicle did not follow the predicted path correctly.

8.2.5 Active Steering Systems

Jujnovich et al. (2006) developed a path-following steering controller to make the rear of the trailer follow a path defined by the fifth wheel. This system was called Conventional Tractor-Active Trailer. The system has steering on all axles including the tractor drive axle. The path following strategy includes a model following controller. If the vehicle develops an off-tracking error, the model following controller allows the vehicle to return to the path defined by the lead point. In order to minimize the lateral tire forces, the controller sets the steer angles of the individual axles of the semitrailer axle group. This was tested using a roundabout path that is standard in the United Kingdom roadways. This system reduced the roundabout swept path width, tail swing, and exit settling distance. Tail swing is the deviation of the rear of the trailer outside the path of the lead point when entering the roundabout. The exit settling distance is an indication of how long after the maneuver the trailer's directional response is affected. The system has been tested only at low speeds.

8.2.6 Electronic Brake Force Distribution System

One of the recent refinements to antilock braking systems has been the addition of electronic brake force distribution (EBD) (Carley 2009). The principle that the weight being supported by the wheels is not distributed evenly is the whole basis of EBD. Wheels that carry a heavier load require more braking force to bring the truck to a controlled stop. During the braking process, the

weight supported by each wheel can shift; therefore, the necessary braking force of each wheel can change rapidly. An EBD system can sense the weight being supported by each wheel, as well as adjust the amount of braking force of each independent wheel continuously. EBD does not detect weight distribution directly, but the system is aware of it through the effect on the slip ratio of the tires. The three primary instruments are necessary for the EBD system are sensors, valves, and an electric control unit. Sensors determine the slip ratio of each independent wheel. Valves regulate the brake force of each wheel and the electronic controller calculates the required actuating force of each brake. EBD is common in modern commercial vehicles in Europe. North American vehicles do not have electronically-controlled braking systems and do not implement EBD.

8.2.7 Anti-Rollover Deployable Axle

An example of a concept for a mechanical rollover-preventing device is Patent No. 6,588,799, the Vehicle Anti-Rollover Device shown in Figure 8-21. This device extends the track width of the vehicle so as to prevent vehicle rollover when the vehicle tilts. The device comprises a sliding steel bar or rod with a wheel or cylindrical ball joint at the terminal end that will slide out from a vehicle when the vehicle begins to tilt. The bar or rod extends to the side of the front and rear of the vehicle to a point where it touches the road to prevent further tilt or rollover. The sliding bar or rod is enclosed in a sleeve that is attached to the frame, bumper or body of the vehicle, so that the load of the vehicle can be absorbed, preventing tilting or rollover.

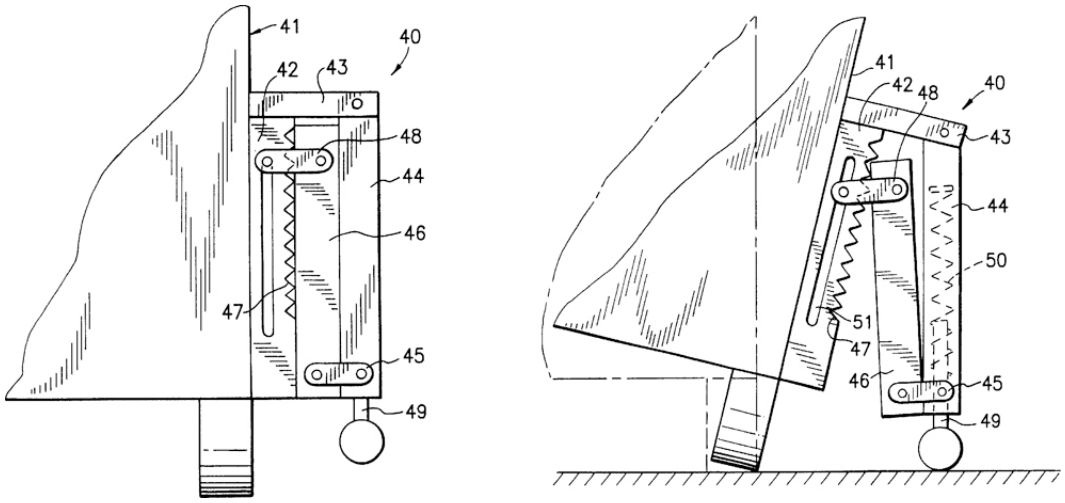

Figure 8-21. Drawing. Vehicle anti-rollover device

A potential improvement on this device uses the same concept but requires no extension beyond the width of the vehicle. This system, shown in , is a modification of Hendrickson lift axle. When the trailer rolls, the air suspensions, or airbags in this case, will be deflected, giving way to the weight of the trailer. But when the tractor trailer is experiencing a sharp turn, the tractor trailer will usually undergo a larger roll angle than a typical turn and as a result, this will cause more deflection on the airbags. To prevent rollover, a pendulum is added on the bottom of the lift axle. The end of the pendulum is in a steel casing with a slot for the pendulum to slide in. The steel case is welded under the axle. When the trailer is rolling, the pendulum will swing so the end of the pendulum will slide along the slot until it is fully extended. The steel case will stop the pendulum from swinging out further, preventing the trailer from tilting any further, and preventing the rollover. For simplicity, the landing gear could be attached together as part of the feature in the lift axle as well, minimizing the number and weight of additional components.

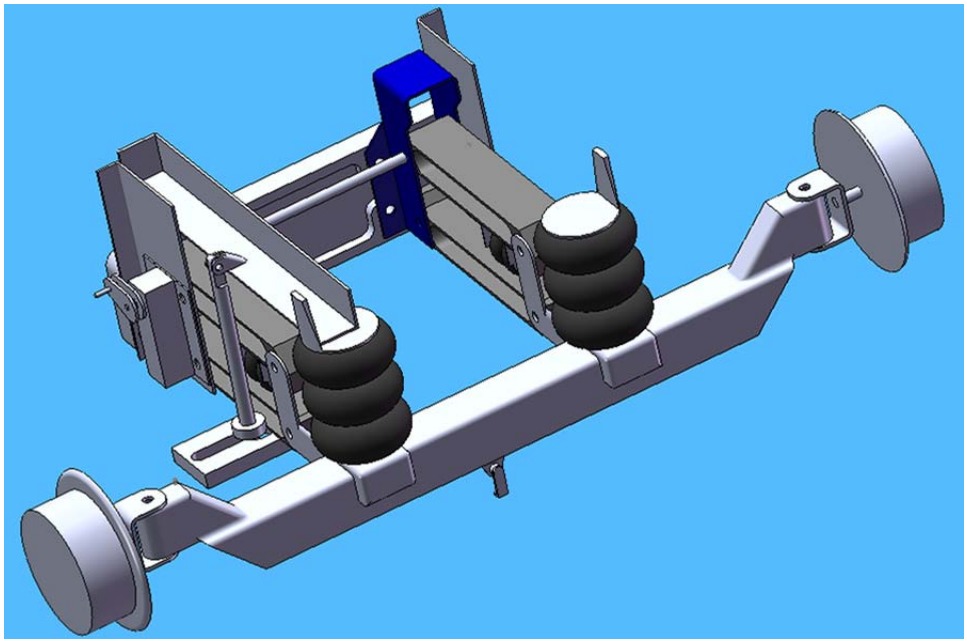

Figure 8-22. Drawing. Modified lift axle

Chapter 9 – Summary of Results

Both the track testing and modeling performed during the Phase C HTRC project increased the understanding of how the suspension system of a cargo tank semitrailer influences its roll performance. Steps were made to develop a modeling methodology that can predict roll performance and to reduce the need for costly track testing. Several suspension design factors were identified as having an important influence on the wheel lift threshold. Detailed analysis of two semitrailer suspensions using TruckSim® showed results that were consistent with the experimental results, and other design factors were modeled to demonstrate the magnitude of benefits of several other designs and technologies.

9.1 Modeling Results

The project included both TruckSim® and Adams model development. TruckSim® is a lumped parameter analysis tool that uses characteristic vehicle performance parameters as inputs predict vehicle performance. The model can simulate user-specified maneuvers and is much less complex than the Adams model. It can be used to evaluate changes in design when the changes do not result in significant differences in the K&C characteristics of the vehicle, or when such differences are precisely known, either as a result of K&C testing of an existing vehicle, or through modeling using software that can account for detailed geometric and stiffness changes to predict the impact on K&C characteristics. Adams modeling can serve to provide the K&C information that TruckSim® requires, and as such, the two software tools are complementary. Even when starting with a known vehicle, the TruckSim® model is sensitive to numerous parameters that must be tuned to develop a high-accuracy baseline model. It does not determine the motions of all components in the vehicle, however, and it cannot predict the effect that component modifications will have on the vehicle performance. Nonetheless, careful model development provides good predictions, and variations to the original model can be expected to provide results that accurately reflect the changes made. In this sense, the tool can be useful for evaluating design changes that have no impact on K&C properties, or for which these changes are known.

Adams modeling can be used to estimate how specific design changes to a vehicle affect its overall performance. The Adams model can therefore provide performance predictions that are specific to individual designs, but the modeling is more complex and requires considerable time for model development. The Adams model can be used to apply the knowledge gained relative to improving the tractor-trailer's roll stability to 1) develop a "buildable" tractor trailer concept that includes design technology options that are relatively easy to implement and that have strong positive stability benefits, and 2) extend the stability evaluations to combination vehicles with multiple trailers.

Specific results from the TruckSim® modeling have improved the HTRC team's understanding of roll stability and the role that the suspension plays in stability. Key successes resulting from the TruckSim® modeling include:

1. When the test design variations in Phase C were selected, it was estimated that the roll stiffness could be significantly increased with the wider beam center spacing of the TC1 axle, and the HTRC team expected that the roll performance of vehicle configuration TC1 would be significantly improved relative to both the Phase B configuration (Tanker T) and configuration TC2, which used the more narrow beam center spacing. The TruckSim® model, gave results that were generally consistent with the track testing results in terms of there being little difference between the wheel lift threshold for the TC1 and TC2 configurations. The wider axle associated with both of the Phase C axle designs provided a much more significant improvement than the roll stiffness change, and it was determined that the coupling between the tractor and tank trailer acted to reduce the benefit that would be expected with the roll stiffness difference between the TC1 and TC2 axles.
2. The effect of the auxiliary roll damping was investigated during Phase C because the TruckSim® model showed poor correlation with test track results in Phase B when only the damping associated with the shock absorbers was included in the model. During model tuning, auxiliary roll damping that was greater than the damping of the shock absorbers, had to be added to the model to achieve results that matched the track testing measurements. Phase C testing confirmed the discovery that additional damping was indeed present in the system and that the shock absorbers play a negligible role in damping roll oscillations (although the shock absorbers are still important for pitch and bounce damping).
3. In addition to the successes achieved in measuring and modeling the vehicle suspensions, the HTRC team was also successful in developing functional curves that accurately reflect the fifth wheel coupling between the tractor and semitrailer. This was not a simple task as the fifth wheel response depends on many parameters including fifth wheel mount design, plate size, kingpin design, and vehicle load. The HTRC team was able to use physical dimension measurements of the tractor's fifth wheel along with video of the fifth wheel separation during testing to establish the fifth wheel lash. Using the known load supported by the fifth wheel and the plate dimensions, the roll moment curve through the fifth wheel was calculated. The fifth wheel characteristics play an important role in the wheel lift and roll behavior of the coupled tractor and semitrailer. Having a properly developed fifth wheel moment curve was essential for the subsequent development of vehicle dynamics models that accurately reflected the vehicle's dynamic behavior.

9.2 Track Testing Results

The track testing in Phase C was developed and conducted primarily to provide new roll stability results that could be compared with modeling results to validate the TruckSim® and Adams models. The desire was to include "clean" comparisons that would include only one design variation relative to some other configuration for which test results were available. Starting with the Tanker T configuration from Phase B as a baseline, two additional configurations were

developed that included a wider axle, but the same beam center spacing (i.e., suspension TC2) and the wider beam spacing in addition to the wider axle (i.e., suspension TC1). The wider track improved the roll performance. The initial expectation was that the greater roll stiffness provided by the wider beam spacing would improve the roll performance as well. A greater roll stiffness was indeed measured, both by the K&C and the strain gages on the axle. However, the TC2 suspension (wider track but narrower beam spacing) actually showed a small improvement over the wider beam TC1 in the data from some of the transient maneuvers. Load sharing between the tractor and trailer axles and differences in roll center height limited to the performance improvement of the stiffer TC1.

The auxiliary roll damping was characterized by performing a modified step steer maneuver to place the trailer on one of its outriggers and then allowing it to drop back onto all wheels in a controlled and repeatable fashion. The damping was quantified by evaluating the damping ratio during the period immediately following the return of the tractor-tank trailer onto all wheels. There was no discernible difference between the roll damping when the shock absorbers were installed and when the shock absorbers were removed, indicating that the shock absorbers do not contribute significantly to the roll damping of the tractor semitrailer. Although fully consistent with the TruckSim® modeling results, this result was not anticipated. Analysis of the airbag pressure measurements showed that a pressure differential developed between the left and right side airbags during transient events and that this provided a significant contribution to the auxiliary roll damping. This pressure differential is likely a function of the valves and plumbing that connect the airbags, so the design could be readily adjusted to either increase or decrease the airbag contribution to auxiliary roll damping.

Chapter 10 – Conclusions and Recommendations

The research conducted during HTRC Phase C project furthered the knowledge base relative to the roll stability of tractor-tank trailers, and efforts were made to advance modeling capabilities to a higher level. The ultimate goal of this research with respect to modeling is to enable accurate assessments of roll stability for design changes using comprehensive vehicle models, as opposed to building and testing prototype vehicles that include the new design features. A primary focus of Phase C was the role that modern suspension systems play on the stability of Class 8 tractor and cargo tank semitrailer combination vehicles. The testing, modeling, and analysis that were conducted all provided new insights into how the suspension influences the roll performance of these vehicles. The knowledge accumulated from this research can be applied to other semitrailer body styles (e.g. van, flatbed, tank) that use similar suspension systems. The modeling and testing complemented each other, and results from each activity served to improve the HTRC team's understanding of the suspension system influence on roll performance. The modeling efforts included both TruckSim® and Adams model development. These two are complementary with TruckSim® better suited for system-level changes and Adams better for changes in the designs of individual components.

Results from the project provided several insights into the influence of the suspension design on roll performance. Based on initial analysis of the different designs that were to be tested in Phase C, some of the testing results were unexpected, but the TruckSim® modeling results matched the experimental trends quite well when the characteristics of the different axle designs were input into the model. This demonstrates the value of the TruckSim® model and also exhibits the complementary relationship between the testing and modeling components of this research program.

Using the wider track axle improved the roll stability of the tractor-semitrailer. Increasing the track of the axle to the maximum practical limit should provide the greatest safety benefits. Furthermore, a wider track may enable other design modifications that can provide additional safety or other performance gains. The beam spacing did not have a significant effect on the roll performance. The ESC system performance was not extensively evaluated, but it did reduce the occurrence of wheel lift for the maneuvers tested, and its behavior was not found to be degraded in any way with the wider axle design or the changes in beam center spacing. Additional Adams modeling to assess other design parameters would allow a better understanding and optimization of the roll stability of a tractor-semitrailer without having to measure the K&C characteristics.

A number of specific designs and technologies have been identified and are expected to provide substantial improvements in inherent vehicle stability. These options can be further developed and optimized using the models so that the maximum safety benefits can be achieved. The team recommends that continued research with the following objectives:

1) Develop a “buildable” tractor trailer concept that includes design technology options that are relatively easy to implement and that have strong positive stability benefits. This concept development effort should be achieved through modeling, and will be considered for future development and testing.

2) Initiate a study of the dynamics associated with combination vehicles with multiple trailers. Such configurations are beneficial in terms of fuel efficiency, but involve new vehicle dynamics challenges that should be studied in more depth.

3) Develop advanced ESC algorithms that involve ESC coordination between the tractor and trailer. Such systems have the potential to provide significantly greater safety benefits than ESC systems on the tractor and trailer(s) that operate independently of each other.

4) Develop ESC hardware to validate the algorithm advancements. Development of such a prototyping system would permit multiple ESC strategies to be validated and offer a standard platform for the inception of commercial systems.

The HTRC team includes expertise among its members in modeling, analysis, testing, manufacturing and design that no single organization could have brought to the table by itself. The member organizations provided valuable contributions to the project, including donations of equipment and expertise, without which the research conducted would not have been possible. In short, the composition of the team brought synergies to the project that have made high-quality research possible, at a cost that was well below the benefits obtained, making this research a valuable use of American tax dollars, which ultimately funded the project.

Chapter 11 – References

Arant, M., S. Nelson, U. Attanayake, R. Hathaway, M.Keil, K. Ro, O. Franzese, H. Knee, T. LaClair, and D. Pape. 2009. U19: Heavy truck rollover characterization (Phase-B) final report. Final report to National Transportation Research Center, Inc., University Transportation Center, Contract No. DTRT06G-0043. Accessed August 2010 at http://www.ntrci.org/library/U19-Heavy_Truck_Rollover_Characterization_Phase_B_1259081915.pdf. http://www.ntrci.org/library/U19-Heavy_Truck_Rollover_Characterization_Phase_B_1259081915.pdf

Arant, M. "Heavy Truck Measurement, Modeling and Evaluation." Presented at SAE May 5-7, 2009. Heavy Truck Handling, Dynamics & Control, Symposium, Clemson University – ICAR, Greenville, South Carolina.

Arant, M. "Assessing the effect of chassis torsional stiffness on the accuracy of heavy vehicle understeer and rollover modeling." Clemson University. 2010. M.S. thesis.

Carley, L. 2009. Electronic Brake Distribution: Emerging Technology Offers Service Opportunities. Import Car, Feb. 1, 2009.

Davenport, J. M., and J. T. Webster. 1975. The Behrens-Fisher problem, an old solution revisited. Metrika 22: 47-54.

Jujnovich, B.A., R.L. Roebuck, A.M.C. Odhams, D. Cebon. 2006. Implementation of Active Rear Steering Of A Tractor – Semi-Trailer. Cambridge University Engineering Department. Cambridge.

Knee, H.E., G. Capps, O. Franzese, P. Pollock, D. Coleman, I. Janajreh, S. Haas, N. Frey, E.H. Law, E. Johnson, J. Petrolino, and D. Rice. 2005. Heavy truck rollover characterization: New-generation single tires vs. standard duals. Paper presented at the Truck and Bus Safety and Security Symposium, November 14-16, in Alexandria, Virginia.

Miege, A., and D. Cebon. 2003. Active Roll Control of an Experimental Articulated Vehicle. Cambridge University Engineering Department. Cambridge.

Pape, D., M. Arant, D. Hall, S. Nelson, J. Petrolino, O. Franzese, H. Knee, N. Wood, S. Yeakel, R. Hathaway, M. Keil, and P. Pollock. 2008. U02: Heavy truck rollover characterization (Phase-A) final report. Final report to National Transportation Research Center, Inc.; University Transportation Center, Contract No. DTRT06G-0043. Accessed August 2010 at http://www.ntrci.org/library/U02-_Heavy_Truck_Rollover_Characterization_Phase_A_1239201531.pdf.

Satterthwaite, F. E. 1946. An approximate distribution of estimates of variance components. Biometrics Bull 2: 110-114.

Smith, H. 1936. The problem of comparing the results of two experiments with unequal means. J. Council Sci. Industr. Res. 9: 211-212. [Cited in: Davenport, J. M., and J. T. Webster. 1975. The Behrens-Fisher problem, an old solution revisited. Metrika 22: 47-54.]

Stone, E. D. Cebon. 2002. "A Preliminary Investigation of Semi-active Roll Control," 6th International Symposium on Advanced Vehicle Control Hiroshima, Japan. Page 6, AVEC2002.

Stone, E. D. Cebon. 2009. "Control of Semi-Active Anti-Roll Systems on Heavy Vehicles," Vehicle System.

Welch, B. L. 1938. The significance of the difference between two means when the population variances are unequal. Biometrika 29: 350-361.

U24: Heavy Truck Rollover Characterization (Phase C)

Appendices A-H

Appendices A-H – Table of Contents

Appendices A-H – List of Figures

Appendices A-H – List of Tables

Appendix A – Test Plan

OVERVIEW OF TESTING EFFORTS FOR: HEAVY TRUCK ROLLOVER CHARACTERIZATION – PHASE-C

HEAVY TRUCK RESEARCH CONSORTIUM (HTRC)
Oak Ridge National Laboratory
Michelin Americas Research Company
Western Michigan University
Battelle
Hendrickson
LBT, Inc.
Volvo Trucks of North America

Sponsor: National Transportation Research Center, Inc. (NTRCI)
February 2, 2010

Approach

This document addresses the testing of a class 8 over-the-road tractor with a tank trailer at the Transportation Research Center (TRC) test track in Marysville, Ohio as part of the (U24) Heavy Truck Rollover Characterization (Phase C) project.

The same test vehicle, consisting of a Volvo VT830 tractor and a LBT tank trailer based on a typical petroleum tanker with five compartments, that was used for testing in Phase B of the project will again be used in this phase, although the tanker has been modified somewhat to meet the needs of this phase of testing. The primary change is based on using a wider axle width, which results in a wider track width on the vehicle. The rollover testing of the test vehicle will be accomplished using three planned vehicle configurations that use three variations of the suspension system, and a fourth variation may be tested as an option depending on the results of the third vehicle configuration. Two of the configurations use different axles and the complete set of tests will be performed for each. The third configuration involves simply removing the shock absorbers from the tank trailer with one of the axle configurations, and only limited testing will be completed with this vehicle configuration. The fourth configuration involves using high damping shock absorbers to characterize the role of the shocks on roll performance. If the results of the third configuration testing are favorable, the fourth vehicle configuration will be tested for the transient maneuvers of the test plan. The four tank trailer configurations are named TC1, TC2, TC3, and TC4 to have simple names and avoid the need to define the complete axle or shock configuration when discussing them. The configurations are as follows:

Table A- 1. Vehicle Configurations for Phase C testing

Tank Trailer Configuration	Axle Name	Axle Specifications			Shock Absorber
		Wall Thickness	Beam Center Spacing	Axle Width	
TC1	TC1 Axle	0.310"	43.5"	77.5"	Hendrickson Original
TC2	TC2 Axle	0.310"	37.5"	77.5"	Hendrickson Original
TC3	TC2 Axle	0.310"	37.5"	77.5"	Shock Removed
TC4 (optional)	TC2 Axle	0.310"	37.5"	77.5"	Hendrickson High Damping

All testing will be performed using New Generation Wide Base Single Tires (NGWBSTs) except for the steer axle, which will use normal steer tires. No testing will be conducted in this phase using dual tires. All of the configurations will use a vehicle loading that is quite similar to the high center of gravity (CG) configuration used in Phase B testing so that the results of this phase can be directly compared to those of Phase B. In order to achieve this CG height using water as opposed to petroleum, two of the tanks will be completely filled (to minimize sloshing effects) with water, and the remaining load will be provided by attaching sandbags on top of the tank trailer, which must be securely strapped in place to prevent movement of the bags. This high CG configuration approximates a standard CG height that is characteristic of today's tanker trailer designs. The weight of sandbags needed for testing is estimated to be between 1820 and 2270 kg (4000-4500 lbs.), based on phase B loading. Water mass in the two tanks is estimated to be 17,900 kg (39,500 lbs.), and the sand will be loaded to provide a total vehicle mass—including tractor and trailer, of 36,290kg (80,000 lbs.)—which is the maximum gross vehicle weight allowable on Federal Highways for combination trucks without a permit. The main objective of this test effort is to observe the impact of the vehicle stability performance due to the changes in the suspension system. The impact of the electronic stability control (ESC) system on the vehicle stability performance is not a primary focus of the testing, but the team wishes to verify that the modifications to the vehicle do not negatively affect the ability of the ESC system to provide its normal stability benefits. As such, a small number of tests will be conducted with the ESC system enabled on the tractor and the trailer, but the majority of the testing will be performed with the ESC system disabled on both the tractor and trailer.

Link-Radlinski must supply the sand and bags for this load and will be responsible for loading and positioning of the sandbags for the different vehicle configurations and filling the tanks with water. Testing with the tanker configurations described above requires that the axles be changed after completing the testing for the TC1 configuration so that the TC2 axles are on the vehicle for the tanker configurations TC2 and TC3. Link-Radlinski personnel must do the axle changeout and all required instrumentation connections, reconfigurations and calibrations that are needed to collect the same test data before and after the axle conversion. The removal of the shock absorbers for the TC3 configuration will be performed at the test track during testing, and the change will be made by members of the HTRC test team. An appropriate wrench and torque

wrench will be required at the test track for the shock absorber removal and replacement and should be provided by Link-Radlinski.

Three different test maneuvers will be performed: two transient and one steady-state. The two transient maneuvers are:

- step steer maneuver, and
- open loop double lane change maneuver

The steady-state test is a:

- ramp steer maneuver.

All three maneuvers will be conducted for tanker configurations TC1 and TC2. For configuration TC3, only the modified step steer maneuver aimed at characterizing the auxiliary roll damping will be performed. Additional testing may be performed using a high rebound damping shock (the TC4 configuration), but only testing of the transient maneuvers will be performed for the TC4 configuration since the shock absorber properties should not affect the steady state roll performance of the tractor-trailer. The TC4 configuration will only be tested if the team determines that the TC3 configuration results indicate that the shock absorbers have a significant impact on the roll performance of the tractor-tank trailer. The specific test condition variations that will be employed in each test maneuver are detailed in the complete specification of each maneuver later in this document.

For the planned testing, there will be several condition variations that require no modification to the vehicle and only represent operational changes that will be modified for the various test cases. These are referred to in this document as test condition variations and include the following:

- Electronic Stability Control (ESC) includes two settings that will be tested: (1) Tractor and trailer ESC “on” (both systems enabled), and (2) tractor and trailer ESC “off” (both systems disabled).
- Test Speed: The ramp steer and step steer maneuvers include both a low speed and high speed conditions, while the open loop double lane change maneuver is performed only at a high speed condition. The low speed is selected so that the vehicle operates in a sub-limit manner in which the ESC would not normally intervene, whereas the high speed condition is selected so that wheel liftoff will occur. For the test condition variations in which the ESC system is enabled, it is expected that ESC intervention will occur for the high speed cases. For safety purposes, all high speed conditions will be determined using small increments in the actual vehicle speed until liftoff is achieved. For the step steer maneuver, bracketing of the high speed condition will also be conducted to determine the speeds at which liftoff occurs for trailer only wheel lift vs. both tractor and trailer wheel lift.

- The ramp steer maneuver will be performed in both clockwise and counter-clockwise directions. All other maneuvers will be performed without varying the direction of travel employed during the procedure.

Sequence And Details Of Testing

All maneuvers will be conducted for vehicle configurations TC1 and TC2, and the condition variations that will be tested are identical for the two configurations. The TC3 configuration is intended only to evaluate the auxiliary roll damping, and only the modified step steer maneuver will be performed for this configuration. For the TC4 configuration, no steady state maneuvers will be performed since the shock absorbers do not influence the vehicle's steady state performance. Testing should begin with the TC1 vehicle configuration. All maneuvers for this configuration will be performed for all of the test condition variations specified. After verifying that all data from the first vehicle configuration has been successfully recorded and meets the needs of the project, the axle will be changed and all necessary instrumentation modifications and re-calibrations will be performed so the vehicle is ready to test in the TC2 configuration. All of the maneuvers, test condition variations and data verification will be repeated for this configuration. After completing all testing for the TC2 configuration, the shock absorbers will be removed at the test track to test the TC3 configuration for the modified step steer maneuver. Finally, contingent upon the results observed in the TC3 configuration testing, the high rebound damping shock absorbers will be installed and the specified test maneuvers, corresponding test condition variations and data verification will be completed for configuration TC4. In this way, all of the maneuvers and operating conditions will be tested for all of the vehicle configurations in sequence.

The following summarizes the variations that will be performed through this testing:

Table A- 2. General summary of all testing variations

Vehicle configurations	Tanker Configuration TC1 • Wide beam spacing axle, baseline shocks Tanker Configuration TC2 • Narrow beam spacing axle, baseline shocks Tanker Configuration TC3 • Narrow beam spacing axle, no shock absorbers Tanker Configuration TC4 • Narrow beam spacing axle, high damping shocks
Maneuvers	Step steer Open loop double lane change Ramp steer
Test condition variations	Electronic stability control (ESC) • Tractor and Trailer ESC On • Tractor and Trailer ESC Off Speed • By maneuver

Both the ramp steer maneuver and the step steer maneuver will be performed at low and high speed conditions. For the ramp steer maneuver, the low speed condition will be tested once in the clockwise (CW) direction and once in the counter-clockwise (CCW) direction. For all of the maneuvers other than the low speed ramp steer, the testing will be performed in only one direction of travel. The low speed condition for the step steer maneuver will be repeated 6 times. The low speed conditions will be selected by the project team prior to the start of testing. For the high speed maneuvers, several attempts will be made to find a speed at which wheel lift will be experienced. Once wheel lift speed is achieved, repetitions at the wheel-lift speed will be conducted per the list below. Data checks will be made in the field to assure that all data was properly collected and extra repetitions may be needed on occasion in the event of missed data due to improper behavior of instrumentation or the data acquisition system.

A steering robot, which improves reliability of the testing, will be used for all maneuvers. For the step steer maneuver, testing will be conducted using a "lift throttle" approach. The maneuver speed is specified and programmed into the steering robot, and the driver accelerates to a speed slightly above the specified speed. He activates the robot and at the same time removes accelerator input, allowing the vehicle to coast to a slower speed. The robot begins the programmed maneuver as soon as the vehicle decelerates to the specified maneuver speed. The ramp steer and lane change maneuvers require the driver to maintain a steady speed throughout the test, however. For these maneuvers, the driver must actively control the vehicle speed, which introduces some additional variability. If test results show high repeatability for the maneuvers, the number of repetitions may be reduced, at the discretion of the HTRC team.

The following table presents the specific test cases that will be performed and the expected number of runs and total time estimate for each variation. The "ESC System Activation" column indicates whether the ESC for both the tractor and trailer systems is enabled (on) or disabled (off). The "Vehicle Config" column indicates the number of vehicle configurations that will be tested. Where the value is '2,' only the TC1 and TC2 configurations will be tested for that test case, while a value of '3' indicates that the TC4 configuration will also be tested (contingent on the TC3 results, as described above). A value of '4' indicates that all vehicle configurations will be tested.

Table A- 3. List of test cases to be performed among the variations in configuration and test conditions. The time estimate is included only for information.

Maneuver	Runs (Low speed)	Runs (High speed)	ESC System	Vehicle Config	Time per pass (min)	Total Time (min)
Ramp Steer	2	5	Off	2	10	140
Step Steer (low speed)	6	0	Off	2	5	60
Step Steer (high speed)	0	12	Off	3	5	180
Modified Step Steer	0	5	Off	4	5	100
Double Lane Change	0	12	Off	3	5	180
Ramp Steer	0	5	On	2	5	50
Double Lane Change	0	5	On	3	5	75

The order of the testing should follow the vehicle configurations so that physical modifications required to the tanker during testing (axle change and shock changes) will be minimized. For each vehicle configuration, the test maneuvers should be scheduled to be performed in order of least-aggressive to most-aggressive, relative to tire wear and damage. However, it is understood that scheduling of maneuvers may need to be adjusted during each day of testing to take advantage of limited resources on the test track when they become available.

Vehicle Setup and Instrumentation

For the loading of the tanker, the first and sixth compartments will be filled with approximately 2,100 and 2,650 gallons of water, respectively (completely filling these compartments in order to eliminate sloshing during testing). Filled sandbags will be placed on the tank trailer to achieve a total vehicle weight of 80,000 pounds. The sandbags will be placed on the rails along the top of the tanker, and must be securely attached to the rails to prevent loss of any of the sandbags during testing. The distribution of the sandbag load along the length of the tanker should be such that the longitudinal position of the center of mass of the sand is approximately at the middle of the center compartment of the tanker.

Outriggers will either come attached to the tanker-trailer requiring them to be “unfolded,” or will be attached per recommendations provided by LBT. Link-Radlinski will be responsible for installing anti-jackknifing equipment provided for the testing. Note that the outriggers are the same as those used in Phase B testing.

The tank trailer will be transported to Link-Radlinski with NGWBS tires already mounted on the trailer. Michelin will ship to Link-Radlinski additional NGWBSTs for the tractor and a new set of steer tires so that they can be mounted on the tractor for testing. Michelin will also ship dual tires for the tank trailer, which will replace the NGWBSTs when testing is completed. All of these tires will arrive already mounted on their appropriate rims. The Volvo tractor will arrive with dual tires. Link-Radlinski will need to mount the NGWBS tires and the new steer tires on the tractor when the tires arrive. NGWBSTs will be used on both the tractor and trailer to perform all testing. If additional tires are needed at the test track (e.g., in the event of a damaged

or flat tire), spare tires will be made available by Michelin. After the testing is completed, Link-Radlinski will mount the original dual drive tires and steer tires on the tractor and the dual tires sent by Michelin on the tank trailer before returning them to Volvo and LBT, respectively, and all remaining tires will be returned to Michelin (MARC) on their rims.

The tank trailer will arrive with the TC1 axles mounted to the vehicle, and the other set of axles (TC2) will be shipped directly to Link-Radlinski by Hendrickson or LBT. After the TC1 vehicle configuration testing is completed, Link-Radlinski will replace the TC1 axles with the TC2 axles and prepare the vehicle for subsequent testing in the TC2 configuration. Link-Radlinski personnel must replace the axles, re-mount wheels on the TC2 axle, align the axles, and perform all required instrumentation connections, reconfigurations and calibrations that are needed to collect the same test data before and after the axle conversion. Link-Radlinski will follow standard alignment procedures and recommendations from Hendrickson (see http://www.hendrickson-intl.com/pdfs/trailer_PDFs/L579.pdf) and will verify that the axles are properly aligned on the trailer before the subsequent testing is performed. All data channels that must be removed for the axle changeout must be reconnected and any necessary re-calibration of the sensors will be performed by Link-Radlinski personnel. Proper functioning of the data acquisition system and all sensors should be verified by Link-Radlinski before proceeding with additional testing.

Instrumentation for the requested data channels (32 analog channels, an IR camera, plus over 100 individual CAN channels from 3 sources) and the data acquisition system must be installed on the test vehicle and properly configured by Link-Radlinski staff, including any auxiliary hardware required for making the measurements, prior to the arrival of the HTRC team. The ranges and bandwidth of the sensors will be sufficient to capture the data with an accuracy acceptable to the HTRC test team. The Somat eDAQ data acquisition system must be configured to collect all of the data at a frequency specified by the HTRC test team (100Hz).

All project-related test-track testing equipment and sensors shall be provided by Link-Radlinski, except for specific sensors identified below that members of the HTRC research team will provide. Link-Radlinski will provide a means for verifying that all testing equipment, sensors and data acquisition system are functioning properly, and to allow for a quick check that the data, within the right range, was collected for each repetition engaged in. Link-Radlinski will provide the HTRC research team with data when requested by the HTRC team, generally after the first test-run of the day and at the end of each test maneuver set.

The same sample frequency, 100 Hz, will be used for all data collection channels. Specific channels along with the data voltage range, equipment/sensor used, and sensor locations for each data type shall be provided by Link-Radlinski staff and will be listed in a table for reference by the HTRC research team. A list of planned sensors for the project is documented in Tables A-4 through A-5, which also specify who will supply each device. The three Somat eDAQ data acquisition modules that will be used to acquire and store all data will be provided by NTRCI

and WMU for the project. The data acquisition system will be the same configuration of the eDAQ devices used in Phase B testing, with two base modules that store data independently and a secondary module, which allows additional channel inputs, that is connected to one of the base modules.

The complete set of measurement channels required for testing is provided in tables below, but the following is a preliminary list of instruments needed for the testing that will not be provided by the HTRC project team:

- Steering Robot
- String Potentiometers (4) for measurement of road wheel angle (steer axle), articulation angle between tractor and trailer at 5th wheel, and the suspension axle-to-frame ride heights (on both sides of axle 5)
- Height sensors (4) to measure the ride height on both sides of axle 3 and axle 5
- Pressure gages (6) to measure brake pressure on axle 2 and axle 4, and for the suspension (airbag) pressure on both sides of axle 4 and axle 5

Any items needed to complete the testing that will not be provided by the test contractor will have to be acquired by the HTRC. Link-Radlinski staff must create a list of any necessary sensors, hardware or other equipment that they do not have available or that will not be provided for the testing. Link-Radlinski will provide this list of items not included in the test quote, along with a price quotation for the necessary items, to the HTRC at the time that the test quotation is provided.

The following tables include the list of data channels that will be measured during testing:

List Of Sensors / Measurement Devices And Other Hardware

Table A- 4. Analog sensors

Channel Name	Channel Units	Description	Sensor or Device from:	Sensor
STANGROB	degrees	Angle of steering wheel in cab	Link	Output from Steering robot
ROBTRG1	logic	Robot Trigger Edaq 101	Link	Output from Steering robot
ROBTRG2	logic	Robot Trigger Edaq 102	Link	Output from Steering robot
RDWHLANG	degrees	Angle of wheels of steer axle relative to the tractor body	Link	Unimeasure Model LX-PA String Potentiometers
STRN_L2	kg	Strain gauge - left side Axle2	WMU (already on tractor drive axles (?) - to be verified)	Multiple Vishay Micromeasure linear strain gages
STRN_R2	kg	Strain gauge - right side Axle2		
STRN_L3	kg	Strain gauge - left side Axle3		
STRN_R3	kg	Strain gauge - right side Axle3		
STRN_L4	kg	Strain gauge - left side Axle4	WMU (will be installed on trailer axles)	Multiple Vishay Micromeasure linear strain gages
STRN_R4	kg	Strain gauge - right side Axle4		
STRN_L5	kg	Strain gauge - left side Axle5		
STRN_R5	kg	Strain gauge - right side Axle5		
STRN_T4	μStrain	Axle torsion strain gage rosette (full bridge), Axle4	WMU (will be installed on trailer axles)	Multiple Vishay Micromeasure strain gage rosettes
STRN_T5	μS	Axle torsion strain gage rosette (full bridge), Axle5		
STRN_F4	μS	Axle flexion strain gage rosette (half bridge), Axle4		
STRN_F5	μS	Axle flexion strain gage rosette (half bridge), Axle5		
AXRH_L3	mm	Height sensor - left side Axle3 (drive axle)	Link	Wenglor HT66MGV80 or HT77MGV80
AXRH_R3	mm	Height sensor - right side Axle3 (drive axle)	Link	Wenglor HT66MGV80 or HT77MGV80

Channel Name	Channel Units	Description	Sensor or Device from:	Sensor
AXRH_L5	mm	Height sensor - left side Axle5	Link	Wenglor HT66MGV80 or HT77MGV80
AXRH_R5	mm	Height sensor - right side Axle5	Link	Wenglor HT66MGV80 or HT77MGV80
BKPRS_L2	psi	Wheel end brake line pressure, Axle2, left	Link	Sensata 83HP/84HP pressure transducer
BKPRS_L4	psi	Wheel end brake line pressure, Axle4, left	Link	Sensata 83HP/84HP pressure transducer
SUSPRSL4	psi	Suspension pressure, Axle4 left	Link	Sensata 83HP/84HP pressure transducer
SUSPRSR4	psi	Suspension pressure, Axle4 right	Link	Sensata 83HP/84HP pressure transducer
SUSPRSL5	psi	Suspension pressure, Axle5 left	Link	Sensata 83HP/84HP pressure transducer
SUSPRSR5	psi	Suspension pressure, Axle5 right	Link	Sensata 83HP/84HP pressure transducer
SUSHT_L5	mm	Suspension ride height, axle-to-frame, Axle5 left	Link	Unimeasure Model LX-PA String Potentiometers
SUSHT_ R5	mm	Suspension ride height, axle-to-frame, Axle5 right	Link	Unimeasure Model LX-PA String Potentiometers
ARTICANG	degrees	Trailer articulation angle, measured at 5th wheel	Link	Unimeasure Model LX-PA String Potentiometers
DRSFTTRQ	N-m	Drive shaft torque	WMU	Torque Trak 10k torque telemetry system
CAMERA_IR	--	IR camera to detect rotation of 5th wheel	WMU	Stable Imaging Solutions IR camera and recorder (IDRS 2000)

Table A- 5. CAN channel inputs from Tractor ECU

eDAQ Channel #	Channel Name	Channel Units	Description
CAN input set1 (from Tractor ECU), connected to digital I/O module of eDAQ1	Sp_Ax1	km/h	Front Axle Speed
	SpRelWhl_L1	km/h	Relative Speed; Front Axle, Left Wheel
	SpRelWhl_R1	km/h	Relative Speed; Front Axle, Right Wheel
	SpRelWhl_L2	km/h	Relative Speed; Rear Axle #1, Left Wheel
	SpRelWhl_R2	km/h	Relative Speed; Rear Axle #1, Right Wheel
	SpRelWhl_L3	km/h	Relative Speed; Rear Axle #2, Left Wheel
	SpRelWhl_R3	km/h	Relative Speed; Rear Axle #2, Right Wheel
	SpHiRes_FL	km/h	Front Axle Left Wheel Speed, high res
	SpHiRes _FR	km/h	Front Axle Right Wheel Speed, high res
	SpHiRes _RL	km/h	Rear Axle Left Wheel Speed, high res
	SpHiRes _RR	km/h	Rear Axle Right Wheel Speed, high res
	SpVehWh	km/h	Wheel Based Vehicle Speed
	BrakeSwitch	on/off	Brake Switch
	WarningLamp	on/off	Amber Warning Lamp Status
	VDCBrake	on/off	VDC Brake Light Request
	VDCOperatio	on/off	VDC Fully Operational
	VDCInfo	on/off	VDC Information Signal
	ABSActive	on/off	ABS Active
	ASRBrake	on/off	ASR/ATC Brake Control
	ASREngine	on/off	ASR/ATC Engine Control
	YCBrakeActi	on/off	YC Brake Control Active
	YCEngineAct	on/off	YC Engine Control Active
	RSPBrakeAct	on/off	RSP Brake Control Active
	RSPEngineAct	on/off	RSP Engine Control Active
	SteerAngle	degrees	Steering Wheel Angle

eDAQ Channel #	Channel Name	Channel Units	Description
	Yaw	deg/sec	Yaw Rate
	LatAccel	m/s^2	Lateral Acceleration
	TorqueDemand	%	Driver Demand Engine Percent Torque
	TorqueActual	%	Actual Engine Percent Torque
	EngSpeed	RPM	Engine Speed
	AccelPositon	%	Accelerator Pedal Position
	FrictionTor	%	Nominal Friction Percent Torque
	RetardTorque	%	Actual Retarder Percent Torque
	ParkBrake	on/off	Parking Brake Switch
	ClutchSwitch	on/off	Clutch Switch
	ShiftInProc	on/off	Shift in Process
	CurrentGear	--	Current Gear
	BrakePres1	kPa	Service Brake Air Pressure, Circuit #1
	BrakePres2	kPa	Service Brake Air Pressure, Circuit #2

Table A- 6. CAN channel inputs from Oxford RT units

eDAQ Channel #	Channel Name	Channel Units	Description	Sensor or Device from:	Sensor
CAN input set2 (RT3100), connected to digital I/O module of eDAQ2	tcTimeSec	s	Tractor Time Second	NTRCI	Oxford RT3100, GPS Inertial Unit
	tcLat	°	Tractor Position Latitude		
	tcLong	°	Tractor Position Longitude		
	tcVelNorth	m/s	Tractor Velocity North		
	tcVelEast	m/s	Tractor Velocity East		
	tcVelDown	m/s	Tractor Velocity Down		
	tcVelHor	m/s	Tractor Velocity Horizontal Vector		
	tcVelFor	m/s	Tractor Velocity Forward Component		
	tcVelLat	m/s	Tractor Velocity Lateral Component		
	tcAccX	m/s^2	Tractor Acceleration Body X Component		
	tcAccY	m/s^2	Tractor Acceleration Body Y Component		
	tcAccZ	m/s^2	Tractor Acceleration Body Z Component		
	tcAccFor	m/s^2	Tractor Acceleration Forward Component		
	tcAccLat	m/s^2	Tractor Acceleration Lateral Component		
	tcAccDown	m/s^2	Tractor Accelerate Down Component		
	tcHeading	°	Tractor Angular Heading		
	tcPitch	°	Tractor Angular Pitch		
	tcRoll	°	Tractor Angular Roll		
	tcAnSpBX	°/s	Tractor X Angular Rate		
	tcAnSpBY	°/s	Tractor Y Angular Rate		
	tcAnSpBZ	°/s	Tractor Z Angular Rate		
	tcAnSpLF	°/s	Tractor Level Forward Axis Angular Rate		
	tcAnSpLP	°/s	Tractor Level Pitch Angular Rate		

eDAQ Channel #	Channel Name	Channel Units	Description	Sensor or Device from:	Sensor
	tcAnSpLY	°/s	Tractor Level Yaw Angular Rate		
	tcAnTrac	°	Tractor Track Angle		
	tcAnSlip	°	Tractor Slip Angle		
	tcDistHold	m	Tractor Distance With Hold		
	tcPosXLoc	m	Tractor X Position Local Coor		
	tcPosYLoc	m	Tractor Y Position Local Coor		
	tcVelXLoc	m/s	Tractor X Velocity Local Coor		
	tcVelYLoc	m/s	Tractor Y Velocity Local Coor		
	tcAnYLoc	°	Tractor Yaw Angle Local Coor		
	tcAnTLoc	°	Tractor Track Angle Local Coor		
	tcAnAcBX	°/s²	Tractor X Angular Acceleration		
	tcAnAcBY	°/s²	Tractor Y Angular Acceleration		
	tcAnAcBZ	°/s²	Tractor Z Angular Acceleration		
	tcAnAcLF	°/s²	Tractor Angular Acceleration Forward		
	tcAnAcLP	°/s²	Tractor Angular Acceleration Pitch		
	tcAnAcLY	°/s²	Tractor Angular Acceleration Yaw		

eDAQ Channel #	Channel Name	Channel Units	Description	Sensor or Device from:	Sensor
CAN input set3 (RT2500), connected to digital I/O module of eDAQ2 (Note that both Oxford RT units are connected in parallel to the same input on eDAQ2)	tlTimeSec	s	Trailer Time Second	WMU	Oxford RT2500, GPS Inertial Unit
	tlLat	°	Trailer Position Latitude		
	tlLong	°	Trailer Position Longitude		
	tlVelNorth	m/s	Trailer Velocity North		
	tlVelEast	m/s	Trailer Velocity East		
	tlVelDown	m/s	Trailer Velocity Down		
	tlVelHor	m/s	Trailer Velocity Horizontal Vector		
	tlVelFor	m/s	Trailer Velocity Forward Component		
	tlVelLat	m/s	Trailer Velocity Lateral Component		
	tlAccX	m/s²	Trailer Acceleration Body X Component		
	tlAccY	m/s²	Trailer Acceleration Body Y Component		
	tlAccZ	m/s²	Trailer Acceleration Body Z Component		
	tlAccFor	m/s²	Trailer Acceleration Forward Component		
	tlAccLat	m/s²	Trailer Acceleration Lateral Component		
	tlAccDown	m/s²	Trailer Accelerate Down Component		
	tlHeading	°	Trailer Angular Heading		
	tlPitch	°	Trailer Angular Pitch		
	tlRoll	°	Trailer Angular Roll		
	tlAnSpBX	°/s	Trailer X Angular Rate		
	tlAnSpBY	°/s	Trailer Y Angular Rate		
	tlAnSpBZ	°/s	Trailer Z Angular Rate		
	tlAnSpLF	°/s	Trailer Level Forward Axis Angular Rate		
	tlAnSpLP	°/s	Trailer Level Pitch Angular Rate		
	tlAnSpLY	°/s	Trailer Level Yaw Angular Rate		

eDAQ Channel #	Channel Name	Channel Units	Description	Sensor or Device from:	Sensor
	tlAnTrac	°	Trailer Track Angle		
	tlAnSlip	°	Trailer Slip Angle		
	tlDistHold	m	Trailer Distance With Hold		
	tlPosXLoc	m	Trailer X Position Local Coor		
	tlPosYLoc	m	Trailer Y Position Local Coor		
	tlVelXLoc	m/s	Trailer X Velocity Local Coor		
	tlVelYLoc	m/s	Trailer Y Velocity Local Coor		
	tlAnYLoc	°	Trailer Yaw Angle Local Coor		
	tlAnTLoc	°	Trailer Track Angle Local Coor		
	tlAnAcBX	°/s²	Trailer X Angular Acceleration		
	tlAnAcBY	°/s²	Trailer Y Angular Acceleration		
	tlAnAcBZ	°/s²	Trailer Z Angular Acceleration		
	tlAnAcLF	°/s²	Trailer Angular Acceleration Forward		
	tlAnAcLP	°/s²	Trailer Angular Acceleration Pitch		
	tlAnAcLY	°/s²	Trailer Angular Acceleration Yaw		

Pre-Test Warmup And ESC System Initialization

A warm-up period of the test vehicle will be required before each series of testing is performed (and after every significant downtime, as determined by HTRC project team members present during testing). The vehicle under test shall be operated for a period of 30-minutes prior to the start of the test. The warm-up operation is performed to allow the tire temperature and pressure to reach normal operating levels before the test maneuvers are initiated. The tire pressure shall be monitored and maintained at 7.9 bar (hot) for all tires during testing.

Any time that the vehicle is not driven for a period of 15 minutes or more, or when the ESC system is enabled after previously being disabled, an initialization of the ESC system must be completed prior to continuation of testing. The procedure for conducting this ESC system initialization is as follows: From a stop, the truck must be accelerated to 30mph. At this speed, a left to right hand turn of normal maneuvering severity must be performed, and then the vehicle should be decelerated to a complete stop. This procedure is not necessary when the warm-up procedure defined above has been recently completed.

Vehicle Test Events (Maneuvers)

A series of four test maneuvers have been selected to maximize the desired data while minimizing testing time and resources. The three test events are described in detail below.

The speeds, steering input angles, and articulation angles proposed in this test plan are estimates and may be refined during the testing process, if necessary.

It is planned to use the steering robot for all test maneuvers. The specification of the steering inputs required to perform all maneuvers will be made by the HTRC team based on the testing performed in Phases A and B and preliminary system evaluation at the start of testing. Some modification to the programming of the steering robot may be required during testing for some of the maneuvers in order to achieve the desired trajectories for those maneuvers, but it is intended to use the same steering programs as used during Phase B testing.

Ramp Steer Maneuver

Background: This test is conducted to determine the maximum lateral acceleration that can be achieved by a vehicle under “near-steady-state” cornering conditions. This test was selected in lieu of a constant radius turn maneuver so that the steering robot could be used for maximum reliability. The results of a ramp steer maneuver provide very similar information to a constant radius turn, but the ramp steer maneuver only requires the driver to maintain constant speed as opposed to manually steering the vehicle to maintain the specified radius arc.

Setup: The surface coefficient of friction shall be measured by Link-Radlinski and documented, or otherwise obtained from TRC.

Vehicle Control: Driver with steering robot for steer control. For this maneuver, lift throttle is not used, and the driver must maintain a constant vehicle speed through manual accelerator control.

Procedure: The vehicle is driven at a set speed (to be determined at the test site) at which point a fixed steering rate is input to the steering system using the steering robot. The test concludes when the vehicle lifts an axle. The steering rate will be negotiated with Link but will probably be 10 deg/s. The test speed during Phase B testing was 30 mph for the high speed ramp steer maneuver and 20 mph during the low speed ramp steer maneuver. It is intended to use the same test speeds, but this could change depending on the stability of the vehicle configurations.

If the turning radius of the vehicle becomes too small for safety, the maneuver will be repeated at a higher speed to generate wheel liftoff at a larger radius.

Step Steer Maneuver

Background: The Step Steer test will provide information regarding sensitivity between the steering wheel input and the resulting yaw rate, lateral acceleration and roll of the vehicle as a function of steering input. This information will better facilitate the understanding of the total vehicle system response. The Step Steer maneuver used for this test set is based on ISO 7401.

Setup: This is a straight-line test with a single quick turn to a specified steering wheel angle. Sufficient test area is required to operate the test vehicle at a constant speed for approximately 30 seconds, with room to attain the test speed and to decelerate at the end of the test.

Vehicle Control: Steering robot for steer control with lift throttle accelerator control

Procedure: A steering robot will provide the steering input angle of 170 degrees/sec up to an angle of 170 deg. The vehicle's speed is expected to be about 30-35 mph during this test, based on Phase B testing, but this could change depending on the stability of the Phase C vehicle configurations. The test should be conducted using the "lift throttle" approach. The driver must accelerate the vehicle to slightly above the desired test speed, then place the truck in neutral and maintain a straight heading with no steering input. The steering robot is then activated, and the steering program must trigger when the correct test speed is reached (as the vehicle coasts to the correct speed). The steering robot controls the vehicle throughout the maneuver and the test data will only be recorded during this same period.

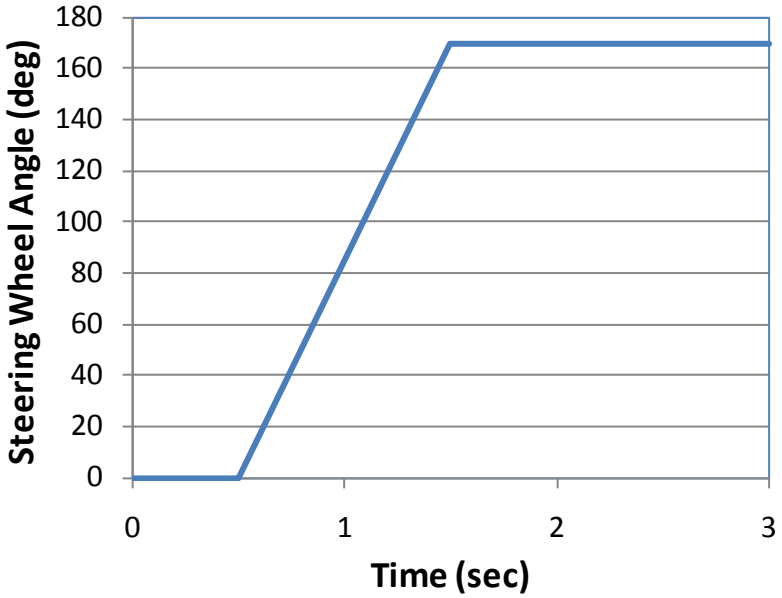

Figure A- 1. Steering Program for the Step Steer Maneuver.

Open-Loop Double Lane Change Maneuver

Background: This test is conducted to determine the transient response of a vehicle when subjected to a sudden maneuver similar to a double lane change (an evasive maneuver in which the driver rapidly steers the vehicle into the adjacent lane to avoid an obstacle, and subsequently steers the vehicle back to the original lane after passing the obstacle). By using a steering robot, repeatable test results may be achieved.

Setup: Sufficient test area is required to operate the test vehicle at a constant speed with room to attain the test speed and to decelerate at the end of the test. The surface coefficient of friction shall be measured by Link-Radlinski and documented.

Vehicle Control: Driver with steering robot for steer control. For this maneuver, lift throttle is not used, and the driver must maintain a constant vehicle speed through manual accelerator control.

Procedure: Steering inputs will be based on the steering program selected for this maneuver during Phase B testing. It is intended to use the same steering inputs for Phase C testing of this maneuver as were used in Phase B testing, but due to the vehicle configuration changes made, some modifications to the steering program could be necessary. During the first pass of each test condition, the original steering program will be used, but alternate programs may be selected in order to obtain a trajectory of the truck that is as close as possible to the desired double lane-change maneuver if the trajectory of the vehicle is significantly different from that desired by the HTRC team. The team expects that the steering inputs will not be modified from what was used in Phase B testing, however. Once the appropriate program is selected for each test case, the maneuver will be performed for the specified number of repetitions for that test condition. This

test will be performed with the driver making a best effort to maintain constant speed control. The test speeds during Phase B testing were in the range of 32-38 mph. It is expected that the same test speeds will be experienced, but this could change depending on the stability of the vehicle configurations in Phase C.

The following description is for the reference steering robot program (from Phase B testing). The maneuver starts with a turn to the left. From an initial steer input of zero deg, the robot increases the steer angle linearly to 240 deg, with this segment of the program lasting a duration of 0.9 seconds. This is followed by a return of the steering angle to the right to -160 deg, which returns the vehicle to a path essentially parallel to the original path with the vehicle in the lane adjacent to the beginning lane. This steering change is input over a one-second interval. The steering is further increased to the right over the next 1.5 seconds to a maximum steering input of -224 deg, which moves the vehicle back to the original lane. Over the next 0.9 second, the steering returns again to the left in order to steer the vehicle in the same direction in which it initially started, with a steering input to the left to 230 deg. Finally, the steering is returned to zero deg, with the change occurring over the final 1.2 seconds. The vehicle should be traveling in the same direction and lane as at the beginning of the maneuver. The steering wheel inputs described above are presented in the graph below.

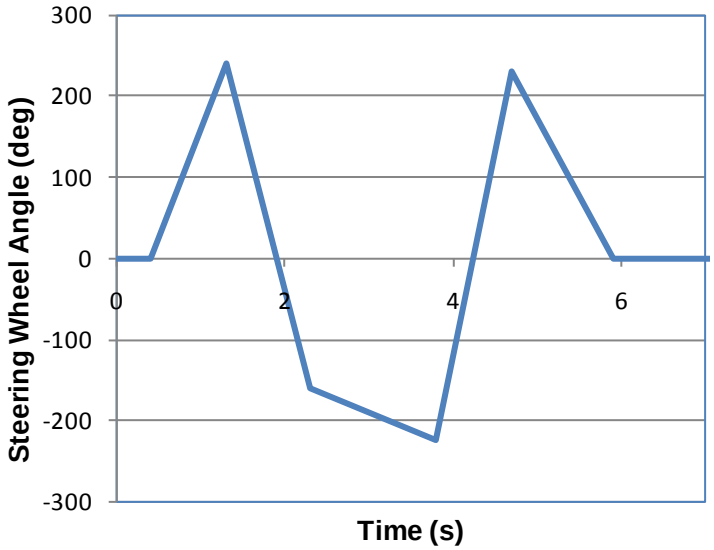

Figure A- 2. Reference Steering Program for the Open Loop Double Lane Change Maneuver (Program number 7 from Phase B testing).

Modified Step Steer Maneuver (to evaluate the auxiliary roll damping of the tractor trailer):

Background: This test is conducted to evaluate the auxiliary roll damping of the test vehicle. The auxiliary roll damping is the damping inherently present in the tractor and trailer due to

bushings, air bags, etc., but the level of damping is not precisely controlled or well known (as in the case of the shock absorbers). Data from this test will allow an indirect evaluation of the auxiliary roll damping through modeling. The oscillations of the vehicle will be measured after completing a step steer maneuver with a sufficient dwell time at the full steer input so that the vehicle rolls completely onto the outriggers and stabilizes. The measurement period of interest is following the return to neutral steering when the vehicle rolls back onto all of its wheels and rocks side to side in an oscillatory manner.

Setup: (Same as for the Step Steer Maneuver) This is a straight-line test with a single quick turn to a specified steering wheel angle. Sufficient test area is required to operate the test vehicle at a constant speed for approximately 30 seconds, with room to attain the test speed and to decelerate at the end of the test.

Vehicle Control: Steering robot with lift throttle accelerator control.

Procedure: Starting at an initial zero steering angle, the steering robot will provide steering input at a rate of 170 deg/s up to an angle of 170 deg, nominally. Programs incorporating several variations in the maximum input angle will be available so that the test can be conducted safely at the same test speed for the different vehicle configurations. Also, the first time this maneuver is performed, an appropriate dwell time (duration of the maximum steering input angle) will be determined that allows the vehicle to roll entirely onto the outriggers and to stabilize. Steering program variations with several dwell times will be available. After holding the maximum steering angle for the selected dwell time, the robot returns to zero deg input steering angle at the rate of 170 deg/s and the neutral steering is maintained for a period of 5 seconds. The vehicle's speed is expected to be about 35 mph during this test, but a test speed that produces a safe and progressive lift in the TC1 configuration will be selected and used for all subsequent testing. It is planned that the test will be conducted using the "lift throttle" approach, but if significant variations in test speed occur due to running on the outriggers, or if different speeds occur during the different vehicle configurations, it may be requested that the driver actively control the speed to achieve the same speed when the vehicle rolls back into contact with the ground on all wheels. The following graph shows the baseline case for the steering program input.

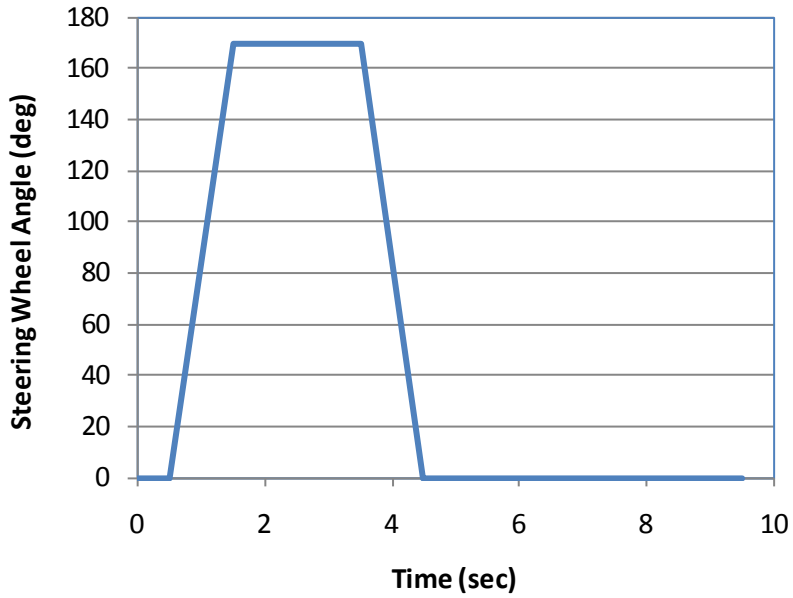

Figure A- 3. Reference Steering Program for the Auxiliary Roll Damping Evaluation Maneuver.

Other Miscellaneous Test Track Requirements

- During testing, the HTRC team will need to have use of the garage and/or conference room in the building by the VDA pad at the TRC facilities. Three tables and chairs for the HTRC team members present will be needed for verification and initial analysis of test data while the testing operations are taking place.

- Link will provide DVDs of all data files acquired during testing to the team as a deliverable for the project. Also, photos showing the instrumentation and hardware added to the vehicle and of the tractor-trailer when it is fully configured should be provided to the HTRC team.

Appendix B – Phase 1 And 2 Summary (Van Semitrailer)

Abstracted from the Executive Summary from final report for Phases 1 and 2 of this Program; *Truck Rollover Characterization for Class-8 Tractor-Trailers Utilizing Standard Dual Tires and New-Generation Single Tires*, July 2005

Phases 1 and 2 of the Heavy Truck Rollover Characterization Project was a major research effort conducted by the National Transportation Research Center, Inc. (NTRCI) in partnership with the Oak Ridge National Laboratory (ORNL), Dana Corporation (Dana), Michelin Americas Research and Development Corporation (Michelin) and Clemson University (Clemson), and was conducted for the Federal Highway Administration (FHWA). ORNL provided the day-to-day management of the project. The expertise mix of this team coupled with complementary research needs and interests, and a positive "can-do" attitude provided an extremely positive experimental research opportunity for all involved. Furthermore, this team supplied significant and valuable resources that provided a strong positive benchmark regarding the ability to conduct research within a public-private partnership. The work conducted by this team focused on initial efforts to generate data and information on heavy truck rollover not currently available in the industry. A 1999 Peterbilt 379 class-8 tractor and 2004 Wabash dry freight van trailer were the test vehicles utilized in this effort. Both were instrumented with a number of sensors to capture the dynamics of the tractor and van trailer as it engaged in various testing maneuvers that included: an evasive maneuver, swept sine, constant radius, and a run-off-the-road maneuver. The run-off-the-road maneuver was discontinued because the test-track at which the testing could not safely accommodate such a maneuver. These maneuvers were carried out utilizing both standard dual tires and new-generation wide base tires in six test series. Two test series also included the use of a wider slider suspension. Outriggers were placed on the test vehicle to assure that an actual rollover would not occur; however, the tests were designed to generate wheel lift of tires during the tests. One of the main objectives of the tests for Phases 1 and 2 was to understand how different elements (e.g., dual tires and new-generation wide base single tires, different trailer suspension types, etc.) affect the overall vehicle roll stability. Tilt-table tests were also performed to characterize the static rollover propensity of the tractor-van trailer.

For all of the tests, the vehicle was loaded with ballast for a gross vehicle weight rating of 79,000 lb., and the speeds were gradually increased so that wheel lift was experienced both visually and via instrumentation. A significant amount of data was collected on all of the maneuvers performed (1.2 Gigabytes of data from 45 data channels sampled at 0.01 sec) and information was also captured via videotaping (one camera inside the cabin and three others outside; plus one off-board camera). Due to a number of issues related to the sensors, and idiosyncrasies in the data itself, a statistically meaningful data set was not possible. However, sufficient data was collected to demonstrate the trends and patterns in the heavy truck rollover phenomenon.

Analyses of the data were performed by the partners. ORNL analyzed the evasive maneuver and constant radius data. Although the lack of data did not allow for the performance of statistical

tests over the data collected, the results of both tests analyzed seem to indicate that the tractor-trailer tire configurations that included the new generation wide base single tire consistently performed better (except for one case involving a constant radius test) than the standard layout (both tractor and trailer with dual tires). The results also indicate that for the tests that included the use of a wider slider suspension for the van trailer, improved stability and increased the effective stiffness of the van trailer.

Dana also analyzed the evasive maneuver using a different analysis methodology. Their analysis indicated that for those tests run with new generation wide base single tires on the van trailer (and dual tires on the tractor in one case, and new generation wide base single tires on the tractor in another), when the results were compared to standard dual tires on the tractor and trailer, a clear improvement in vehicle stability could be seen. Dana also found large contributions to increasing roll stability by using the wider-slider van trailer suspension.

Michelin analyzed the data from swept sine maneuver. Michelin computed six frequency response functions (FRFs) to include an analysis of the coherent frequency range of each of the six test series. The swept sine test can be used, for example, to calculate yaw rate-to-steering wheel angle, and lateral acceleration-to-steering wheel angle. In general, Michelin found that differences between the test series for the swept sine maneuver were small with the exception of those cases in which the wider slider suspension configuration was used. The estimated van trailer roll gain was noticeably lower with the wider-slider suspension configuration.

Clemson University analyzed the constant radius maneuvers conducted at radii of 150 ft and 400 ft. Different variables were analyzed including Trailer Roll Gradient (deg/g), Fifth Wheel Roll Moment Sensitivity, and Axle 5 Absolute Roll Angle Sensitivities. For the Trailer Roll Gradient analysis, the data indicated that for the case with new generation wide base single tires on the tractor and van trailer (with the wider-slider suspension), the test vehicle rolled less per unit g than the other series. This was followed closely by the case of standard dual tires on the tractor and new generation wide base singles on the van trailer (with a wider slider suspension), (similar to the results found by ORNL for this maneuver). In Clemson's analysis of the Fifth Wheel Roll Moment Sensitivity, results indicated that new generation wide base tires on the tractor and van trailer (with the wider slider suspension) gave the best overall performance in terms of roll moment generation, followed somewhat closely by the case of standard duals on the tractor and new generation wide base single tires on the van trailer (with a wider slider suspension). A similar result was obtained in Clemson's analysis of the understeer gradient and lateral acceleration.

Lastly, Clemson investigated, analytically, which design and loading variables had the largest impact in minimizing rollover propensity. They accomplished this via a computer program which was written to study the effect of these variables on the rollover propensity. The design variables that were found to be most influential on rollover were identified and include: payload

placement, roll bump stop clearance, payload distribution, track width, and torsional stiffness of the tractor sprung mass.

Overall, for this study, it was concluded that the use of new generation wide base single tires and wider-slider suspensions seem to provide improved roll stability for class-8 tractor-van trailers. Further quantification of this effect should be conducted through additional research, and similar studies should be conducted on flat-bed trailers and tank trailers. Lastly, other technologies exist and are emerging that could also contribute to improved roll stability.

Appendix C – Phase A Summary (Flatbed Semitrailer)

Abstracted from the Executive Summary from the final report of Phase A of this Program, U02: Heavy Truck Rollover Characterization (Phase A)

Background

This Heavy Truck Rollover Characterization Program is a major research effort conducted by the National Transportation Research Center, Inc. (NTRCI) in partnership with Oak Ridge National Laboratory (ORNL), Michelin Americas Research Company (Michelin), Western Michigan University (WMU), and Battelle Memorial Institute (Battelle). This research is one of the major projects conducted by the NTRCI in its role as a University Transportation Center (UTC) for the Research and Innovative Technology Administration (RITA), an agency within the Department of Transportation (DOT). This research also involved, via subcontract, Volvo Trucks North America, Inc., Clemson University, and the Transportation Research Center, Inc. (TRC). This work, entitled Heavy Truck Rollover Characterization – Phase A, addresses truck rollover issues dealing with a tractor and flatbed trailer, and follows similar work that was conducted by NTRCI on a tractor-van trailer in 2004-2005 [1].

Brief Overview

The overall objectives of this research were to:

- Contribute to the understanding of the dynamics of heavy truck rollover,
- Contribute to the development of advanced models of heavy truck vehicle dynamics that reflect project experiences, and
- Develop recommendations for improvement of the roll stability of heavy vehicles in preparation for realizing and testing such concepts in future phases of heavy truck rollover characterization research.

This project involved four major types of activities;

1) Tractor and flatbed trailer characterization,
2) Simulation modeling,
3) On-track testing, and
4) Data analyses.

The tractor and flatbed trailer characterization was necessary in order to generate kinematic and compliance data for later use in the development of simulation models of the vehicle.

Simulation modeling was conducted in order to better understand the dynamic behavior of the test vehicle, and if successful, would allow for the conduct of various “what if” design studies. Initial solid-body models, finite element models, and kinematic models were also developed and will prove to be important as this project moves into the design recommendation phase.

On-track testing was conducted to:

- Better understand the behavior of the test vehicle in a quasi-real-world environment,
- Allow the research team to study and experience the performance of the test vehicle while varying several control parameters, and
- Generate data for baseline comparison purposes with the simulation models.

Data analyses were conducted to assess the potential benefits of new generation wide base single (NGWBS)tires, Electronic Stability Control (ESC) on the tractor, and variation in the Center-of-Gravity (CG) of the payload.

For the Phase A research a tractor-flatbed trailer was studied. This configuration was considerably more torsionally compliant than the tractor-van trailer. When the test-track experiences with the tractor-van trailer were compared with those of the tractor-flatbed trailer, the tractor-van trailer demonstrated a more systematic and linear approach to axle lift as the vehicle speed was increased. In contrast, the torsionally compliant tractor-flatbed trailer combination went from no wheel lift to a dramatic wheel lift (that is from zero to 24 in. of wheel lift) within just a few miles-per-hour. As a result, much greater test design detail was required for the tractor-flatbed trailer than the tractor-van trailer.The testing conducted in this Phase A of the HTRC Program is an extension of the previous work done in Phases 1 and 2. In the previous work, a van trailer was tested with dual tires and NGWBS tire configurations as well as with standard and wide axles for the van trailer. While dispersion in the testing results limited the statistical assessment of the data collected in Phases 1 and 2, the data indicated that some combinations of axles and tires, such as wider axles and NGWBS tires, offered the potential to raise the rollover threshold of the vehicle. The testing in Phase A was conducted using an aluminum flatbed trailer and was limited to standard axle widths (78 in.) for both the tractor and flatbed trailer. For Phase A, the data was sufficient to provide statistically valid conclusions indicating that the performance of the dual tires and NGWBS tires were equivalent, and that modifications in payload did change the vehicle's roll threshold.

Regarding the use of the tractor ESC system; in all cases for which the tractor ESC system was engaged, it provided a rapid reduction in the lateral acceleration and vehicle speed. Because of safety concerns and resource limitations, determination of the speed margin gained in terms of the wheel lift threshold through the use of the tractor ESC system was not possible for all load configurations. However, the wheel lift duration was shown to be reduced for all test cases when the tractor ESC system was engaged.

Behavior of the vehicle as the payload CG height changed resulted in the expected behavior. That is, higher CG payloads elicit wheel lift at slower speeds.

The team also attempted to utilize a simulation model, set up with test-track data collected for the tractor-flatbed trailer, to emulate the performance experienced during the on-track testing. For this effort, TruckSim®, developed by Mechanical Simulation Corp., was used. If such

performance could have been emulated, the research team would have a significant capability to address the impact of "what if" design changes in software rather than testing them in the more expensive on-track testing mode. Unfortunately, the behavior of the on-track vehicle for the various maneuvers could not be well emulated in the TruckSim® modeling environment. The reason for the differences is not known. This suggests that: 1) the modeling of vehicle stability is complex, especially for multiple degree of freedom articulated vehicles, 2) the test vehicle needs to be characterized and/or modeled in more depth than is currently capable, and/or 3) the modeling assumptions and associated equations of motion used in this analysis cannot effectively treat a tractor and flatbed trailer with the low torsional stiffness properties observed in this case. Using the combined tests of the prior phases of research in this Program, it appears that some tire and axle combinations hold the potential for improving class 8 tractor-trailer rollover threshold limits. However, there are many other parameters that may be reflected in the testing results, such as the torsional compliance of the flatbed trailer, the torsional compliance of the tractor, the trailer length, and the load arrangement, to name a few. These limit the definitive assessment of axle or tire effects on roll stability. It may be possible to assess if there is any interaction between chassis stiffness and tire selection that increases or decreases the global vehicle stability limits.

Research Team

ORNL was the overall lead of the Phase A research and provided project oversight, and management, and expertise to support vehicle instrumentation; on-track testing; data collection, management and quality assurance of the collected data; and data analyses. Michelin led the research involving the Kinematics and Compliance (K&C) Testing, and developed a procedure to conduct torsional stiffness testing of the test tractor and flatbed trailer, which they subsequently carried out. Michelin was also intimately involved with the design of the test-track testing, its execution, physical characterization of the tractor and flatbed trailer, and reflecting all of these efforts within their TruckSim® model. WMU also provided their expertise in the design of the test-track testing, creating solid-body models, and the development of their TruckSim® model of the tractor and flatbed trailer. WMU also developed several unique roll stability design concepts that they studied via their modeling tools. WMU's analyses suggested that such concepts could provide a reduced rollover propensity for a tractor-flatbed trailer combination. Battelle conducted an initial investigation into run-off-the-road events, and provided invaluable insights into truck rollover stemming from their experience in the cargo tank rollover area [2].

The research team for this effort built on the relationships that were formed during the Phase 1 and Phase 2 efforts conducted in the 2004-2005 timeframe. Each organization contributed actively to the successful execution of this project, and was able to address associated and complementary research needs and interests. This team also supplied significant and valuable resources that leveraged the NTRCI-UTC/DOT funding and was a great example of a strong and successful public-private partnership.

Context of the Phase A Research

The work conducted by the Phase A HTRC team focused on efforts to generate data and information on heavy truck rollover not currently available in the industry. The lessons learned and results from this research will be merged with the lessons learned and results of the tractor-box-trailer (Phases 1 and 2), and tractor-flatbed trailer efforts (Phase A); with industry experience and expertise; and in conjunction with tractor and trailer original equipment manufacturers (OEMs); to provide a basis for recommending design enhancements that would support enhanced roll stability and safety in future class 8 combination vehicle concept. This phase of the project (Phase A) was conducted to understand the roll stability and roll characteristics of a 2007 Volvo model, VN 64T830, class 8 heavy-duty tractor with a fully-loaded 48 ft aluminum Utility flatbed-trailer with Intraax air suspension.

Testing Overview

Testing was conducted at the TRC in East Liberty, Ohio. TRC was also contracted to provide the data acquisition system; to collect data during the test maneuvers and for executing the on-track testing conducted in May, 2008. For the on-track testing, TRC designed and constructed new load racks per the specifications provided by the Phase A project team. There were four test maneuvers selected by the project team for on-track testing, and a detailed test plan was developed as a roadmap for test execution. The test maneuvers selected for rollover testing were:

- Constant radius,
- Ramp steer,
- Step steer, and
- Lane change (highway evasive maneuver).

The ramp steer maneuver was subsequently eliminated because of the successful execution of the high-speed constant radius maneuver. Three different elements of the tractor-flatbed trailer configuration were varied during the testing;

1) Tires (standard dual tires versus NGWBS tires),
2) Flatbed trailer payload CG height (two different payload CG heights), and
3) Tractor ESC system (on and off).

It should also be noted that test-track testing was conducted at low speeds and at lift threshold limit speeds.

The first three attempts to collect truck rollover data at TRC were unsuccessful. The first attempt (October 25-26, 2007) revealed that when wheel lift was achieved, it was experienced at the drive axles of the tractor. Because the drive axle lifted first, the outriggers mounted in the center of the flatbed trailer were felt to be inadequate to prevent the tractor from rolling over in the event that a more severe wheel lift was to occur; and the testing was therefore halted. The research team decided that if wheel lift was to be experienced first on the drive axle, that an

alternative outrigger placement was necessary in order to assure that the test vehicle would not rollover during testing.

For the second attempt (November 16, 2007), the outriggers were moved forward on the flatbed trailer in order to minimize the potential for the tractor to rollover. However, due to the flexibility inherent in the flatbed trailer, the outriggers, now located at a more-forward location and providing more protection for the tractor, did not adequately protect the rear of the flatbed trailer from rollover. The testing resulted in a larger than desired flatbed trailer axle lift which was deemed too severe for testing conditions, and the testing was again halted.

For the third attempt (January 10-12, 2008), a second set of outriggers was added to the rear of the flatbed trailer so that the tractor-flatbed trailer was protected for both the drive axle and the flatbed trailer axle lift. However, during the third attempt at the on-track testing, the tractor-flatbed-trailer speed reached relatively high levels without achieving wheel lift. TRC halted further testing because further increases in speed would have resulted in too much energy being in the system, and if a violent wheel lift would have occurred, the integrity of the outriggers might have been compromised.

After considerable discussion within the team and with subject matter experts outside of the team, it was concluded that in order to achieve a more controllable wheel lift, the CG of the ballast had to be raised, allowing for wheel lift to occur at slower speeds. It was also decided that the ballast should be grouped into two elements located over the drive axle and the flatbed trailer axles. In order to accommodate this new ballast system, a rack system was designed to raise the ballast blocks above the deck. It should be noted that the racks would also allow the CG of the ballast to be changed which added an additional study variable, and would allow the tests to be conducted within a speed and articulation angle envelope that was acceptable by TRC. The fourth attempt (May 15 – 21, 2008) to perform rollover testing was successful.

The low-speed maneuvers were conducted for the purposes of establishing a baseline assessment for the vehicle, and to generate data of relevance to model validation. The high-speed maneuvers were conducted at speeds at which wheel lift was achieved for a particular maneuver. The highest speed attained during the May test campaign was less than 40 mph (64.4 km/h). The low-speed maneuvers were executed at several miles per hour slower than the high-speed maneuvers. For the step steer and lane change maneuvers, low-speed was 15 mph (24.1km/h); for the constant radius the low-speed varied from 5-to-25 mph (8.1-to-40.2 km/h). The vehicle was able to perform all of the maneuvers at the low-speed, in a very stable manner.

Both the low-CG and high-CG payload conditions were tested using conventional 275/80 R22.5 dual tires on the drive and flatbed-trailer axles. An additional test with the high-CG payload case only was evaluated using 445/50 R2.5 NGWBS tires.

Data Acquired

During the test maneuvers, the TRC-owned eDAQ data acquisition system was used to collect 33 channels of data at a sampling rate of 102.4 Hz. This resulted in over 168 megabytes of data in the SIF file format (i.e., the format used by eDAQ). The SIF files were converted to over 310 megabytes of data in the more common “comma separated variable” ASCII format for distribution to the team members.

Summary of Results

Constant Radius Test

To support simulation model validation, steady-state constant radius testing was completed at a low speed to quantify the understeer characteristics of the tractor-flatbed-trailer combination. For the low-speed testing, the data indicated that at low lateral acceleration levels, the vehicle needed approximately three degrees of steering input at the steering wheel above that which would be dictated by the Ackermann geometry in order to maintain the measured radius of curvature. At higher lateral acceleration levels, the steering input approached the Ackermann requirement. This indicates that the vehicle was slightly understeering, but at a very slowly decreasing rate with respect to its lateral acceleration. All of the tested payload and tire combinations had very similar understeer curves. Due to the high-CG payload condition, the steady-state testing was limited to accelerations below 0.2 g. Changing tires or payload heights did not change the understeer response significantly.

For the high-speed constant radius maneuver, the Duncan Multiple Range test was used to analyze the data. It showed that the reduction of the payload height by 1 ft was statistically significant, but the selection of tires was not (similar conclusions were derived from the step steer and lane-change maneuvers analysis). The ability to discern a statically significant change in vehicle lift response of a 1 ft payload height change indicated a reasonably well-controlled test method. The tests were repeated with the tractor ESC system engaged with the expected result that wheel lift was prevented for all of the constant radius runs at higher speeds.

The high-speed constant radius test data also showed that for the high-CG payload case, the drive axles lifted at a slightly lower lateral acceleration level than the flatbed trailer axles. This is in contrast to the low-CG payload case wherein the flatbed trailer axles lifted with the drive axles. Because of the flatbed trailer’s flexibility, which severely limits its ability to effectively transmit torque from one end to the other, it was deduced that the front and rear portions of the flatbed-trailer have very similar roll limits.

The drive axle lift sensitivity was 0.06 g/ft of height change in the payload; 0.12 g/ft in system CG height change (includes the masses of the axle, outrigger, load rack, etc.). The flatbed trailer axle lift sensitivity was 0.04 g/ft of height change in the payload; 0.067 g /ft in system CG height change. Given that the mass of the unloaded tractor is greater than the unloaded flatbed trailer,

the amount of payload which can be carried over the flatbed trailer axles is greater than the payload at the drive axles.

Step Steer Test

The step steer test was designed to evaluate the transient behavior of the vehicle using a repeatable steering input. Testing was initially performed without the tractor ESC system engaged to evaluate the vehicle's stability, and then with the tractor ESC system engaged, to assess the benefits of such a system.

Several key vehicle metrics were selected as potential lift indicators including vehicle velocity, lateral acceleration, roll rate, yaw rate, roll angle, and vehicle side slip angle. The results of the statistical analysis showed that payload height and lateral acceleration were well-correlated to the wheel lift event, while the remaining parameters were not. The analysis also showed that it was possible to determine with 95% confidence that the low-CG payload vehicle response was statistically different from the response of the high-CG payload vehicle for both the drive and flatbed trailer axle sets. It was not possible to distinguish between the behaviors of the dual tires and the NGWBS tires for either the drive or flatbed trailer axle sets. The indication is that the dual tires and the NGWBS tires have similar performance in roll stability for a torsionally compliant flatbed trailer.

For the cases where the tractor ESC system was engaged with a high-CG payload configuration, the analysis of the data showed that, although the axle lift thresholds for speed or lateral acceleration were similar to those observed with the tractor ESC system off condition, the duration of the observed wheel lift decreased. This would be expected since the engagement of the tractor ESC system should tend to bring the vehicle back into a stable operating situation sooner. The data, however, could not be used to statistically quantify the lift duration reduction because the driver's response after a wheel lift occurred varied significantly. For the low-CG payload case, the tractor ESC system was effective in preventing wheel lift under the same conditions and speeds that wheel lift was observed for this maneuver when the tractor ESC system was not engaged.

Lane Change Maneuver Test

For the lane change maneuver, roll stiffness (***RS***), computed as the ratio of the maximum roll angle divided by the maximum lateral acceleration was used as the analysis variable (the variable ***RS*** was computed for the tractor, and the front and rear of the flatbed trailer). For each lane-change maneuver (a total of 70 runs), two ***RS*** values were computed: one for the first half of the maneuver (left turn) and one for the second half (right turn). Since in the majority of the cases (more than 85%) the distributions of ***RS*** had very dissimilar variances for the different treatments analyzed, a Smith-Satterthwaite Test was used to test the null hypothesis that the means of each pair of compared distributions of ***RS*** (e.g., dual tire ***RS*** vs. NGWBS tire ***RS***, for high-CG payload and high-speed) were the same. Concentrating on the first part of the maneuver, the

results showed that the null hypothesis could only be rejected with a low level of confidence (less than 95%) when the dual tires were compared against the NGWBS tires for the cases of high-CG payload/high-speed/tractor ESC-off, high-CG payload/low-speed/tractor ESC-off, and high-CG payload/high-speed/tractor ESC-on. This indicates no statistically significant differences between the two types of tires regarding roll stability with this torsionally compliant flatbed trailer. The tests also seem to indicate that the engagement of the tractor ESC system made the ***RS*** distributions of the dual tires and the NGWBS tires "more equal," since the null hypothesis could only be rejected at lower confidence levels than when the system was not engaged. This difference was more pronounced in the second half of the maneuver, when the tractor ESC system had some time to act (i.e., the first half of a lane change maneuver consisted of an abrupt change in the direction of travel that cannot be predicted by the tractor ESC system). However, because only five runs were conducted with the tractor ESC on (three with dual tires and two with NGWBS tires), those tests are not as powerful as those conducted with the tractor ESC off (12 runs; seven with dual tires and five with NGWBS tires).

Regarding the effect of payload CG height change; the results showed that for the high-speed case, the null hypothesis could be rejected at a very high level of confidence (close to 99.99%+, except for the tractor ***RS*** comparison in the second half of the maneuver where the null hypothesis could be rejected with 96.9% confidence). This strongly indicates that the 1 ft decrease in the height of the CG payload increases the roll stability of the vehicle substantially (average decreases in ***RS*** of 16% for the tractor and 13%-17%-to-20%-30% for the flatbed trailer, for the first and second half of the maneuver, respectively, were observed). For the low-speed runs, the null hypothesis could only be rejected at the 99% confidence level when considering the ***RS*** distributions for the rear of the flatbed trailer, indicating that the 1 ft payload CG height decrease showed statistically significant gains in roll stability for the flatbed trailer. For the tractor and the front of the flatbed trailer, the null hypotheses could be rejected with 98% and 90% confidence level, respectively.

In summary, the results of the test-track testing showed that, in terms of roll stability, the reduction of the payload height by 1 ft was statistically significant in affecting the roll stability for all of the maneuvers, but the selection of tires was not. Although there were very few runs conducted with the tractor ESC system engaged, the results of the tests seem to indicate that there is a positive contribution of this system in terms of roll stability. However, the testing also indicated that the tractor ESC system would not prevent wheel lift under some situations (i.e., for some speed, steering and load combinations) but appears to reduce the duration of the wheel lift. The results suggest that the effect of the tractor ESC system needs to be further and specifically investigated, for the lane change maneuver. Additionally, to address the issue of wheel lift duration, a different vehicle test strategy and set of measurements will be required.

Modeling Results

For the modeling analysis, TruckSim® was utilized as the platform to develop a functional model of the vehicle using the kinematics and compliance data as well as manufacturers' design/build data sheets that were gathered for the tractor and flatbed trailer in this phase of the project. Particular attention was paid to inputs such as axle motions and suspension stiffness, as well as chassis rigidity.

Constant Radius Test

Both the low- and high-speed constant radius tests were evaluated in the model to determine if the model could reproduce the performance of the vehicle as observed during the test-track testing. The low-speed model was executed using a constant radius turn of 75 m (the same as the test-track test), and a speed increment of 1 km/h (0.62 mph) every 3 sec (slightly slower than that observed in the test-track tests). The model was found to be sensitive to the torsional stiffness parameters for the tractor and flatbed trailer. When the measured vehicle torsional stiffness was used, the model did not correctly predict the understeer response of the vehicle. Artificially stiffening the chassis in the model helped to reproduce the correct slope in the steering vs. lateral acceleration plot, but it over-predicted the amount of understeer by about 5 deg at the steering wheel.

The high-speed model was evaluated using a slow constant steering rate of 5 deg/s at the steering wheel, with the test vehicle traveling at 61 km/h (37.9 mph) (this speed was selected because it was the lift speed that was realized in the test-track testing). Using the measured torsional stiffness values for the test vehicle, the simulation model significantly under-predicted the wheel lift threshold for both the tractor and the flatbed trailer in both the high-CG and low-CG payload configurations. Increasing the torsional stiffness of the model by an order of magnitude accurately emulated the same drive axle lift threshold for the high-CG payload condition, but not for the low-CG payload condition. The flatbed trailer axle lift threshold was not correctly predicted for either load condition using the stiffened chassis. Further investigation is needed into the model representation of torsional stiffness and the vehicle system sensitivity to this parameter.

Step Steer Test

As in the previous case, the modeling efforts for the step steer were also affected by torsional stiffness questions which, in general, were the same as those in the high-speed constant radius testing. The simulation model was fairly close at predicting the lift threshold of the tractor for the artificially stiffened chassis case, as well as the flatbed trailer lift point for the "as-measured" chassis case. However, the remaining lift points were not correctly estimated, and neither chassis model correctly predicted the lift sequence of flatbed trailer axle lift before drive axle lift.

In summary, the torsional stiffness of the flatbed-trailer used in the TruckSim® model has a significant impact on the overall modeled vehicle behavior. Understanding how the chassis of a

flexible vehicle behaves is important for understanding the overall vehicle's response to various inputs. Furthermore, modeling such torsional flexibility takes considerable care, is not trivial, and is a significant area for future research.

Solid Modeling

The flatbed trailer used in this study was scanned by WMU using an ATOS II white light scanning system. This system produces a point cloud from which very precise computer models can be generated. The scan produced a highly precise, material specific model which can be used in a library for the development of a future truck concept. With the precise representation obtained, the WMU team was able to produce a finite element model for structural analysis testing. The structural model matched the experimentally determined torsional characteristics of the actual flatbed trailer used in the test-track testing.

WMU also developed an ADAMS kinematic model of the flatbed trailer suspension which allows selected parameters to be varied to assess their influence on the overall tractor-flatbed trailer model. The solid models, finite element models, and kinematic models will prove to be important as this project moves into the design recommendation phase. These models provide the foundation for full flex body modeling which will enable the assessment of road surface encounters and their influence throughout the model.

Advanced Design Concepts

Advanced design concepts were explored that extend beyond the current-day tractor-trailer design. As part of this study several tractor-trailer design concepts were suggested and initially investigated. These included: a moveable 5^{th} wheel for the tractor, a deployable third trailer axle, and an active suspension concept; all of which were addressed through modeling efforts. Although these are still considered to be in the initial stages of a feasibility study, all have shown, at least conceptually, some potential for improvement of the roll stability of a combination vehicle. These concepts, as well as others that might present themselves in future phases, will be further studied for their applicability.

Vehicle Handling Characteristics

The as-tested tractor-flatbed trailer was modeled and evaluated using a simulation program as well as studied from a parametric perspective. As part of this study, the importance of looking at the class 8 tractor-flatbed trailer as a system was stressed. To assist in evaluating parameters in the tractor-flatbed trailer design that might ultimately lead to improvements in the rollover threshold, a unique software program was developed by WMU. The program predicts quite well some of the handling characteristics of the tractor and flatbed trailer, and has design attributes that allows one to study, conceptually, the influence of a selected attribute on stability. Design parameters such as axle wall thickness, suspension bushing characteristics, etc. can be altered to benchmark their influence on the dynamics of the tractor-flatbed trailer. This program allows variations in load placement, frame structural properties, and details of the suspension.

Appendix D – Phase B Summary (Tank Semitrailer)

Abstracted from the Executive Summary from the final report of Phase B of this Program, U19: Heavy Truck Rollover Characterization (Phase B), October 2009

Background

This Heavy Truck Rollover Characterization Program is a major research effort conducted by the National Transportation Research Center, Inc. (NTRCI) in partnership with the Oak Ridge National Laboratory (ORNL), Michelin Americas Research Company (Michelin), Western Michigan University (WMU), Battelle Memorial Institute (Battelle), LBT, Inc. (LBT), and Bendix Commercial Vehicle Systems (Bendix). This research is one of the major projects conducted by the NTRCI in its role as a University Transportation Center (UTC) for the Research and Innovative Technology Administration (RITA), an agency within the U.S. Department of Transportation (DOT). This research also involved, via subcontract, Volvo Trucks North America, Inc., Clemson University and Link-Radlinski, Inc. This work, entitled Heavy Truck Rollover Characterization – Phase B, addresses truck rollover issues dealing with a tractor and tank trailer, and follows similar work that was conducted by NTRCI on a tractor-van trailer in 2004-2005, and on a tractor-flatbed trailer in 2007-2008.

Brief Overview

The overall objectives of this research were to:

- Contribute to the understanding of the dynamics of heavy truck rollover and stability,
- Contribute to the development of advanced models of heavy truck vehicle dynamics that reflect project experiences, and
- Develop recommendations for the improvement of the roll stability of heavy vehicles in preparation for realizing and testing such concepts in future phases of heavy truck rollover characterization research.

This project involved four major types of activities:

1. Tractor and tanker-trailer characterization,
2. Computer simulation modeling,
3. On-track testing, and
4. Data analysis.

The tractor and tank trailer characterization were necessary in order to generate kinematic and compliance (K&C) data for later use in the development of simulation models of the vehicle (the combination tractor and tank trailer). Each unit (tractor or tank trailer) of the vehicle was characterized individually under conditions that accurately represented the as-tested vehicle arrangement.

The tank railer used for the on-track testing (designated as Tanker T) was designed and fabricated by LBT, so that the desired test load distributions could be obtained with minimal complexity in terms of loading the tanks with water and sand. The outriggers were also developed by LBT with design support from Bendix and other research team members. LBT also manufactured two other tank railers (designated Tanker M and Tanker W). Tankers M and W were functionally identical and typical of commercial petroleum tanks and were not modified for the project. Tanker T used the same aluminum tank barrel as Tanker M and Tanker W. Tankers M and W were used for K&C characterization and torsion testing by Michelin, and rigidity and dimensional characterization by WMU, respectively.

Simulation modeling was conducted in order to better understand the dynamic behavior of the test vehicle, and these models will allow for the conduct of various "what if" design studies in future phases of this Program. This activity involved the development of solid-body models, finite element models, and kinematic models that will be important as this project moves into the design recommendation phase.

On-track testing was conducted to:

- Better understand the behavior of the test vehicle in a real-world environment,
- Allow the research team to study and experience the performance of the test vehicle while varying a selected number of control parameters, and
- Generate data for baseline comparison purposes with the simulation models.

Data analyses were conducted to assess the potential benefits of New Generation Wide-Base Single (NGWBS) tires, Electronic Stability Control (ESC) on the tractor and tank trailer, and variations in the Center-of-Gravity (CG) of the tank trailer.

For the Phase B research, the tractor that was used was the same tractor that was used in the Phase A research; a 2007 Volvo model, VT64T830, Class 8 heavy-duty tractor.

The tank trailers used in Phase B were considerably stiffer in torsion than the flatbed trailer studied in Phase A of this Program. When the test-track experiences with the tractor-tank trailer are compared with those of the tractor-flatbed trailer, the effect of the torsionally stiff tank trailer chassis is evident. In the flatbed trailer testing, the front and rear ends of the flatbed trailer rolled independently of each other with the result that the wheel lift threshold was the lower limit of the two ends of the flatbed trailer. For the tank trailer, the chassis could pass restoring moments from one end of the tank trailer to the other so that the wheel lift threshold was defined by the total overturning moments and the total restoring moments. The consequence of this is that when the front of the flatbed trailer began to roll over, it would quickly run through the fifth wheel lash, and then the drive axles would resist the overturning moment. For the tank trailer, the front overturning moment was resisted primarily by the rear axles through the chassis torsion until the tank trailer axles lifted and the tank trailer rolled through the fifth wheel lash, and the drive axles began to impart a significant restoring moment.

The testing conducted in Phase B is an extension of the previous work done in Phases 1, 2 and A. In Phases 1 and 2, a van trailer was tested with dual tire and NGWBS tire configurations as well as with standard and wide axles (wider-sliders) for the van-trailer. In Phase A, a flatbed trailer was tested with dual tire and NGWBS tire configurations, tractor ESC on and off, and two different tank trailer CG heights. While data dispersion in the testing of Phases 1 and 2 limited the statistical assessment of the data, it indicated that some combinations of axles and tires, such as wider axles and NGWBS tires (tested in Phases 1 and 2), and ESC (tested in Phase A) offered the potential to raise the wheel lift threshold of the vehicle.

The testing in Phase B was conducted using a tank trailer that used a 1,816 mm (71.5 in.) axle width for both the tractor and tank trailer (the axle width is the distance between the rim mounting faces on either end of the axle). Both the dual tires, and the NGWBS tires using standard 2 in. offset rims, were mounted on the test vehicle as they are typically mounted and used in the industry. This results in a 74.7 in. track width for the NGWBS tires, which is approximately 2.0 in. wider than the track width of the dual tire assemblies. This track width increase can be achieved using NGWBS tires without exceeding the overall width limitations (exterior face-to-exterior face) of the vehicle (the track width is defined as tire center to tire center for the NGWBS tires, and from the midpoint between the two tires on one axle end to the midpoint between the two tires on the other axle end for dual tires). Figure D-1 below provides an illustration of the comparison in track width and overall width for dual tires and NGWBS tires for the specific case of the tank trailer used in Phase B testing. The 71.5 in. axle represents the narrowest axle width commonly used in heavy duty trucks. Although the trends shown in Figure D-1 are generally true across commercial vehicles, the actual measurements for other common axle and component configurations will frequently be different than the specific values shown here. For Phase B, the data was sufficient to draw valid conclusions concerning the effect on vehicle stability of small tank trailer CG height changes and dual tire vs. NGWBS tire configurations. The testing showed generally that the NGWBS tires were, at a minimum, equivalent in roll stability when compared to the dual tire arrangement. The data also confirmed the effects of differing tank trailer CG heights on roll stability, and addressed the benefits of ESC on the tractor and tank trailer.

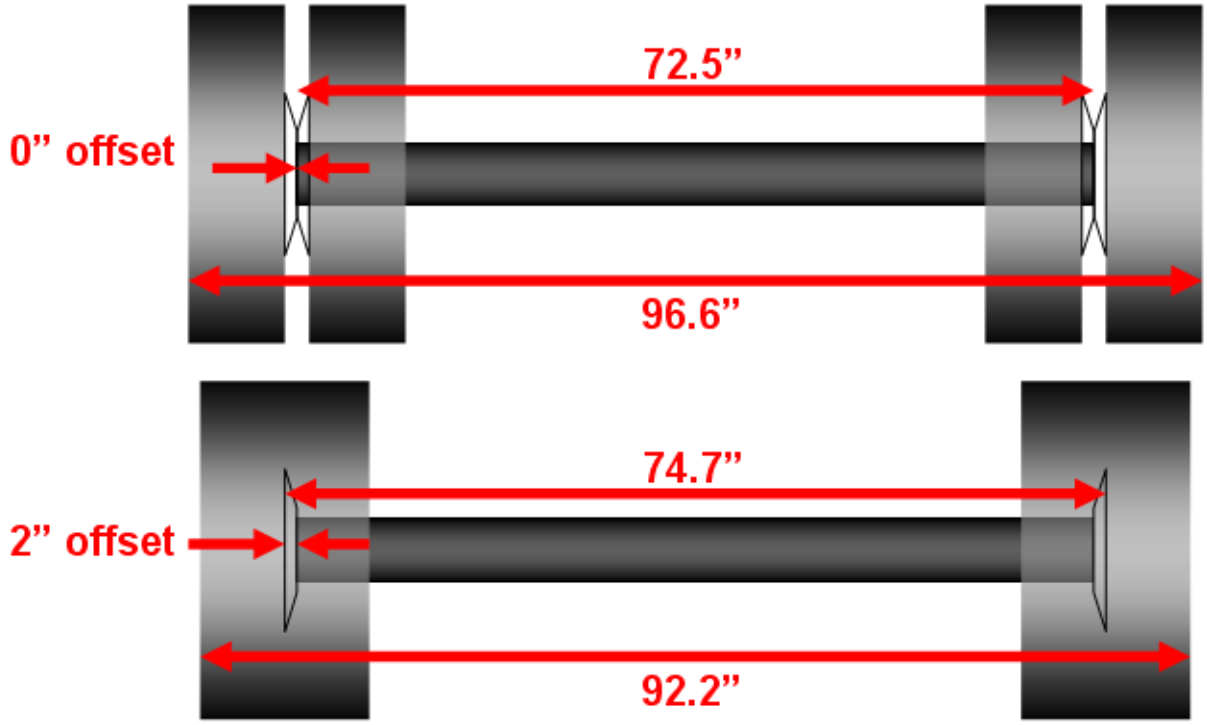

Figure D- 1. Track Width and Overall Width of Dual Tires and NGWBS Tires when both are Mounted on the Phase B Trailer.

The Phase B testing and analysis fulfilled the objectives of the research and provided further evidence and quantification of the benefits of the ESC system, CG height variation and NGWBS tires on truck rollover stability, particularly for a tractor-tank trailer configuration. Conclusions regarding the rollover performance of the tractor-tank trailer relative to several system parameters were made based on statistical assessments of wheel lift among the various vehicle configurations tested. With more complete measurements of some of the parameters influencing rollover behavior of the truck— such as the fifth wheel lash and orientation—and more accurate measurement of roll angle and other kinematic characteristics, a more complete understanding of the roll dynamics of Class 8 tractor-trailers has been developed from this research. The collected data was used in developing and validating vehicle dynamics models to demonstrate the ability of the model to predict improvements in rollover performance.

Research Team

ORNL was the overall lead of the Phase B research and provided:

- project oversight and management;
- support for vehicle instrumentation, on-track testing, data collection, and the management quality assurance of the collected data;
- and data analyses.

Michelin led the research involving the K&C testing and developed simulation models from the K&C data which were used to assess project modeling potentials. Michelin was also involved with the design of the on-track testing and its execution. These efforts included preparation of the test plan; executing the testing at the Transportation Research Center (TRC) located in East Liberty, Ohio; test data analysis; model development using TruckSim®; and modeling assessment. Michelin's efforts were graciously and generously donated to this project at Michelin's expense.

WMU also provided their expertise in the design of the on-track testing, instrumentation of the tank trailer with WMU-provided strain gages, provision of a third eDAQ data acquisition system for use during testing, creation of solid-body models of the tractor and tank trailer, and physical characterization of the tank trailer.

Battelle provided project review support in all aspects of the project.

LBT graciously and generously donated the use of two of their tank trailers for characterization efforts conducted by Michelin and WMU respectively, and designed and fabricated the custom-built third tank trailer used for the on-track testing. In addition, LBT designed (with input from Bendix and other research team members) and paid for the fabrication of the outriggers used for the on-track testing, arranged for the movement of the tank trailers to and from the respective test sites (Kalamazoo, Michigan for Tanker W characterization; Greenville, South Carolina for K&C testing of Tanker M; and Marysville, Ohio for on-track testing of Tanker T). LBT also provided significant insight related to tank trailer dynamics.

Bendix provided the ESC system for Tanker T, provided engineering insights for its functionality, and supported the design of the outriggers used in the on-track testing.

Each partner-organization contributed actively to the successful execution of this project, and was able to address associated and complementary research needs and interests. This team also supplied significant and valuable resources that leveraged the NTRCI-UTC/DOT funding and was again, a great example of a strong and successful public-private partnership.

Context of the Phase B Research

The work conducted by the Phase B research team focused on efforts to generate data and information on heavy truck rollover not currently available in the industry. It is part of a longer-term research Program that will take the lessons learned in Phases 1, 2, A and B involving Class 8 tractors and a van trailer, flatbed trailer and tank trailer; and the experiences of engaging in on-track testing, vehicle dynamics modeling, and analysis of the on-track data, to provide a basis for the development of an advanced Class 8 tractor-trailer concept that will be more stable and therefore safer.

K&C Testing

Michelin conducted a K&C test on Tanker M using their heavy vehicle test rig located in Greenville, South Carolina. The tank trailer that was evaluated was an aluminum fuel-hauling unit manufactured by LBT in 2008, and was functionally identical to the LBT tanker used in the on-track testing at the facilities of TRC, located in East Liberty, Ohio. The main difference between Tanker T and the units characterized by Michelin and WMU was that Tanker T's fuel delivery plumbing was not fitted but was replaced with a set of outriggers. It should be noted that the outriggers contributed some additional net weight to Tanker T.

The K&C testing performed by Michelin encompassed the evaluation of Tanker M's response to applied loads and motions in roll in vertical, lateral, and longitudinal directions. The tank trailer chassis was also evaluated for torsional stiffness. The data collected consisted of kinematics curves (such as toe change under jounce), and compliance curves (such as wheel deflection under load). In addition to the K&C data, weight measurements were taken of the tank trailer using a known tractor for the tow vehicle in order to obtain the tank trailer's loaded and unloaded mass. The longitudinal and lateral CG location of the tank trailer was also determined. The data was compiled into a document that was distributed to the project partners for use in the development of simulation models.

On-Track Testing Overview

On-track testing was conducted at TRC from May 18-22, 2009. The testing was conducted by Link-Radlinski, Inc., of East Liberty, Ohio under a subcontract to NTRCI. Representatives from all of the research team organizations were present for some or all of the testing. A Test Plan was prepared by the research team that:

- defined the specific maneuvers to be completed, which included all of the maneuvers needed by the research team and the Co-Simulation (CS) team (the CS team conducts research for NTRCI on another project). In many cases both groups used the same maneuvers resulting in significant cost savings for the projects. The maneuvers conducted at TRC were:
    - steady-state ramp steer maneuver,
    - step steer maneuver,
    - dry open loop double lane change maneuver, and a
    - wet open loop double lane change maneuver
- specified how to best perform the maneuvers,
- defined the vehicle configurations for which testing should be conducted,
- specified the measurements to be made during testing,
- defined the data channels, including the specific information to be measured and how to best measure them, and
- provided information for organizing the team and the testing contractor, for performing these tasks.

Table D-1 shows the maneuvers performed during the on-track testing, including an indication of the project that was the primary user of the data from the maneuver. In reality, much of the data taken from each of the linked projects can be useful for the other project, which indicates the synergies among the NTRCI project teams.

Table D- 1. List of Maneuvers Performed During On-Track Testing.

Request	Maneuver	Number of Runs (low-speed)	Number of Runs (high-speed)	ESC (tractor-tanker-trailer)	Vehicle Config. **
HTRC	Steady-state ramp steer	2	10	OFF-OFF	3
HTRC	Steady-state ramp steer	0	5	ON-ON	3
HTRC	Steady-state ramp steer	0	5	ON-OFF	2
HTRC	Steady-state ramp steer	0	5	OFF-ON	2
HTRC	Step steer	6	15	OFF-OFF	3
HTRC	Step steer	0	5	ON-ON	3
HTRC	Step steer	0	5	ON-OFF	3
HTRC	Step steer	0	5	OFF-ON	2
CS	Step steer (alt)	0	5	OFF-OFF	2
CS	Step steer (alt)	0	5	ON-OFF	2
HTRC	Double lane change (dry)	6	15	OFF-OFF	3
HTRC	Double lane change (dry)	0	5	ON-ON	3
HTRC	Double lane change (dry)	0	5	ON-OFF	3
HTRC	Double lane change (dry)	0	5	OFF-ON	2
CS	Double lane change (wet)	0	5	OFF-OFF	2
CS	Double lane change (wet)	0	5	ON-ON	2
CS	Double lane change (wet)	0	5	ON-OFF	2
CS	Double lane change (wet)	0	5	OFF-ON	2

* HTRC = Heavy Truck Rollover Characterization project, CS = Co-Simulation project

** A ‘2’ under the Vehicle Config. Column indicates that only the dual tire, low-CG and high-CG configurations were tested, while a ‘3’ indicates the NGWBS tire, high-CG configuration was also tested.

Prior to the testing, the research team also worked to develop and refine software for data reduction and analysis in order to enable rapid review of the test data in the field.

Coordination of the test-track efforts was led by ORNL but was ultimately shared among the team members for the project. From April 30 through May 15, 2009, Link-Radlinski, Inc. performed the primary instrumentation of the tractor-tank trailer, and engaged in other activities to prepare the tractor-tank trailer for the on-track testing. WMU provided the strain gages and mounted these on the tractor-tank trailer. “Shakedown testing” was performed during May 16-17, 2009. For the shakedown testing, research team members worked with Link-Radlinski, Inc., to:

- finalize the vehicle setup prior to testing,
- verify that all sensors and hardware used for the testing were working as expected,

- program the operation of the steering robot used for the Phase B test maneuvers which required its use,
- make measurements of various configuration parameters of the vehicle and identify instrumentation locations, and
- ensure that everything was configured correctly for the testing.

A steering robot was used in order to ensure high test repeatability as it resulted in maneuvers which were easier to repeat accurately. This improved the quality of the test data.

A total of 73 separate tests were performed during the on-track testing, with between one and 20 runs for each of the tests (3-5 repetitions were typical). These tests covered three different vehicle configurations (low-CG and high-CG with dual tires, and high-CG with NGWBS tires), and various combinations of the ESC system activation (tractor off-tank trailer off (i.e., ESC off-off), tractor on-tank trailer on (i.e., ESC on-on), tractor on-tank trailer off (i.e., ESC on-off), and tractor off-tank trailer on (i.e., ESC off-on)) were also tested. In this way, the 73 test conditions represent a matrix of combinations among the vehicle configurations, ESC system status, and speeds across the different test maneuvers. The specific combinations tested were selected to cover those parameters considered most relevant.

Data Acquired

During the test maneuvers, three eDAQ data acquisition systems were used; two from NTRCI and one from WMU. A total of 165 data channels were configured for the testing, and data was recorded at a sampling rate of 100 Hz for each channel.

Data Analyses

Data analyses of the on-track test data were conducted by ORNL, Michelin and WMU. Data analysis of each selected maneuver was accomplished by the organizations indicated below:

- Steady-State Ramp Steer Maneuver (Michelin and WMU),
- Step Steer Maneuver (Michelin and ORNL),
- Open-Loop Double Lane Change, dry surface (ORNL and WMU)
- Open-Loop Double Lane Change, wet surface (Clemson University's (CU's) Co-Simulation team); note: this maneuver, while performed during the test period was not required by the HTRC and was conducted to support the Co-Sim research. Details of the Co-Sim testing and analyses are presented in reference.

Summary of Results and Conclusions

Steady State Ramp Steer Maneuver – Major Findings

The ramp steer maneuver is a decreasing radius turn performed at a near constant velocity. A constant steering rate-of-change is provided while the tractor-tank trailer is traveling at a constant speed. The test data was used to evaluate the vehicle's sub-limit (normal driving) and

rollover behavior (note: limit testing involves the condition where wheel forces on an axle combination go to zero).

Two major conclusions were derived from the analysis of the low-speed (sub-limit) execution of the steady state ramp steer maneuver. First, the selection of the tires did not appear to have a significant impact on the understeer behavior of the vehicle because all of the high-CG configurations had similar understeer responses (for both clockwise (CW) and counter-clockwise (CCW) maneuvers) as well as similar understeer gradients. The second conclusion was that the movement of 4,300 lb of payload from the bottom of the center tank to the top of the tank trailer, which shifted the CG of the tank trailer up by about 4.5 inches (115 mm), produced only a small change in the understeer behavior of the vehicle, and the impact on the handling behavior was not significantly impacted. This is a rather important observation, since it was desirable not to adversely change the handling performance for conducting the project testing. The ability to see the small change in the tractor-tank trailer's understeer performance, furthermore, provided a good indication that the instrumentation was sufficient for assessing the vehicle's handling behavior.

The objective of the rollover testing was to evaluate the limit stability of the vehicle under various test conditions. To maximize the quality of the testing, Phase B efforts attempted to minimize the sub-limit behavior changes to the vehicle from the test cases. The small changes in observed sub-limit behavior indicate that the differences in wheel lift thresholds should be functions of limit stability and not the sub-limit behavior of the vehicle leading up to the wheel lift threshold.

Analysis of the steady state wheel lift threshold testing (i.e., the high-speed, steady-state ramp steer tests, which resulted in wheel liftoff) showed that the selection of dual tires or NGWBS tires did not have a statistically significant effect on the vehicle's lift point. The analysis also indicted that the movement of 4,300 lb of ballast had a statistically significant effect on the vehicle wheel lift threshold. That is, the higher CG tank trailer configuration lowered the wheel lift threshold of the tank trailer. For the nominal vehicle configuration (high-CG, dual tires) with the ESC off-off, the lateral acceleration of the tank trailer was increased by 0.18 m/s^2.

For the Phase B testing, the tractor and tank trailer had similar track widths, and the tractor's suspension roll stiffness was roughly equal to the tank trailer's suspension roll stiffness. With a very stiff tank trailer chassis, the tank trailer was able to transmit torque from the front to the rear of the tank trailer (and vice-versa) very effectively. Given that the roll stiffness at the front of the tank trailer was reduced by the fifth wheel compliance, the tank trailer axles acted to resist the bulk of the tank trailer's overturning moment during a given maneuver as long as the required restoring moment was below the peak restoring moment that the tank trailer axles could provide. With a fifth wheel lash of about 2.0 deg, the tank trailer would saturate its rear axle restoring roll moment before it would begin to transmit substantial moments to the tractor through the fifth wheel.

The result of the tank trailer's design and loading was that increases in the overturning moment would increase the roll moment applied to the tank trailer axles until the vehicle lifted the tank trailer axles. At this point, the tank trailer chassis roll angle would increase quickly as the tank trailer passed through the remaining fifth wheel lash. When the fifth wheel lash was traversed, the restoring moment from the tractor axles through the fifth wheel increased quickly, preventing further roll. From this point on, any increasing overturning moment was resisted by the drive axles alone until they also lifted. This is the point of impending rollover.

Step Steer Maneuver – Major Findings

Analysis of the vehicle's wheel lift threshold in a step steer maneuver indicated that the NGWBS tires had a statistically significant higher lift threshold than the dual tires for the rear tank trailer axle. Unfortunately, the dispersion in the test data prevented similar conclusions from being drawn for the remaining axles in the step steer maneuver. As a result, the selection of the tire fitment was deemed to not be a statistically significant parameter for determining wheel lift thresholds.

As with the ramp steer maneuver, the step steer maneuver data also indicated that the low-CG case had a statistically significant higher wheel lift threshold when compared to the high-CG case. While this was an expected outcome, the observable effect of a tank trailer CG height change of 115 mm or 4.5 in. indicates the sensitivity of the test. Finally, the tank trailer axles continued to lift first, similar to the ramp steer maneuver.

Open- Loop Double Lane Change Maneuver – Major Findings

The open-loop double lane change maneuver mimics a rapid approach to slow moving traffic where the driver is attempting to avoid a collision. The vehicle is rapidly steered left, then right to straighten the path, a "progressive" pause, followed by a 2nd turn to the right and then to the left to return to the original "lane of travel." Results of the testing with ESC off-off indicated that the change in the tank trailer CG height was statistically significant. The lateral acceleration at initial wheel lift was higher for the low-CG configuration than it was, at initial lift, for the high-CG configuration. However, the test speed for the low-CG was higher than that with the high-CG. This speed difference explains the difference in the results for lateral acceleration.

Overall Data Analysis Conclusions

The following seven general conclusions resulted from the analysis of the data from the on-track testing.

- Conclusion-1: With regard to the performance of the ESC systems on the tractor and tank trailer, the ESC on-on configuration increased the rollover threshold for all of the maneuvers when compared to the ESC off-off configuration.
- Conclusion-2: The effect on roll stability of the variation in tank trailer CG height was experienced as expected, and was statistically significant.

- Conclusion-3: The experienced and expected behavior of the vehicle with regard to the tractor-tank trailer CG height change helps to confirm that the on-track testing was of good quality.
- Conclusion-4: The tire selection did not have a statistically significant effect on the vehicle's overall stability.
- Conclusion-5: For steady-state maneuvers, the tank trailer ESC had the dominant impact on roll stability.
- Conclusion 6: For transient maneuvers, the tractor ESC had the dominant impact on roll stability.
- Conclusion7: The ESC on-on configuration significantly improved roll stability when compared to the ESC off-off case and reflected the most behaviorally stable configuration of those tested within this project.

Both the dual tires, and the NGWBS tires using standard 2 in. offset rims, were mounted on the test vehicle as they are typically mounted and used in the industry. This results in a 74.7 in. track width for the NGWBS tires, which is approximately 2.0 in. wider than the track width of the dual tire assemblies. This track width increase can be achieved using NGWBS tires without exceeding overall width limitations of the vehicle. The high torsional rigidity of the tank trailer tested in Phase B provided an opportunity for the team to validate the differences between high torsional stiffness and low torsional stiffness chassis structures by referencing the flatbed trailer testing from Phase A. One finding during the testing and data analysis phase was the importance of understanding the impact of 5th wheel lash on the tanker roll rates, and the influence on the tractor when the lash was taken up during a wheel lift event. On the rigid tank trailer, once the tank trailer's 5th wheel plate separated from the tractor's 5th wheel, the tank trailer experienced an increase in roll velocity which then was abruptly limited when the lash was taken up as the kingpin "topped out." The increase in roll velocity was caused by the tank trailer tandems offering the only roll resistance to the roll moment during the last phase. The total roll moment of the tank trailer was acting against the tank trailer tandem roll stiffness. If the tank trailer tandems were lifted, the roll moment would be solely balanced against gravitational forces without the benefit of suspension roll stiffness. The abrupt take-up re-coupled the tractor roll stiffness to the tank trailer and, if the tank trailer axles had not lifted, it would have been re-coupled to the tandem roll stiffness. The abruptness of the take-up leads to an unloading of the tractor drive axles on the inside of the turn, which has the potential to destabilize the tractor. By comparison, the low torsional stiffness of the flatbed trailer allowed the discretely located flatbed trailer loads to essentially act independently in roll. The load independence allowed the front load to act against the tractor suspension roll stiffness while the rear load acted against the flatbed trailer tandem roll stiffness. This decoupling of the two loads allowed the flatbed trailer to run through the lash at a lower lateral acceleration, which provided a smoother transition (lower impact loads) during lash take-up. This gained knowledge enabled the HTRC research team to pay particular attention to the 5th wheel characteristics in the modeling phase. It was proven that the 5th wheel characteristics are critically important when modeling a torsionally rigid trailer.

Challenges were also identified in “field testing” of the torsional characteristics of the torsionally rigid tank trailer. In the prior phases both a van trailer and flatbed trailer were successfully measured using the field technique described in the Phase B final report. With the tank trailer, the suspension roll stiffness could be measured; however, the chassis and tank stiffness could not be accurately evaluated. The method described herein can be successfully applied to vehicles that fall within a range of torsional stiffness where the stiffness may influence the modeling results, such as in low-to-medium torsional stiffness trailers. The method is a valuable tool to characterize trailers where trailer torsional stiffness influences the modeling and possibly the tractor-trailer dynamics. It has limited application when the trailer characteristics are such that modeling as a rigid vehicle is appropriate.

Since Phase B testing included axle mounted height sensors, it was possible to use this information to detect subtle differences in the axle behavior between the NGWBS tires and the dual tires. One of the differences noted was a small increase in the axle roll angle with the NGWBS tires when compared with the dual tires in the lane change maneuver. Factors that played into this difference may include the lower combined radial stiffness of the NGWBS Tires compared to the combined radial stiffness of the dual tires, and the higher cornering stiffness of the NGWBS tires as the lift threshold is entered, leading to a higher articulation angle at iso-steering input.

The testing also revealed the need to accurately match the ESC system to the particular characteristics of the tank trailer. In some configurations, ESC system intervention, with the axle brake cycling, excited a wheel hop on the tank trailer. Although not yet proven, it appears that the geometry of the tank trailer suspension, which leads to high anti-dive for the tank trailer under braking, can be the cause of wheel hop during ESC system intervention. This observed characteristic will need to be further studied in the future work of the HTRC research team.

Modeling Results

TruckSim®

The modeling efforts conducted by WMU and Michelin using TruckSim® were successful in accurately reproducing the dynamic behavior of the vehicle. The TruckSim® models were able to predict the appropriate wheel lift thresholds for the step steer and ramp steer cases with good accuracy. The models were also able to accurately reproduce the vehicle roll behavior and wheel lift points in the lane change maneuvers.

There were two significant modeling parameters needed for the evaluation of TruckSim® simulations which could not be directly measured and which needed to be estimated in order to successfully complete the modeling efforts. These were the inertia of the vehicle (tractor and tank trailer), and the fifth wheel torsional response characterization. To complete the modeling, these parameters were estimated using available engineering data. The dimensional and mass measurements taken during testing were used to evaluate the vehicle's inertia. For the fifth

wheel, the tank trailer load, its dimensions, and the kingpin design were used to estimate the roll moment transmitted through the fifth wheel as a function of relative tractor and tank trailer roll angles. The model was able to produce good results with reasonable estimates of the non-measured parameters.

The TruckSim® model was quite successful at predicting the wheel lift thresholds for both the ramp steer and the step steer maneuvers. These modeling exercises were completed with the same payload configurations that were used in the understeer analysis and are believed to be accurate reflections of the actual low-CG and high-CG configurations. For the open loop double lane change maneuver, the model was able to predict the correct vehicle wheel lift points using two sets of standardized loads; one with the center load set above the water tanks (high-CG tank trailer), and the other with the center load below the water tanks (low-CG tank trailer). The loads used in the modeling efforts matched the on-track test loads in location and mass. Lift points predicted by the model were within the 95% confidence intervals observed in the on-track data results for all but two measurements and these two were off by less than 1.5%.

SimMechanics

The model of a coupled lateral/directional motion of a tractor-tank trailer configuration is being developed at WMU using MATLAB/Simulink/SimMechanics. The simulation test results subject to the three steering input signals used during the actual on-track vehicle testing were used to study the transient characteristics of the tank trailer. The simulation results agree, in general, with the test results for the low-speed maneuver during on-track testing, but exhibits instability for some maneuver testing at higher speeds. This may be due to the uncertainties in the system parameters used in the model, especially associated with the high torsional stiffness of the tank trailer. Much of these data should be further investigated and validated with other efforts including static and dynamic measurement and solid modeling.

The tank trailer frame was much stiffer than the van trailer and flatbed trailer, and the torsional stiffness showed a strong influence on the stability of the vehicle. A trailer with high stiffness is more susceptible to rollover. The liquid sloshing effect (not tested during the on-track testing) was modeled with a flexible tanker model, and its effect aggravates unstable motion. Thus, for a tank trailer with high torsional stiffness and a moving payload such as liquid sloshing or hanging weight, it is recommended that the tank trailer be modeled as a rigid-body with a moving pendulum.

Solid and Finite Element Modeling Toward Fully Flexible Dynamic Models

Models have been developed which will support fully flexible dynamic models of the tractor and tank trailer system (e.g. frame, axles, trailing arms) in ADAMS. For Phase B, this process began by digitally scanning the Volvo tractor and the LBT tank trailer. Solid models of the tractor and tank trailer structures were developed in Pro/Engineer solid modeling software using these scans. These solid models were then passed to ABAQUS where finite element models were developed

and analyzed for flexural and modal frequency content. The models were converted to modal neutral files which are used in Phase C.

ADAMS will use the modal neutral files as flexible structures in a full vehicle analysis environment. This full flexible model will make it possible to investigate the interaction of the flexible structures as a dynamic system. Stress and fatigue studies will be possible as well.

Appendix E – Step Steer Maneuver Data

Table E- 1. Step Steer –Maneuver initial speed and lateral accelerations at wheel lift (Tanker TC1)

Run	Initial Speed (km/h)	Tractor Lateral Acceleration (g)		Trailer Lateral Acceleration (g)	
		Axle 2L	Axle 3L**	Axle 4L	Axle 5L
33 STEP 1_041210_094937_RN_001_filt.csv	52.8	#N/A	#N/A	-0.379	-0.379
34 STEP 1_041210_095012_RN_001_filt.csv	54.3	#N/A	#N/A	-0.387	-0.387
34 STEP 2-4_041210_095130_RN_001_filt.csv	54.4	#N/A	#N/A	-0.351	-0.351
34 STEP 2-4_041210_095130_RN_002_filt.csv	54.3	#N/A	#N/A	-0.369	-0.369
34 STEP 2-4_041210_095130_RN_003_filt.csv	54.4	#N/A	#N/A	-0.375	-0.375
35 STEP 1_041210_095209_RN_001_filt.csv	55.9	-0.439	-0.433**	-0.362	-0.366
35 STEP 2-4_041210_095325_RN_001_filt.csv	56.0	-0.431	-0.429**	-0.371	-0.366
35 STEP 2-4_041210_095325_RN_002_filt.csv	56.0	-0.424*	-0.412**	-0.364	-0.364
35 STEP 2-4_041210_095325_RN_003_filt.csv	56.0	-0.406*	-0.406**	-0.365	-0.364
36 STEP 1_041210_095403_RN_001_filt.csv	57.6	-0.458*	-0.458**	-0.373	-0.373

* The observed Axle 2 left minimal vertical forces were above the threshold used to determine wheel lift; these lateral accelerations were not used in the analysis.

** The observed Axle 3 left minimal vertical forces were between three and four times the threshold used to determine wheel lift these lateral accelerations were not used in the analysis.

Table E- 2. Step Steer –Maneuver initial speed and lateral accelerations

Run	Initial Speed (km/h)	Lateral Acceleration (g)	
		Tractor	Trailer
30 STEP 1_041210_094707_RN_001_filt.csv	47.9	-0.334	-0.305
32 STEP 1_041210_094742_RN_001_filt.csv	51.1	-0.371	-0.357
32 STEP 2-4_041210_094858_RN_001_filt.csv	51.2	-0.372	-0.331
32 STEP 2-4_041210_094858_RN_002_filt.csv	51.1	-0.368	-0.325
32 STEP 2-4_041210_094858_RN_003_filt.csv	51.1	-0.364	-0.330

Table E- 3. Step Steer –Maneuver initial speed and lateral accelerations at wheel lift (Tanker TC2)

Run	Initial Speed (km/h)	Tractor Lateral Acceleration (g)		Trailer Lateral Acceleration (g)	
		Axle 2L	Axle 3L**	Axle 4L	Axle 5L
TC2 HIGH SPEED STEP_041210_173646_RN_005_filt.csv	54.4	#N/A	#N/A	-0.397	-0.385
TC2 HIGH SPEED STEP_041210_173646_RN_006_filt.csv	54.4	#N/A	#N/A	#N/A	-0.379
TC2 HIGH SPEED STEP_041210_173646_RN_007_filt.csv	54.3	#N/A	#N/A	-0.394	-0.394
TC2 HIGH SPEED STEP_041210_173646_RN_008_filt.csv	54.4	#N/A	#N/A	-0.373	-0.401
TC2 HIGH SPEED STEP_041210_173646_RN_009_filt.csv	56.0	-0.440	-0.440**	-0.387	-0.390
TC2 HIGH SPEED STEP_041210_173646_RN_010_filt.csv	56.0	-0.438	-0.438**	-0.396	-0.394
TC2 HIGH SPEED STEP_041210_173646_RN_011_filt.csv	56.0	-0.435	-0.425**	-0.378	-0.372
TC2 HIGH SPEED STEP_041210_173646_RN_012_filt.csv	56.0	-0.429	-0.428**	-0.371	-0.384
TUESDAY RUNS TC2_041310_091945_RN_005_filt.csv	56.1	-0.436*	-0.436**	-0.379	#N/A
TUESDAY RUNS TC2_041310_091945_RN_006_filt.csv	56.1	-0.447	-0.447**	-0.391	#N/A

* The observed Axle 2 left minimal vertical forces were above the threshold used to determine wheel lift; these lateral accelerations were not used in the analysis.

** The observed Axle 3 left minimal vertical forces were between three and four times the threshold used to determine wheel lift these lateral accelerations were not used in the analysis.

Table E- 4. Step Steer –Maneuver initial speed and lateral accelerations

Run	Initial Speed (km/h)	Lateral Acceleration (g)	
		Tractor	Trailer
TC2 HIGH SPEED STEP_041210_173646_RN_001_filt.csv	51.2	-0.379	-0.349
TC2 HIGH SPEED STEP_041210_173646_RN_002_filt.csv	51.2	-0.373	-0.349
TC2 HIGH SPEED STEP_041210_173646_RN_003_filt.csv	51.2	-0.373	-0.339
TC2 HIGH SPEED STEP_041210_173646_RN_004_filt.csv	51.2	-0.383	-0.340

Table E- 5. Step Steer – Maximum lateral acceleration and maximum roll angle (Tanker TC1, tractor)

Run	Max Ay (g)	Max RA (deg)	RC (deg/g)
33 STEP 1_041210_094937_RN_001_filt.csv	-0.40	3.09	-7.77
34 STEP 1_041210_095012_RN_001_filt.csv	-0.42	3.18	-7.63
34 STEP 2-4_041210_095130_RN_001_filt.csv	-0.42	3.26	-7.77
34 STEP 2-4_041210_095130_RN_002_filt.csv	-0.42	3.17	-7.50
34 STEP 2-4_041210_095130_RN_003_filt.csv	-0.42	3.08	-7.36
35 STEP 1_041210_095209_RN_001_filt.csv	-0.44	4.53	-10.30
35 STEP 2-4_041210_095325_RN_001_filt.csv	-0.46	4.85	-10.63
35 STEP 2-4_041210_095325_RN_002_filt.csv	-0.44	4.46	-10.16
35 STEP 2-4_041210_095325_RN_003_filt.csv	-0.44	4.56	-10.37
36 STEP 1_041210_095403_RN_001_filt.csv	-0.49	5.68	-11.69

Table E- 6. Step Steer – Maximum lateral acceleration and maximum roll angle (Tanker TC1, trailer)

Run	Max Ay (g)	Max RA (deg)	RC (deg/g)
33 STEP 1_041210_094937_RN_001_filt.csv	-0.39	3.63	-9.32
34 STEP 1_041210_095012_RN_001_filt.csv	-0.41	4.08	-9.93
34 STEP 2-4_041210_095130_RN_001_filt.csv	-0.41	5.58	-13.77
34 STEP 2-4_041210_095130_RN_002_filt.csv	-0.42	5.26	-12.52
34 STEP 2-4_041210_095130_RN_003_filt.csv	-0.41	4.68	-11.36
35 STEP 1_041210_095209_RN_001_filt.csv	-0.44	9.48	-21.62
35 STEP 2-4_041210_095325_RN_001_filt.csv	-0.47	9.71	-20.64
35 STEP 2-4_041210_095325_RN_002_filt.csv	-0.52	9.39	-18.20
35 STEP 2-4_041210_095325_RN_003_filt.csv	-0.45	9.45	-20.94
36 STEP 1_041210_095403_RN_001_filt.csv	-0.50	10.19	-20.37

Table E- 7. Step Steer – Maximum lateral acceleration and maximum roll angle (Tanker TC2, tractor)

Run	Max Ay (g)	Max RA (deg)	RC (deg/g)
TC2 HIGH SPEED STEP_041210_173646_RN_005_filt.csv	-0.44	3.30	-7.55
TC2 HIGH SPEED STEP_041210_173646_RN_006_filt.csv	-0.43	3.26	-7.59
TC2 HIGH SPEED STEP_041210_173646_RN_007_filt.csv	-0.43	3.19	-7.38
TC2 HIGH SPEED STEP_041210_173646_RN_008_filt.csv	-0.43	3.31	-7.69
TC2 HIGH SPEED STEP_041210_173646_RN_009_filt.csv	-0.46	4.92	-10.73
TC2 HIGH SPEED STEP_041210_173646_RN_010_filt.csv	-0.46	4.92	-10.73
TC2 HIGH SPEED STEP_041210_173646_RN_011_filt.csv	-0.45	4.70	-10.54
TC2 HIGH SPEED STEP_041210_173646_RN_012_filt.csv	-0.44	4.61	-10.39
TUESDAY RUNS TC2_041310_091945_RN_005_filt.csv	-0.47	5.16	-11.08
TUESDAY RUNS TC2_041310_091945_RN_006_filt.csv	-0.47	5.15	-10.95

Table E- 8. Step Steer – Maximum lateral acceleration and maximum roll angle (Tanker TC2, trailer)

Run	Max Ay (g)	Max RA (deg)	RC (deg/g)
TC2 HIGH SPEED STEP_041210_173646_RN_005_filt.csv	-0.43	7.41	-17.08
TC2 HIGH SPEED STEP_041210_173646_RN_006_filt.csv	-0.43	5.77	-13.51
TC2 HIGH SPEED STEP_041210_173646_RN_007_filt.csv	-0.41	5.55	-13.47
TC2 HIGH SPEED STEP_041210_173646_RN_008_filt.csv	-0.42	6.53	-15.52
TC2 HIGH SPEED STEP_041210_173646_RN_009_filt.csv	-0.46	9.68	-21.08
TC2 HIGH SPEED STEP_041210_173646_RN_010_filt.csv	-0.46	9.70	-21.13
TC2 HIGH SPEED STEP_041210_173646_RN_011_filt.csv	-0.46	9.53	-20.90
TC2 HIGH SPEED STEP_041210_173646_RN_012_filt.csv	-0.46	9.43	-20.43
TUESDAY RUNS TC2_041310_091945_RN_005_filt.csv	-0.46	9.83	-21.23
TUESDAY RUNS TC2_041310_091945_RN_006_filt.csv	-0.46	9.77	-21.30

Appendix F – Lane Change Maneuver Data

Table F- 1. Lane Change/ESC Disabled –Maneuver initial speed and lateral accelerations at wheel lift (Tanker TC1)

Run	Initial Speed (km/h)	Trailer Lateral Acceleration (g)			
		Axle 4L	Axle 4R	Axle 5L	Axle 5R
34 LANE CHANGE_040910_175059_RN_001_filt.csv	54.4	-0.317	0.418	-0.317	0.373
34 LANE CHANGE_040910_175059_RN_002_filt.csv	55.4	#N/A	0.426	#N/A	0.384
34 LANE CHANGE_040910_175059_RN_003_filt.csv	55.4	-0.263	0.429	-0.263	0.382
VARIED SPEED LANE CHANGE_040910_165926_RN_005_filt.csv	55.2	-0.184	0.412	-0.188	0.396
VARIED SPEED LANE CHANGE_040910_165926_RN_006_filt.csv	55.5	-0.294	0.421	-0.294	0.389

Table F- 2. Lane Change/ESC Disabled –Maneuver initial speed and lateral accelerations at wheel lift (Tanker TC2)

Run	Initial Speed (km/h)	Trailer Lateral Acceleration (g)			
		Axle 4L	Axle 4R	Axle 5L	Axle 5R
TC 2 34 LANE CHANGE_042010_141511_RN_001_filt.csv	54.2	#N/A	0.409	#N/A	0.342
TC 2 34 LANE CHANGE_042010_141511_RN_002_filt.csv	54.9	#N/A	0.427	#N/A	0.443
TC 2 34 LANE CHANGE_042010_141511_RN_003_filt.csv	54.9	#N/A	0.409	#N/A	0.412
TC 2 34 LANE CHANGE_042010_141511_RN_004_filt.csv	55.1	#N/A	0.416	#N/A	0.426
TC 2 34 LANE CHANGE_042010_141511_RN_005_filt.csv	54.9	#N/A	0.402	#N/A	0.394
TC2 34 LANE CHANGE 5-9_042010_141640_RN_001_filt.csv	56.1	#N/A	0.415	#N/A	0.404
TC2 34 LANE CHANGE 5-9_042010_141640_RN_002_filt.csv	55.4	#N/A	0.422	#N/A	0.412
TC2 34 LANE CHANGE 5-9_042010_141640_RN_003_filt.csv	55.6	#N/A	0.412	#N/A	0.403
TC2 34 LANE CHANGE 5-9_042010_141640_RN_004_filt.csv	55.2	#N/A	0.411	#N/A	0.446
TUESDAY RUNS TC2_041310_091945_RN_001_filt.csv	55.5	#N/A	0.394	#N/A	0.397
TUESDAY RUNS TC2_041310_091945_RN_002_filt.csv	55.0	#N/A	0.427	#N/A	0.392
TUESDAY RUNS TC2_041310_091945_RN_003_filt.csv	55.4	#N/A	0.396	#N/A	0.409
TUESDAY RUNS TC2_041310_091945_RN_004_filt.csv	55.1	#N/A	0.423	#N/A	0.402

Table F- 3. Lane Change/ESC Disabled – Maximum lateral acceleration and maximum roll angle (Tanker TC1, tractor)

Run	First Part			Second Part		
	Max Ay (g)	Max RA (deg)	RC (deg/g)	Max Ay (g)	Max RA (deg)	RC (deg/g)
34 LANE CHANGE_040910_175059_RN_001_filt.csv	-0.41	3.06	-7.52	0.52	-3.61	-6.94
34 LANE CHANGE_040910_175059_RN_002_filt.csv	-0.42	2.99	-7.04	0.49	-3.33	-6.83
34 LANE CHANGE_040910_175059_RN_003_filt.csv	-0.42	3.21	-7.63	0.51	-3.59	-6.98
VARIED SPEED LANE CHANGE_040910_165926_RN_005_filt.csv	-0.42	3.07	-7.33	0.52	-3.51	-6.82
VARIED SPEED LANE CHANGE_040910_165926_RN_006_filt.csv	-0.44	3.29	-7.54	0.52	-3.67	-7.10

Table F- 4. Lane Change/ESC Disabled – Maximum lateral acceleration and maximum roll angle (Tanker TC1, trailer)

Run	First Part			Second Part		
	Max Ay (g)	Max RA (deg)	RC (deg/g)	Max Ay (g)	Max RA (deg)	RC (deg/g)
34 LANE CHANGE_040910_175059_RN_001_filt.csv	-0.34	3.28	-9.65	0.45	-7.74	-17.22
34 LANE CHANGE_040910_175059_RN_002_filt.csv	-0.33	3.53	-10.53	0.46	-5.94	-13.05
34 LANE CHANGE_040910_175059_RN_003_filt.csv	-0.38	3.65	-9.57	0.45	-7.46	-16.47
VARIED SPEED LANE CHANGE_040910_165926_RN_005_filt.csv	-0.38	3.38	-8.79	0.46	-7.08	-15.26
VARIED SPEED LANE CHANGE_040910_165926_RN_006_filt.csv	-0.33	3.59	-10.78	0.46	-7.03	-15.12

Table F- 5. Lane Change/ESC Disabled – Maximum lateral acceleration and maximum roll angle (Tanker TC2, tractor)

Run	First Part			Second Part		
	Max Ay (g)	Max RA (deg)	RC (deg/g)	Max Ay (g)	Max RA (deg)	RC (deg/g)
TC 2 34 LANE CHANGE_042010_141511_RN_001_filt.csv	-0.42	3.01	-7.24	0.47	-3.10	-6.57
TC 2 34 LANE CHANGE_042010_141511_RN_002_filt.csv	-0.41	3.06	-7.46	0.50	-3.27	-6.51
TC 2 34 LANE CHANGE_042010_141511_RN_003_filt.csv	-0.42	3.19	-7.55	0.50	-3.38	-6.75
TC 2 34 LANE CHANGE_042010_141511_RN_004_filt.csv	-0.41	3.30	-7.99	0.51	-3.43	-6.71
TC 2 34 LANE CHANGE_042010_141511_RN_005_filt.csv	-0.41	3.30	-7.97	0.49	-3.40	-6.93
TC2 34 LANE CHANGE 5-9_042010_141640_RN_001_filt.csv	-0.44	3.12	-7.06	0.49	-3.56	-7.34
TC2 34 LANE CHANGE 5-9_042010_141640_RN_002_filt.csv	-0.43	3.12	-7.25	0.50	-3.66	-7.38
TC2 34 LANE CHANGE 5-9_042010_141640_RN_003_filt.csv	-0.43	3.11	-7.27	0.49	-3.61	-7.34
TC2 34 LANE CHANGE 5-9_042010_141640_RN_004_filt.csv	-0.43	3.10	-7.27	0.50	-3.55	-7.14
TUESDAY RUNS TC2_041310_091945_RN_001_filt.csv	-0.45	3.09	-6.93	0.47	-3.74	-7.89
TUESDAY RUNS TC2_041310_091945_RN_002_filt.csv	-0.45	3.19	-7.13	0.48	-3.61	-7.50
TUESDAY RUNS TC2_041310_091945_RN_003_filt.csv	-0.46	3.12	-6.83	0.49	-3.69	-7.52
TUESDAY RUNS TC2_041310_091945_RN_004_filt.csv	-0.44	3.22	-7.32	0.49	-3.71	-7.53

Table F- 6. Lane Change/ESC Disabled – Maximum lateral acceleration and maximum roll angle (Tanker TC2, trailer)

Run	First Part			Second Part		
	Max Ay (g)	Max RA (deg)	RC (deg/g)	Max Ay (g)	Max RA (deg)	RC (deg/g)
TC 2 34 LANE CHANGE_042010_141511_RN_001_filt.csv	-0.34	3.50	-10.36	0.41	-4.53	-11.08
TC 2 34 LANE CHANGE_042010_141511_RN_002_filt.csv	-0.33	3.59	-10.85	0.46	-6.98	-15.08
TC 2 34 LANE CHANGE_042010_141511_RN_003_filt.csv	-0.34	3.59	-10.53	0.45	-6.91	-15.26
TC 2 34 LANE CHANGE_042010_141511_RN_004_filt.csv	-0.35	3.72	-10.55	0.45	-6.57	-14.67
TC 2 34 LANE CHANGE_042010_141511_RN_005_filt.csv	-0.36	3.69	-10.15	0.44	-6.29	-14.21
TC2 34 LANE CHANGE 5-9_042010_141640_RN_001_filt.csv	-0.37	3.96	-10.84	0.45	-6.14	-13.77
TC2 34 LANE CHANGE 5-9_042010_141640_RN_002_filt.csv	-0.36	3.95	-10.94	0.44	-6.66	-15.14
TC2 34 LANE CHANGE 5-9_042010_141640_RN_003_filt.csv	-0.34	3.88	-11.30	0.43	-6.30	-14.53
TC2 34 LANE CHANGE 5-9_042010_141640_RN_004_filt.csv	-0.37	3.88	-10.54	0.45	-6.39	-14.31
TUESDAY RUNS TC2_041310_091945_RN_001_filt.csv	-0.35	3.97	-11.22	0.42	-4.93	-11.85
TUESDAY RUNS TC2_041310_091945_RN_002_filt.csv	-0.37	4.09	-10.99	0.46	-6.26	-13.76
TUESDAY RUNS TC2_041310_091945_RN_003_filt.csv	-0.37	4.08	-11.10	0.44	-6.73	-15.25
TUESDAY RUNS TC2_041310_091945_RN_004_filt.csv	-0.38	4.20	-11.09	0.44	-6.44	-14.62

Appendix G – Adams Modeling

Simulations of the ramp steer in the Adams model are presented here for three vehicles—Tanker T, Tanker TC2, and a modified Tanker T having a rigid tractor frame and no fifth wheel lash. The ramp steer maneuver was selected for tuning the Adams model because it progresses to wheel lift as the steering angle increases for at a steady speed. The vehicle speed was 45 km/h, and the ramp steer rate of the hand wheel of 10 deg/s, nominally the same conditions as the experiments on the test track. The trailer track width is the only difference in the model between the Tankers T and TC2; see Table 6-1 of the main text.

In the images of the vehicles in the maneuver, the positions of two or three vehicles are overlaid. Tanker T is shown in solid red, and Tanker TC2 is shown with a blue tractor cab and hood with a silver trailer. The horizontal bar in the figures represents the outrigger. The mass of the entire outrigger assembly was included in the model, but the outrigger tires were not modeled, so the model's roll angle was not limited.

The longer axle of Tanker TC2 deflects more than that of Tanker T under the same static vertical load of the trailer. The static rest position of the rear of Tanker TC2 in the model was 4 mm below that of Tanker T, as illustrated in Figure G-1.

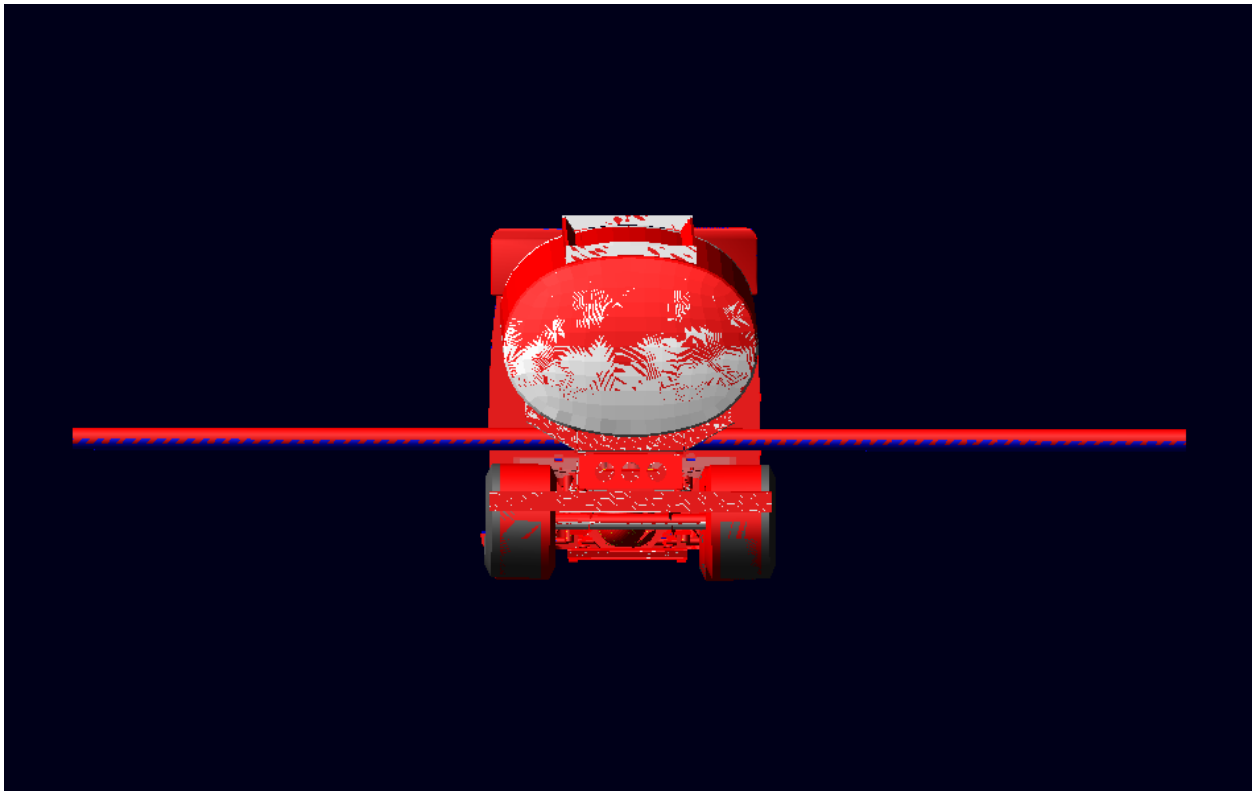

Figure G- 1. Screen capture. Rear view of Tanker T (in red) overlaid on Tanker TC2 (silver trailer and blue outrigger) showing the lower static position of Tanker TC2.

Tanker T had a slightly greater understeer than Tanker TC2, as evidenced by Tanker T tracking outside and slightly behind the path of Tanker TC2. Figures G-2 and G-3, both taken at 18 s into the ramp steer maneuver, show the difference from two angles.

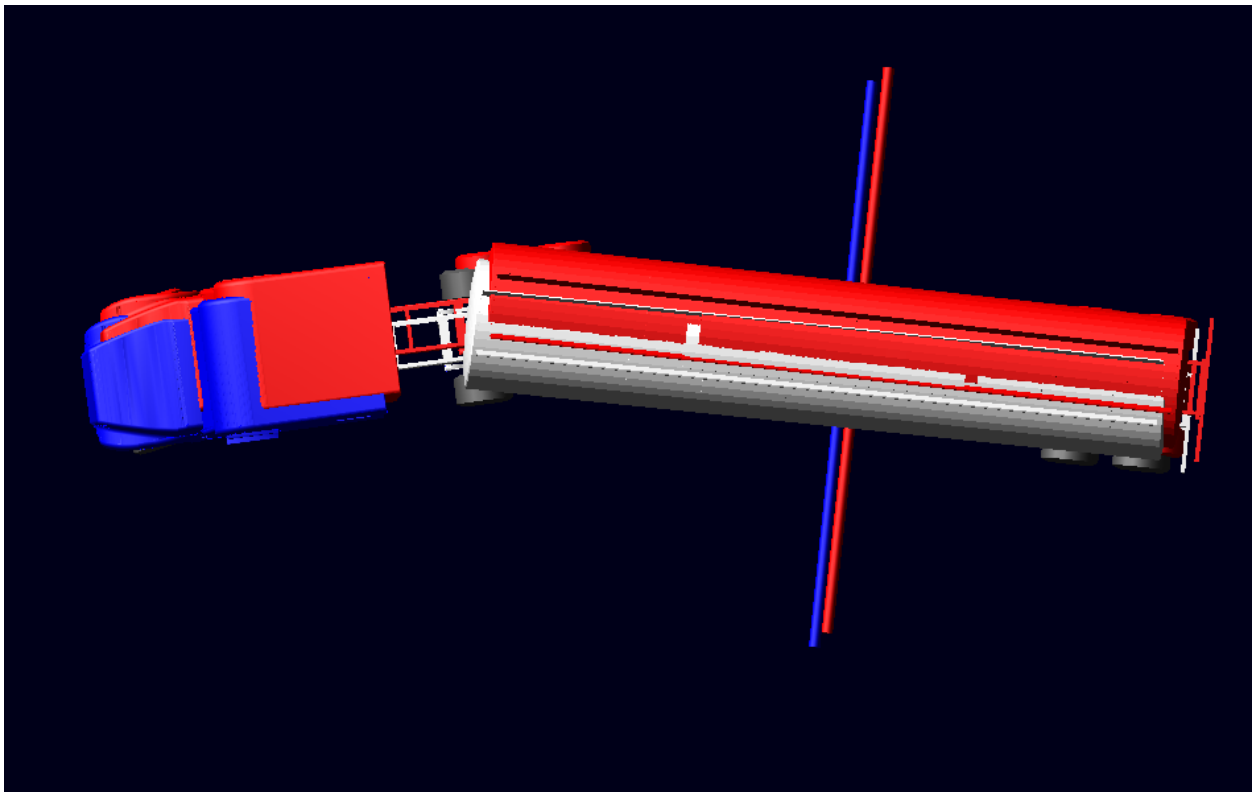

Figure G- 2. Screen capture. Top view at 18 s into the ramp steer maneuver showing the greater understeer of Tanker T (red) than of Tanker TC2 (blue cab and silver tank).

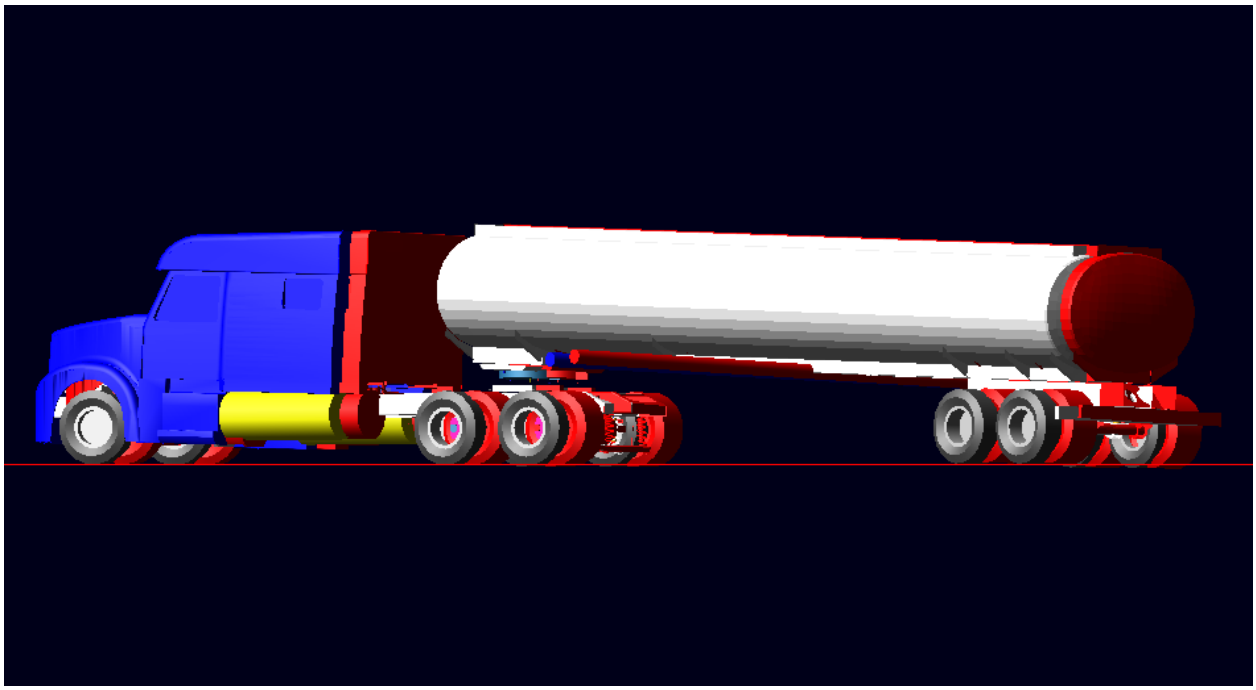

Figure G- 3. Screen capture. Same conditions as Figure G-2, from a different perspective.

The left tire on axle 5 lifted first in all three runs. The first tire of Tanker T lifted about 3 s before Tanker TC2. When the maneuver was continued to 23 s, Tanker T rolled over, as shown in Figure G-4.

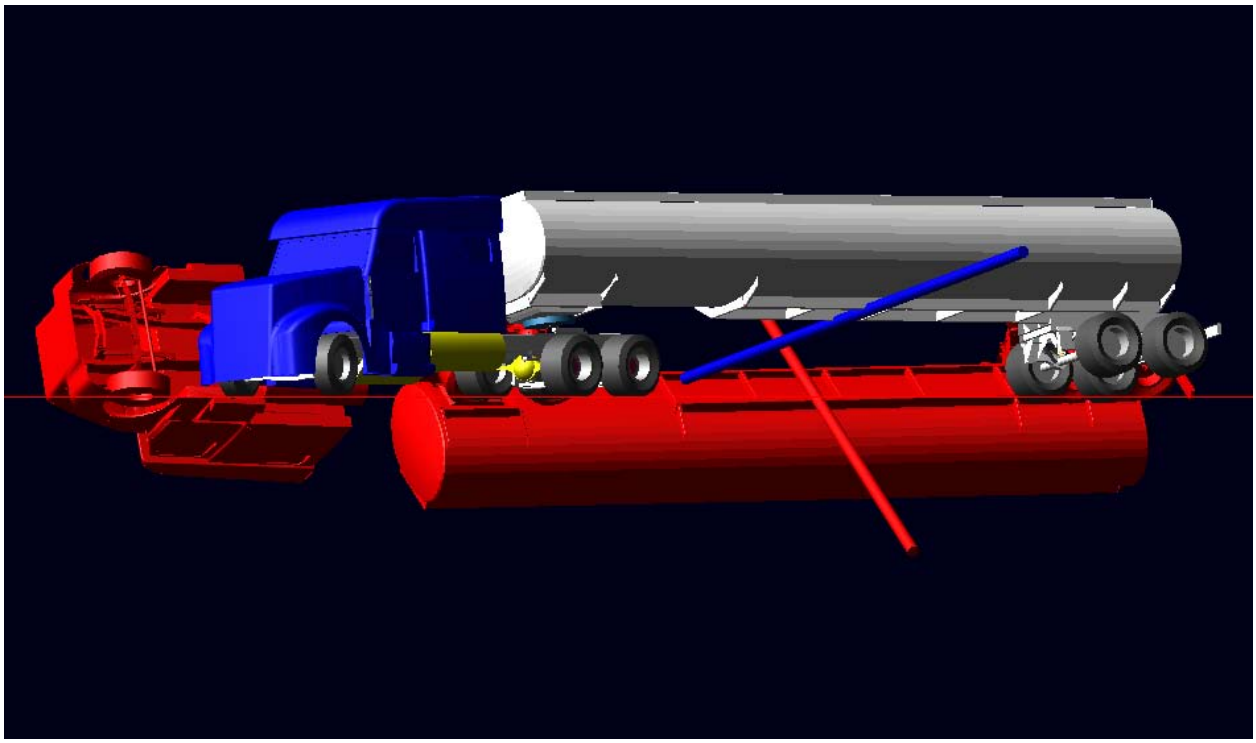

Figure G- 4. Screen capture. Complete rollover of Tanker T at 23 s into the ramp steer

At the pictured instant, model has 2.5 deg lash in the fifth wheel attachment significant flex in the tractor frame, as shown in Figure G-5.

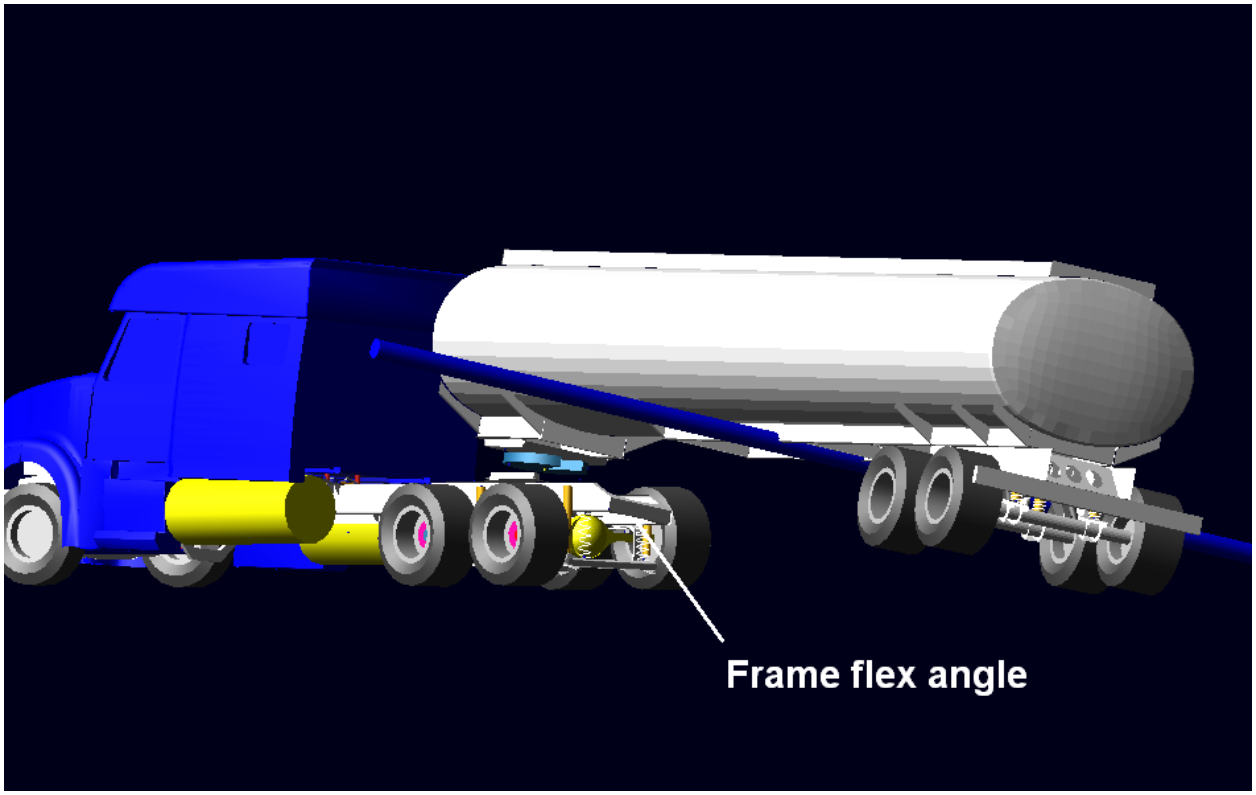

Figure G- 5. Screen capture. A left rear corner view of the tractor showing the flex angle of the tractor frame.

The lift sequence of the tires matched experimental data, and the path was close to field data. Table G-1 lists the lateral acceleration at wheel lift on the fifth axle during the ramp steer for Tankers T and TC2. One column lists the experimentally measured values (See Table 7-1 of the main text.) and another lists the corresponding values predicted by the Adams model. The model predicted the trends in wheel lift threshold, but the values were between 14% and 16% lower than test track measurements.

Table G- 1. Lateral acceleration at wheel lift in the Ramp Steer maneuver, from Adams model and test track

Condition	**Overall Width** in *mm*	**Lift Threshold, g**	
		Test Track	Adams Model
Tanker T (nominal)	92.2 *2342*	.364	.307
Tanker TC2 (wider track)	97.875 *2486*	.388	.333
difference	5.675 *144*	6.6%	8.5%

A short study of the effect of frame flexure and fifth wheel lash was done on Tanker T. The simulation of Tanker T was run again with a rigid tractor frame and with the fifth wheel lash locked out. Figure G-6 illustrates that the left wheel on axle 5 lifted at approximately the same time for Tanker TC2 and the modified Tanker T. The left wheel on Axle 5 lifted 2 s earlier for the original Tanker T. For a design aimed at stiffening the tractor frame and eliminating fifth wheel lash, the black line in Figure G-6 would serve as theoretical limit for controlling the start of wheel lift on axle 5. Thus, the start of rollover might be delayed.

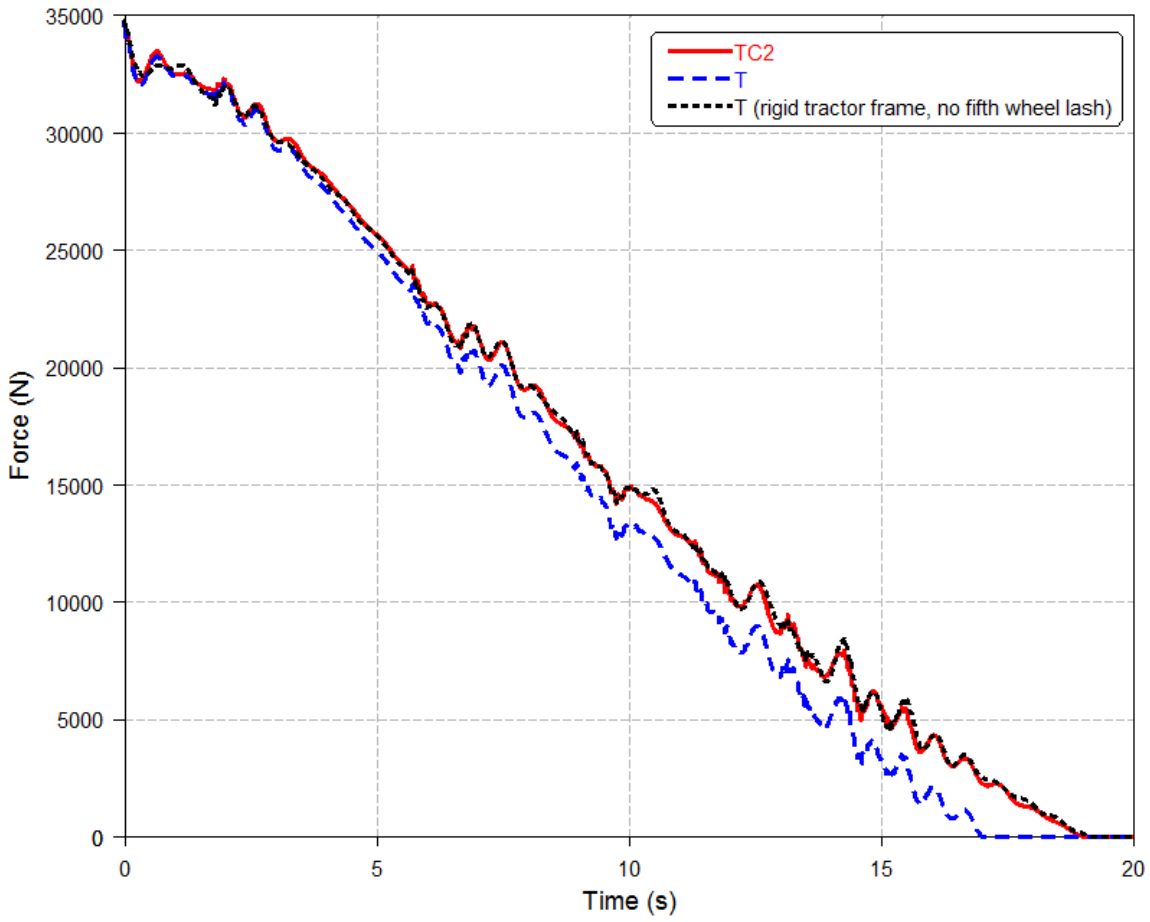

Figure G- 6. Graph. Vertical force on the left (inside) tire on Axle 5 during the ramp steer for the three modeled vehicles.

Perhaps the most dramatic effect of the rigid tractor frame and the elimination of all fifth wheel lash on the Tanker T vehicle is shown in Figure G-7. Here, top and rear views clearly show that this combination has caused the modified Tanker T to significantly drift wide of the paths of the two original vehicles. While the rigid vehicle was more stable in roll, this caused significant understeer.

The Adams model predicts that the wider axle of Tanker TC2 will provide a clear improvement over over Tanker T in delaying wheel lift. The model also predicts that increased tractor frame

stiffness will also delay wheel lift, but it will also increase understeer. These are obviously a topic for further study.

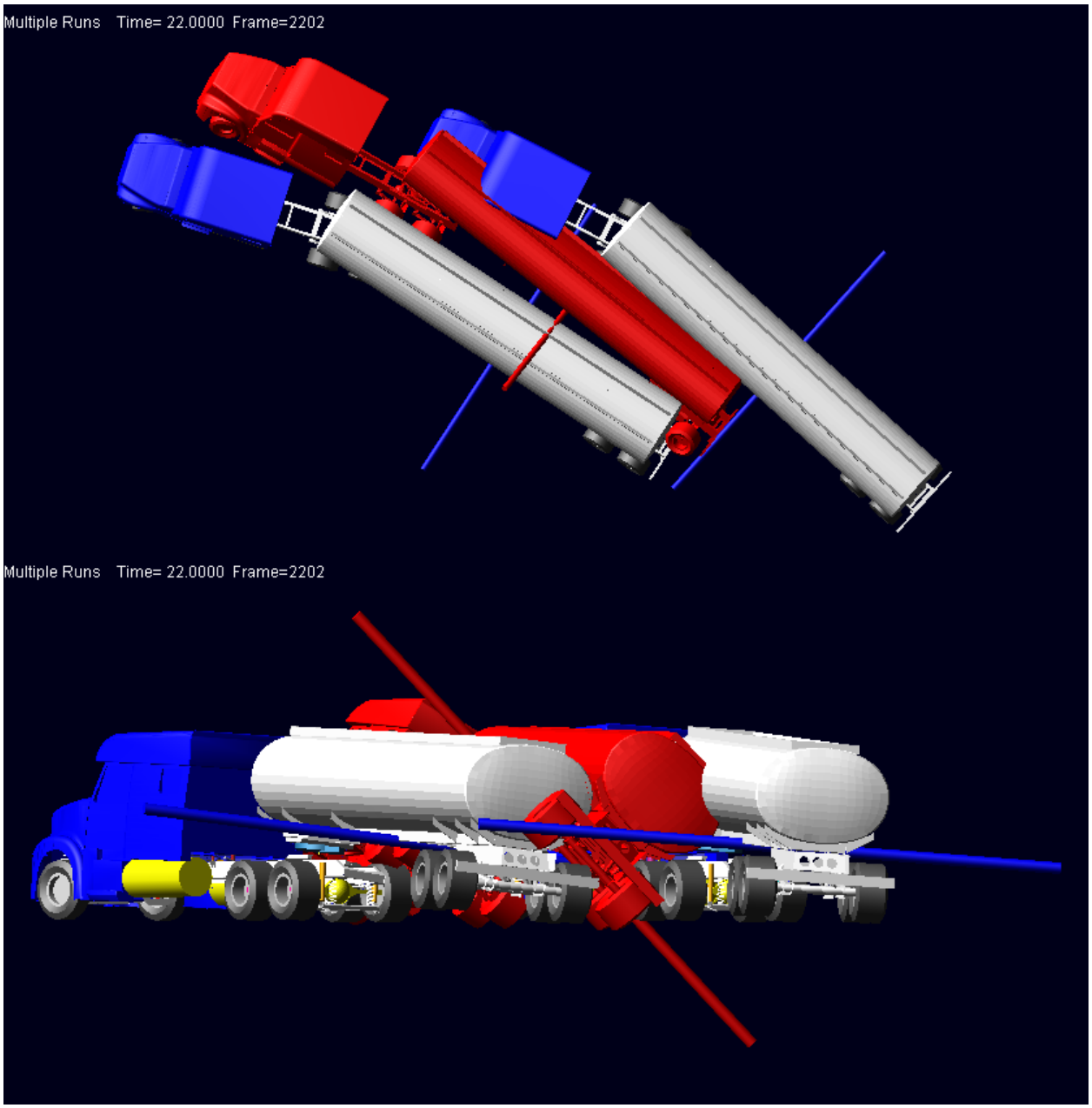

Figure G- 7. Screen capture. The modified Tanker T vehicle on the far right drifts outside the paths of Tanker TC2 on the far left and Tanker T shown in red.

As of this writing the Adams model is in the process of being tuned for validation. It has shown the ablity to predict differences between rigid body and flexible body vehicles. The Adams model shows promise in its ability to model discrete and flexible components.

Appendix H – Kinematics and Compliance (K&C) Data

Line Item	
	Equivalent or similar, very close in performance.
	Not a meaningful measurement
	Large or significant difference
	Difference but significance is unknown

no color

	Leading Trailer Axle				
	Vertical Deflection	**Tanker T**	**Tanker TC1**	**Units**	**Diff Ind**
1	The middle axle suspension vertical spring rate is equivalent between the trailers	270.8	280.1	N/mm	3%
2	The middle axle suspension vertical spring rate hysteresis is equivalent between the trailers	327.4	319.4	kg	-3%
3	The Mmiddle axle toe change and steer due to vertical loading is similar between the trailers and near zero	0	0		
4	The middle axle camber change due to vertical loading is equivalent between the trailers	-0.003	-0.003	deg/ mm	
5	The middle axle track change due to vertical loading is equivalent between the trailers	0.051	0.051	mm/ mm	
6	The middle axle wheel center lateral displacement due to vertical loading is similar between the trailers and near zero	-0.003	0.002	mm/ mm	
7	The middle axle wheel center longitudinal displacement due to vertical loading is similar between the trailers	-0.365	-0.394	mm/ mm	7%
8	The middle axle locked wheel rotation due to vertical loading is similar between the trailers	0.115	0.117	deg/ mm	2%
9	The middle axle roll center height due to vertical loading is equivalent between the trailers (Line 32 is a better measurement of roll center height)	20	21	mm	5%
10	The middle axle roll center height gradient due to vertical loading is equivalent between the trailers	0.08	0.08	mm/ mm	

	Rear Trailer Axle				
	Vertical Deflection				
11	The rear axle suspension vertical spring rate is equivalent between the trailers	240.3	234.9	N/mm	-2%
12	The rear axle suspension vertical spring rate hysteresis is equivalent between the trailers	332.9	314	kg	-6%
13	The rear axle toe change and steer due to vertical loading is similar between the trailers and near zero	0	0	deg/ mm	
14	The rear axle camber change due to vertical loading is equivalent between the trailers	-0.003	-0.003	deg/ mm	

15	The rear axle track change due to vertical loading is equivalent between the trailers	0.046	0.049	mm/ mm	6%
16	Tanker TC1 has slightly more rear axle wheel center lateral displacement due to vertical loading, but both are near zero	0.001	0.008	mm/ mm	88%
17	The rear axle wheel center longitudinal displacement due to vertical loading is similar between the trailers	-0.347	-0.367	mm/ mm	5%
18	The rear axle locked wheel rotation due to vertical loading is similar between the trailers	0.114	0.116	deg/ mm	2%
19	The rear axle roll center height due to vertical loading is similar between the trailers	18	21	mm	14%
20	The rear axle roll center height gradient due to vertical loading is similar between the trailers	0.05	0.06	mm/ mm	17%
	Leading Trailer Axle				
	Responses Due To Braking Forces				
21	The vertical load change due to braking forces is equivalent between the trailers	118.8	114.5	kg/kN	-4%
22	Tanker T demonstrates more toe out under braking forces	0.021	0.015	deg/ kN	-40%
23	The axle steer due to braking forces is equivalent between the trailers and near zero	-0.001	0	deg/ kN	
24	The wheel center longitudinal displacement due to braking forces is greater for Tanker TC1	0.83	1.02	mm/ kN	19%
25	Tanker TC1 shows more locked wheel rotation due to braking forces	-0.22	-0.26	deg/ kN	15%
	Rear Trailer Axle				
	Responses Due To Braking Forces				
26	The vertical load change due to braking forces is similar between the trailers	116.4	109.8	kg/kN	-6%
27	Tanker T demonstrates slightly more toe out under braking forces	0.018	0.014	deg/ kN	-29%
28	The axle steer due to braking forces is equivalent between the trailers and near zero	0.001	-0.001	deg/ kN	
29	The wheel center longitudinal displacement due to braking forces is slightly greater for Tanker TC1	0.81	0.88	mm/ kN	8%
30	Tanker TC1 shows more locked wheel rotation due to braking forces	-0.21	-0.24	deg/ kN	13%

	Leading Trailer Axle				
	Responses Due To Lateral Forces				
31	Tanker T demonstrates more vertical load change due to lateral forces	57.9	42.8	kg/kN	-35%
32	Tanker T has a higher roll center height	520	430	mm	-21%
33	Tanker T demonstrates more toe change axle steer due to lateral forces	-0.029	-0.021	deg/ kN	-38%
34	Both trailers are equivalent for camber change due to lateral forces	0.029	0.029	deg/ kN	
35	Tanker T demonstrates a less linear lateral axle shift over center due to lateral forces	0.92	0.7	mm/ kN	-31%
36	Tanker T demonstrates a less linear lateral axle shift over center due to lateral forces	0.67	0.46	mm/ kN	-46%
	Rear Trailer Axle				
	Responses Due To Lateral Forces				
37	Tanker T demonstrates more vertical load change due to lateral forces	58.9	41.4	kg/kN	-42%
38	Tanker T has a higher roll center	529	417	mm	-27%
39	Tanker T demonstrates more toe change axle steer due to lateral forces	-0.026	-0.018	deg/ kN	-44%
40	Both trailers are equivalent for camber change due to lateral forces	0.029	0.029	deg/ kN	
41	Tanker T demonstrates a less linear lateral axle shift over center due to lateral forces	0.81	0.67	mm/ kN	-21%
42	Tanker T demonstrates a less linear lateral axle shift over center due to lateral forces	0.56	0.43	mm/ kN	-30%
	Responses Due To Roll				
43	The vertical suspension spring rate of the leading trailer axle is similar between these two trailers	520.8	543.4	N/mm	4%
44	The leading axle of Tanker TC1 demonstrates higher hysteresis than the leading axle of Tanker T	197.4	254.4	kg	22%
45	The leading axle of Tanker T demonstrates more roll steer than the leading axle of Tanker	-0.061	-0.051	deg/	-20%

	TC1			deg	
46	The CP-based, yaw corrected roll steer of the leading axle is similar between the trailers with Tanker T showing slightly more	-0.171	-0.161	deg/ deg	-6%
47	The leading axle of Tanker TC1 has much more camber change due to roll	0.178	0.267	deg/ deg	33%
48	The leading axle roll stiffness is higher on Tanker TC1	11559	12873	Nm/ deg	10%
49	The leading axle roll stiffness hysteresis is similar between the trailers	0.22	0.23	deg	4%
50	The vertical suspension spring rate of the rear trailer axle is similar between these two trailers	504.4	533.2	N/ mm	5%
51	The rear axle of Tanker TC1 demonstrates higher hysteresis than the rear axle of Tanker T	197.1	217.7	kg	9%
52	The rear axle of Tanker T demonstrates more roll steer than the rear axle of Tanker TC1	-0.046	-0.036	deg/ deg	-28%
53	The CP-based, yaw corrected roll steer of the rear axle is similar between these two trailers with Tanker TC1 showing slightly more	-0.156	-0.147	deg/ deg	-6%
54	The leading axle of Tanker TC1 has much more camber change due to roll	0.181	0.262	deg/ deg	31%
55	The rear axle roll stiffness is higher for Tanker TC1	11587	12641	Nm/ deg	8%
56	Tanker T has higher roll stiffness hysteresis	0.24	0.21	deg	-14%